"THE ELECTRONIC STRUCTURE OF SOME LINEAR MOLECULES."

A

Thesis

presented for the degree of

Ph.D.

in the

University of Glasgow

by

Andrew McKendrick B.Sc.

October 1968.

ProQuest LLC.
789 East Eisenhower Parkway
P.O. Box 1346
Ann Arbor, MI 48106 – 1346

SUMMARY.

This thesis contains an account of molecular electronic structure calculations performed on the linear nitrile molecules CN^-, HCN and FCN. The effect on the CN residue of varying X in the XCN system was observed by analysing the migration of electronic charge with the aid of population analyses and pictorial representations of the electron density distribution.

The calculations were performed as accurately as was feasible using the linear combination of atomic orbitals, molecular orbital, self-consistent field procedure. The only approximation made to this scheme was that the three-centre integrals were evaluated according to approximate formulae. All other integrals were evaluated accurately either by numerical integration or by analytical methods.

A minimal basis set was employed, each atomic orbital being a linear combination of Slater type orbitals of the 'double zeta' type, the orbital exponents of which had been optimally chosen in atomic calculations. These natural atomic orbitals were transformed to an orthogonalised basis set to simplify the mathematical analysis of the iterative procedure by which the energy minimisation was effected. In this work the iteration scheme, to provide a self-consistent wave function, was elaborated in terms of density matrix theory.

In chapter one, a brief account of the various quantum chemical techniques which have been used to study chemical systems, is given, together with an appraisal of the problems involved in such calculations. The standard and aims of the present work are also presented here.

Chapter two contains a fuller account of the theory upon which the present calculations are based. Particular attention is paid to the approximate methods by which the multicentre integrals are calculated. Two of these methods, based on an asymmetric partitioning of the overlap charge densities, have not been evaluated to any extent before.

Experimental information such as the internuclear separations, the double zeta functions and the various units and conversion factors employed in this work, is detailed in chapter three.

The results of the molecular electronic structure calculations performed are presented in chapter four. Population analyses, pictorial representations of the electron density distribution, together with a few molecular properties are presented for each of five internuclear separations of C-N in CN^-, of H-C in HCN and of F-C in FCN. Where possible comparisons are made with calculations of other workers.

The predicted minimum energies for CN^-, HCN and FCN are respectively, -92.18149 a.u. at an internuclear separation of 2.348 a.u.; -92.74494 a.u. at a C-H separation of 2.086 a.u.;

and -191.6180 a.u. at a C-F separation of 2.48 a.u. The calculated dipole moments, in Debye's, for HCN and FCN are respectively 2.59 and 1.54 and are to be compared with the experimental values of 3.00 and 2.17.

An evaluation is made of the Mulliken and two variants of the Löwdin multicentre integral approximations with special reference to the validity of ab initio calculations performed with their aid in integral evaluation. It is shown that both Löwdin approximations give markedly improved results as compared with the Mulliken approximation, and even in the case of the twenty-two electron system of FCN the results are encouragingly close to those of the most accurate calculations. A comparison of some accurate three-centre one-electron integrals for HCN and FCN with the values resulting from the multicentre integral approximations, shows that the full Löwdin method is the best approximation in most cases and often yields values accurate to about three decimal places.

Contour diagrams of the probability charge density and its profile along the internuclear axis are presented for each of the five calculations on CN^-, HCN and FCN. The trends shown are compared with those arising from the population analyses of Mulliken, Löwdin and Doggett. The gross atom charge densities resulting from two of the population analyses, reproduce the molecular dipole moment when account is taken of any atomic

dipoles present. The results of these two different methods of analysing the electronic charge distribution are often at variance, but in general the overall trends are similar. Various contour diagrams of the charge density difference, for example, between the molecular and atomic densities or between two molecular species, are presented, and they clearly show the resultant migration of electronic charge.

The system of computer programs which was written to perform the various stages of the SCF calculations, is described in chapter five. Flow diagrams are presented for each program.

Finally, proposals as to future work using the information and experience obtained in the present calculations, are put forward in chapter six.

There are two appendices. The first describes the method of Gaussian quadrature which was used as the basis of the numerical integration technique by which most of the molecular integrals were evaluated. Appendix two contains the values of all the integrals required to perform the calculation on HCN at its equilibrium configuration, the multicentre integrals being evaluated by the full Löwdin approximation.

Acknowledgements.

I wish to express my gratitude to Dr. G. Doggett not only for his invaluable guidance and encouragement, but also for his many interesting and helpful discussions throughout the course of this work.

In addition, I would like to thank Dr. Doggett for allowing me to use his electron densities computer program and his procedure for the numerical integration of the one-electron integrals.

I would like to thank Dr. J. Sime, Mrs D. Jeffreyes and Miss N. Renfrew for their help with various computing problems. Also I acknowledge with gratitude the support of a Science Research Council research studentship for the duration of this work.

Finally I would like to thank my wife for her help in preparing this thesis.

LIST OF CONTENTS.

NOMENCLATURE.

In order to simplify the text of this thesis, symbols and abbreviations for some common phrases and quantities are used where possible. The nomenclature adopted is presented below: the symbol or abbreviation is listed first followed by a short explanation.

MO : molecular orbital.
VB : valence bond.
SCF : self-consistent field.
LCAO : linear combination of atomic orbitals.
$\underset{\sim}{R}$: representation of the one-particle density matrix.
MC : multiconfiguration.
CI : configuration interaction.
SCGF : self-consistent group function.
ZDO : zero differential overlap.
CNDO : complete neglect of differential overlap.
NDDO : neglect of diatomic differential overlap.
STO : Slater type (atomic) orbital.
GTF : Gaussian type function.
MSO : molecular spin orbital.
OAO : orthogonal atomic orbital.
NAO : natural atomic orbital.
LOAO : Löwdin orthogonalised atomic orbital.

MA : Mulliken approximation.

IMA : invariant Mulliken approximation.

PLA : partial Löwdin approximation.

FLA : full Löwdin approximation.

DZ : double zeta.

DZ+P : double zeta + polarisation.

BA+P : big atom + polarisation.

ϕ : symbol used for an MO.

χ : symbol used for an AO in the NAO basis; χ_a (1) may be abbreviated to χ_a for compactness.

$\underset{\sim}{M}$: a tilda beneath a symbol denotes a matrix, e.g. $\underset{\sim}{R}$.

$\bar{M}$: a bar above a symbol denotes the OAO basis, e.g. $\bar{\chi}$ is the symbol for an AO in the OAO basis.

tr : symbol for the trace of a matrix.

δ_{ij} : the Kronecker Delta; $\delta_{ij} = 1$ when $i = j$ and $\delta_{ij} = 0$ when $i \neq j$.

Chemical symbols such as C for carbon, etc., are also used in the text.

The AO's on an atom are represented by 1s, 2s, $2p_z$, $2p_x$, $2p_y$; for simplicity the p orbitals may be written as 2z, 2x, 2y.

CHAPTER ONE

INTRODUCTION

The title of this research work first appeared in the literature in 1935 as one of a series of papers on the electronic structure of molecules by R. S. Mulliken [1]. His paper deals specifically with linear triatomic molecules whose electronic structure he tried to elucidate by using simple MO theory and additional chemical concepts such as electronegativity. Mulliken was mainly interested in correlating the electronic structures of isoelectronic species.

Since then many workers have investigated molecular electronic structures by various means in an attempt to uncover the factors which affect chemical reactivity. Perhaps the best known is the 1938 treatise on "The Nature of the Chemical Bond" by Linus Pauling [2].

With the increasing availability of computers in the late 1950's, quantum mechanical calculations on small molecules became possible, thus stimulating investigation of molecular electronic structures and the chemical bond. The early work of B. J. Ransil [3] on certain first row diatomic molecules set the standard for future years.

By the early 1960's successful calculations had been achieved for a number of diatomic molecular systems; interest then turned to larger molecules. The problem of effecting such calculations was tackled in two ways; firstly by finding satisfactory approximate methods particularly with regard to integral evaluation, and secondly by improving computing and mathematical techniques, thus gradually increasing the size of molecule whose structure could be elucidated.

One of the first ab initio calculations on a linear triatomic molecule was performed by A. D. McLean [4] in 1962. The molecule was hydrogen cyanide, HCN.

It was to this background that it was decided to attempt an elucidation of the electronic structures of the linear nitrile molecules, CN^-, HCN and FCN. FCN is particularly interesting because of the unusually short CF bond.[5] In choosing the XCN system, the intention was to examine the effect on the CN residue of varying X. In order to achieve this with any success the calculations were performed as accurately as possible. However, some approximate methods had to be used and an attempt was made to evaluate their effect on the accuracy of the calculated molecular parameters. This was achieved by comparison with McLean's work on HCN. The calculations were then performed at a variety of X-C distances.

The basic problem in wave mechanics is to solve the equation

$$H\Psi = E\Psi \qquad (I.1)$$

where E and Ψ are the total energy and wave function, respectively, of the system under discussion and H is the Hamiltonian operator. This equation is insoluble for all but the very simplest problems and accurate approximations have to be invoked to simplify the more interesting situations. The most important of these is the fixed-nucleus approximation which provides the basis for performing molecular electronic structure calculations. The wave-mechanical basis for this approximation was given by Born and Oppenheimer [6] in 1927. Basically it means that the vibrational and rotational motions of a molecule are effectively quite separate from the electronic motions. This approximation is valid provided that the electronic ground state is not degenerate or nearly degenerate. Consequently, for fixed nuclear coordinates there is a definite set of electronic energies which can be obtained by solving the appropriate wave equation. The solution of this equation for all possible nuclear configurations gives the total electronic energy as a function of the nuclear coordinates, a plot of which yields an energy hypersurface. For diatomic molecules this hypersurface is a plane curve since the distance between the atoms is the only internal coordinate. These hypersurfaces are important since they represent the potential energy which governs the motion of the nuclei.

The complexity of the wave equation is thus reduced by eliminating the terms involving nuclear motion, but it is still rather complex for direct solution. As a result, further approximations have to be made. The two most commonly used are the molecular orbital and valence-bond approximations.

The VB method was historically the first and was developed by Heitler and London [7]. This theory considers a molecule to be composed of atoms to some extent retaining their individuality even when chemically bonded. It is particularly designed to consider a molecule as being characterised by a series of structures based on the simple chemical concept of the localised electron pair bond.

The MO method was originated by Hund [8] and developed in a series of papers by Mulliken [9]. It is essentially an extension of the quantum theory of atoms. Each electron is assigned to a one-electron wave function, but this now extends over the whole molecule. The corresponding one-electron orbitals are also obtained in an analogous manner by an SCF procedure.

Since both the MO and VB methods are approximations, neither is the ideal solution yet each has its special merits. Chemical concepts such as valence, the two-electron bond and resonance are more easily seen in the VB scheme while processes such as excitation and ionization are more readily shown in MO theory. This follows since for closed shell molecules, the one-electron MO's transform according to the irreducible representations of the molecular point group. It should be stated that, although in their simpler forms the two theories lead to different results, when each is refined, the two methods yield the same molecular wave function. The main difference really is in the starting points.

The disadvantages of the two methods are also well known. VB theory is difficult to apply especially to large molecules, mainly because of orthogonality problems, and molecular properties are not so easily obtained. The simple VB method also overestimates the effect of electron correlation, but it does give the correct lowest energy dissociation products allowing only radical formation on dissociation.

The simple MO method fails at large internuclear distances by predicting both radical and ionic dissociation products i.e. it under-estimates electron correlation by allowing two electrons of opposite spin too great a possibility of being in the same region of space.

A reasonably complete treatment of oxygen requires 495 configurations in MO theory and many thousands of ionic structures in VB theory. Consequently, for most molecules it is not a feasible proposition to carry each theory to its limits and one is forced to make a choice of either a VB or MO approach. Because MO theory is conceptually the simpler and is also easier to work with it was decided to use it as a basis for the present work.

About twenty years after its origin, a rigorous mathematical analysis of the MO method was given by Roothaan [10]. His analysis for the LCAO-MO-SCF method has been used in the majority of molecular calculations performed since then.

Despite the success of this method it was decided to follow the more recent analysis of McWeeny [11]. Here the LCAO-MO-SCF method is elaborated in terms of density matrix theory. In the Roothaan scheme each cycle of the SCF iteration procedure requires a matrix diagonalisation which can be rather time consuming. In the density matrix method this is replaced merely by a set of matrix operations and one final diagonalisation. In addition to the increase in speed there is a saving in time arising from the fact that fewer iterations are usually required to reach the minimum.

McWeeny uses the method of steepest descents to descend the energy surface and determines the best correction to $\underset{\sim}{R}$, $\Delta\underset{\sim}{R}$, which gives the maximum lowering in energy. The corrected $\underset{\sim}{R}$ may no longer be idempotent and small departures from idempotency are eliminated by a simple iterative procedure. The process is repeated until $\Delta\underset{\sim}{R}$ is as small as desired. More recently Hoffmann [12] has indicated that a smoother descent of the energy surface is obtained by keeping $\underset{\sim}{R}$ rigorously idempotent during the descent. However, little trouble was experienced in the present work using the McWeeny method and consequently, there was no need to employ Hoffmann's more rigorous and more involved procedure. It must be kept in mind, however, that it might be necessary to change the minimisation procedure when studying more complicated molecules, perhaps those containing more than twenty electrons.

It was mentioned above that the simple VB and MO theories converged to the same molecular wave function if the necessary refinements were made. These refinements, of course, also improve the resulting wave function. While the VB wave function is improved by including ionic terms, the MO wave function is improved by allowing for configuration interaction. This involves performing a variational calculation by considering the mixing of selected excited states with the ground state. These excited states must have the same symmetry as the ground state. This technique improves the total wave function by admitting better electron correlation than in the simple MO wave function made up of one-electron functions which place no limit on the relative positions of the electrons of opposite spins. A limited amount of correlation for electrons of parallel spins is built into the wave function, however, by the use of an antisymmetric product of these one electron functions.

Many configuration interaction calculations have been performed using the virtual orbitals arising out of a normal ground state SCF MO calculation, but it is now becoming more widely realised that because of their nature the improvement in energy and wave function is limited. The MC SCF method is an improved technique recently developed by Veillard and Clementi [13,14]. It incorporates the feature of configuration interaction thus decreasing the error arising from the neglect of electron correlation. Instead of merely finding the best molecular wave function for the ground state, ψ_0, MC SCF theory constructs the doubly excited state wave functions ψ_1, ψ_2, etc., as well as ψ_0 and determines the best total wave function in the form $\Psi = a_0\psi_0 + a_1\psi_1 + a_2\psi_2 + \cdots\cdots$. The variation principle is applied to optimise both the a's, the CI coefficients, and the AO coefficients in the MO's: a fast convergence results.

Although the correlation of electrons of opposed spins is not taken fully into account in simple MO theory, Brillouin's theorem[15] ensures that the one-electron properties will be reasonably well represented by the SCF wave function. This follows since the matrix elements between the ground and singly excited states are zero for MO's determined by an SCF procedure. Consequently, by performing a CI, it is the two-electron properties which will be improved through the inclusion of the doubly-excited configurations.

The disadvantages of simple MO theory could be summed up as the physical unrealism of mono-electronic molecular spin orbitals. It is much more realistic to consider larger groups of electrons together as for example the two-electron bond or the lone pair. A theory based on this concept has been elaborated in density matrix notation by McWeeny [11]. A recent evaluation of the technique, the self-consistent group function method, was performed by Cook et al [16] and a comparison was made with ordinary SCF MO theory as applied to the water molecule and some simple hydrocarbons. The SCGF method, which has much of the chemical interest of VB theory in it yet maintains a simple orbital notation, was found to be very successful and it is possible that future work will find this a most useful tool.

It is also very possible that the correlation problem could be solved by the use of two-electron molecular functions, now called geminals [17]. This avenue has not been explored to any great extent, or with much success, due to the numerical complexity involved but it is possible that if the same effort were applied in this direction as is being applied to conventional LCAO-MO-SCF calculations even more useful results would be obtained.

Until recently all-electron ab initio calculations on molecules containing between thirty and fifty electrons were impossible and there was the obvious need to develop more approximate methods for dealing with such molecular systems. Indeed the SCGF method, as used by Cook et al [16], is the latest attempt to perform accurate calculations using an approximate technique.

By reducing the number of electrons considered, the quantum mechanical problem is simplified. For example, in the study of conjugated hydrocarbons this is done by considering the sigma electrons as part of the core in the potential field of which the pi electrons move. A rigorous mathematical framework for the pi-electron approximation was given by Lykos and Parr [18]. This approach has had wide application and can be seen as the forerunner of the SCGF method since it recognises specific groups of electrons.

The semi-empirical methods due to Pariser and Parr [19] and Pople [20] are examples of theories based on the pi-electron approximation. An AO basis set of pi orbitals is chosen explicitly but some of the integrals are evaluated empirically to agree with certain known experimental quantities such as the first ionisation potential or the lowest energy pi-pi* transition. An integral part of this method is the ZDO approximation. This allows for the neglect of all two-electron integrals involving one or two-centre overlap charge densities. The hope, which has some justification, is that the neglected integrals will be small or at least very much smaller than the one- or two-centre coulomb integrals which remain.

Despite some limited success, the need to extend such an approximate method to include all electrons was apparent. A technique having a good mathematical foundation was given by Pople, Segal and Santry [21,22] in 1965. These authors distinguish two levels of the ZDO approximation since it is now possible to neglect integrals containing one-centre overlap charge densities. The CNDO approximation which, like the ZDO approximation, is normally applied to pi-electron systems, neglects all two-electron integrals involving overlap charge densities even if they are associated with one centre. In pi-electron theory the ZDO approximation can be written as

$$(\pi_p \pi_q | \pi_r \pi_s) = \delta_{pq} \delta_{rs} \gamma_{pr} \qquad (I.2)$$

It is found to be quite accurate provided the 2p orbitals on each centre are chosen to be symmetrically orthogonalised [23] AO's. However, when there are several AO's on each centre some of the one-centre integrals neglected in CNDO theory are quite large.

This rather important disadvantage is overcome in Pople's second level of the ZDO approximation. In his NDDO approximation only those two-electron integrals involving bicentric overlap charge distributions are neglected. In recent work [16] it was shown that the NDDO method was vastly superior to the CNDO method and reproduced the electron density and bond polarities of full non-empirical calculations on the methane and water molecules surprisingly well. In contrast, the CNDO approximation caused the bond polarities to be incorrect in both magnitude and direction. In Pople's method the one-electron integrals are often chosen semi-empirically whereas Cook, Hollis and McWeeny evaluated all the integrals theoretically.

Pople has since developed an improvement on the CNDO method called the intermediate neglect of differential overlap approximation [24]. Here, one-centre overlap densities are allowed only in completely monocentric integrals. This method, however, still contains the rather drastic approximations imposed by the integral invariancy conditions imposed in the first paper of their series.

One of the most unsatisfactory procedures in these methods is in attempting to justify the empirical values of some integrals, without reference to a basis set and then choosing AO's to evaluate other integrals.

One of the first problems in LCAO-MO-SCF theory is to choose a specific AO basis set. Although many mathematical functions have been tried in molecular calculations, the most widely used basis function is the STO having the form

$$(n,l,m) = N_n(\zeta)r^{n-l}e^{-\zeta r}S_l^m(\theta,\phi) \qquad (I.3)$$

where n, l, m are the quantum numbers defining the real AO, $N_m(\zeta)$ is a normalising factor, ζ is the orbital exponent and the S functions are the normalised real spherical harmonics. ζ is now seldom calculated according to the original rules given by Slater, but is instead optimised in some manner. Ransil [3] has defined the various choices of STO: e.g. Slater AO, best atom AO, best AO etc. In molecular calculations it has been usual to use the minimum number of STO basis functions which could reasonably represent the structure of each of the atoms in the molecule. It is also fairly common practice to use best atom ζ's, which are determined variationally, so that an atomic wave function comprised of best atom AO's will minimise the energy of the atom.

However, there is no reason why best atom zeta's used in molecules will give the best molecular energy. When the zeta's are chosen to minimise the molecular energy they are normally termed best MO zeta's [3]. Such an optimisation is very time consuming as can be seen, for example, from the method outlined by Sahni and Sawhney [25] who were studying the ground and ionised states of N_2. Because nonlinear exponent optimisation is so expensive in computer time, some workers, for example, Matcha [26], doubt if a molecular zeta optimisation is justified at present.

There is a second method for improving the basis set which is becoming more common. This involves increasing the number of AO's in the basis set. This method is much more economical in computing terms. Such basis sets are known as accurate AO, SCF AO or Hartree-Fock AO bases. Enough STO's are used in these sets to reproduce the true Hartree-Fock numerical solutions for atoms. Clementi [27] has tabulated these functions and also includes a very useful contracted set of double-zeta functions for molecular calculations. It is well known that double ζ functions can represent the SCF AO quite closely and Clementi believed they would be useful in calculations where the size of basis set which could be used was limited. Matcha has since shown that the Clementi double ζ functions yield results in good agreement with those obtained by the use of more accurate AO basis sets.

There has been a recent tendency to replace the minimal basis set by an extended basis set in molecular calculations. Here extra-valence shell AO's are added to allow a better representation of the electron distribution in the molecule. However, as a molecular system can be completely determined by a mathematically complete set of functions centred at a given point in space, care must be taken in adding extra-valence shell AO's to minimal basis sets on many centres in space to avoid the ill-conditioning of the SCF equations which could arise through having effectively an overcomplete set. In addition the extra-valence shell AO's which are added must form a well balanced basis set as described by Mulliken [28].

Interesting comparisons of some of these basis sets have been made by Mulliken [28] and Ballinger [29] for HF. Karo and Allen [30] found a large improvement in energy resulted by using free atom SCF AO's instead of best atom AO's. Ballinger using STO's optimised the orbital exponents for the molecule but obtained only a slight improvement in total energy. He also found that overlap populations, excitation energies and the dipole moment were not greatly improved.

Recently growing numbers of molecular electronic calculations have been performed using a linear combination of Gaussian orbitals to approximate the MO's, as for example by Clementi [31]. GTF's were initially introduced by Boys [32] and have the form,

$$\xi(A,\alpha,a) = X_A^{a_1} Y_A^{a_2} Z_A^{a_3} (r_A^2)^{a_4} e^{-\alpha r_A^2} \qquad (I.4)$$

where $X_A = X-A_X$, etc., $r_A^2 = X_A^2 + Y_A^2 + Z_A^2$, a_1, a_2, a_3 and a_4 have integral values and α is positive.

The use of GTF's has the distinct advantage over STO's that the multicentre integrals are much more easily evaluated. There is an overcompensating disadvantage in the fact that convergence to a good wave function is very much slower. Two recent calculations on HCN [33,34] have shown that the number of GTF's required to reproduce the best total energy obtained using STO's would be very large indeed; probably at least fifty.

In the present work it was decided to use a minimal basis set of double-zeta functions comprised of STO's whose exponents had been chosen to minimise the atomic energies. The limitation to a minimal basis set was made partly for computational economy reasons and partly from the hope that quite accurate calculations could be carried out from a simple chemical orbital picture.

Clementi double zeta functions [27] were chosen as the most economical way of improving the AO basis set as discussed above.

The recent work of Matcha [26] also shows that it is probably more important to improve the double zeta basis set by adding orbitals to allow for polarisation rather than by replacing it with accurate Hartree-Fock AO's.

One of the initial objectives of this work was to find an approximate method of performing molecular calculations which would reproduce many of the results of accurate ab initio calculations to a reasonable degree of precision. The use of an STO basis set also complicated the evaluation of the three-centre integrals. Since it was not economically possible to evaluate these integrals exactly, approximate methods had to be used or, alternatively, they could be neglected as for example in the CNDO scheme.

It was felt that the CNDO scheme was rather too approximate to yield useful results, an opinion which has been to some extent justified by the work of Cook et al [16]. Therefore it was decided to perform and evaluate an ab initio SCF method with the single limitation that the multicentre integrals would be calculated by an approximate method. Indeed the question must be answered whether the improvement in the basis set can be justified when integral approximations are used.

As far as approximate methods are concerned, the problem of the multicentre integrals has been tackled mainly by replacing a two-centre charge distribution $\chi_a^*(1)\,\chi_b(1)$ by one or more carefully chosen one-centre distributions. The first method which had any success was given by Sklar [35], who replaced the two-centre orbital product by the product of two identical orbitals located at the midpoint between the centres.

$$\chi_a^*(1)\chi_b(1) \doteqdot S_{ab}\chi_m^*(1)\chi_m(1) \tag{I.5}$$

where $S_{ab}=\int \chi_a^*(1)\chi_b(1)dv_1$ is the overlap integral between the orbitals.

The second important method which has an accuracy similar to Sklar's method was given by Mulliken [36] who simply averaged two mono-centric distributions located at the two centres involved.

$$\chi_a^*(1)\chi_b(1) \doteqdot \tfrac{1}{2}S_{ab}[\chi_a^*(1)\chi_a(1)+\chi_b^*(1)\chi_b(1)] \tag{I.6}$$

Rudenberg [37] showed the Mulliken approximation to be the first term of an infinite series whose sum was $\chi_a^*(1)\chi_b(1)$. When the right hand side of (I.6) was the dominant term, the Mulliken approximation was quite good but when other terms of the series become important, or even dominant, the accuracy was poor. Rudenberg's method uses the fact that an AO on any centre, a, can be expanded in terms of a complete set of AO's on another centre, b:

$$\chi_{a\alpha}(1) = \sum_{k=1}^{\infty} S_{a\alpha bk}\chi_{bk}(1) \tag{I.7}$$

$$\chi_{a\alpha}\chi_{b\beta} = \tfrac{1}{2}\sum_{k=1}^{\infty} [S_{a\alpha bk}\chi_{b\beta}\chi_{bk}+S_{b\beta ak}\chi_{a\alpha}\chi_{ak}] \tag{I.8}$$

Although there have been many attempts to improve these methods, perhaps the most interesting from an intuitive point of view was the method proposed by Löwdin [38]. He modified the Mulliken approximation by weighting the relative contributions of the monocentric distributions in order that the approximated charge distribution should have the correct dipole moment.

$$\chi_a^*(1)\,\chi_b(1) = \mu_1 S_{ab}\,\chi_a^*(1)\,\chi_a(1) + \mu_2 S_{ab}\,\chi_b^*(1)\,\chi_b(1) \qquad (I.9)$$

where $\mu_2 = \dfrac{\int \chi_a^*(1) z_a \chi_b(1) dv_1}{R_{ab} S_{ab}}$, $\mu_1 + \mu_2 = 1$ and R_{ab} is the internuclear separation.

Recently two improved approximate methods have been proposed which are based on the representation of a bicentric charge distribution as a truncated expansion of monocentric distributions. The first was given by Cizek [39]. His approximation was again a linear combination of two single-centre distributions but whose locations and relative weightings were chosen to reproduce the lower multipole moments up to and including the octupole moment. The second was proposed by Harris and Rein [40]. They used symmetry criteria in selecting the one-centre products in the expansion; the coefficients of which were determined by requiring agreement for certain key integrals.

Each of these methods is, however, rather cumbersome to apply in practice. Also, the evaluation of their accuracy is given almost exclusively for two-centre integrals mainly of the hybrid and exchange type although Cizek also gives comparisons for certain two-centre one-electron integrals. Admittedly there are very few accurate three and four centre integral values available in the literature. The respective authors of these last two methods are hopeful, however, that the extension of their approximations to multicentre integrals will be almost as successful. Roach [41]has shown from practical experience in evaluating three-centre integrals that, in a few cases, certain of the intermediary equations in Cizek's analysis have complex roots. The approximation breaks down in these cases.

It would appear that although many approximate methods exist for multicentre integral evaluation, few detailed examinations of these methods appear to have been made. Indeed the whole purpose of their existence seems thwarted as very few molecular calculations have been performed which make use of the above integral approximations. As is pointed out by Cizek, no trace of an evaluation of the simple Löwdin [38] method is apparent except for a short note by Ellison [42] who compares the Löwdin and exact values of two two-centre one-electron integrals for the water molecule. He also compares the Löwdin and Mulliken approximations for one three-centre one-electron integral, but no exact value was available for a more interesting comparison. An even greater mystery is the lack of reference to Löwdin's improved method [43]. This method is also based on the expansion of a function on one centre in terms of a complete set of functions on another centre. For practical applications, however, it is necessary to limit the size of this set to involve only those

AO's which occur in the given basis set. Löwdin's improved method bears a comparable relationship to his simpler method given in (I.9) as the Rudenberg method bears to the Mulliken approximation. It takes the form:

$$\chi_a \chi_b = \lambda_1 \sum_{A \leq a} \chi_a \chi_A S_{Ab} + \lambda_2 \sum_{B \leq b} \chi_B \chi_b S_{aB} \qquad \text{(I.10)}$$

where $\lambda_1 + \lambda_2 = 1$ and A runs over all AO's having a principal quantum number equal to or less than that of a etc. λ_1 and λ_2 are further chosen so that the total electric dipole moment along the line a—b is given correctly.

The Mulliken approximation is the major exception, however, as it has been widely used in electronic structure calculations. This obviously arises from the ease of its application. For similar reasons it was decided to use this approximation as the basic integral approximation procedure in the present work. Also, conscious of the fact that, even as the sole approximation in an ab initio type calculation, the use of Mulliken's method might yield rather inaccurate results, it was decided to evaluate the improved approximation of Löwdin, given in (I.10), as an alternative method.

One of the major roles of the theoretical chemist is to feed back simple yet useful concepts to the experimentalist. Wahl [44] has pointed out that results presented in the form of vast numerical tables are nearly always incomprehensible. It is surely a recognition of these facts which has led to the recent increase in papers which display wave functions in pictorial form as contour diagrams of electronic probability densities [45,46]. Perhaps the other most thought provoking concept to arise from the analysis of the wave function, as opposed to its use in calculating various molecular properties, is the effective charge on an atom in a molecule. The population analysis of molecular wave functions is not new and since it was introduced by Mulliken [47] it has been widely used to yield quantities such as the atom and bond populations and the effective atomic charges. Löwdin [23] had previously defined the charge on an atom derived from a molecular wave function using a basis set of orthogonalised AO's but this has had little usage. Its main disadvantage is that, having mixed AO's from other atoms into those of the atom being considered to obtain orthogonality, the charge assigned to that atom is to some extent delocalised over the other atoms.

It has since become apparent that these methods have certain limitations and it is dubious to what extent the concept of atomic charge can be taken. Mulliken has since shown [28] how the choice of basis set can affect the atom and bond populations. Cusachs and Politzer [48] have recently highlighted the question of the physical significance of atom charges after noting that quite different wave functions result when the Mulliken or Löwdin definitions of atomic charge are used as self-consistency criteria in their SCF computations.

Doggett [49] has recently proposed an alternative method of performing a population analysis. It has the distinct advantage over other methods in that the resulting gross atom charge densities will reproduce the calculated molecular dipole moment when atomic contributions are included. This new method partitions the bond charge density asymmetrically in order to reproduce the bond dipole moments and is based on Löwdin's [38] original partitioning as given in (I.9). Doggett also gives the analysis in a matrix notation which lends itself well to computer calculation. He studied the first row diatomic hydrides and shows with the aid of contour diagrams that, although it is difficult to justify any absolute validity in the atom charge concept, when a series of related molecules is considered the trends shown by the charge densities are indeed significant.

It is a further aim of this work to show how the use of contour diagrams and population analyses, can aid the elucidation of the electronic structures of the molecular series CN^-, HCN, FCN.

CHAPTER TWO

THEORY

2.1. General Theory.

Within the Born-Opperheimer [6] approximation and neglecting spin-orbit and spin-spin interactions, the wave functions, Ψ_A, for the stationary states of an N-electron molecule are solutions of the equation

$$H\Psi_A(1,2,\ldots,N) = \mathcal{E}_A\Psi_A(1,2,\ldots,N) \qquad \text{(II.1)}$$

where A = 0,1,2,..... labels the various electronic states and 1,2,...N represents the four space and spin coordinates of each of the electrons 1,2,...N. The Hamiltonian operator, H, is given in atomic units by

$$H = -\sum_{i=1}^{N}\left(\tfrac{1}{2}\nabla_i^2 + \sum_{\beta=1}^{M}\frac{Z_\beta}{r_{i\beta}}\right) + \tfrac{1}{2}\sum_{i,j=1}^{N}\frac{1}{r_{ij}} + \tfrac{1}{2}\sum_{\alpha,\beta=1}^{M}\frac{Z_\alpha Z_\beta}{r_{\alpha\beta}} \qquad \text{(II.2)}$$

$$= \sum_{i=1}^{N} f(i) + \sum_{i>j=1}^{N}\frac{1}{r_{ij}} + \sum_{\alpha>\beta=1}^{M}\frac{Z_\alpha Z_\beta}{r_{\alpha\beta}} \qquad \text{(II.3)}$$

where β labels the M nuclei of nuclear charge Z_β in the molecule; i labels the electrons; $r_{i\beta}$, r_{ij} and $r_{\alpha\beta}$ are respectively the distances between electron i and nucleus β, between electrons i and j and between nuclei α and β. The eigenvalue $\mathcal{E}_A$ corresponding to an exact solution Ψ_A of (II.1) is given by

$$\mathcal{E}_A = \frac{\int \Psi_A^* H \Psi_A \, d\tau}{\int \Psi_A^* \Psi_A \, d\tau} = E_A + \sum_{\alpha>\beta=1}^{M}\frac{Z_\alpha Z_\beta}{r_{\alpha\beta}} \qquad \text{(II.4)}$$

Since exact solutions are seldom possible, approximate solutions Ψ_A' are sought and an approximate value to E_A, E_A', can be obtained by using Ψ_A' in (II.4). The stationary state of lowest energy is the ground state and it can be shown that for this state $\mathcal{E}_0' \geqslant \mathcal{E}_0$, equality occurring only for the exact solution where $\Psi_0' = \Psi_0$.

The approximate total wave function is normally built from a set of monoelectronic wave functions ψ_i called molecular spin orbitals and the simplest antisymmetric wave function is the Slater determinant obtained by antisymmetrising the product of the N (where N is even) lowest energy MSO's $\psi_1(1)\psi_2(2)\psi_3(3)\ldots\psi_N(N)$:

$$\Psi = \sqrt{\frac{1}{N!}} \begin{vmatrix} \psi_1(1) & \psi_1(2) & \cdots & \psi_1(N) \\ \psi_2(1) & \psi_2(2) & \cdots & \psi_2(N) \\ \vdots & \vdots & & \vdots \\ \psi_N(1) & \cdots & \cdots & \psi_N(N) \end{vmatrix} \tag{II.5}$$

Since the MSO's are orthonormal, substitution of (II.5) into (II.4) leads to the following expression for the electronic energy:

$$E_0 = \sum_{i=1}^{N} f_i' + \sum_{i>j=1}^{N} (J_{ij}' - K_{ij}') \tag{II.6}$$

For a closed-shell state, (II.6) reduces to (II.7):

$$E_0 = 2\sum_{i=1}^{n} f_i + \sum_{i,j=1}^{n} (2J_{ij} - K_{ij}) \tag{II.7}$$

where now N=2n, and f_i, J_{ij} and K_{ij} represent the following integrals over MO's:

$$f_i = \int \phi_i^*(1)\, f(1)\, \phi_i(1)\, dv_1 \tag{II.8}$$

$$J_{ij} = \int \phi_i^*(1)\, \phi_i(1) \frac{1}{r_{12}} \phi_j^*(2)\, \phi_j(2)\, dv_1 dv_2 \tag{II.9}$$

$$K_{ij} = \int \phi_i^*(1)\, \phi_j(1) \frac{1}{r_{12}} \phi_j^*(2)\, \phi_i(2)\, dv_1 dv_2 \tag{II.10}$$

Normally in Hartree-Fock theory the best MO's are determined variationally by the self-consistent field method. The result of performing a variational calculation on (II.7) is the set of equations, (II.11).

$$h^F \phi_i = \sum_j \phi_j\, \varepsilon_{ji} \tag{II.11}$$

where h^F is the Hartree-Fock Hamiltonian operator and ε_{ji} is a lagrangian multiplier. For atoms, the problem of solving these equations is simplified by the central symmetry, but for molecules it is a very difficult mathematical problem. Consequently, it is necessary to use approximations to the best MO's. The most common method is to take a linear combination of atomic orbitals, χ_p, for each of the MO's, ϕ_i:

$$\phi_i = \sum_p \chi_p\, T_{pi} \tag{II.12}$$

for i = 1,2,.....n. It is convenient, though not essential, to choose the AO's to be mutually orthogonal such that

$\int \bar{\chi}_p^*(1)\, \bar{\chi}_q(1)\, dv_1 = \delta_{pq}$. Thus,

$$\phi_i = \sum_p \bar{\chi}_p \, \bar{T}_{pi} \tag{II.13}$$

or in matrix notation:

$$\underset{\sim}{\phi} = \underset{\sim}{\bar{\chi}} \; \underset{\sim}{\bar{T}} \tag{II.14}$$

where the row matrix, $\underset{\sim}{\phi}$, is the collection of occupied MO's, $\underset{\sim}{\bar{\chi}}$ is the row matrix of OAO's, and $\underset{\sim}{\bar{T}}$ is the matrix of OAO coefficients arranged in columns.

The operator equation (II.11) is then transformed into the matrix equation (II.15).

$$\underset{\sim}{\bar{h}}^F \, \underset{\sim}{\bar{T}} = \underset{\sim}{\bar{T}} \, \underset{\sim}{\varepsilon} \tag{II.15}$$

The conventional solution of (II.15) is effected by an SCF method as described by Roothaan [10]. But, as discussed in the introduction, it was decided to perform the SCF calculation using the density matrix formulation as outlined by McWeeny [11]. In this method it is not necessary to determine the MO's themselves at each cycle, since, for a closed shell, the total wave function is completely determined by the one-electron density matrix for electrons of given spin, $\underset{\sim}{\bar{R}}$:

$$\underset{\sim}{\bar{R}} = \underset{\sim}{\bar{T}} \, \underset{\sim}{\bar{T}}^{\dagger} \tag{II.16}$$

where $\underset{\sim}{\bar{T}}^{\dagger}$ is the transpose of the conjugate complexes of the elements of $\underset{\sim}{\bar{T}}$. $\underset{\sim}{\bar{R}}$ is calculated directly by iterative matrix methods as discussed by McWeeny and briefly reiterated below.

The orthonormality conditions take the form

$$\sum_r \bar{T}_{rR}^{*} \bar{T}_{rS} = \sum_r \bar{T}_{Rr}^{\dagger} \bar{T}_{rS} = (\bar{T}^{\dagger} \bar{T})_{RS} = \delta_{RS}$$

i.e. $$\underset{\sim}{\bar{T}}^{\dagger} \underset{\sim}{\bar{T}} = \underset{\sim}{1} \qquad \text{(II.17)}$$

This is equivalent to saying that $\underset{\sim}{\bar{R}}$ is idempotent since

$$\underset{\sim}{\bar{R}} \underset{\sim}{\bar{R}} = \underset{\sim}{\bar{T}} \underset{\sim}{\bar{T}}^{\dagger} \underset{\sim}{\bar{T}} \underset{\sim}{\bar{T}}^{\dagger} = \underset{\sim}{\bar{T}} \underset{\sim}{\bar{T}}^{\dagger} = \underset{\sim}{\bar{R}} \qquad \text{(II.18)}$$

By substituting (II.13) in (II.8), (II.9), (II.10) and (II.7), and using (II.16), the total energy reduces to

$$E_0 = 2 \operatorname{tr} \underset{\sim}{\bar{R}} \underset{\sim}{\bar{f}} + \operatorname{tr} \underset{\sim}{\bar{R}} \underset{\sim}{\bar{G}} \qquad \text{(II.19)}$$

where

$$\bar{f}_{pq} = (\bar{\chi}_p | f | \bar{\chi}_q) \qquad \text{(II.20)}$$

and

$$\bar{G}_{pq} = \sum_r \sum_s \bar{R}_{sr} \left\{ 2(\bar{\chi}_p \bar{\chi}_q | g | \bar{\chi}_r \bar{\chi}_s) - (\bar{\chi}_p \bar{\chi}_s | g | \bar{\chi}_r \bar{\chi}_q) \right\} \qquad \text{(II.21)}$$

(II.20) and (II.21) use a Dirac-type abbreviation for the one- and two-electron matrix elements:

$$(\bar{\chi}_p | f | \bar{\chi}_q) = \int \bar{\chi}_p^{*}(1)\, f(1)\, \bar{\chi}_q(1)\, dv_1 \qquad \text{and}$$

$$(\bar{\chi}_p \bar{\chi}_q | g | \bar{\chi}_r \bar{\chi}_s) = \int \bar{\chi}_p^{*}(1)\, \bar{\chi}_q(1) g(1,2)\, \bar{\chi}_r^{*}(2)\, \bar{\chi}_s(2)\, dv_1 dv_2$$

The variational problem of determining the best MO's is thus equivalent to finding the stationary value of (II.19) subject to the condition $\underset{\sim}{\bar{R}}^2 = \underset{\sim}{\bar{R}}$. By considering a variation in $\underset{\sim}{\bar{R}}$, $\Delta\underset{\sim}{\bar{R}}$, the corresponding change in energy, ΔE_0, is determined and for the stationary energy condition, the first-order change $(\Delta E_0)_1 = 0$. Neglecting second-order terms,

$$\Delta E_0 \;=\; 2 \operatorname{tr} \underset{\sim}{\bar{h}}^F \Delta\underset{\sim}{\bar{R}} \;=\; 0 \tag{II.22}$$

where $\underset{\sim}{\bar{h}}^F$, the matrix of the Hartree-Fock Hamiltonian, is given by

$$\underset{\sim}{\bar{h}}^F \;=\; \underset{\sim}{\bar{f}} + \underset{\sim}{\bar{G}} \tag{II.23}$$

Since first-order terms vanish at the turning point, (II.22) subsequently yields the condition that at the minimum, provided $\underset{\sim}{\bar{R}}$ is idempotent,

$$\underset{\sim}{\bar{R}}\,\underset{\sim}{\bar{h}}^F - \underset{\sim}{\bar{h}}^F\,\underset{\sim}{\bar{R}} \;=\; 0 \tag{II.24}$$

i.e. $\underset{\sim}{\bar{R}}$ commutes with $\underset{\sim}{\bar{h}}^F$.

Because $\underset{\sim}{\bar{h}}^F$ depends through $\underset{\sim}{\bar{G}}$ on the matrix $\underset{\sim}{\bar{R}}$, the problem must be solved iteratively. $\underset{\sim}{\bar{h}}^F$ is recalculated from each new $\underset{\sim}{\bar{R}}$ obtained. Starting from an arbitrary idempotent matrix $\underset{\sim}{\bar{R}}$, and using a method of steepest descent of the energy surface, the best single descent correction $\Delta\underset{\sim}{\bar{R}}$ is determined in the manner outlined by McWeeny [11]. The new matrix, $\underset{\sim}{\bar{R}}'$, is then given by

$$\underset{\sim}{\bar{R}}' \;=\; \underset{\sim}{\bar{R}} + \Delta\underset{\sim}{\bar{R}} \tag{II.25}$$

and the whole process is repeated until self-consistency is obtained.

After each descent of the energy surface, the idempotency of $\bar{\underset{\sim}{R}}_0$ is maintained using the relationship

$$\bar{\underset{\sim}{R}}_{n+1} = \bar{\underset{\sim}{R}}_n^2 (3 \underset{\sim}{1} - 2 \bar{\underset{\sim}{R}}_n) \qquad \text{(II.26)}$$

where $\bar{\underset{\sim}{R}}_n$ is the n'th term in the convergent sequence $\bar{\underset{\sim}{R}}_0$, $\bar{\underset{\sim}{R}}_1$..... derived via the steepest descent method, and whose limit $\bar{\underset{\sim}{R}}$ is rigorously idempotent.

2.2. Symmetric Orthogonalisation of the AO Basis Set.

As discussed in the introduction, the natural atomic orbitals in the AO basis set were chosen to be Clementi double-zeta functions. These functions are not orthogonal to each other when situated on different centres. Since it is much simpler to perform the iteration procedure with a completely orthogonalised basis set, it was decided to use the symmetric orthogonalisation procedure of Löwdin [23] to transform from the NAO basis to the Löwdin orthogonalised atomic orbital basis. At the end of the calculation the reverse transformation can be applied to return to the basis of NAO's. The LOAO basis has the additional advantage of being a more valid basis for neglecting integrals in any future approximate calculations based on a neglect of differential overlap. If the AO's are orthogonal, (II.17) can be written in the form

$$\bar{\underset{\sim}{T}}^{\dagger} \int \underset{\sim}{\chi}^{\dagger} \underset{\sim}{\chi} \, d\tau \, \bar{\underset{\sim}{T}} = \underset{\sim}{1}.$$

However, when the basis is comprised of NAO's (II.17) no longer holds and if the unbarred symbols denote matrices in the NAO basis, the normalisation condition (II.17) becomes

$$\utilde{T}^{\dagger}\utilde{S}\utilde{T} = \utilde{1} \tag{II.27}$$

where $\utilde{S}$ is the matrix of overlap integrals in the NAO basis. From (II.17) and (II.27) it follows that

$$\utilde{T} = \utilde{S}^{-\frac{1}{2}}\bar{\utilde{T}} \tag{II.28}$$

and

$$\utilde{T}^{\dagger} = \bar{\utilde{T}}^{\dagger}\utilde{S}^{-\frac{1}{2}} \tag{II.29}$$

By substituting for $\utilde{T}$ in the relationship $\utilde{\phi} = \utilde{\chi}\,\utilde{T}$ and comparing with (II.14) the LOAO's are given in terms of the NAO basis set by

$$\bar{\utilde{\chi}} = \utilde{\chi}\,\utilde{S}^{-\frac{1}{2}} \tag{II.30}$$

This orthogonalisation is not unique [43] but is a convenient choice for the present analysis.

2.3. Transformation of the Matrices over NAO's to Matrices over LOAO's.

The matrices which appear in the McWeeny iteration scheme are defined with respect to an orthogonal basis, but the matrices which are formed initially are given in terms of molecular integrals calculated in an NAO basis. Before commencing the calculations, it is necessary, therefore, to transform the $\utilde{f}$, $\utilde{G}$

and $\underset{\sim}{h}^F$ matrices from the NAO basis to the LOAO basis.

For example, consider the (pq)th element of the $\bar{\underset{\sim}{f}}$ matrix as given in (II.20):

$$\bar{f}_{pq} = \int \bar{\chi}^*_p \, f \, \bar{\chi}_q \, dv$$

Using (II.30) in the form $\bar{\chi}_p = \sum_i \chi_i \, S_{ip}^{-\frac{1}{2}}$ and substituting in (II.20)

$$\bar{f}_{pq} = \int \sum_i \chi^*_i \, S_{ip}^{-\frac{1}{2}*} \, f \, \sum_j \chi_j \, S_{jq}^{-\frac{1}{2}} \, dv$$

$$= \sum_i \sum_j S_{ip}^{-\frac{1}{2}*} \int \chi^*_i f \chi_j \, dv \; S_{jq}^{-\frac{1}{2}}$$

$$= \sum_i \sum_j S_{pi}^{-\frac{1}{2}} \; f_{ij} \; S_{jq}^{-\frac{1}{2}}$$

$$= \sum_i S_{pi}^{-\frac{1}{2}} \; (\underset{\sim}{f}\underset{\sim}{S}^{-\frac{1}{2}})_{iq}$$

$$= (\underset{\sim}{S}^{-\frac{1}{2}} \underset{\sim}{f} \underset{\sim}{S}^{-\frac{1}{2}})_{pq}$$

i.e.

$$\bar{\underset{\sim}{f}} = \underset{\sim}{S}^{-\frac{1}{2}} \underset{\sim}{f} \underset{\sim}{S}^{-\frac{1}{2}} \qquad \text{(II.31)}$$

In a similar manner it can be shown that

$$\bar{\underset{\sim}{G}} = \underset{\sim}{S}^{-\frac{1}{2}} \underset{\sim}{G} \underset{\sim}{S}^{-\frac{1}{2}} \qquad \text{(II.32)}$$

$$\bar{\underset{\sim}{h}}^F = \underset{\sim}{S}^{-\frac{1}{2}} \underset{\sim}{h}^F \underset{\sim}{S}^{-\frac{1}{2}} \qquad \text{(II.33)}$$

and

$$\underset{\sim}{R} = \underset{\sim}{S}^{-\frac{1}{2}} \bar{\underset{\sim}{R}} \underset{\sim}{S}^{-\frac{1}{2}} \qquad \text{(II.34)}$$

As discussed above when two-electron integrals are being neglected in some form of neglect of differential overlap scheme, it is more valid to neglect integrals in an orthogonalised basis, than in a non-orthogonal basis. With the possibility of performing future calculations of this kind in mind it is necessary to find an interbasis transformation for the two-electron integrals. Another reason for obtaining such a transformation is that it affords one method of calculating $\underset{\sim}{\bar{G}}$, as given in (II.21), using the elements of $\underset{\sim}{\bar{R}}$ and $\underset{\sim}{\bar{\gamma}}$, where

$$\bar{\gamma}_{pqrs} = (\bar{\chi}_p \bar{\chi}_q | g | \bar{\chi}_r \bar{\chi}_s) \qquad \text{(II.35)}$$

Alternatively, $\underset{\sim}{\bar{G}}$ can be evaluated by (II.32) i.e. $\underset{\sim}{G}$ is first calculated from the elements of $\underset{\sim}{R}$ and $\underset{\sim}{\gamma}$, where

$$\gamma_{pqrs} = (\chi_p \chi_q | g | \chi_r \chi_s) \qquad \text{(II.36)}$$

and then transformed according to (II.32).

The elements of $\underset{\sim}{\gamma}$ and $\underset{\sim}{\bar{\gamma}}$ are interrelated in the following way:

$$\bar{\gamma}_{pqrs} = \iint \bar{\chi}_p^* \bar{\chi}_q \frac{1}{r_{12}} \bar{\chi}_r^* \bar{\chi}_s \, dv_1 dv_2$$

Substituting for $\bar{\chi}_p$ etc. gives

$$\bar{\gamma}_{pqrs} = \iint \sum_i \chi_i^* S_{ip}^{-\frac{1}{2}*} \sum_j \chi_j S_{jq}^{-\frac{1}{2}} \frac{1}{r_{12}} \sum_k \chi_k^* S_{kr}^{-\frac{1}{2}*} \sum_l \chi_l S_{ls}^{-\frac{1}{2}} \, dv_1 dv_2$$

$$= \sum_i \sum_j \sum_k \sum_l S_{pi}^{-\frac{1}{2}} S_{jq}^{-\frac{1}{2}} \iint \chi_i^* \chi_j \frac{1}{r_{12}} \chi_k^* \chi_l \, dv_1 dv_2 \quad S_{rk}^{-\frac{1}{2}} S_{ls}^{-\frac{1}{2}}$$

$$\bar{\Upsilon}_{pqrs} = \sum_i \sum_j \sum_k \sum_l S^{-\frac{1}{2}}_{pi} S^{-\frac{1}{2}}_{jq} S^{-\frac{1}{2}}_{rk} S^{-\frac{1}{2}}_{ls} \Upsilon_{ijkl} \qquad \text{(II.37)}$$

Since $\underset{\sim}{S}^{-\frac{1}{2}}$ is a real symmetric matrix $S^{-\frac{1}{2}}_{pi} = S^{-\frac{1}{2}}_{ip}$ etc., (II.37) can be rewritten

$$\bar{\Upsilon}_{pqrs} = \sum_i \sum_j \sum_k \sum_l (\underset{\sim}{S}^{-\frac{1}{2}} x \underset{\sim}{S}^{-\frac{1}{2}})_{pqij} \Upsilon_{ijkl} (\underset{\sim}{S}^{-\frac{1}{2}} x \underset{\sim}{S}^{-\frac{1}{2}})_{klrs}$$

where matrix direct product nomenclature is used:

$\underset{\sim}{C} = \underset{\sim}{A} x \underset{\sim}{B}$ if $C_{ik,jl} = A_{ij} . B_{kl}$, and $\underset{\sim}{C}$ is of order n^2 where $\underset{\sim}{A}$ and $\underset{\sim}{B}$ are of order n. Hence,

$$\bar{\Upsilon}_{pqrs} = \sum_i \sum_j (\underset{\sim}{S}^{-\frac{1}{2}} x \underset{\sim}{S}^{-\frac{1}{2}})_{pqij} [\underset{\sim}{\Upsilon} (\underset{\sim}{S}^{-\frac{1}{2}} x \underset{\sim}{S}^{-\frac{1}{2}})]_{ijrs}$$

$$= [(\underset{\sim}{S}^{-\frac{1}{2}} x \underset{\sim}{S}^{-\frac{1}{2}}) \underset{\sim}{\Upsilon} (\underset{\sim}{S}^{-\frac{1}{2}} x \underset{\sim}{S}^{-\frac{1}{2}})]_{pqrs}$$

i.e. $$\underset{\sim}{\bar{\Upsilon}} = (\underset{\sim}{S}^{-\frac{1}{2}} x \underset{\sim}{S}^{-\frac{1}{2}}) \underset{\sim}{\Upsilon} (\underset{\sim}{S}^{-\frac{1}{2}} x \underset{\sim}{S}^{-\frac{1}{2}}) \qquad \text{(II.38)}$$

(II.38) is a neater expression than (II.37) and is faster to perform in the computer as well, but it suffers from the fact that it requires too much computer store. Consequently (II.37) has to be used, although it requires further modification for efficient computer evaluation as it requires all elements of Υ_{ijkl} instead of only the unique elements. The technique for evaluating $\underset{\sim}{\bar{\Upsilon}}$ from the unique elements of $\underset{\sim}{S}^{-\frac{1}{2}}$ and $\underset{\sim}{\Upsilon}$ is described in chapter five.

Berthier [50] and Moreau and Serre [51] have performed semi-empirical pi electron calculations involving an LOAO basis in which they suggest the following transformation for the coulomb integrals from an STO basis to those from an LOAO basis:

$$\bar{\underset{\sim}{Y}} = (\underset{\sim}{S}^{-\frac{1}{2}} x \underset{\sim}{S}^{+\frac{1}{2}}) \, \underset{\sim}{Y} \, (\underset{\sim}{S}^{-\frac{1}{2}} x \, \underset{\sim}{S}^{+\frac{1}{2}}) \qquad \text{(II.39)}$$

They claim that this equation is valid for coulomb integrals and at the same time say that the other integrals are made negligible. However, the hybrid and exchange integrals are not made negligible by the transformation (II.39) although the coulomb integrals are reasonably well represented.

Experience has shown that if (II.38) is used, the coulomb integrals are exact while the exchange and hybrid integrals really are negligible. Table II.1 compares the values of these integrals in the NAO basis and in the LOAO basis according to both (II.38) and (II.39) for the pi orbitals of the allyl system with the geometry shown below.

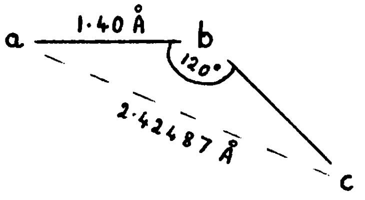

Table II.1.

Comparison of Integrals in NAO and OAO Bases.

Integral	Value in NAO Basis	Value in OAO Basis by (II.39)	Value in LOAO Basis by (II.38)
(aa|aa)	0.3937058	0.3956127	0.3956586
(aa|ab)	0.0886391	0.0964766	-0.0000261
(aa|ac)	0.0101987	0.0129208	-0.0004893
(aa|bb)	0.3321897	0.3321960	0.3321962
(aa|bc)*	0.0659371	0.0812180	0.0000940
(aa|cc)	0.2077917	0.2038792	0.2038665
(ab|ab)	0.0216475	0.0235276	0.0000002
(ab|ac)$^+$	0.0026209	0.0031520	-0.0000006
(ab|bb)	0.0886391	0.0809604	0.0000685
(ab|bc)	0.0188754	0.0197938	0.0000001
(ab|cc)*	0.0659371	0.0497644	0.0000940
(ac|ac)	0.0003459	0.0004286	0.0000076
(ac|bb)	0.0112649	0.0102950	-0.0009871
(ac|bc)$^+$	0.0026209	0.0025167	-0.0000006
(ac|cc)	0.0101987	0.0064473	-0.0004893
(bb|bb)	0.3937058	0.3976911	0.3976241
(bb|bc)	0.0886391	0.0971868	0.0000685
(bb|cc)	0.3321897	0.3321960	0.3321962
(cc|cc)	0.3937058	0.3956127	0.3956586

From Table II.1 it is seen that when (II.39) is used the OAO integrals, instead of tending to zero, actually increase in value in most cases. The one- and two-centre coulomb integrals are reasonably well represented but, in some cases, only to four decimal places. What is much more disturbing is that the symmetry of the system is not maintained as can be seen, for example, by comparing the rows marked * or $^+$. Although not shown in the table, even the integrals (aa|ab) and (aa|ba) do not have the same value when (II.39) is used. In contrast, if (II.38) is used, the symmetry is maintained, the integrals are all accurate and the hybrid and exchange integrals are negligible.

Experience has shown that, although the transformation in (II.38) is useful for pi orbitals, it is not useful for sigma orbitals where there are more than one orbital on each atom.

2.4. Evaluation of the Molecular Integrals.

In molecular structure calculations the eventual basic problem is the evaluation of the molecular integrals which arise in (II.20) and (II.21). For example, the elements of the one-electron matrix, $\underset{\sim}{f}$, are evaluated by the algebraic addition of their constituent one electron integrals.

$$f_{pq} = \int \chi_p \, f \, \chi_q \, dv = \int \chi_p \left[-\tfrac{1}{2}\nabla^2 - \sum_{\alpha} \frac{Z_\alpha}{r_\alpha} \right] \chi_q \, dv \qquad \text{(II.40)}$$

(II.40) contains integrals of the following types:

Kinetic Energy : $(\chi_p| -\frac{1}{2}\nabla^2|\chi_q) = -\frac{1}{2}\int \chi_p(1)\nabla^2\chi_q(1)dv_1$ (II.41)

Nuclear Attraction: $(\chi_p|\frac{Z}{r_q}|\chi_p) = Z\int \chi_p(1)\frac{1}{r_q}\chi_p(1)dv_1$ (II.42)

Resonance (Split Nuclear Attraction) : $(\chi_p|\frac{Z}{r_p}|\chi_q) = Z\int \chi_p(1)\frac{1}{r_p}\chi_q(1)dv_1$ (II.43)

Three-Centre: $(\chi_p|\frac{Z}{r_a}|\chi_q) = Z\int \chi_p(1)\frac{1}{r_a}\chi_q(1)dv_1$ (II.44)

The one-electron integral with unit operator is the

Overlap Integral: $(\chi_p|\chi_q) = \int \chi_p(1)\chi_q(1)dv_1$ (II.45)

The two-electron integrals which arise in (II.21) can be classified according to four main types:

Coulomb:

$$(\chi_p\chi_p|\frac{1}{r_{12}}|\chi_q\chi_q) = \iint \chi_p(1)\chi_p(1)\frac{1}{r_{12}}\chi_q(2)\chi_q(2)dv_1dv_2 \qquad \text{(II.46)}$$

Hybrid:

$$(\chi_p\chi_p|\frac{1}{r_{12}}|\chi_p\chi_q) = \iint \chi_p(1)\chi_p(1)\frac{1}{r_{12}}\chi_p(2)\chi_q(2)dv_1dv_2 \qquad \text{(II.47)}$$

Exchange:

$$(\chi_p\chi_q|\frac{1}{r_{12}}|\chi_p\chi_q) = \iint \chi_p(1)\chi_q(1)\frac{1}{r_{12}}\chi_p(2)\chi_q(2)dv_1dv_2 \qquad \text{(II.48)}$$

Multicentre:

$$(\chi_p \chi_q | \frac{1}{r_{12}} | \chi_r \chi_s) = \iint \chi_p(1)\chi_q(1)\frac{1}{r_{12}}\chi_r(2)\chi_s(2)dv_1dv_2 \qquad \text{(II.49)}$$

In the present work all integrals are evaluated by numerical integration techniques, although a small number of one centre coulomb integrals, involving highly contracted 1s AO's, are evaluated by analytical means if the values obtained numerically are of insufficient accuracy. Numerical values for a few of these integrals, obtained both numerically and analytically, are presented in Tables V.2 and V.3 in chapter five.

Of the one- and two-centre integrals the exchange integrals are the most difficult to evaluate. Their values were obtained using Corbato and Switendick's [52] MIDIAT diatomic molecular integral program, originally coded for the MIT I.B.M. 704 computer, but adapted by F. R. A. Hopgood for the S.R.C. ATLAS computer at Chilton. All other integrals are evaluated by programs developed in Glasgow. These programs use the Gaussian quadrature method, as discussed in chapter five and appendix one, to set up the integration mesh as opposed to the MIDIAT program which uses Simpson's Rule. The Gaussian method is more economical in giving the required accuracy using fewer mesh points.

The STO's, χ', in the Clementi expansion, χ, are used in the normalised real form,

$$(2\zeta)^{n+\frac{1}{2}}\,[(2n)!]^{-\frac{1}{2}}\,r^{n-1}\,e^{-\zeta r}\,S_{l,|m|}(\theta,\phi)$$

where the functions $S_{l,|m|}(\theta,\phi)$ are the normalised real spherical harmonics defined by Roothaan [53]. For the numerical integration procedure the integrals are first expressed in prolate spheroidal coordinates defined in appendix one. Integration over ϕ is then performed analytically and the remaining integrations are performed by two applications of Gaussian quadrature. This is also discussed in appendix one. The method and algebraic form of the integrals are illustrated below for the case of the overlap integral between two $2p_x$ Clementi functions on centres a and b,

$$I = \int \chi_{2x_a}(1)\,\chi_{2x_b}(1)\,dv_1$$

Now $\chi'_{2x_a} = c_a(2k_a)^{5/2} r_a\, e^{-k_a r_a}\left[\frac{3}{2\pi}\cdot\frac{1}{2}\right]^{\frac{1}{2}} \sin\theta_a \cos\phi\, \frac{1}{2\sqrt{6}}$

$$= \frac{1}{\sqrt{\pi}}\, c_a\, k_a^{5/2}\, r_a\, e^{-k_a r_a} \sin\theta_a \cos\phi$$

and $\chi_{2x_a} = \sum_p \frac{1}{\sqrt{\pi}}\, c_{ap}\, k_{ap}^{5/2}\, r_a\, e^{-k_{ap} r_a} \sin\theta_a \cos\phi$

$$I = \iiint \sum_p \sum_q \frac{1}{\pi} c_{ap} c_{bq} k_{ap}^{5/2} k_{bq}^{5/2} r_a r_b e^{-k_{ap} r_a} e^{-k_{bq} r_b} \sin\theta_a \sin\theta_b \cos^2\phi\, dr\, d\theta\, d\phi$$

On changing to elliptical coordinates using (A1.4), (A1.5), (A1.8), (A1.9) and (A1.10),

$$I = \iiint \sum_p \sum_q \frac{1}{\pi} c_{ap} c_{bq} k_{ap}^{5/2} k_{bq}^{5/2} \frac{R}{2}(\mu+\nu)\frac{R}{2}(\mu-\nu) \frac{(\mu^2-1)(1-\nu^2)}{(\mu+\nu)(\mu-\nu)} \frac{R^3}{8}(\mu^2-\nu^2) \times$$

$$e^{-k_{ap}\frac{R}{2}(\mu+\nu)} e^{-k_{bq}\frac{R}{2}(\mu-\nu)} \cos^2\phi \; d\mu\, d\nu\, d\phi$$

The ϕ integration is performed analytically since

$$\int_0^{2\pi} \cos^2\phi \; d\phi = \pi$$

Hence,

$$I = \int_{-1}^{+1}\int_{+1}^{\infty} \sum_p \sum_q c_{ap} c_{bq} k_{ap}^{5/2} k_{bq}^{5/2} \frac{R^5}{32}(\mu^2-1)(1-\nu^2)(\mu^2-\nu^2) \times$$

$$e^{-k_{ap}\frac{R}{2}(\mu+\nu)} e^{-k_{bq}\frac{R}{2}(\mu-\nu)} \; d\mu\, d\nu$$

The Gaussian quadrature mesh is then set up and the integrand is evaluated at each point and summed with the necessary weighting factors to give the required value for the integral. Further details are given in appendix one.

The two-electron integrals can be written in the form

$$\iint \chi_p(1)\chi_p(1)\frac{1}{r_{12}}\chi_q(2)\chi_q(2)\,dv_1 dv_2 = \int V_p(2)\chi_q(2)\chi_q(2)\,dv_2 \tag{II.50}$$

where

$$V_p(2) = \int \chi_p(1)\chi_p(1)\frac{1}{r_{12}}\,dv_1 \tag{II.51}$$

In (II.51) the integration over the coordinates of electron 1 yields a known function of the coordinates of electron 2.

These potential functions for the constituent STO's are tabulated in the paper of Barnett and Coulson [54]. The integral evaluation is then similar to that given for the overlap integrals.

2.5. Evaluation of the Multicentre Integrals by Approximate Methods.

In the above section it was mentioned that the multicentre integrals which arise in LCAO MO SCF theory are difficult to evaluate accurately. In the present work three approximate methods for the evaluation of these integrals are compared: the Mulliken method, and Löwdin's simple and improved methods.

The Mulliken approximation (MA) is very simple and has the form

$$(\chi_i^A \chi_p^B| \doteq \tfrac{1}{2} S_{ip} [(\chi_i^A \chi_i^A| + (\chi_p^B \chi_p^B|] \qquad \text{(II.52)}$$

i.e. a bicentric charge distribution is replaced by the weighted sum of two monocentric distributions. Its application to a four centre two-electron integral gives

$$(\chi_i^A \chi_j^B|g|\chi_p^C \chi_q^D) \doteq \tfrac{1}{4} S_{ij} S_{pq} [\gamma_{ip}+\gamma_{iq}+\gamma_{jp}+\gamma_{jq}] \qquad \text{(II.53)}$$

where the simplified nomenclature for a two-centre coulomb integral, γ_{ab}, is used.

$$\gamma_{ab} = (\chi_a^P \chi_a^P|g|\chi_b^Q \chi_b^Q) \qquad \text{(II.54)}$$

As far as can be ascertained, the MA has been used in this form in nearly all applications to date. In the present work it has been used rather carefully. Ruttink [55] found that different results were obtained for some molecular properties in a molecular calculation invoking the MA. Bearing in mind Pople and co-worker's [21] invariancy requirements in CNDO theory, Ruttink [55] investigated the invariancy conditions for two multi-centre integral approximations. He found that when the Rudenberg [37] approximation is used the results of LCAO MO SCF calculations are invariant to orthogonal transformations of the AO basis set. He also found that the MA itself is not invariant and pointed out that for (II.54) to be invariant it has to take the form

$$(\chi_i^A \chi_j^B | g | \chi_p^C \chi_q^D) \doteq \tfrac{1}{4} S_{ij} S_{pq} [\gamma_{AC} + \gamma_{AD} + \gamma_{BC} + \gamma_{BD}] \qquad \text{(II.55)}$$

where the values of γ_{AC} etc., are invariant to changes in the corresponding orbitals caused by an orthogonal transformation. To obtain this invariancy he suggested taking averages of the two-centre coulomb integrals

e.g.
$$\gamma_{AC} = \frac{1}{n_A n_C} \sum_i^{n_A} \sum_p^{n_C} \gamma_{ip} \qquad \text{(II.56)}$$

In the present work the use of an invariant Mulliken approximation (IMA) will be considered. However, it seems likely that such invariancy procedures are of dubious value. These methods yield often totally unrealistic values for integrals and it is quite possible that the MA may be closer to physical reality than the IMA. That is what is chemically important. A similar viewpoint to this was in fact made by R. R. Hart in a discussion immediately following Pople and Segal's work [22]. It is really the experimental observables and the total wavefunction which must be invariant under orthogonal transformations of the basis set and not necessarily the integral approximation itself. However, the balance between mathematical rigour and integral reality needs much more investigation. An evaluation of the effect of using the IMA and MA, on the molecular properties of HCN, is presented in 4.1.

The second method used in this work is Löwdin's first approximation [38], hereafter called the partial Löwdin approximation (PLA). It has a similar form to the MA and is also quite simple to apply. It is written as

$$(\chi_i^A \chi_p^B | \doteq \mu_1 S_{ip} (\chi_i^A \chi_i^A | + \mu_2 S_{ip} (\chi_p^B \chi_p^B | \qquad \text{(II.57)}$$

The basis of this method recognises that an equi-partitioning of the overlap charge, as used in the MA, is not realistic in a heteronuclear system.

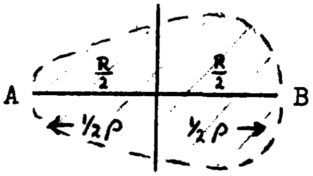

Mulliken Approximation

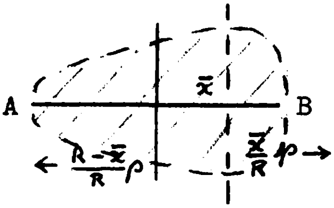

Löwdin Approximation

It is obviously better to divide the charge asymmetrically. The asymmetrical partitioning suggested by Löwdin has the additional advantage of preserving the orbital bond dipole moment. If the centroid of the normalised overlap charge, measured from the left hand atom A, is defined thus

$$\bar{x} = \frac{1}{S_{AB}} \int \chi_A(1) z_A \chi_B(1) dv_1 = \frac{X_{AB}}{S_{AB}} \qquad \text{(II.58)}$$

then the overlap charge is shared between nuclei A and B in the ratio $\frac{R-\bar{x}}{R} : \frac{\bar{x}}{R}$, respectively.

μ_1 and μ_2 in (II.57) are then given by

$$\mu_2 = \frac{\bar{x}}{R} = \frac{X_{AB}}{RS_{AB}} \qquad \text{(II.59)}$$

and

$$\mu_1 + \mu_2 = 1 \qquad \text{(II.60)}$$

In order to use this approximation it is necessary to evaluate the dipole moment integrals for each bond orbital pair.

These integrals are obtained in an analogous manner to the split nuclear attraction integrals mentioned in the last section, but the operator is now the coordinate z_A, measured from A, rather than the operator $\frac{1}{r_A}$.

The third method to be investigated is Löwdin's improved method [43], hereafter referred to as the full Löwdin approximation (FLA). The PLA like the MA is not invariant to orthogonal transformations of the AO basis set, but the FLA, like the Rudenberg method which it resembles, is invariant. This invariancy arises out of the formulation and is not enforced unnaturally. Consequently it is expected to be a better method than any of the others described so far. The FLA takes the form,

$$(\chi_i^A \chi_p^B | \doteq \lambda_1 \sum_a (\chi_i^A \chi_a^A | S_{ap} + \lambda_2 \sum_b (\chi_p^B \chi_p^B | \ S_{bi} \qquad \text{(II.61)}$$

where a runs over all orbitals having principle quantum number equal to or less than that of i; λ_1 and λ_2 are not equal to μ_1 and μ_2 respectively, but they are again chosen to reproduce the orbital bond dipole moment. Since

$$(\chi_i^A | z_A | \chi_p^B) = \lambda_1 \sum_a (\chi_a^A | z_A | \chi_i^A) S_{ap} - \lambda_2 \sum_b (\chi_b^B | z_A | \chi_p^B) S_{bi}$$

the expression for λ_2 is as follows:

$$\lambda_2 = \frac{\sum_a (\chi_a^A|z_A|\chi_i^A)S_{ap} - (\chi_i^A|z_A|\chi_p^B)}{\sum_a (\chi_a^A|z_A|\chi_i^A)S_{ap} - \sum_b (\chi_b^B|z_A|\chi_p^B)S_{bi}} \qquad \text{(II.62)}$$

λ_1 can then be derived since

$$\lambda_1 = 1 - \lambda_2 \qquad \text{(II.63)}$$

The evaluation of λ_1 and λ_2 also requires the bond dipole moment integrals. λ_1 and λ_2 are also more tedious to evaluate than μ_1 and μ_2. In any calculations using the integral approximations described above it is expected that the relative ordering of accuracy would be

ab initio > FLA > PLA > MA > IMA.

A detailed investigation of these approximations is presented for HCN in chapter four.

2.6. Calculation of the MO's and their Energies.

The one-electron MO energies are the eigenvalues of the $\bar{\underset{\sim}{h}}^F$ matrix corresponding to the minimum energy, and are obtained by diagonalising $\bar{\underset{\sim}{h}}^F$.

$$\bar{\underset{\sim}{U}}^{\dagger}\, \bar{\underset{\sim}{h}}^F\, \bar{\underset{\sim}{U}} = \underset{\sim}{\varepsilon} \qquad \text{(II.64)}$$

The components of the eigenvectors of $\bar{\underset{\sim}{h}}^F$ are contained in $\bar{\underset{\sim}{U}}$ whose columns are therefore the various MO LOAO coefficients of both occupied and virtual MO's. The AO coefficients in the natural basis are obtained by performing the transformation

$$\underset{\sim}{U} = \underset{\sim}{S}^{-\frac{1}{2}}\bar{\underset{\sim}{U}} \qquad \text{(II.65)}$$

The ordering of the one-electron energies is very interesting and important especially when they are obtained from an approximate calculation. They are very sensitive to integral approximations and may even change their relative order when compared with a completely *ab initio* calculation.

An interesting property which may be obtained from the orbital energies is the first ionisation potential of the molecule. By Koopman's [56] theorem, the lowest energy ionisation potential is the negative of the highest occupied ε_i. Koopman's theorem has been more widely applied, often without justification, for calculating higher energy ionisation potentials. Also the anti-bonding MO's are frequently used as approximations to excited state orbitals in a configuration interaction calculation: a procedure which assumes there is no reorganisation of the orbitals after excitation.

There has been a recent reinterpretation of Koopman's theorem by Newton [57]. It turns out that the theorem is much more general than was originally thought. He concludes that the ground state is stable under any one-electron excitation obtained by removing an electron from the ground state of the un-ionised system.

2.7. Evaluation of Molecular Dipole Moment.

For molecules represented by a Slater determinant composed of doubly occupied LCAO MO's, ϕ_i, where

$$\phi_i = \sum_p \chi_p \, T_{pi}$$

as given in (II.12), the component of the molecular moment along the internuclear axis z, with origin on the left hand atom (See 3.3), can be expressed in a.u.'s as

$$\mu_z = 2\sum_i \int \phi_i \, z \, \phi_i \, dv - \sum_\alpha Z_\alpha z_\alpha \qquad \text{(II.66)}$$

By substituting (II.12) in (II.66) and defining

$$X_{pq} = \int \chi_p \, z \, \chi_q \, dv \qquad \text{(II.67)}$$

then,

$$\mu_z = 2 \operatorname{tr} \underset{\sim}{R}\underset{\sim}{X} - \sum_\alpha Z_\alpha z_\alpha \qquad \text{(II.68)}$$

$$= \sum_{pq} P_{pq} X_{qp} - \sum_\alpha Z_\alpha z_\alpha \qquad \text{(II.69)}$$

tr $\underset{\sim}{P}\underset{\sim}{X}$ is composed of one-centre and two-centre terms, and the one-centre terms, particularly the $(2s|z_\alpha|2z)$ integrals, give rise to an atomic dipole contribution to the molecular dipole.

For ionic systems, e.g. CN^-, the dipole moment depends on the origin of the axis reference frame and care must be taken over the choice of origin when making comparisons with other work.

2.8. Population Analyses.

The spinless one-electron density function is expressed in terms of $\underset{\sim}{R}$ and the basis set AO's as follows;

$$P_1(1) = 2 \sum_i \sum_j \chi_i (1) \chi_j (1) R_{ij} \qquad \text{(II.70)}$$

Now $\int P_1(1)dv = n$, the number of electrons in the system

$$n = \int \sum_i \sum_j \chi_i (1) \chi_j (1) P_{ij} \, dv$$

$$= \sum_i \sum_j P_{ij} \int \chi_i (1) \chi_j (1) \, dv$$

$$= \sum_i \sum_j P_{ij} S_{ij} \qquad \text{(II.71)}$$

Since $\underset{\sim}{S}$ is symmetric

$$n = \sum_i (\underset{\sim}{P}\underset{\sim}{S})_{ii} = \text{tr } \underset{\sim}{P}\underset{\sim}{S} \qquad \text{(II.72)}$$

(II.71) can be partitioned however to yield more interesting results.

$$n = \sum_i P_{ii} S_{ii} + \sum_{i \neq} \sum_j P_{ij} S_{ij} \qquad \text{(II.73)}$$

The electronic charge in the system has been subdivided into one- and two-centre terms: $Q_{ii} = P_{ii}$ is a partial atom population and $Q_{ij} = P_{ij} S_{ij}$ is a partial bond population. If Q_{ii} is summed over all orbitals χ_i on an atom, the result is the atom population $Q_{\alpha\alpha}$. Similarly $Q_{\alpha\beta}$ is termed the bond population. In order to perform the population analysis, the 1s and 2s AO's on an atom must be orthogonal.

There has always been a desire to represent the electron density in a molecule by point charges situated at the nuclei; i.e. the gross atom charge densities. This is achieved by replacing the bicentric overlap charge distribution $\chi_i(1)\ \chi_j(1)$ by two monocentric charge distributions associated with the two atoms involved in the bonding.

Historically the first method was given by Löwdin [23] using a completely orthogonalised basis set: i.e. $S_{ij} = \delta_{ij}$. In this case the gross atom charge densities, q_α, are given by

$$q_\alpha = \sum_{i \in \alpha} \bar{P}_{ii} \qquad \text{(II.74)}$$

This method has had little usage since it is difficult to accept the q_α as representing an atom charge since AO's on other nuclei are mixed in to achieve the required orthogonality.

Mulliken's method [47] has had much wider application. The overlap density $\chi_i(1)\ \chi_j(1)$ is approximated by (I.6) and the gross atom charge densities are obtained by substitution into (II.70).

$$q_\alpha = Q_{\alpha\alpha} + \sum_{i \in \alpha} \sum_{j \neq i} P_{ij}\, S_{ij} \qquad \text{(II.75)}$$

The main objection to this type of population analysis is that the overlap densities $\chi_i(1)\ \chi_j(1)$ are apportioned equally to each atom contributing the AO's χ_i and χ_j, a situation which might only be true in general if the AO's χ_i and χ_j are of a similar size and symmetry.

The method recently proposed by Doggett [49] eliminates this criticism since the overlap densities are apportioned between the two atoms according to the asymmetric bond parameters μ_1 and μ_2 defined in (I.9). If the value of μ_2 for each orbital bond pair $\chi_i(1)\ \chi_j(1)$ is denoted by μ_{ij}, i.e. an element of the bond asymmetry matrix $\underset{\sim}{\mu}$, then the contributions to the gross atom charge densities on the atoms α and β from each diatomic overlap density are given by

$$\sum_{i\epsilon\alpha} \sum_{j\epsilon\beta} (1 - \mu_{ij})\ P_{ij}\ S_{ij} \qquad \text{for } \alpha \text{ and}$$

$$\sum_{i\epsilon\alpha} \sum_{j\epsilon\beta} \mu_{ij}\ P_{ij}\ S_{ij} \qquad \text{for } \beta \text{ where } \beta$$

is the right hand atom.

The gross atom charge densities are then obtained by summing up all these diatomic contributions along with the atom population itself. This method is hereafter referred to as the Doggett I method.

The fourth method is similar to the last one given above except that the bond asymmetry parameters are now given by the λ_{ij} elements of the full Löwdin bond asymmetry matrix, $\underset{\sim}{\lambda}$; i.e. the overlap density $\chi_i(1)\ \chi_j(1)$ has been replaced by the FLA as given in (I.10). This method is hereafter referred to as the Doggett II method.

Although it is unrealistic to represent the three-dimensional electron density distribution of a polyatomic molecule by a number of point charges, situated at the atomic nuclei, it is intuitively felt that they may have some relative meaning when discussing trends in charge distribution along a series of molecules. For example, Doggett [49] has shown this to be so in a series of first-row diatomic hybrides. Certainly, a method which yields gross atom densities capable of reproducing the calculated dipole moment of the molecule, providing atomic dipoles are also included, must be more acceptable than a method which does not have this property.

The relative ease of performing the population analyses must be considered as an important point also. The Löwdin method is slightly easier to perform than the Mulliken and Doggett I methods which are in turn easier to perform than the full Löwdin variation of Doggett's method. Comparing the two methods which preserve the bond dipole moment there is no question that the Doggett I method is far easier to apply than the Doggett II modification, and since both methods must yield the same dipole moment, the Doggett I is always used in preference to the FLA modification for this purpose.

If it is shown, however, that the FLA to multicentre integrals is superior to the PLA, it could be argued that the FLA gives a better approximation to the division of the overlap densities between the atoms. It would, therefore, be expected in a population analysis that the gross atom charge densities from the Doggett II method might be superior to those of the Doggett I method.

The four methods described above are compared in more detail in chapter four.

2.9. Pictorial Representation of the One-Electron Density Function.

For a closed shell molecule, the spinless one-electron density function is given in terms of the occupied real MO's by [11]

$$P_1(1) = 2 \sum_i \phi_i(1)\, \phi_i(1) \qquad (II.76)$$

and since $\phi_i(1) = \sum_p \chi_p(1)\, T_{pi}$, $P_1(1)$ is given in terms of the NAO's by

$$\begin{aligned} P_1(1) &= 2 \sum_i \sum_p \sum_q \chi_p(1)\, \chi_q(1)\, T_{pi}\, T_{qi} \\ &= 2 \sum_p \sum_q \chi_p(1)\, \chi_q(1)\, R_{pq} \\ &= \sum_p \sum_q \chi_p(1)\, \chi_q(1)\, P_{pq} \qquad (II.77) \end{aligned}$$

The drawing of contour diagrams gives a simple visual picture of the electronic structure of the molecule under investigation. The method used in the present work differs from other cases in that the diagrams were plotted by hand and not on a computer controlled graph plotter.

The electronic probability density is evaluated at each point on a variable mesh superimposed on the xz plane of the linear molecules. Since they possess cylindrical symmetry, rotation about the internuclear z axis would give the 3D situation.

From the table of electron probability densities, in units of electrons/a.u.^{3}, $P_1(1)$ is displayed by drawing selected contours of constant density, and it is a simple, though tedious matter of interpolating between the grid points to obtain the position of the required contour. Ransil and Sinai [45] call these plots, ρ diagrams or ρ maps. They also define ρ profiles which are plots of the electron probability density along a selected molecular axis which is often an internuclear axis. These profiles show in relief the charge density maxima and minima along the chosen axis. Ransil and Sinai also define $\Delta\rho$ diagrams and $\Delta\rho$ profiles which are analogous plots to ρ diagrams and ρ profiles for a difference electron density which can be defined as

$$\Delta P_1(1) = \sum_p \sum_q \chi_p(1)\, \chi_q(1)\, [P_{pq} - P'_{pq}] \qquad \text{(II.78)}$$

If necessary, dummy rows and columns of zeros are added to

P' to give it the same order as P. In most situations the density function being subtracted is given in terms of the same AO basis set e.g. as with $P_{HCN} - P_{CN^-}$.

These difference diagrams are very useful since they show immediately how the charge density has rearranged between two static molecular systems or situations. The results of the present work are presented in terms of various P and ΔP diagrams and profiles in chapter four in an attempt to elucidate trends of charge transfer among related molecules.

CHAPTER THREE

EXPERIMENTAL DETAILS

3.1. Units.

Unless otherwise stated, all numerical values quoted in this thesis are in atomic units (a.u.). Dipole moments are quoted in Debye units. In obtaining the numerical values of the a.u. conversion factors, use was made of the values of $\hbar$ and e given by Cohen et al [58]:

$$\hbar = 1.05443 \times 10^{-27} \text{ erg. sec.}$$

$$e = 4.80286 \times 10^{-10} \text{ esu.}$$

Using the value for m_e of 9.1083×10^{-28} gm., the atomic unit of distance, a_o, was calculated from the relationship

$$a_o = \frac{\hbar^2}{m_e e^2}$$

Using the energy conversion factor $1\text{eV} = 1.60206 \times 10^{-12}$ erg., the atomic unit of energy was evaluated as e^2/a_o.

The numerical values of the units obtained are

$$1\text{a.u. of distance} = 0.529172 \times 10^{-8} \text{ cm.}$$

$$1\text{a.u. of energy} = 27.20963 \text{ eV.}$$

The conversion factor for dipole moments from a.u.s to Debye units is

$$1\text{a.u.} = 2.5416 \text{ Debye.}$$

3.2. Choice of Nuclear Configurations.

The equilibrium internuclear distances for XCN molecules used in this thesis are the microwave values reported by Tyler and Sheridan [5]. The results for X = H, F are given in Table III.1 in both Å and atomic units.

Table III.1.

Equilibrium Internuclear Distances for HCN and FCN.

	HCN		FCN	
Internuclear Distance	Å	a.u.	Å	a.u.
N - C	1.155	2.1826551	1.159	2.1902141
C - X	1.063	2.0087986	1.262	2.3848578

However, to simplify comparisons between the XCN systems, the C - N distance in CN^-, HCN and FCN is chosen to be 1.159Å. Future calculations on the molecules ClCN, BrCN and ICN would then be open to direct comparisons since the C - N equilibrium distance of ClCN and ICN is 1.159Å and in BrCN is 1.158Å [5].

Calculations are performed at five different internuclear distances of C - N in CN^-, of C - H in HCN and of C - F in FCN. The distances used are given in a.u.s in Table III.2.

Table III.2.

Internuclear Distances used in Calculations.

Calc. No.	C – N distances in CN	C – H distances in HCN	C – F distances in FCN
1	1.8000000	1.6000000	2.0000000
2	2.0000000	1.8000000	2.2000000
3	2.1902141	2.0087986	2.3848578
4	2.4000000	2.2000000	2.6000000
5	2.6000000	2.3848578	2.8000000

In addition, four calculations on HCN, each utilising a different multicentre integral approximation, were performed at the internuclear distances chosen by McLean [4]: namely $R_{CH} = 2.000$ a.u. and $R_{CN} = 2.187$ a.u.

3.3. Molecular Axis Convention.

The electronic structure calculations are performed with the molecules oriented so that nitrogen is always the left hand atom. All the local z axes are taken in the same direction along the internuclear axis. The z axis on N is directed towards C, and the origin is taken at N when required, for example, in the calculation of the dipole moment.

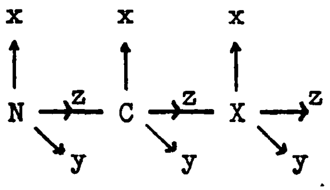

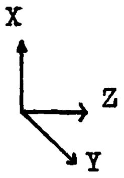

3.4. Atomic Orbital Indexing.

The AO numbering is shown in Table III.3 below. The ordering of the indices is governed by two rules.

a) All AO's of a given symmetry on any atom are indexed sequentially.

b) The atoms are indexed sequentially from left to right.

Table III.3.

Atomic Orbital Indexing for HCN and FCN.

AO type.	HCN Indexing.			FCN Indexing.		
	N	C	H	N	C	F
1s	1	4	7	1	4	7
2s	2	5		2	5	8
$2p_z$	3	6		3	6	9
$2p_x$	8	9		10	11	12
$2p_y$	10	11		13	14	15

3.5. Atomic Orbital Basis Functions in Real form.

Because Clementi quotes his double-zeta functions to only five decimal places, the normalisation and orthogonality integrals are only accurate at best to this level. Since there is no point in introducing any unnecessary error into the integrals, Clementi's values have been extended to values which yield normalisation and orthogonality integrals accurate to eight places of decimals. To this end, the orbital exponents given to five decimal places are assumed exact and normalisation and orthogonalisation are performed by adjusting the orbital coefficients.

The double-zeta AO's are first normalised exactly, and the normalisation constant, N is given by

$$N = 1/\sqrt{\sum_i \sum_j c_i c_j S_{ij}}$$

where S_{ij} is the overlap integral between the STO's χ_i and χ_j of which the double-zeta AO's are composed, and the c_i are the STO coefficients. The normalised coefficients for the 1s AO are then given by

$$n_i^{1s} = A\, c_i^{1s}$$

where A is the appropriate normalisation constant. The orthogonality between the 1s and 2s AO's is extended to eight decimal places by performing a Schmidt orthogonalisation. If B is the normalisation constant for the 2s AO and if the m_i^{2s} are the normalised coefficients where

$$m_i^{2s} = B\, c_i^{2s}$$

then the orthogonalised 2s AO coefficients, z_i^{2s}, are given by

$$z_i^{2s} = \frac{1}{\sqrt{(1-x^2)}} (m_i^{2s} - x n_i^{1s})$$

where $$x = \sum_i \sum_j c_i^{1s}\, c_j^{2s}\, S_{ij}$$

These extended values are listed for C, N and F in Tables III.4, III.5 and III.6 respectively.

The orbital exponent for hydrogen was taken as 1.0.

3.6. Accuracy of Calculations.

The molecular electronic structure calculations were regarded as having reached self-consistency if a given number of cycles had been completed or if the modulus of the difference of two successive electronic energies was less than a given tolerance. In this work initial runs were made using a tolerance of $1_{10}{-5}$ and an upper limit of fifty or sixty cycles. For CN^- and HCN it was found that in production runs a tolerance of $1_{10}{-7}$ or $1_{10}{-8}$ was possible with the limit at sixty cycles. In the case of FCN a tolerance of $1_{10}{-5}$ was roughly equivalent to a limit of

Table III.4.

Double-Zeta AO's for Carbon.

AO type	Orbital Exponent	1s Coefficients	2s Coefficients	AO type	Orbital Exponent	2p Coefficients
1s	5.23090	0.843224702	-0.271764724	2p	1.25572	0.801673552
1s	7.96897	0.165648959	0.015549287	2p	2.72625	0.260477905
2s	1.16782	0.001069993	0.273680848			
2s	1.82031	-0.000499997	0.789072461			

Table III.5.

Double-Zeta AO's for Nitrogen.

AO type	Orbital Exponent	1s Coefficients	2s Coefficients	AO type	Orbital Exponent	2p Coefficients
1s	6.11863	0.811793176	-0.285956754	2p	1.50585	0.782559547
1s	8.93843	0.196390768	0.019130128	2p	3.26741	0.283209836
2s	1.39327	0.001080004	0.308107708			
2s	2.22157	-0.000180001	0.762994320			

Table III.6.

Double-Zeta AO's for Fluorine.

AO type	Orbital Exponent	1s Coefficients	2s Coefficients	AO type	Orbital Exponent	2p Coefficients
1s	7.91788	0.769496759	0.313396771	2p	1.84539	0.725315631
1s	11.01100	0.237272084	-0.029231273	2p	4.17099	0.357542776
2s	1.94665	0.000760007	-0.401630888			
2s	3.09603	0.001090010	-0.680111503			

fifty cycles. To obtain convergence to a tolerance of $1_{10}-7$ or $1_{10}-8$, one hundred cycles were required. A ΔP diagram is presented in chapter four showing the difference in the electron density distributions of FCN in taking convergence at fifty cycles and one hundred cycles. The contours are all small in magnitude, being roughly two orders of magnitude less than the contours in the FCN P diagram. It can be seen that a reasonable representation of the electron density is obtained even after fifty cycles.

In the Jacobi diagonalisation procedure, the off-diagonal elements were required to be zero to a given tolerance. The values $1_{10}-7$ or $1_{10}-8$ were used in this work.

When applying equation (II.23) any improved $\underset{\sim}{R}$ is regarded as being idempotent if the quantity $\mathrm{tr}(\underset{\sim}{R}^2-\underset{\sim}{R})^2 <$ tol where tol is some specified tolerance. In general a value of not less than $1_{10}-7$ was used in this work. It is possible, however, that in favourable cases where the deviation from idempotency is small, it is immaterial what value is chosen as all would probably be satisfied at the first idempotency cycle.

3.7. Contour Diagrams.

It is found that, in general, a mesh of 0.1a.u. is sufficient to accurately represent P contour diagrams. Occasionally, it is necessary to decrease the mesh to values such as 0.04a.u. or 0.025a.u., in order to throw into relief small areas either of rapidly varying electron probability density near the nuclei, or of uncertain contour direction. This is especially true for ΔP contour diagrams.

In calculating difference electron densities the orders of the two $\underset{\sim}{R}$ matrices being subtracted must be compatible. Where the orders are not equal rows and columns of zeros are added to the matrix of smaller order until the orders are identical.

The electron probability densities are evaluated only for positive x ordinates in the xz plane since the molecules have cylindrical symmetry. To standardise the plotting of the contour diagrams for easy comparison, the starting z abscissa is always taken as -2.0a.u. where the N atom is the origin. The final abscissa depends on the molecule but is always at least 2.0a.u. beyond the second or third atom.

3.8. <u>Computation Times.</u>

The total computer calculation times shown in Table III.7 are for complete calculations making no use of previously calculated quantities. The times quoted in minutes are partitioned to show the relative times of the three main sections:

a) the evaluation of the integrals and the setting up of the integral arrays.

b) the SCF energy minimisation (for a tolerance of $1_{10}{-7}$).

c) the evaluation of molecular properties and contour diagrams.

Section a) is also subdivided to show the exchange integral evaluation times on the Atlas computer.

Table III.7.

Sample Calculation Times for CN^-, HCN and FCN.

Molecule	Integral Evaluation KDF9	Integral Evaluation ATLAS	SCF Energy Minimisation	Molecular Properties and Contour Diagrams	Total
CN^-	9	10	10	7	36
HCN	18	12	25	9	64
FCN	23	30	50	14	117

By making use of previously evaluated integrals, for example, in performing the varied internuclear distance calculations in FCN and HCN, it is possible to save a certain amount of computer time: 14 minutes for HCN and FCN. Also when performing the calculations with various multicentre integral approximations an even greater saving in time results for the second and subsequent calculations: 23 minutes for HCN and 42 minutes for FCN.

CHAPTER FOUR

RESULTS AND DISCUSSION

4.1. Comparison of Multicentre Integral Approximations for HCN.

In this section, the results of four molecular electronic structure calculations, using best atom AO's in a minimal basis set, are presented for the molecule HCN at the equilibrium configuration used in McLean's 1962 accurate calculation [4]. The four calculations differ from McLean's calculation in that the three-centre integrals are evaluated by four different multicentre integral approximations. In calculation IMA the invariant Mulliken method is used; in MA the ordinary Mulliken method; in PLA the partial Löwdin method; and in FLA the full Löwdin method is used. These four calculations are compared wherever possible to McLean's accurate calculation designated as MCL. The effect of introducing the sole approximation of the multicentre integrals into an ab initio calculation can thus be evaluated.

Additional comparisons are made where possible with the work of M.P. Melrose [59] who attempted a calculation similar to the one designated in this work as the MA i.e. using the ordinary Mulliken approximation.

A comparison of various calculated molecular properties is given in Table IV.1. The first point to be noted from this table is that the use of a multicentre integral approximation apparently lowers the total energy relative to the ab initio value. This is somewhat surprising since it was expected that, as the integral approximation became less rigorous, the energy would rise

Table IV.1.

Calculated Molecular Properties for HCN (Best Atom AO's).

	IMA	MA	PLA	FLA	MCL
Electronic Energy E_{el}	-116.61593	-116.60790	-116.53140	-116.46920	-116.4236
Total Energy E	-92.73970	-92.73167	-92.65517	-92.59297	-92.5474
Kinetic Energy T	91.25466	91.24116	91.42916	91.49046	91.32089
Potential Energy V	-183.99436	-183.97283	-184.08433	-184.08343	-183.86829
-2T/V	0.99193	0.99190	0.99334	0.99401	0.99333
Dipole Moment μ_{HCN}	1.309	1.304	2.033	1.803	2.100

further above the ab initio value.

After further consideration it was realised that when an integral approximation is invoked the effective Hamiltonian no longer represents the molecule accurately, and there is no theorem which states whether the resultant energy will be above or below the ab initio value. It can also be seen from Table IV.1 that as the integral approximation becomes more rigorous the energy approaches the ab initio value from below. Further to this it would seem that, if the total energy is used as a criterion of accuracy, the full Löwdin method is the best of all the approximates as it gives a total energy within 0.05% of the ab initio value. It is also interesting to notice that the simple Mulliken method, although not invariant, is a slightly better approximation on the basis of total energies, than the IMA.

However, the PLA reproduces $-2T/V$ and μ more satisfactorily. This is significant as E may not be the best criterion; it is important to obtain other molecular properties correctly as well.

Table IV.2 contains a comparison of the one-electron MO energies for all five methods. Also included are the ε's from Melrose's two calculations MPM1 and MPM2. Table IV.2 again shows the improvement obtained over the Mulliken approximation by the Löwdin methods. If the MO energies are used as a criterion of accuracy, the PLA would appear to be better than the FLA or the Mulliken methods. However, two points should be noted which are

Table IV.2.

Comparison of One-Electron MO Energies for HCN.

MO	IMA	MA	PLA	FLA	MCL	MPM1	MPM2
1σ	-15.74270	-15.74694	-15.72871	-15.74789	-15.7402	-15.8222	-15.9891
2σ	-11.39718	-11.39177	-11.40352	-11.41422	-11.4277	-11.5571	-11.7832
3σ	-1.24039	-1.24301	-1.25258	-1.25750	- 1.2522	-1.9721	-2.1230
4σ	-0.82626	-0.81577	-0.79341	-0.78111	-0.7965	-0.7186	-1.1415
5σ	-0.56912	-0.56458	-0.56445	-0.57350	-0.5582	-0.2360	-0.1494
6σ	0.84003	0.68603	0.52148	0.35346	0.3648	0.8664	0.6985
7σ	1.09234	1.15020	1.07993	0.96128	1.0860	3.2533	1.1430
1π	-0.49597	-0.49736	-0.50296	-0.51372	-0.5074	-0.3652	-0.4899
2π	0.25918	0.26031	0.25566	0.24528	0.2516	0.2407	0.0994
G	61.53518	61.51358	61.49718	61.60332	61.5792	-	-
$\sigma-\pi$ gap	0.07315	0.06722	0.06149	0.05978	0.0508	-	-
$\pi-\pi^A$ gap	0.75515	0.75767	0.75862	0.75900	0.7590	-	-
1st I.P. (eV)	13.49	13.53	13.69	13.98	13.81	-	-

not quite so obvious. Firstly, the two orbital energy gaps, defined in the table are slightly better represented by the FLA. Secondly, it can be seen that the MO energies are reasonably well represented in all four approximate calculations with the sole exception of 6σ which appears peculiarly sensitive to the nature of the integral approximation. Only in the FLA calculation is it reasonably well represented. A discussion of Melrose's calculations is deferred to the end of this section.

In Table IV. 3 a comparison is given of the unique non-zero matrix elements of $\underset{\sim}{R}$, and Table IV. 4 contains the results of a Mulliken population analysis of the electron density distribution. Table IV. 5 compares the effective atom charges as given by three different methods; the Mulliken, Doggett I and Doggett II population analyses.

It is difficult to see from Table IV. 3 which of the $\underset{\sim}{R}$ matrices resulting from the approximate calculations is closest to McLean's $\underset{\sim}{R}$, but it is clearly seen that the PLA and FLA $\underset{\sim}{R}$ matrices are closer than the Mulliken $\underset{\sim}{R}$ matrices. This is seen most clearly in the $\underset{\sim}{R}$ matrix elements 88, 89 and 99. However, none of the methods appears to reproduce the 55 or 66 $\underset{\sim}{R}$ elements to any degree of accuracy and this seems to be the main failing of the approximate methods. The off-diagonal elements of $\underset{\sim}{R}$, are reasonably well reproduced in general.

A similar picture is obtained from Tables IV. 4 and IV. 5.

Table IV.3.

R Matrices for Best Atom HCN Calculations.

AO Indices	IMA	MA	PLA	FLA	MCL
11	1.005	1.005	1.005	1.005	1.006
12	0.006	0.006	0.009	0.013	0.012
13	-0.028	-0.027	-0.027	-0.028	-0.032
14	0.001	0.000	0.001	0.000	0.001
15	-0.033	-0.034	-0.028	-0.030	-0.048
16	0.024	0.024	0.024	0.026	0.037
17	0.011	0.014	0.012	0.016	0.009
22	0.857	0.845	0.903	0.952	0.916
23	-0.338	-0.344	-0.307	-0.307	-0.332
24	-0.022	-0.022	-0.027	-0.033	-0.031
25	-0.058	-0.050	-0.055	-0.096	-0.071
26	-0.050	-0.052	-0.032	-0.007	-0.002
27	-0.028	-0.019	-0.021	0.020	0.042
33	0.544	0.537	0.563	0.505	0.522
34	-0.026	-0.025	-0.029	-0.021	-0.032
35	0.247	0.263	0.255	0.309	0.254
36	-0.215	-0.200	-0.210	-0.193	-0.251
37	-0.168	-0.183	-0.165	-0.193	-0.068
44	1.006	1.006	1.006	1.006	1.008
45	-0.023	-0.022	-0.023	-0.022	-0.023

Table IV.3 continued.

AO Indices	IMA	MA	PLA	FLA	MCL
46	0.005	0.002	0.005	-0.001	0.007
47	-0.007	-0.006	-0.005	-0.005	-0.018
55	0.495	0.525	0.486	0.524	0.366
56	0.042	0.053	0.099	0.089	0.064
57	0.148	0.119	0.132	0.080	0.167
66	0.213	0.219	0.231	0.247	0.344
67	0.215	0.224	0.212	0.234	0.213
77	0.241	0.239	0.191	0.223	0.183
88	0.343	0.348	0.359	0.374	0.366
89	0.379	0.380	0.380	0.381	0.381
99	0.419	0.415	0.403	0.388	0.396

Table IV.4.

Mulliken Population Analysis of Best Atom HCN Electron Densities.

		Atom/Bond Populations						Gross Atom Charge Densities		
		N	C	H	NC	CH	NH	N	C	H
IMA	sigma	4.813	3.429	0.481	0.597	0.764	-0.084	5.070	4.109	0.821
	pi	1.373	1.677	0.000	0.950	0.000	0.000	1.848	2.152	0.000
	total	6.186	5.106	0.481	1.547	0.764	-0.084	6.917	6.262	0.821
MA	sigma	4.775	3.499	0.478	0.623	0.713	-0.087	5.042	4.166	0.791
	pi	1.391	1.658	0.000	0.950	0.000	0.000	1.867	2.133	0.000
	total	6.166	5.157	0.478	1.573	0.713	-0.087	6.909	6.300	0.791
PLA	sigma	4.941	3.447	0.398	0.572	0.722	-0.080	5.187	4.094	0.719
	pi	1.437	1.611	0.000	0.952	0.000	0.000	1.913	2.087	0.000
	total	6.378	5.058	0.398	1.524	0.722	-0.080	7.100	6.181	0.719
FLA	sigma	4.925	3.554	0.445	0.506	0.642	-0.074	5.142	4.129	0.730
	pi	1.494	1.552	0.000	0.953	0.000	0.000	1.971	2.029	0.000
	total	6.420	5.107	0.445	1.459	0.642	-0.074	7.113	6.158	0.730
MCL	sigma	-	-	-	0.520	0.801	-0.011	5.143	4.096	0.761
	pi	-	-	-	0.953	0.000	0.000	1.939	2.060	0.000
	total	-	-	-	1.473	0.801	-0.011	7.082	6.156	0.761

Table IV.5.

Effective Atomic Charges for Best Atom HCN Calculations.

	Mulliken			Doggett I			Doggett II		
	N	C	H	N	C	H	N	C	H
IMA	+0.083	-0.261	+0.178	+0.134	-0.102	-0.032	+0.212	-0.272	+0.060
MA	+0.091	-0.300	+0.209	+0.145	-0.135	-0.010	+0.248	-0.308	+0.060
PLA	-0.100	-0.181	+0.281	-0.036	-0.036	+0.072	+0.060	-0.214	+0.154
FLA	-0.113	-0.157	+0.270	-0.005	-0.038	+0.043	+0.157	-0.244	+0.087
MCL	-0.081	-0.155	+0.236	+0.010	-0.038	+0.028	+0.083	-0.226	+0.143

The PLA and FLA reproduce the results of the population analysis on McLean's results a little better than do the MA or IMA. Of these first two the FLA is slightly superior to the PLA, in all but the Doggett II effective atomic charges.

Contour diagrams 1, 2, 3 and 4 present ΔP diagrams and profiles for the difference electron density between McLean's calculation and respectively the FLA, PLA, IMA and MA calculations. The contours have quite small values indicating that there is not much difference between the approximate wave functions and McLean's accurate wave function. The profiles also show this quite clearly. As a generalisation, a given contour covers a smaller area in the PLA and FLA diagrams than it does in the IMA and MA diagrams. The PLA seems to reproduce the electron density distribution particularly well in the vicinity of the H atom. The four diagrams show that the effect of the multicentre integral approximations is to take electronic charge away from the region of the atoms and deposit it in the bonds. The only significant difference among the four diagrams is that the FLA method has deposited charge in the region normally thought of as the N lone pair, whereas charge is depleted from this region in the other three methods.

The result of this evaluation indicates that the full and partial Löwdin approximations to the three-centre integrals lead to results which are a significant improvement over those obtained

CONTOUR DIAGRAM 1.

$P_{MCL} - P_{FIA}$

R(NC) = 2.187a.u.

R(CH) = 2.000a.u.

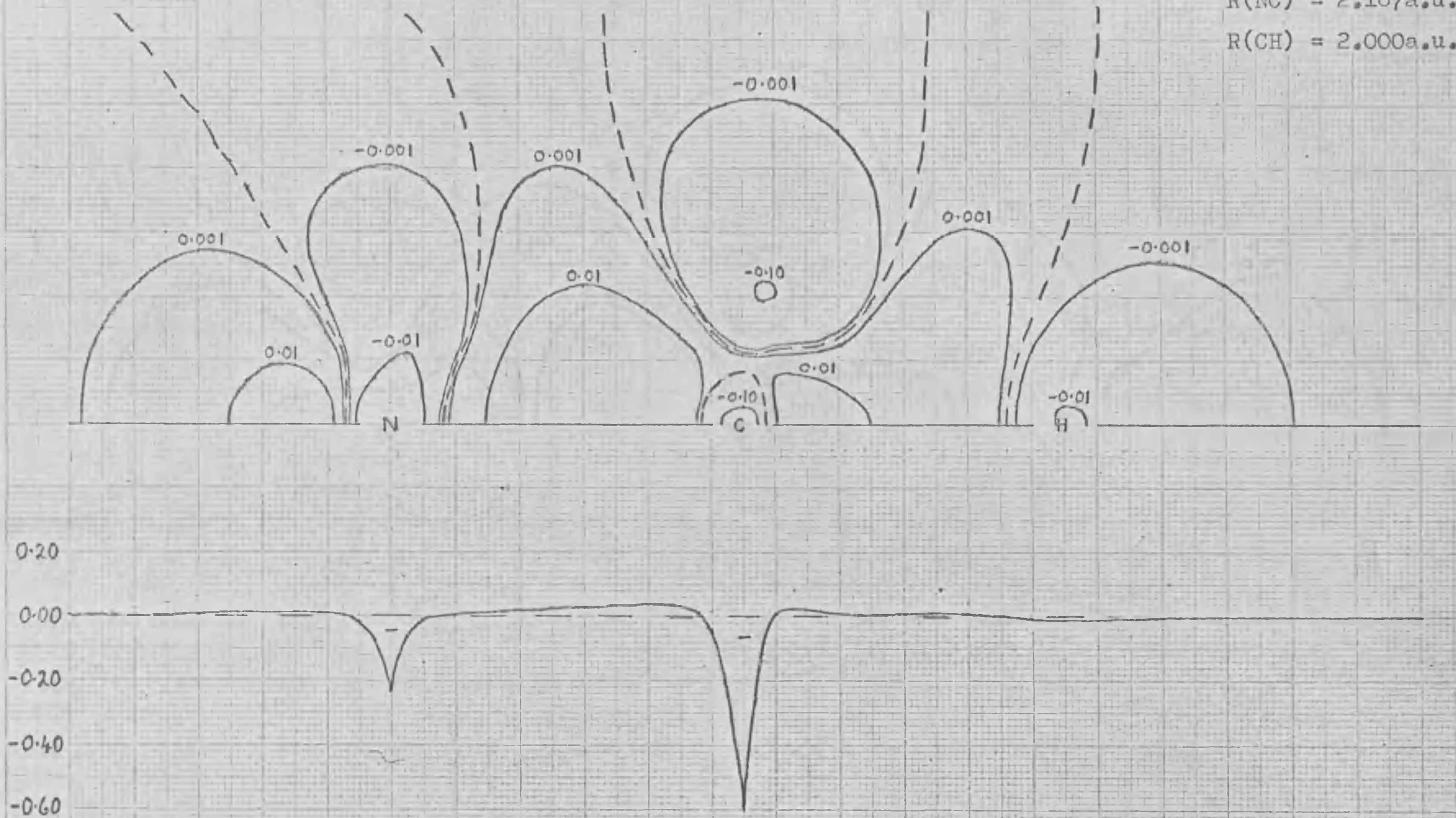

CONTOUR DIAGRAM 2.

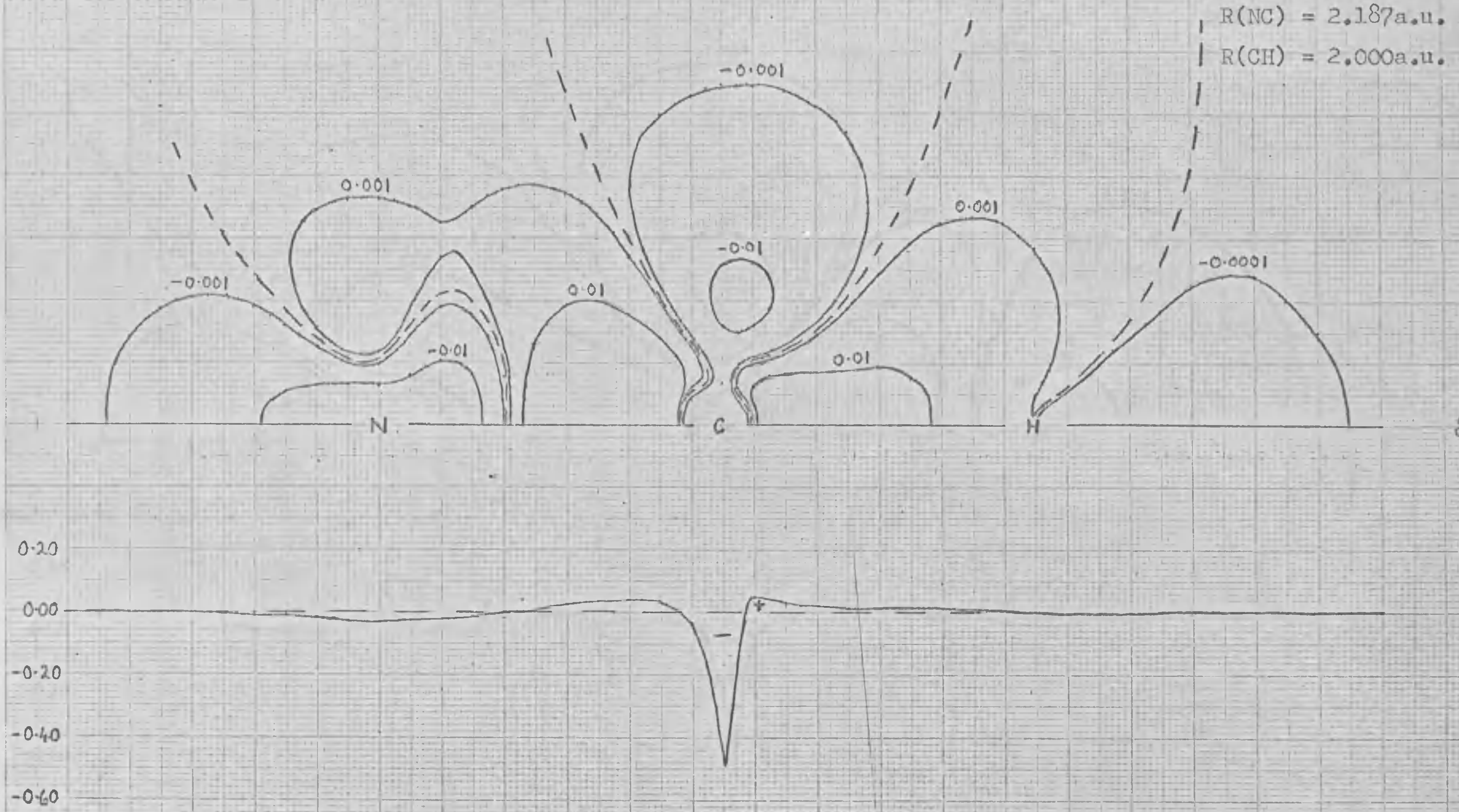

$P_{MCL} - P_{PLA}$

R(NC) = 2.187a.u.

R(CH) = 2.000a.u.

CONTOUR DIAGRAM 3.

$P_{MCL} - P_{IMA}$

R(NC) = 2.187a.u.

R(CH) = 2.000a.u.

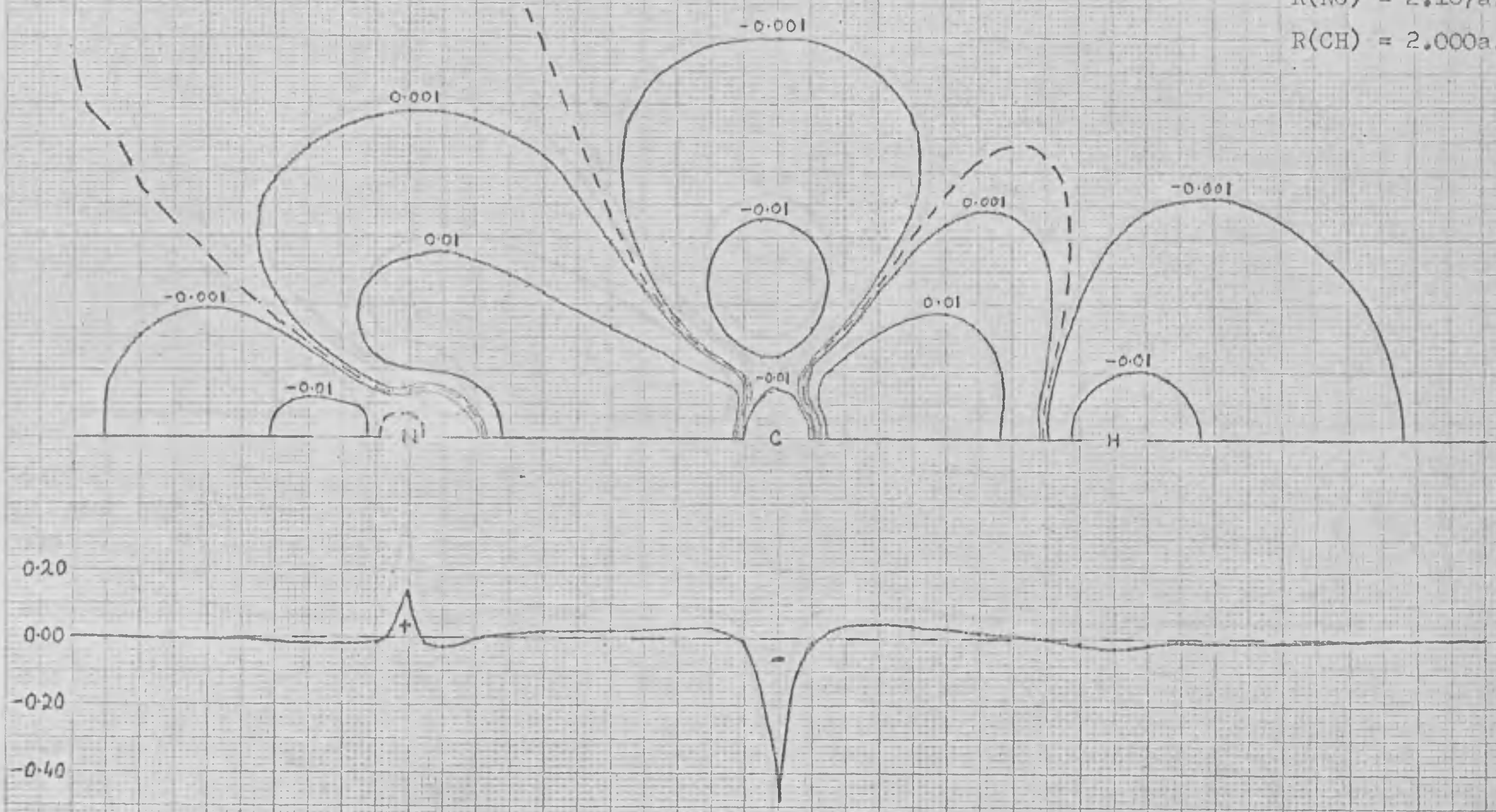

CONTOUR DIAGRAM 4.

$P_{MCL} - P_{MA}$

R(NC) = 2.187a.u.

R(CH) = 2.000a.u.

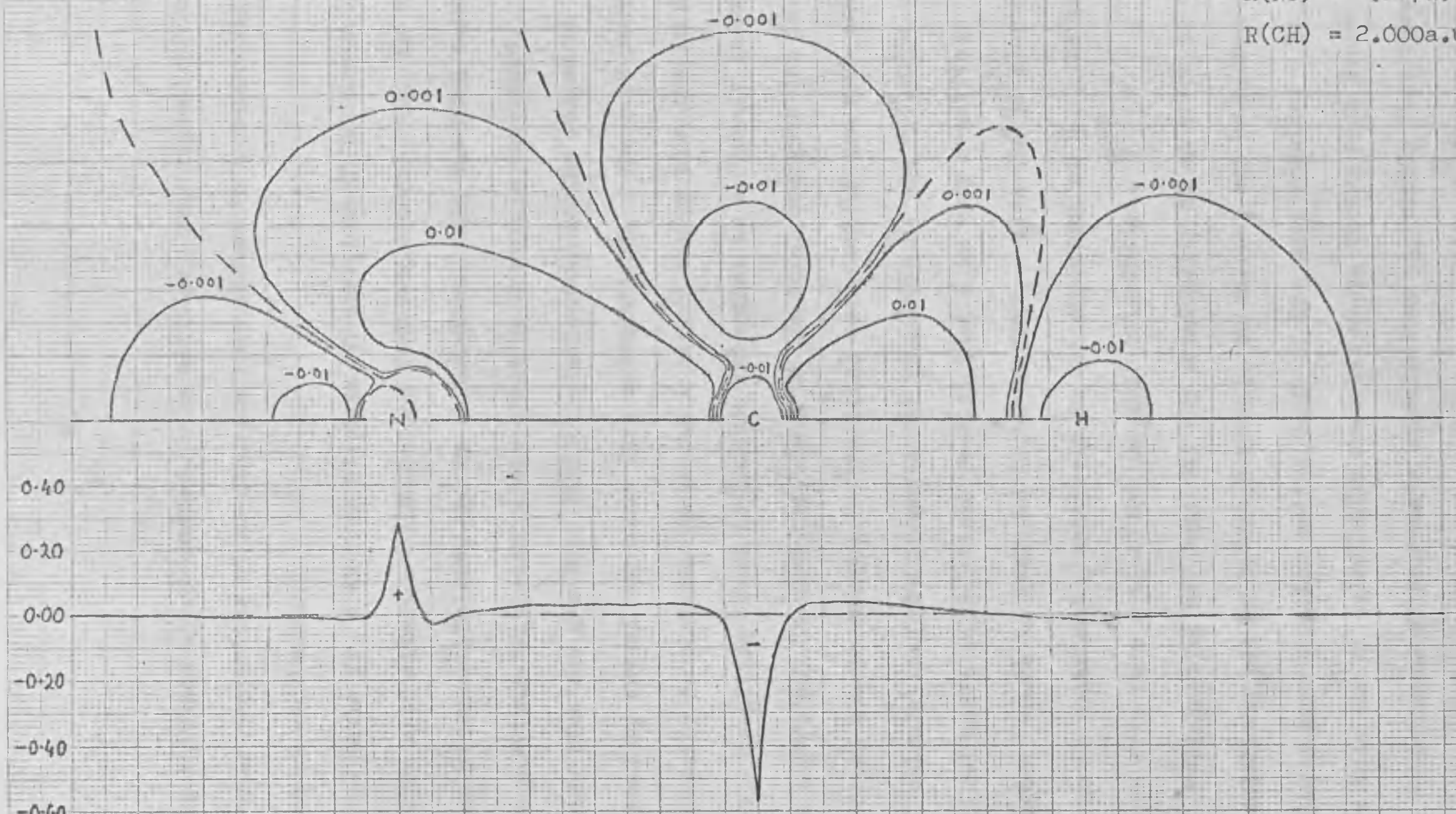

by the Mulliken approximation. In addition, they reproduce the molecular properties of an accurate calculation to a reasonable degree of accuracy.

In Table IV. 2 the one-electron MO energies of Melrose's [59] Mulliken approximation calculations were presented. MPM1 is directly comparable with the MA calculation. In the MPM2 calculation accurate three-centre one-electron integrals were used. It is seen that the ε's bear little relationship to the values obtained by any of the other five calculations. The most serious discrepancy is that the 5σ MO has a higher energy than the 1π MO and the resulting first ionisation potential is seriously in error. This inaccuracy is also reflected in the total energies and in effective atomic charges. The total energies for the MPM1 and MPM2 calculations are respectively -92.5007a.u. and -93.1033a.u. Both Melrose's calculations predict that H is very negatively charged; -0.64 in MPM1 and -2.40 in MPM2. Also the pi electronic charge is polarised excessively in the direction of N. The trends become even more extreme in the MPM2 calculation.

Melrose does not rule out the possibility of an error in his calculations but he believes them to be correct and he blames the Mulliken approximation as the cause of the poor results. It is felt that the MA calculation reported above throws some doubt as to the correctness of Melrose's calculations especially when taken in context with the closeness to McLean's results of all the integral approximation calculations presented above. The rigorous testing carried out on the computer programs, which is discussed in chapter five, is an additional verification of the MA results.

It is possible to go further, as it is doubtful if even errors in Melrose's molecular integrals would cause such drastic results. There are four main failings in the MPM1 and MPM2 calculations; namely, too low an E; the transposition of the 5σ and 1π MO's; the very negative H atom; and the excessive polarity of the pi electronic charge. It has been the experience of this work that exactly these four symptoms are obtained if there are errors in the method of forming the $\bar{\underset{\sim}{G}}$ matrix.

4.2. Molecular Electronic Structure Calculations on CN^-.

In this section, results are presented for molecular electronic structure calculations performed at five internuclear distances of C–N, in CN^-, as given in chapter three. A minimal basis set of double-zeta AO's is employed and all integrals are evaluated accurately.

A comparison of the various calculated molecular properties is given in Table IV.6. This table shows how the molecular properties behave as the C–N internuclear separation is increased. For example, it can be seen that a minimum in the total energy is predicted somewhere between 2.2 and 2.4 a.u., probably closer to 2.4 a.u., and also that the dipole moment increases almost linearly with increasing nuclear separation. The dipole moments are all in the direction C – N, and the origin is taken at N.

Figures IV.1, IV.2 and IV.3 respectively, show the trends in E, μ_{NC} and $-2T/V$ as R_{CN} varies, in more detail. From figure IV.1 the predicted minimum energy at an internuclear separation of 2.32a.u. is -92.17a.u. Figure IV.2 shows that the variation of μ with R_{CN} is indeed almost linear.

A least squares fit of the variation of E with R_{CN}, to the parabola $y = ax^2+bx+c$ yields a minimum E of -92.18149 a.u. at an equilibrium R of 2.348 a.u.

Table IV.7 contains a comparison of the one-electron MO energies for all five distances and includes, G, twice the sum of

Table IV.6.

Some Calculated Molecular Properties for CN^- at Five Internuclear Distances.

Calculation.	1	2	3	4	5
R_{CN}	1.80	2.00	2.1902141	2.40	2.60
Electronic Energy E_{el}	-115.23967	-113.09011	-111.33430	-109.66429	-108.28661
Total Energy E	-91.90634	-92.09011	-92.15809	-92.16429	-92.13276
Kinetic Energy T	93.67963	93.11309	92.78533	92.58322	92.49370
Potential Energy V	-185.58597	-185.20320	-184.94342	-184.74751	-184.62646
-2T/V	1.00956	1.00552	1.00339	1.00227	1.00196
Dipole Moment* μ_{NC}	-2.925	-3.154	-3.341	-3.524	-3.681

* These values are relative to N as origin.

FIGURE IV.1.

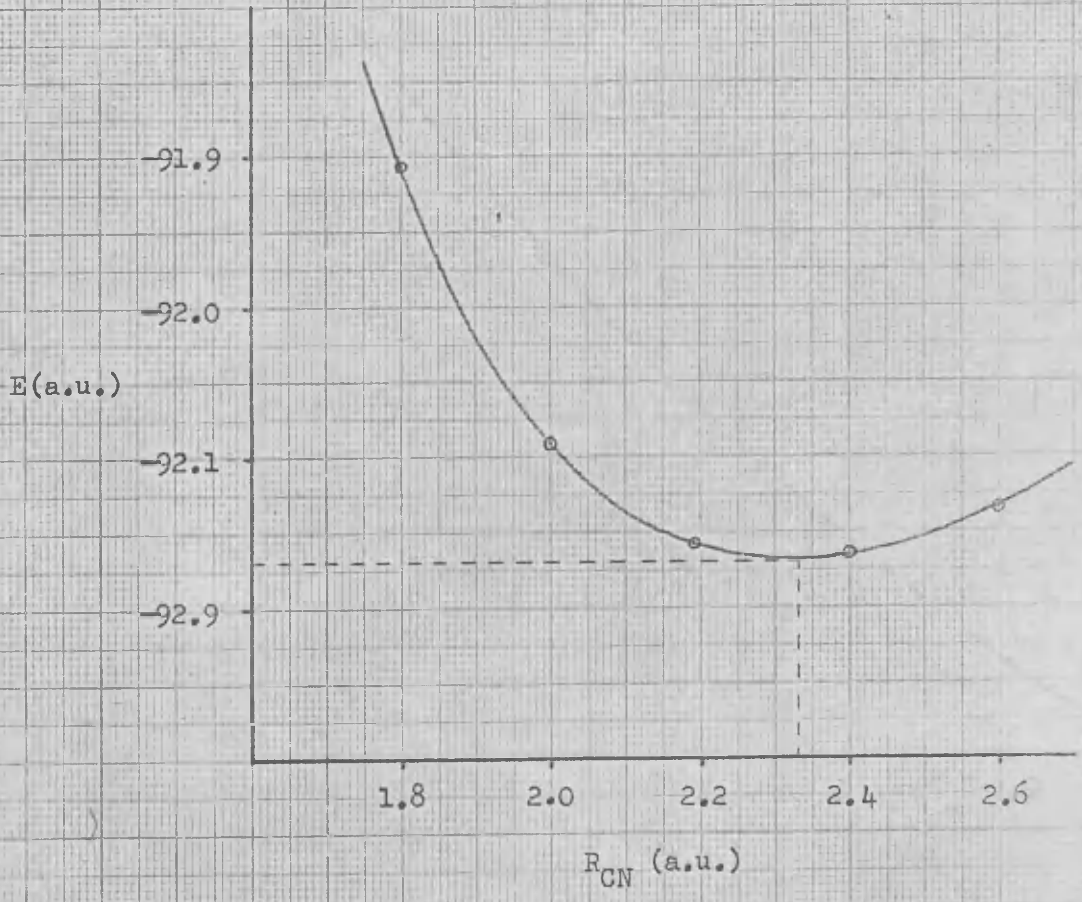

Diagram to show Variation of E with R_{CN} for CN^-.

FIGURE IV.2.

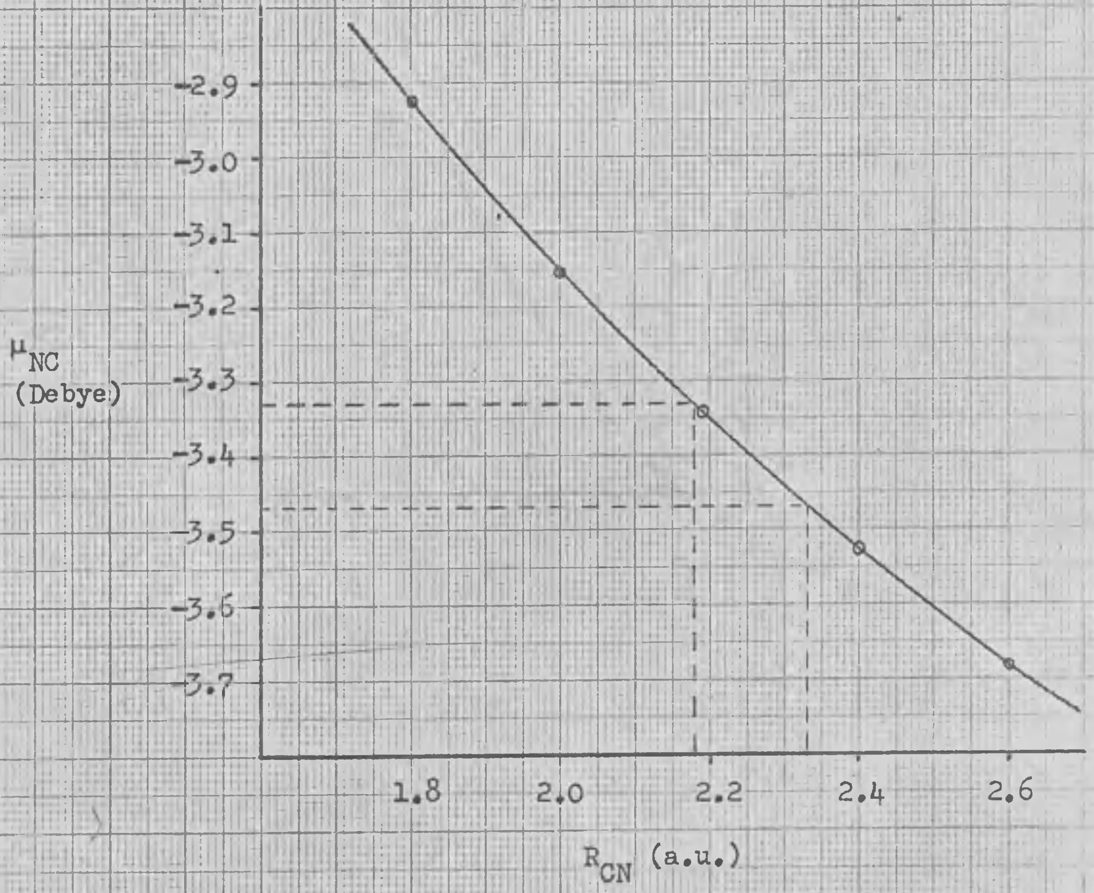

Diagram to show Variation of μ_{NC} with R_{CN} for CN^-.

FIGURE IV.3.

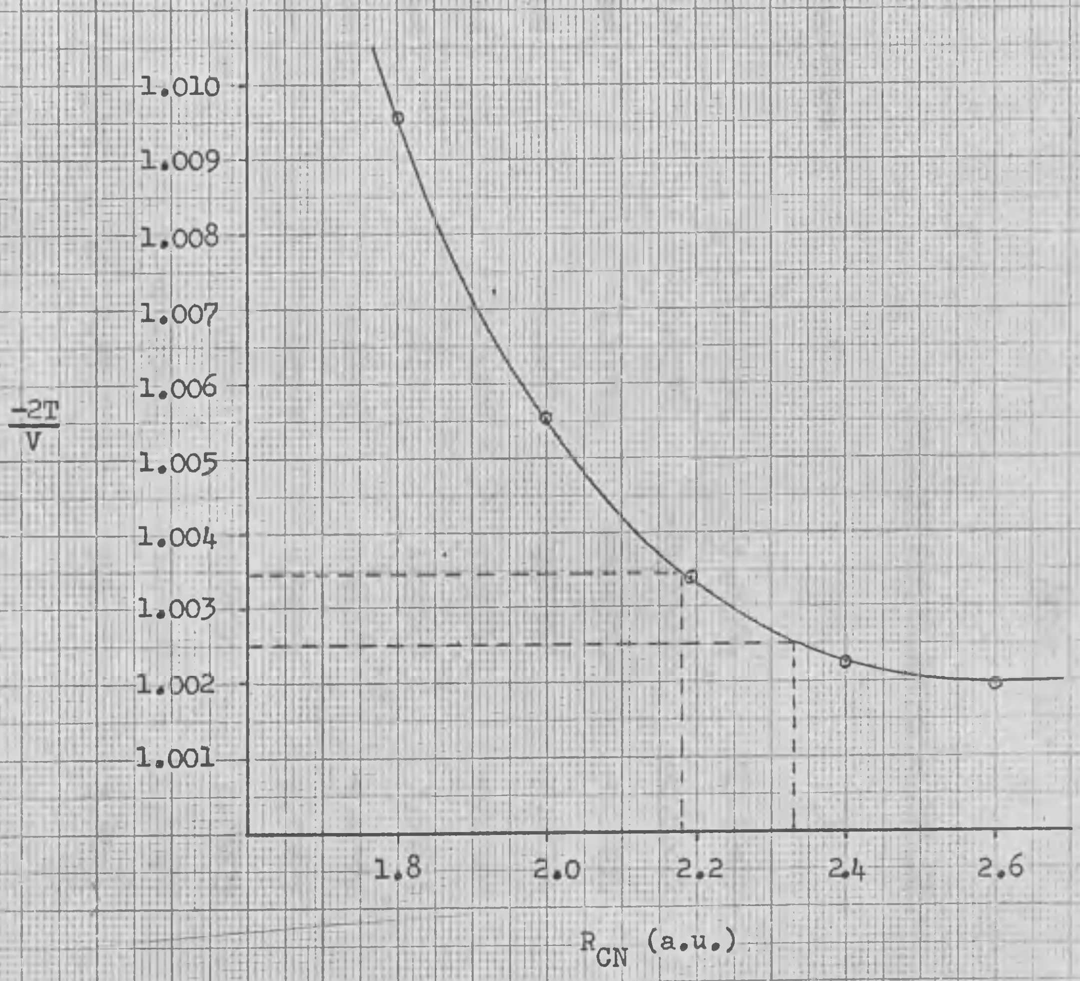

Diagram to show Variation of $-2T/V$ with R_{CN} for CN^-.

Table IV.7.

One-Electron MO Energies for CN^-.

Calculation	1	2	3	4	5
$\varepsilon(1\sigma)$	-15.28361	-15.24584	-15.22047	-15.19945	-15.18278
$\varepsilon(2\sigma)$	-10.99969	-10.95909	-10.93821	-10.92654	-10.92220
$\varepsilon(3\sigma)$	-1.03395	-0.96570	-0.90035	-0.83320	-0.77644
$\varepsilon(4\sigma)$	-0.27332	-0.27978	-0.28734	-0.29699	-0.30703
$\varepsilon(5\sigma)$	-0.14518	-0.13238	-0.12162	-0.11010	-0.09861
$\varepsilon(6\sigma)$	1.82244	1.56749	1.35646	1.16210	1.01326
$\varepsilon(1\pi)$	-0.27018	-0.21520	-0.16972	-0.12637	-0.09082
$\varepsilon(2\pi)$	0.70773	0.64714	0.59857	0.55323	0.51659
$\pi-\pi^A$ gap	0.97791	0.86234	0.76829	0.67960	0.60741
G	-56.55222	-56.02638	-55.61486	-55.23804	-54.93740
1st I.P.(eV)	3.95	3.60	3.31	3.00	2.47

the bonding MO energies to see whether G also has a turning point within the range of R under study.

In figures IV.4 and IV.5, the variations of G, and the ε's respectively, with R are shown. It can be seen from Table IV.7 and figures IV.4 and IV.5 that G and all the bonding MO ε's, with the exception of the 4σ MO, are lowered as the internuclear separation decreases and consequently no minimum is predicted by G.

The first ionisation potential by Koopman's theorem for the equilibrium R_{CN} is about 0.12 a.u. (3.26 eV). This compares fairly well with the experimental value of 3.7 ± 0.2 eV derived from the electron affinity of CN [60].

The results of a Mulliken population analysis are presented in Table IV.8. From the total gross atom charge densities it appears that, as the internuclear separation increases, the electronic charge is displaced progressively more towards C. However, the constituent sigma and pi electronic charges are displaced in opposite senses. Pi electronic charge is displaced from C to N, but this is overcompensated by the sigma charge displacement from N to C. The atom and bond populations show a similar trend. For example, the σ bond population increases as the π bond population decreases. There is no real indication of how CN^- would dissociate although it appears from the above to be tending to dissociate to N and C^-. However the trend is diminishing by 2.60 a.u. and it may well reverse further out.

FIGURE IV.4.

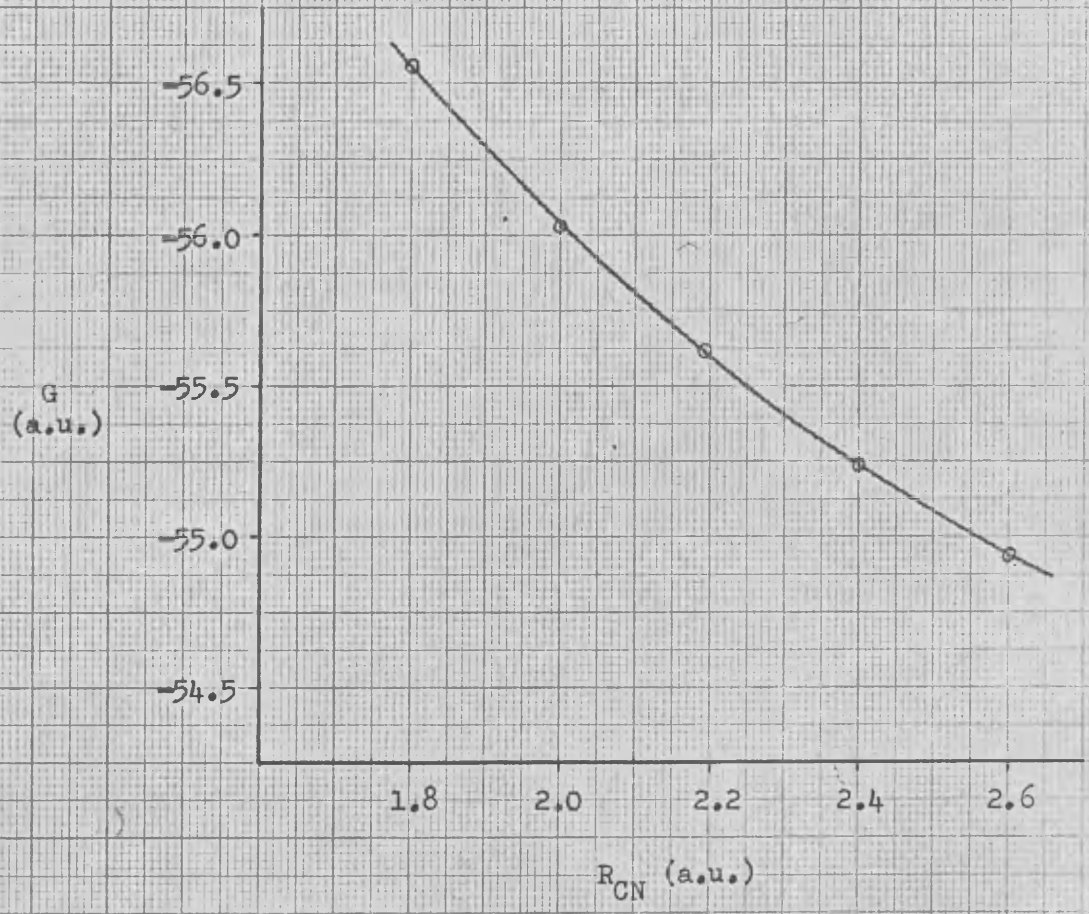

Diagram to show Variation of G with R_{CN} for CN^-.

FIGURE IV.5.

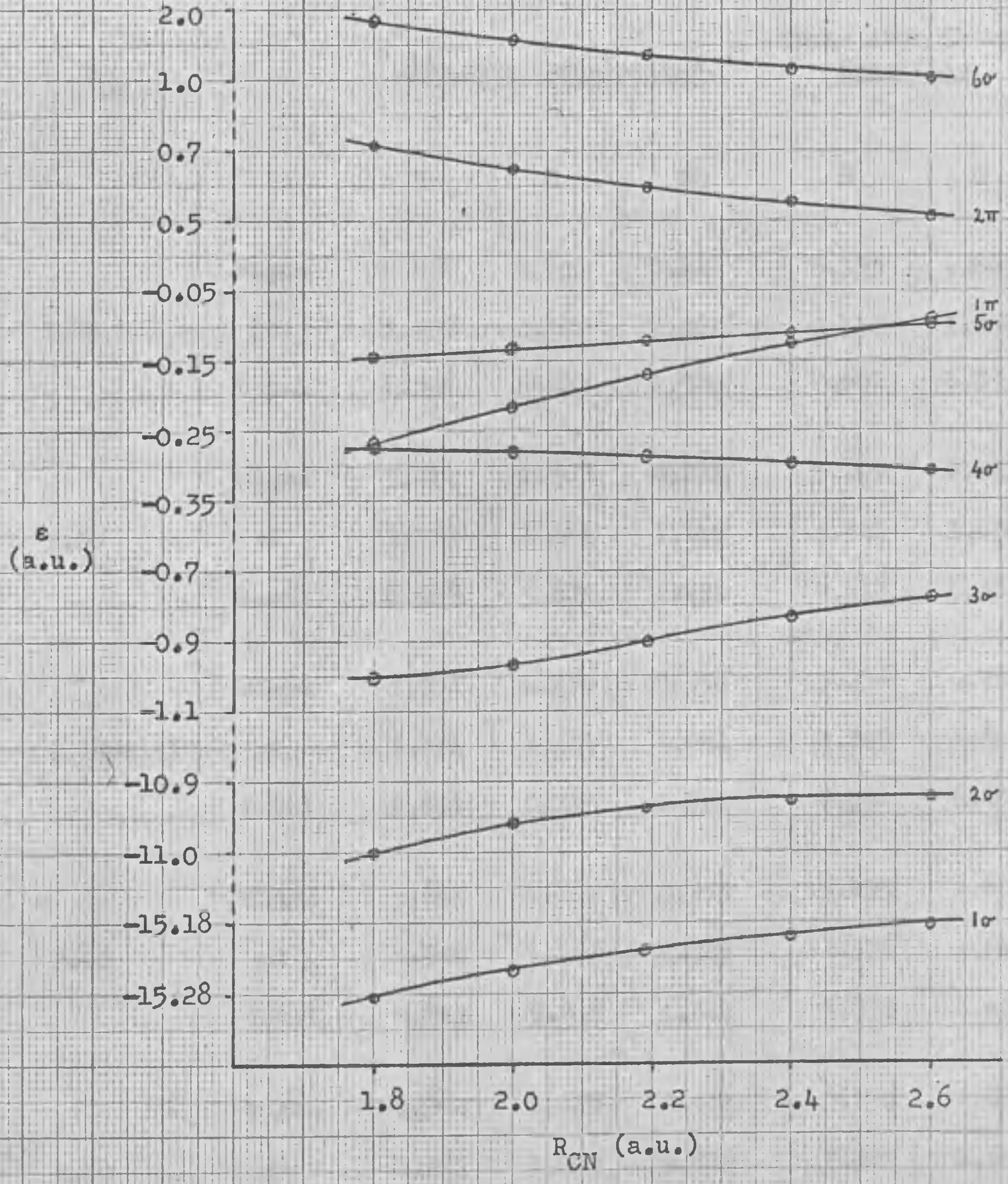

Diagram to show Variation of ε with R_{CN} for CN^-.

Table IV.8.

Mulliken Population Analysis of CN^- Electron Density.

R_{CN}		Atom/Bond Populations.			Gross Atom Charge Densities.	
		N	C	NC	N	C
1.80	sigma	5.276	4.605	0.119	5.335	4.665
	pi	1.702	1.037	1.261	2.332	1.668
	total	6.978	5.642	1.380	7.667	6.333
2.00	sigma	5.141	4.587	0.272	5.277	4.723
	pi	1.767	1.084	1.149	2.341	1.659
	total	6.908	5.671	1.421	7.618	6.382
2.1902141	sigma	5.061	4.589	0.350	5.236	4.764
	pi	1.834	1.124	1.042	2.355	1.645
	total	6.895	5.713	1.392	7.591	6.409
2.40	sigma	5.002	4.604	0.393	5.199	4.801
	pi	1.910	1.162	0.929	2.374	1.626
	total	6.912	5.766	1.322	7.573	6.427
2.60	sigma	4.964	4.625	0.411	5.170	4.830
	pi	1.982	1.193	0.825	2.394	1.606
	total	6.946	5.818	1.235	7.564	6.436

A comparison of the effective atomic charges as evaluated by the Mulliken, Löwdin, Doggett I and Doggett II population analyses is given in Table IV. 9.

As noted by Cusachs and Politzer [48] in a slightly different context, the Mulliken and Löwdin methods lead to opposite results and trends, as electronic charge appears to be displaced from C to N as the internuclear separation increases. The trend of the Mulliken and Doggett I methods is similar but it is seen that the Mulliken method underestimates the polarity of the CN bond because it does not partition the bond charge density according to the bond dipole moment. The Doggett II method exaggerates this polarity even more but also finds a minimum in the N electronic density.

The one-electron density functions $P_1(1)$ corresponding to the wave functions for the five CN^- calculations are shown in pictorial form in Contour Diagrams 5, 6, 7, 8 and 9. Also, the total electron probability density distribution of 7 is divided into its constituent σ and π distributions which are shown in the upper and lower halves, respectively, of Contour Diagram 10.

P diagrams 5 to 9 show that as the C - N internuclear separation increases the probability density decreases in the vicinity of the N atom and in the bond. This is particularly well seen by comparing the 0.4 contours. It is not quite so easily seen that this charge is building up on to the C atom, but by careful examination of the 0.1 contour above and to the right

Table IV. 9.

Effective Atomic Charges for CN^-.

R_{CN}		Mulliken	Löwdin	Doggett I	Doggett II
1.80	N	−0.667	−0.422	−0.859	−1.040
	C	−0.333	−0.578	−0.141	+0.040
2.00	N	−0.618	−0.440	−0.715	−0.853
	C	−0.382	−0.560	−0.285	−0.147
2.1902141	N	−0.591	−0.456	−0.644	−0.775
	C	−0.409	−0.544	−0.356	−0.225
2.40	N	−0.573	−0.476	−0.601	−0.772
	C	−0.427	−0.524	−0.399	−0.228
2.60	N	−0.564	−0.492	−0.581	−1.315
	C	−0.436	−0.508	−0.419	+0.315

CONTOUR DIAGRAM 5.

P_{CN^-}

$R(CN) = 1.80$a.u.

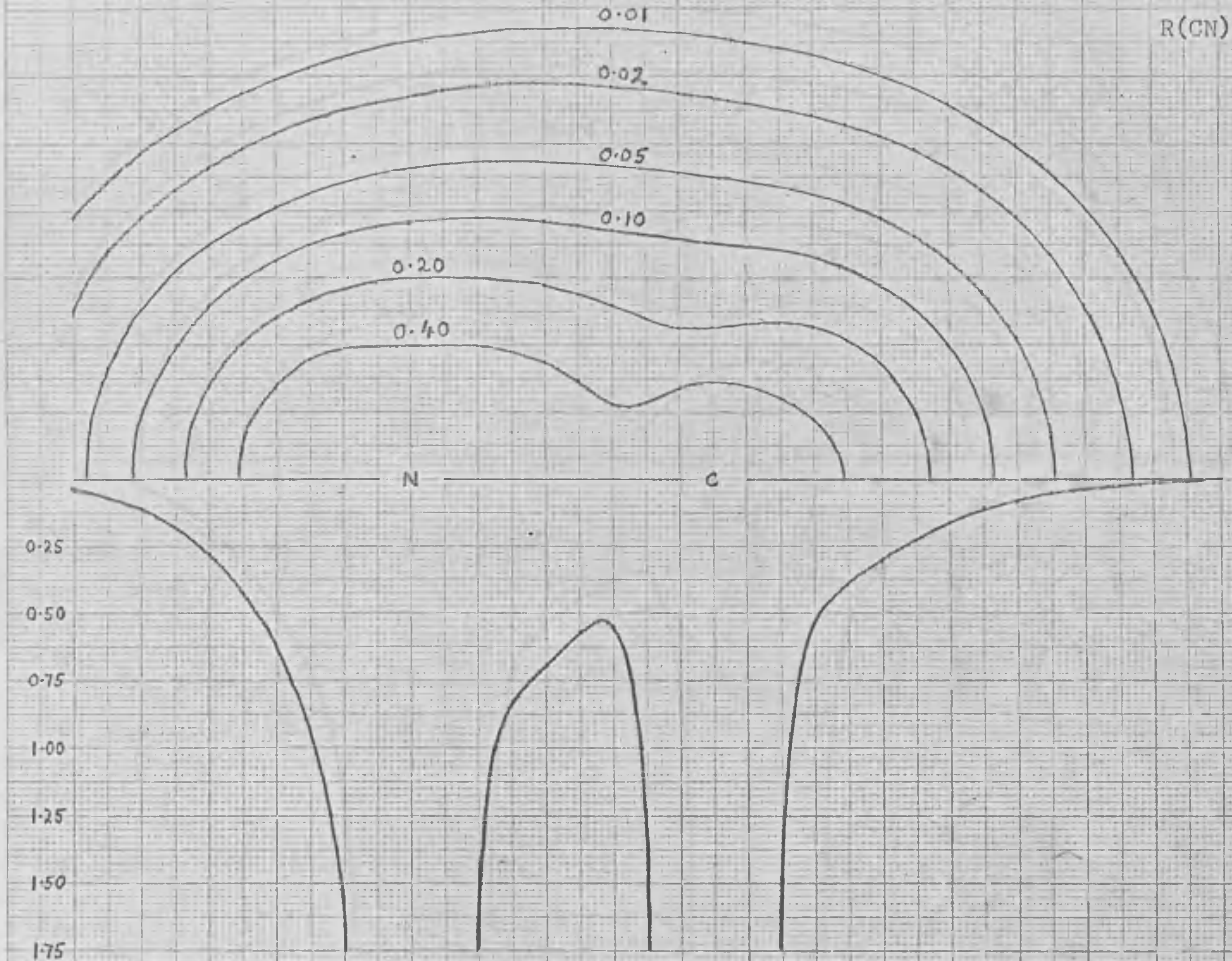

CONTOUR DIAGRAM 6.

P_{CN^-}

$R(CN) = 2.00$a.u.

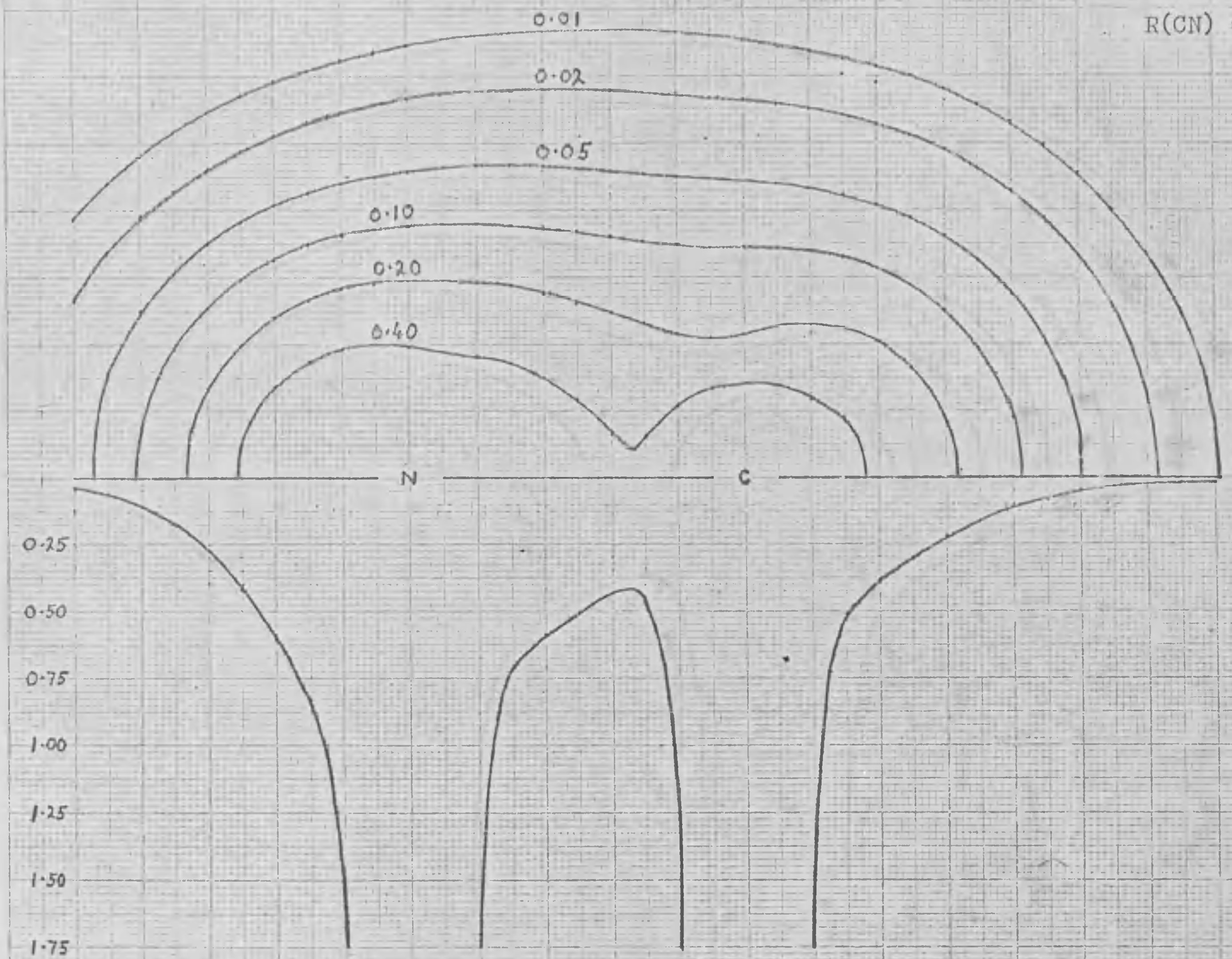

CONTOUR DIAGRAM 7.

P_{CN^-}

R(CN) = 2.1902141a.u.

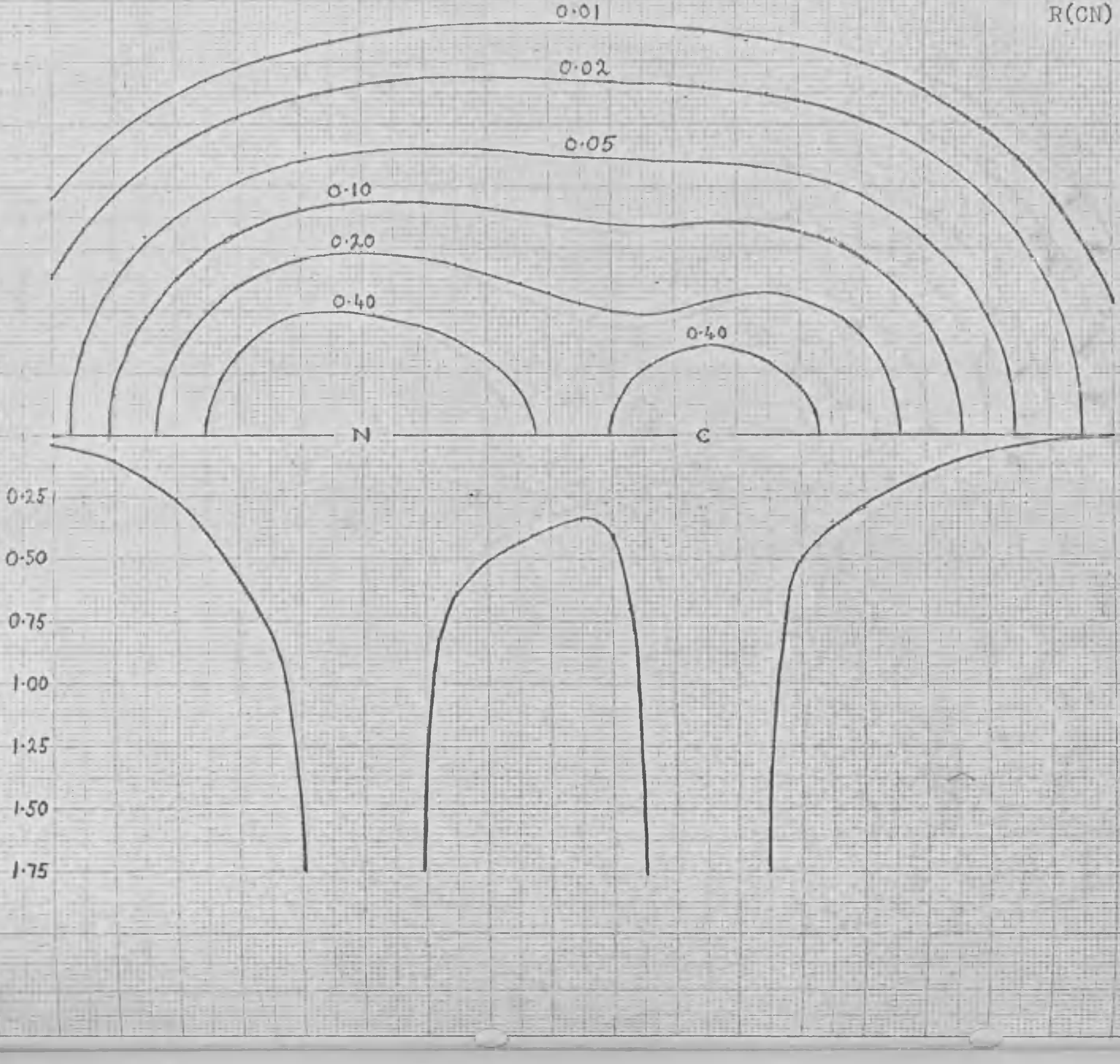

CONTOUR DIAGRAM 8.

P_{CN^-}

R(CN) = 2.40a.u.

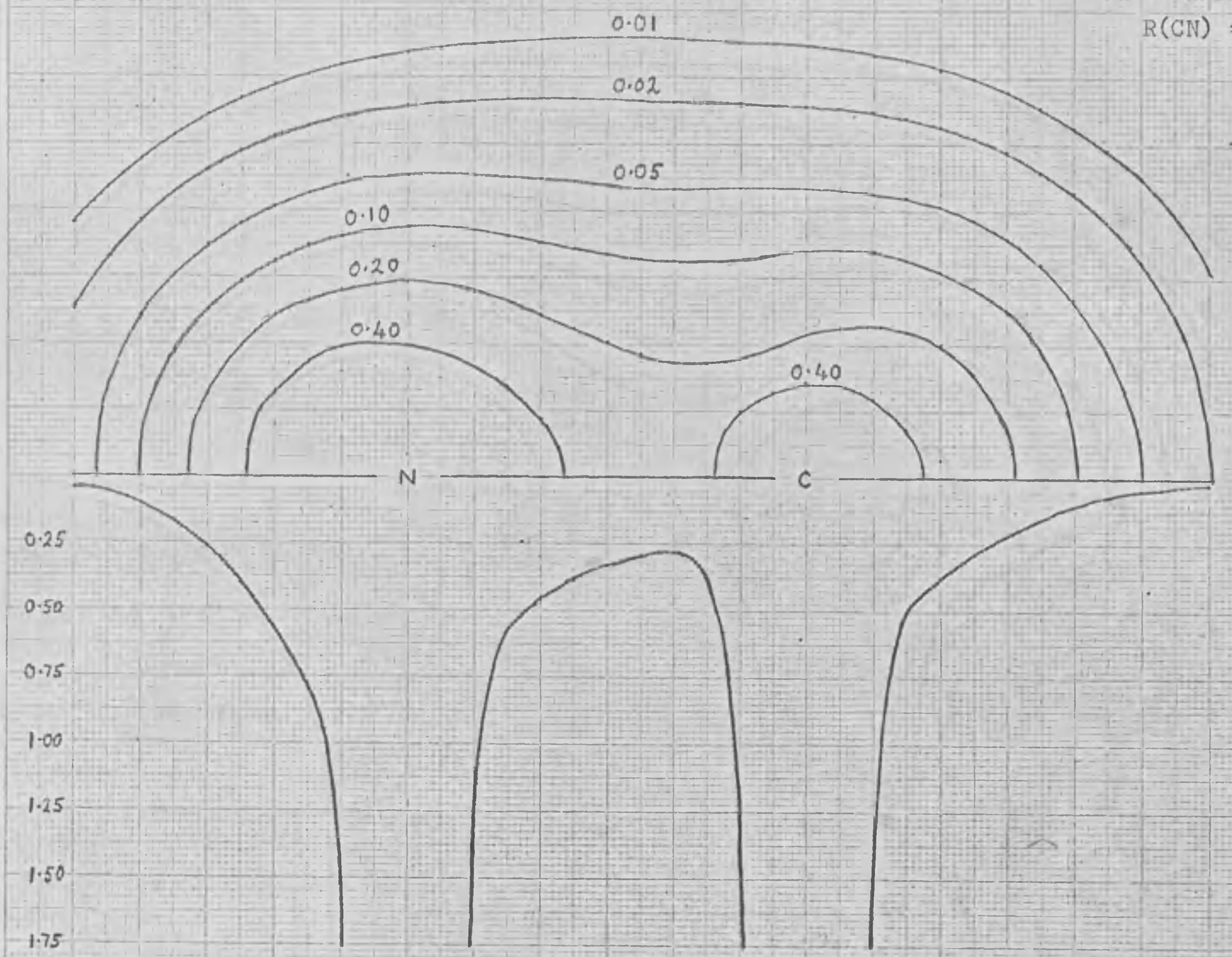

CONTOUR DIAGRAM 9.

P_{CN^-}

R(CN) = 2.60a.u.

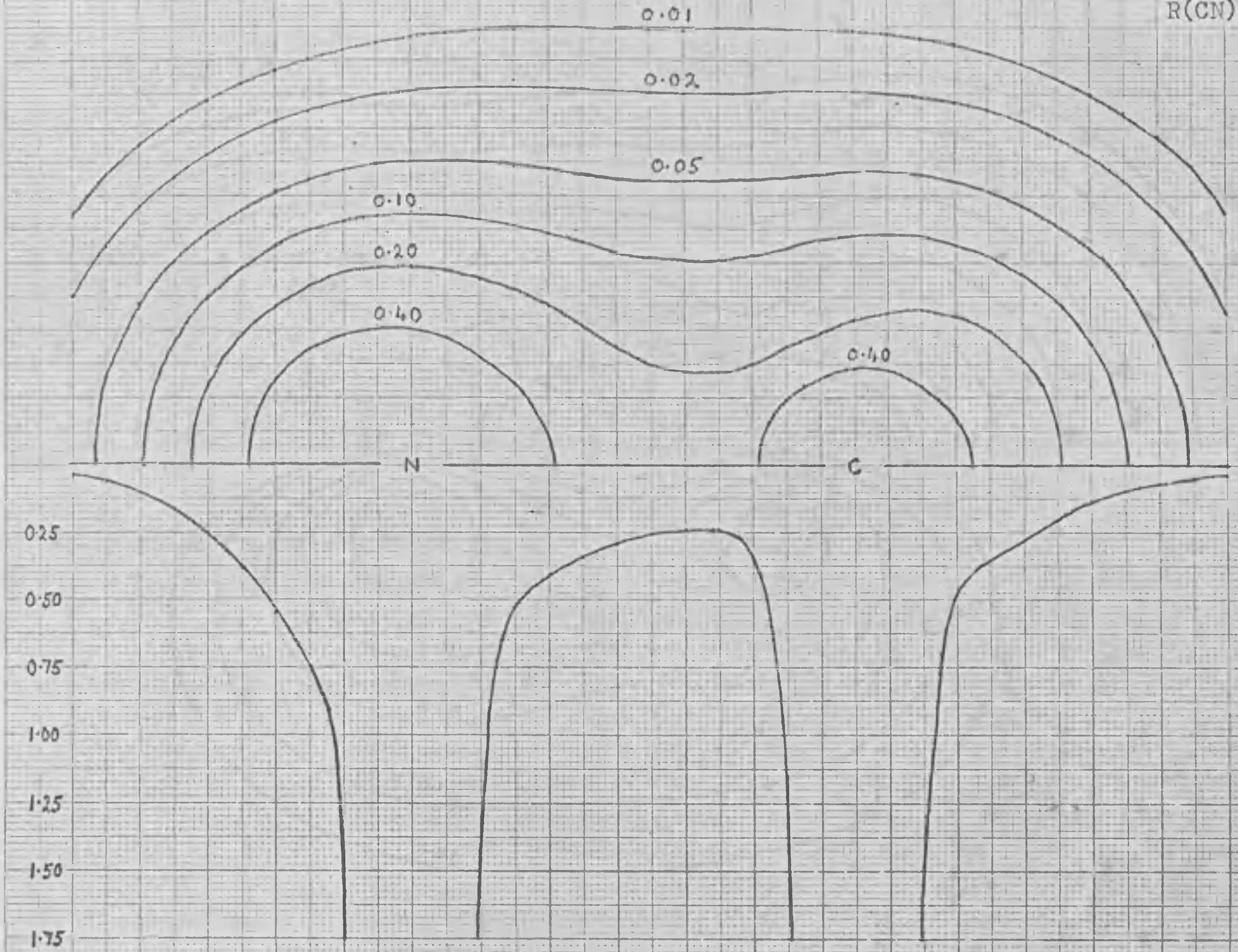

CONTOUR DIAGRAM 10.

R(CN) = 2.1902141a.u.

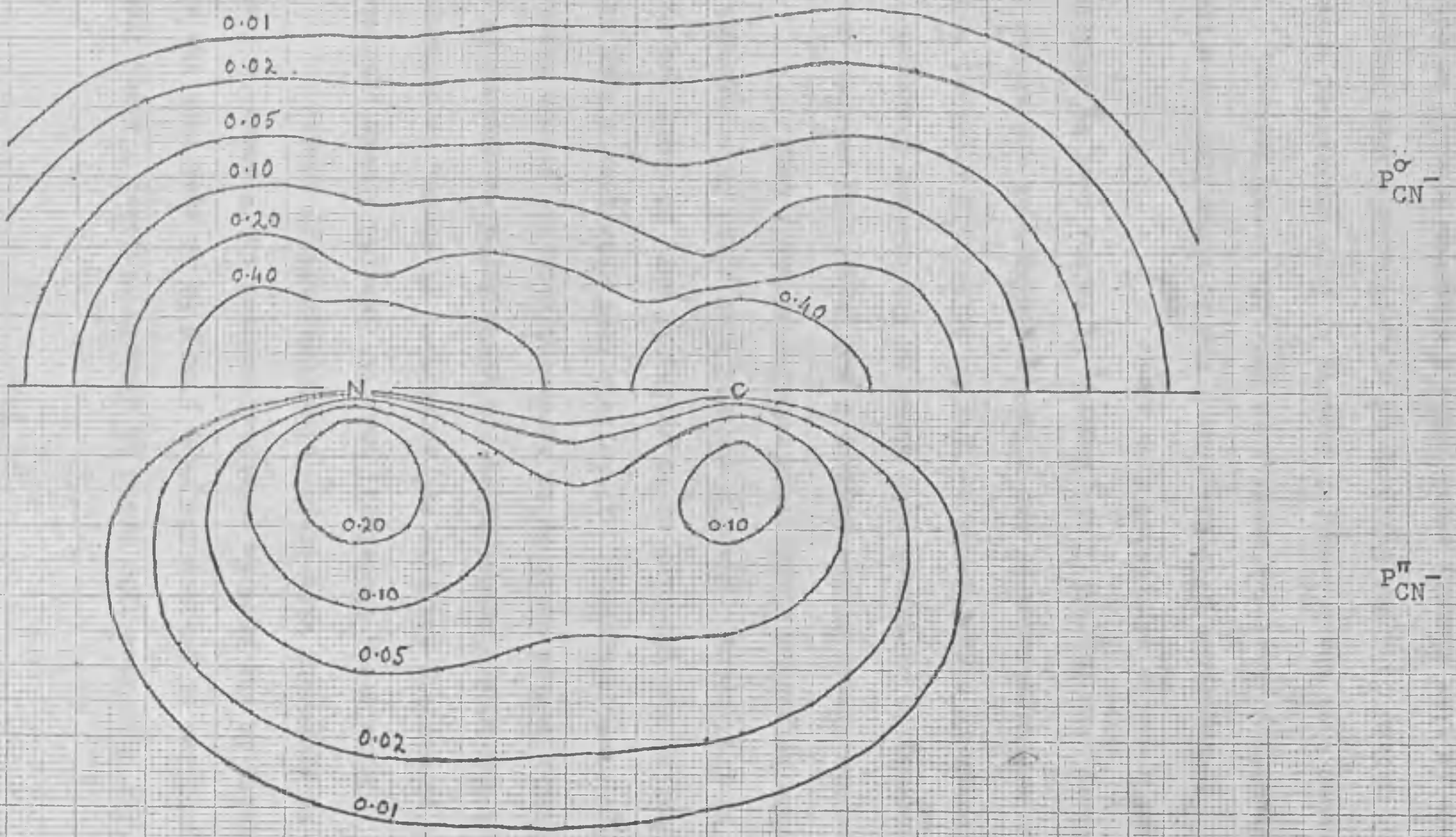

of the C nucleus this trend is clearly visible. Also, from the P profiles of Contour Diagrams 5 to 9 it is seen that the electron density in the bond is polarised towards the N atom: a fact which is in agreement with simple electronegativity ideas.

It is seen, therefore, that the general trends predicted by the population analyses are correct. It shows, in particular, that the Löwdin method gives the wrong trend as opposed to the Mulliken method which is in agreement with the trends displayed in the contour diagrams. It is felt that this goes a long way to answering the question as to which, if any, of these two methods is to be preferred. Cusachs and Politzer posed this question but were unable to answer it from the results of their work.

The trends of the Doggett I and Doggett II methods are generally in agreement with those of the contour diagrams. Although no significance can yet be definitely attached to the absolute magnitudes of the effective charges of any of the four methods, the Doggett I and Doggett II values must be preferred since μ can be reproduced from them.

A comparison of P diagrams 7 and 10 shows how the σ and π probability densities combine to give the total density. It can be seen that the σ electron density is more contracted around N than around C. The build up of σ electronic charge between the atoms is also clearly seen. The π electron density is polarised more towards N as predicted by the Mulliken population analysis, but again only the trend is probably of any use and not the absolute values.

Table IV. 10 contains a comparison of the results of this work, using R_{CN} = 2.19a.u., with the recent work of Bonaccorsi et al [61] who used a minimal basis set of best atom AO's at an internuclear separation of 2.18a.u. Although these internuclear separations are close enough for a direct comparison, the middle column shows the double zeta results for 2.18a.u. obtained by interpolation from figures IV.1 to IV.5.

As expected, it is seen that the total energy is significantly improved by using double-zeta AO's in the basis set. However, the best atom calculation gives a poor estimate for the first ionisation potential in contrast to the calculation using the double-zeta basis. Also, the gross atom populations from the best atom calculation appear to resemble the Löwdin values for the double-zeta calculation rather than the Mulliken values as can be seen from a comparison with Table IV.9.

It should be noted that -2T/V is only a valid test of the Virial Theorem at the equilibrium internuclear separation, which is not at 2.19a.u. From figure IV.3 the value of -2T/V at 2.348a.u. is 1.0025.

Finally, for completeness, the $\underset{\sim}{R}$ matrix for the CN^- calculation with R_{CN} = 2.4a.u. is presented in Table IV.11.

Table IV.10.

Comparison of Double-Zeta and Best Atom Calculations for CN^-.

	Double-Zeta	Interpolated Double-Zeta	Best Atom
R_{CN}	2.1902141	2.18	2.18
E_{el}	-111.33430	-111.332	-111.1934
E	-92.15809	-92.156	-91.9273
T	92.78533	92.802	92.5726
-2T/V	1.00339	1.00345	1.0035
$\varepsilon(1\sigma)$	-15.22047	-15.22	-15.1791
$\varepsilon(2\sigma)$	-10.93821	-10.938	-10.8272
$\varepsilon(3\sigma)$	-0.90035	-0.90	-0.8167
$\varepsilon(4\sigma)$	-0.28734	-0.287	-0.2143
$\varepsilon(1\pi)$	-0.16972	-0.171	-0.0807
$\varepsilon(5\sigma)$	-0.12162	-0.123	-0.0359
1st I.P.(eV)	3.265	-	0.98
Gross atom population on N	7.591	-	7.4984
Gross atom population on C	6.409	-	6.5017
μ_{CN} (Debye)*	2.23	2.24	1.84

*These values are relative to C as origin.

Table IV. 11.

R Matrix for CN^- Calculation 4: R(CN) = 2.40a.u.

$\underset{\sim}{R}_{\sigma}$	1.0027	-0.0008	-0.0318	0.0025	-0.0105	0.0230
		0.8762	-0.2994	-0.0160	-0.0651	-0.0613
			0.6224	-0.0432	0.0354	-0.3660
				1.0048	0.0013	0.0344
					0.8431	0.3633
						0.4543
$\underset{\sim}{R}_{\pi}$	0.4775	0.3724				
		0.2904				

4.3. Molecular Electronic Structure Calculations on HCN.

Results are presented below for molecular electronic structure calculations performed at the five internuclear distances of the C – H bond given in 3.2. A minimal basis set of double-zeta AO's is used and all two-centre integrals are evaluated accurately. The three-centre integrals are evaluated by two methods: the Mulliken Approximation made invariant to orthogonal transformations of the basis set and the Full Löwdin Approximation.

A comparison of various calculated molecular properties is given in Tables IV.12 and IV.13. These tables indicate how the molecular properties vary as the C – H internuclear separation is increased. A minimum in E is predicted somewhere between 1.80 and 2.0088a.u. for the IMA calculation whereas the FLA calculation predicts the minimum to be on the other side of the experimental value, i.e. between 2.0088 and 2.20a.u. but probably closer to the experimental value. The dipole moment again appears to vary almost linearly with increasing C – H distance but it can be seen that the μ_{HCN}'s from the FLA calculations are greater than the IMA values by about 0.7 Debye. The experimental value of μ_{HCN} is known accurately to be 3.00 Debye [5] and the FLA again shows itself to be superior to the IMA by predicting the dipole moment more accurately.

The variation of the total energy E with R_{CH} is shown in Figure IV.6 for each approximation. The IMA is the lower

Table IV.12.

Some Calculated Molecular Properties for HCN at Five Internuclear Distances of the CH Bond (Invariant Mulliken Approximation).

Calculation	1	2	3	4	5
R_{CH}	1.60	1.80	2.0087986	2.20	2.3848578
Electronic Energy E_{el}	-117.63410	-117.15814	-116.72594	-116.37789	-116.07773
Total Energy E	-92.86103	-92.89431	-92.89581	-92.87995	-92.85562
Kinetic Energy T	91.62212	91.54539	91.48752	91.45259	91.43267
Potential Energy V	-184.48315	-184.43970	-184.38333	-184.33254	-184.28829
-2T/V	0.99328	0.99269	0.99236	0.99226	0.99228
Dipole Moment μ_{HCN}	1.153	1.483	1.814	2.102	2.376

Table IV.13.

Some Calculated Molecular Properties for HCN at Five Internuclear Distances of the CH Bond (Full Löwdin Approximation).

Calculation	1	2	3	4	5
R_{CH}	1.60	1.80	2.0087986	2.20	2.3848578
Electronic Energy E_{el}	-117.47016	-116.99350	-116.57417	-111.23870	-115.95002
Total Energy E	-92.69709	-92.72967	-92.74404	-92.74076	-92.72791
Kinetic Energy T	92.17128	91.94941	91.83104	91.76050	91.71115
Potential Energy V	-184.86837	-184.67908	-184.57508	-184.50126	-184.43906
-2T/V	0.99716	0.99578	0.99505	0.99469	0.99449
Dipole Moment μ_{HCN}	1.651	2.097	2.486	2.803	3.090

FIGURE IV.6.

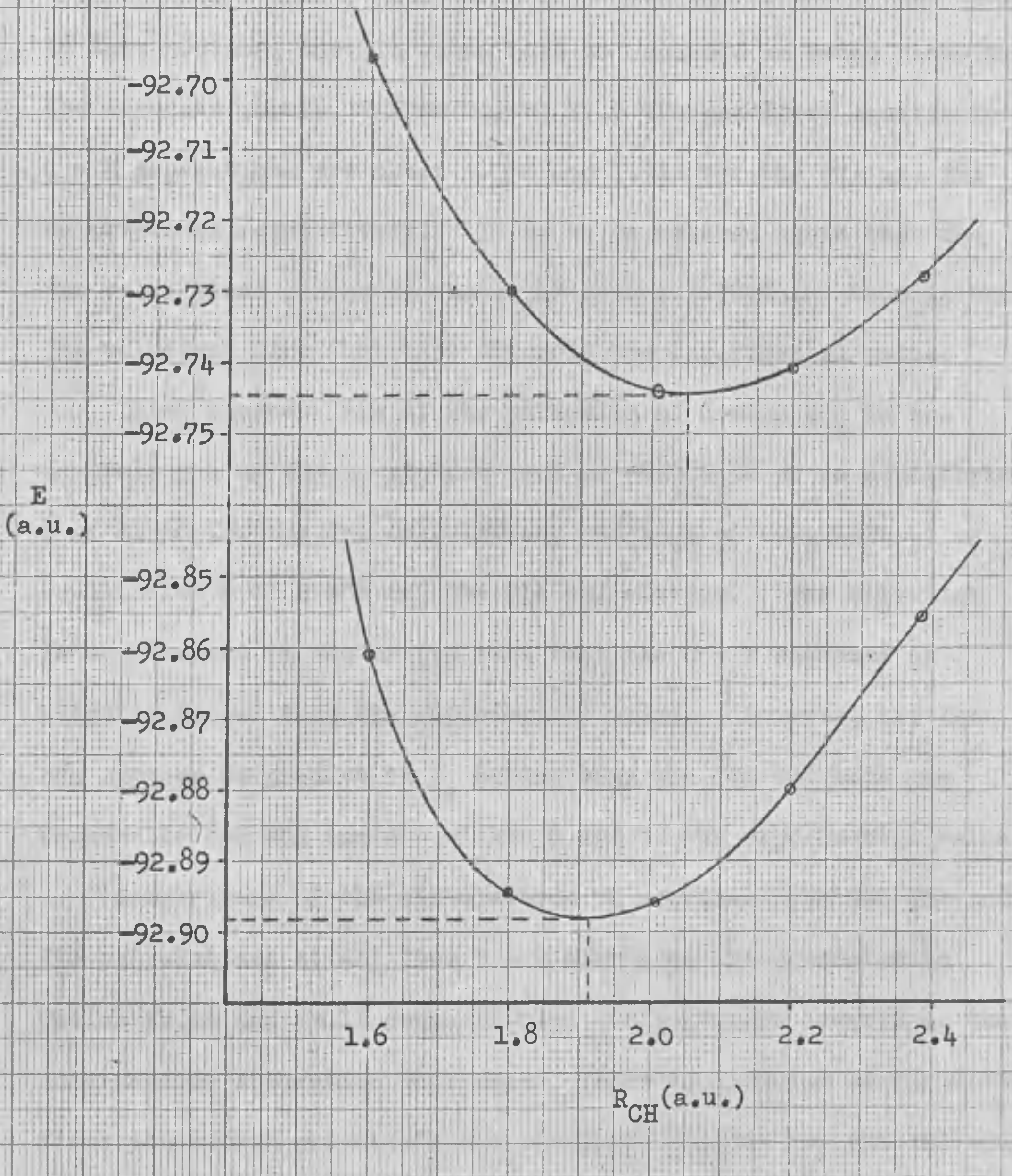

Diagram to show Variation of E with R_{CH} for HCN.

curve. As with the best atom calculations on HCN reported in 4.1. the FLA gives a higher E than the IMA and by the trends shown in that section, the FLA value must be regarded as being close to the accurate result. From figure IV.6 the predicted equilibrium C – H separations are about 2.050 and 1.912 for the FLA and IMA calculations respectively. It is to be noticed again that the FLA value seems closer to the experimental 2.0088a.u. than is the IMA value and also that they straddle the experimental value.

Least squares fits of the variation of E with R_{CH} to the parabola $y = ax^2+bx+c$, yielded an E of –92.89698 at an equilibrium R of 1.968 for the IMA calculation, and an E of –92.74494 at an equilibrium R of 2.086 for the FLA calculation. The situation is complicated in HCN by the fact that the C – N distance is slightly longer than the experimental value. However, the IMA now appears to predict an R_e better than the FLA but both are reasonable for HCN and are within 0.04Å of the experimental value.

Comparisons of the one-electron MO energies from the IMA and FLA calculations at all five C – H distances are presented in Tables IV.14 and IV.15 respectively. All ε's are lowered as the internuclear separation decreases. Both equilibrium configuration first ionisation potentials are similar; 15.43eV for the IMA and 15.67eV for the FLA. These overestimate the experimental value of 13.91eV but this is a common finding in MO calculations. The π bonding – antibonding gap remains almost constant as R_{CH} varies

Table IV. 14.

One Electron MO Energies for IMA Calculations on HCN.

Calculation	1	2	3	4	5
R_{CH}	1.60	1.80	2.0087986	2.20	2.3848578
1σ	-15.81053	-15.79630	-15.78308	-15.77236	-15.76287
2σ	-11.52874	-11.50955	-11.49689	-11.48888	-11.48278
3σ	-1.35979	- 1.33884	-1.32232	-1.31060	-1.30143
4σ	-0.97165	-0.92389	-0.87674	-0.83677	-0.80148
5σ	-0.66507	-0.65272	-0.64162	-0.63235	-0.62356
6σ	1.04366	0.98931	0.82670	0.65652	0.52007
7σ	1.50927	1.18176	1.05046	1.01527	0.99508
1π	-0.59036	-0.57778	-0.56724	-0.55927	-0.55262
2π	0.13835	0.14843	0.15798	0.16593	0.17307
G	-63.03300	-62.75372	-62.51026	-62.31900	-62.15472
$\sigma-\pi$ gap	0.07471	0.07494	0.07438	0.07308	0.07094
$\pi-\pi^A$ gap	0.72871	0.72621	0.72522	0.72520	0.72569
1st I.P.(eV)	16.06	15.72	15.43	15.22	15.04

Table IV. 15.

One Electron MO Energies for FLA Calculations on HCN.

Calculation	1	2	3	4	5
R_{CH}	1.60	1.80	2.0087986	2.20	2.3848578
1σ	-15.79850	-15.78753	-15.77383	-15.76223	-15.75222
2σ	-11.50611	-11.50224	-11.49190	-11.48370	-11.47679
3σ	-1.36887	-1.34285	-1.32598	-1.31482	-1.30616
4σ	-0.90379	-0.86402	-0.82330	-0.78819	-0.75740
5σ	-0.67619	-0.65512	-0.63919	-0.62620	-0.61424
6σ	0.36959	0.34804	0.28841	0.23021	0.17799
7σ	0.84738	0.91814	0.96532	0.98774	0.99795
1π	-0.60897	-0.59005	-0.57615	-0.56610	-0.55792
2π	0.14265	0.14597	0.15536	0.16434	0.17264
G	-62.94280	-62.66372	-62.41300	-62.21468	-62.04530
$\sigma-\pi$ gap	0.06722	0.06507	0.06304	0.06010	0.05632
$\pi-\pi^A$ gap	0.75162	0.73602	0.73151	0.73044	0.73056
1st I.P.(eV)	16.57	16.06	15.67	15.40	15.18

as might be expected since H has no π orbitals. Certainly it would seem that H has little penetration effect on the pi orbitals.

The results of a Mulliken population analysis on the IMA and FLA calculations are presented in Tables IV. 16 and IV. 17 respectively. From the gross atom charge densities of the IMA calculation it is seen that as R_{CH} increases, N loses σ electronic charge to C but gains more π charge to give a net gain in electronic charge at N. Meanwhile the gross atom charge density on H goes through a maximum roughly at the equilibrium R_{CH}. This maximum is also reflected in the CH bond population. It is interesting to see that although the π atom populations change markedly, the bond population remains constant at about 1.065. As R_{CH} increases electronic charge is lost from the NC bond and compensates for the decreasing antibonding NH population.

The gross atom charge densities of the FLA calculation show slightly different trends. The N charge density goes through a minimum at the equilibrium configuration but this time C loses slightly more charge overall, and also loses it from both σ and π contributions. H is markedly more positive at the innermost R_{CH} and gains more electronic charge as the C – H separation increases. But the most startling difference is that the π bond polarity is the reverse of the IMA calculation.

As far as the bond populations are concerned there is now no maximum in the CH bond population and the CH and NH bonds

Table IV.16.

Mulliken Population Analysis of IMA HCN Electron Density.

R_{CH}		Atom/Bond Populations.						Gross Atom Charge Densities.		
		N	C	H	NC	CH	NH	N	C	H
1.60	sigma	4.905	3.364	0.524	0.740	0.707	-0.240	5.155	4.088	0.758
	pi	1.304	1.636	0.000	1.060	0.000	0.000	1.834	2.166	0.000
	total	6.209	5.000	0.524	1.800	0.707	-0.240	6.989	6.254	0.758
1.80	sigma	4.891	3.388	0.470	0.653	0.775	-0.178	5.129	4.103	0.768
	pi	1.342	1.596	0.000	1.063	0.000	0.000	1.873	2.127	0.000
	total	6.233	4.984	0.470	1.716	0.775	-0.178	7.002	6.230	0.768
2.0088	sigma	4.884	3.427	0.443	0.586	0.795	-0.135	5.109	4.118	0.773
	pi	1.377	1.559	0.000	1.064	0.000	0.000	1.909	2.091	0.000
	total	6.261	4.986	0.443	1.650	0.795	-0.135	7.018	6.209	0.773
2.20	sigma	4.880	3.469	0.432	0.539	0.787	-0.107	5.097	4.132	0.772
	pi	1.406	1.529	0.000	1.065	0.000	0.000	1.938	2.062	0.000
	total	6.286	4.998	0.432	1.604	0.787	-0.107	7.035	6.194	0.772
2.3849	sigma	4.879	3.510	0.428	0.506	0.765	-0.087	5.088	4.145	0.767
	pi	1.430	1.505	0.000	1.065	0.000	0.000	1.963	2.037	0.000
	total	6.309	5.015	0.428	1.571	0.765	-0.087	7.051	6.183	0.767

Table IV.17.

Mulliken Population Analysis of FLA HCN Electron Density.

R_{CH}		Atom/Bond Populations.						Gross Atom Charge Densities.		
		N	C	H	NC	CH	NH	N	C	H
1.60	sigma	5.005	4.000	0.621	0.775	−0.128	−0.273	5.256	4.324	0.420
	pi	1.506	1.429	0.000	1.065	0.000	0.000	2.039	1.961	0.000
	total	6.511	5.429	0.621	1.840	−0.128	−0.273	7.295	6.285	0.420
1.80	sigma	4.983	3.721	0.408	0.605	0.442	−0.158	5.206	4.244	0.550
	pi	1.514	1.421	0.000	1.065	0.000	0.000	2.046	1.954	0.000
	total	6.496	5.142	0.408	1.670	0.442	−0.158	7.252	6.198	0.550
2.0088	sigma	4.961	3.662	0.356	0.527	0.600	−0.106	5.172	4.226	0.602
	pi	1.537	1.398	0.000	1.065	0.000	0.000	2.070	1.930	0.000
	total	6.498	5.060	0.356	1.592	0.600	−0.106	7.242	6.156	0.602
2.20	sigma	4.947	3.655	0.342	0.490	0.646	−0.080	5.152	4.222	0.625
	pi	1.558	1.378	0.000	1.064	0.000	0.000	2.090	1.910	0.000
	total	6.505	5.033	0.342	1.554	0.646	−0.080	7.242	6.133	0.625
2.3849	sigma	4.937	3.663	0.340	0.468	0.654	−0.062	5.140	4.224	0.636
	pi	1.574	1.363	0.000	1.063	0.000	0.000	2.105	1.895	0.000
	total	6.511	5.026	0.340	1.531	0.654	−0.062	7.245	6.119	0.636

progressively gain electronic charge at the expense of the NC bond. The negative CH bond population at the innermost R_{CH} is probably a reflection on the unrealistic nature of this internuclear separation. Another interesting point is that the bond population is again constant despite marked changes in atom populations and again has the value 1.065. An apparent anomaly in both calculations is that the H atom population decreases for increasing R_{CH} despite an increasing gross atom density.

A comparison of the effective atomic charges as evaluated by the Mulliken, Löwdin, Doggett I and Doggett II population analyses is presented in Tables IV. 18 and IV. 19 for the IMA and FLA calculations, respectively. The unsatisfactory nature of the concept of effective charges is apparent from these tables as nearly every possible combination of trends in the movement of electronic charge is apparent. There are, however, a few interesting points which appear to yield consistent conclusions. Whichever population analysis is used it is generally true that the IMA calculation leads to a more equable distribution of charge than does the FLA calculation. This is particularly well shown in the Doggett I population analysis where all atoms are close to neutrality in the IMA calculation. In contrast to the case of CN^-, the Mulliken and Löwdin methods appear to overestimate the charge separation between the NC and H molecular fragments, compared with the Doggett I and Doggett II methods. This phenomenon can again

Table IV.18.

Effective Atomic Charges for IMA HCN Calculations.

R_{CH}		Mulliken.	Löwdin.	Doggett I.	Doggett II.
	N	+0.011	+0.108	+0.003	+0.055
1.60	C	−0.254	−0.212	+0.071	+0.445
	H	+0.243	+0.104	−0.074	−0.500
	N	−0.002	+0.082	+0.005	+0.032
1.80	C	−0.230	−0.204	+0.026	+0.020
	H	+0.232	+0.122	−0.031	−0.052
	N	−0.018	+0.054	+0.002	+0.014
2.0088	C	−0.209	−0.194	−0.014	−0.115
	H	+0.227	+0.140	+0.012	+0.101
	N	−0.034	+0.032	−0.003	0.000
2.20	C	−0.194	−0.190	−0.045	−0.170
	H	+0.228	+0.158	+0.048	+0.170
	N	−0.051	+0.016	−0.010	−0.014
2.385	C	−0.182	−0.190	−0.070	−0.198
	H	+0.233	+0.174	+0.080	+0.212

Table IV.19.

Effective Atomic Charges for FLA HCN Calculations.

R_{CH}		Mulliken	Löwdin	Doggett I	Doggett II.
	N	−0.295	−0.080	−0.166	+0.024
1.60	C	−0.285	−0.136	−0.205	+0.191
	H	+0.580	+0.216	+0.371	−0.215
	N	−0.252	−0.086	−0.139	−0.039
1.80	C	−0.198	−0.128	−0.052	−0.010
	H	+0.450	+0.214	+0.191	+0.049
	N	−0.242	−0.100	−0.133	−0.070
2.0088	C	−0.156	−0.126	−0.039	−0.120
	H	+0.398	+0.226	+0.172	+0.190
	N	−0.242	−0.110	−0.134	−0.089
2.20	C	−0.133	−0.128	−0.048	−0.167
	H	+0.375	+0.238	+0.182	+0.256
	N	−0.245	−0.124	−0.138	−0.103
2.385	C	−0.119	−0.128	−0.062	−0.191
	H	+0.364	+0.252	+0.200	+0.294

be attributed to the poorer partitioning of the overlap population in the Mulliken method. A direct result of this is that the Mulliken method never admits the somewhat surprising negative hydrogen atom density exhibited by the asymmetric partitioning methods for both the IMA and FLA calculations. Chemically it would be surprising if H was not positively charged at the HCN equilibrium configuration but there is nothing to say what its polarity should be when it is closer to the C atom. Indeed, because of the more realistic partitioning of the overlap population, the Doggett I and Doggett II results should be more satisfactory.

Generally as R_{CH} increases N gains electrons but the Doggett I method for both calculations and the Mulliken for the FLA calculation have the N effective charge passing through a minimum. There is a sharp division in the trends shown for C by the asymmetric partitioning methods and the Mulliken and Löwdin analyses. The latter two methods generally predict that C loses electronic charge as R_{CH} increases while the Doggett I and Doggett II methods predict a gain or, in one case, a minimum value for the electronic charge associated with the C atom. There is no general trend obvious with respect to the gross atom charges on H. For the IMA calculation the Mulliken population analysis predicts that H just goes through a maximum of electronic charge while the other three predict that it loses electronic charge as the CH distance increases.

The same trend is shown by the Doggett II and the Löwdin analyses for the FLA calculation. The Mulliken analysis gives exactly the opposite trend; namely, that H gains electronic charge as the CH distance increases, while the Doggett I method predicts that the charge on H goes through a maximum.

Contour diagrams 11 to 15 give a pictorial representation of how the electron density distribution changes as the CH internuclear distance increases. The charge distribution is quite stable and only two trends can be discerned. Electronic charge is being displaced from the vicinity of H as the C - H internuclear separation increases, and this charge appears to be moving in to the region of the CN bond. Only the Doggett II method really agrees with this conclusion. However, from Tables IV. 16 and IV. 17 it is seen that the CN bond population decreases as C - H increases.

Contour diagram 16 gives a pictorial representation of the charge distribution for the experimental R_{CH} distance using the IMA and is to be compared with the corresponding FLA diagram, 13. The distributions are similar, but the IMA yields more charge on H and in the CN bond but less on N. These trends corroborate those shown in the atom and bond populations. The polarity of the CN π atom populations, i.e. $C^{\delta +} N^{\delta -}$, predicted in the FLA calculation, is also shown to be substantiated by contour diagram 17.

Contour diagrams 18 and 19 give, for the FLA and IMA

CONTOUR DIAGRAM 11.

P_{HCN}

R(NC) = 2.1902141a.u.

R(CH) = 1.60a.u.

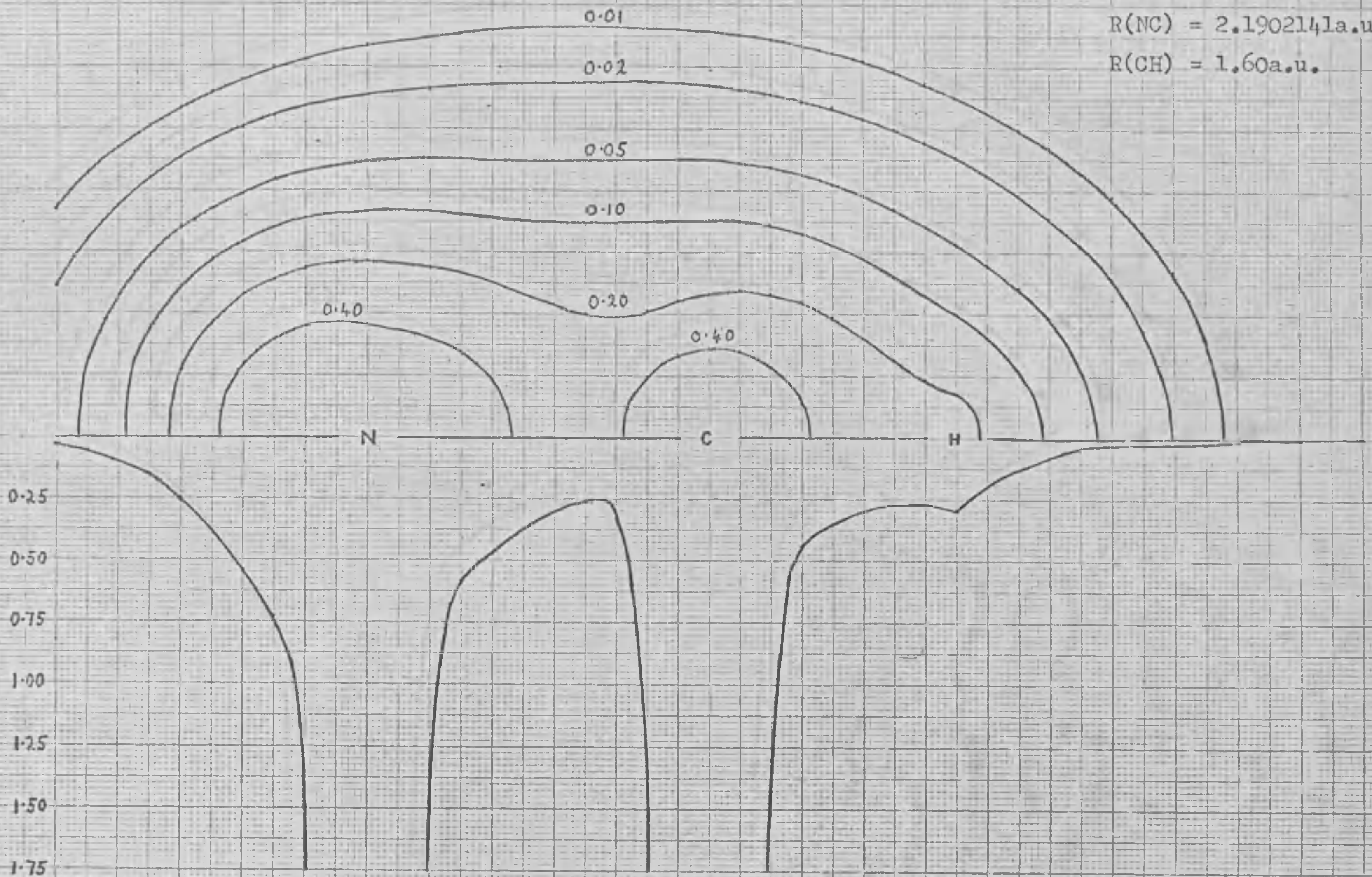

CONTOUR DIAGRAM 12.

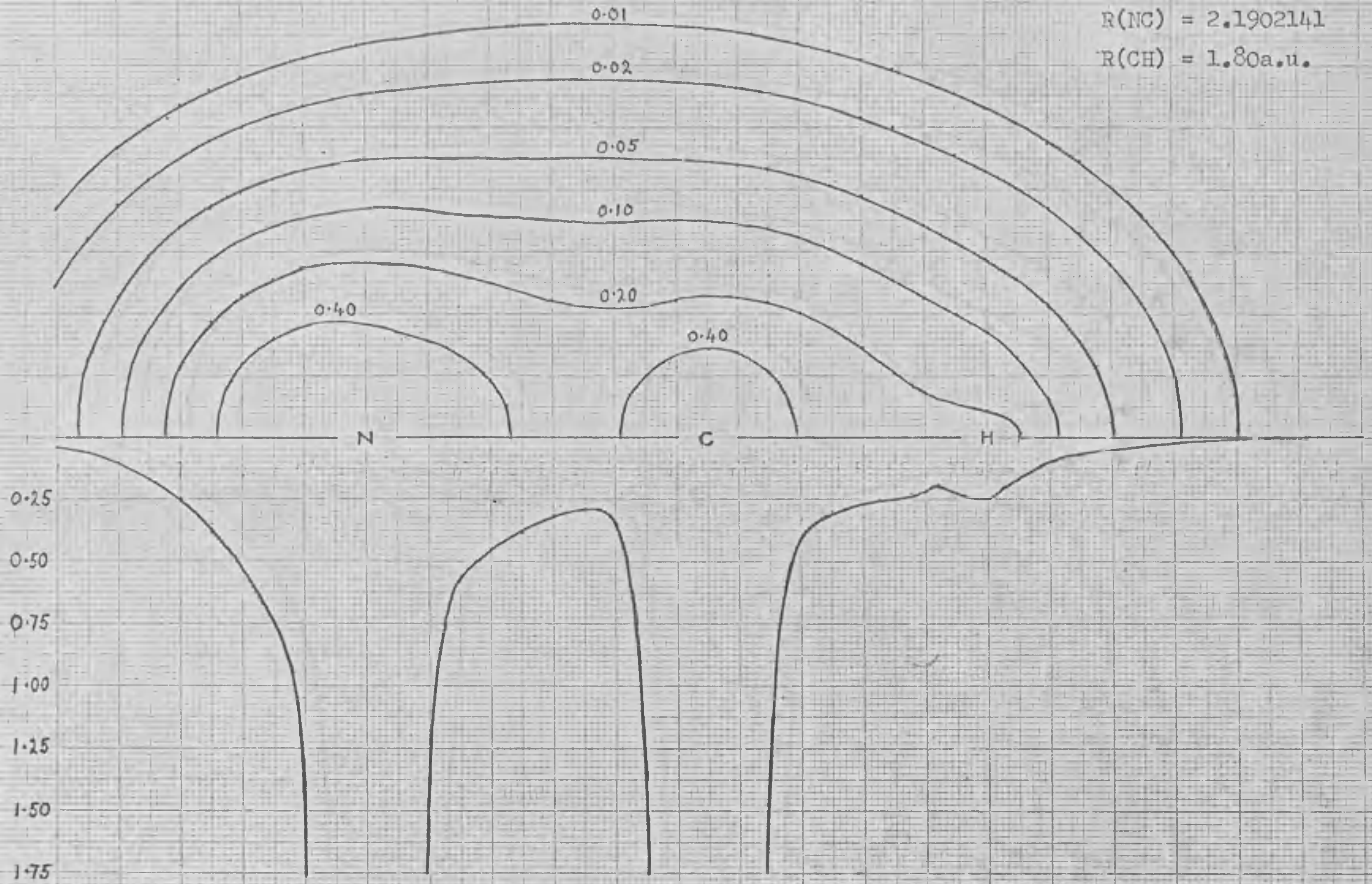

P_{HCN}

R(NC) = 2.1902141

R(CH) = 1.80a.u.

CONTOUR DIAGRAM 13.

P_{HCN}

R(NC) = 2.1902141a.u.

R(CH) = 2.0087986a.u.

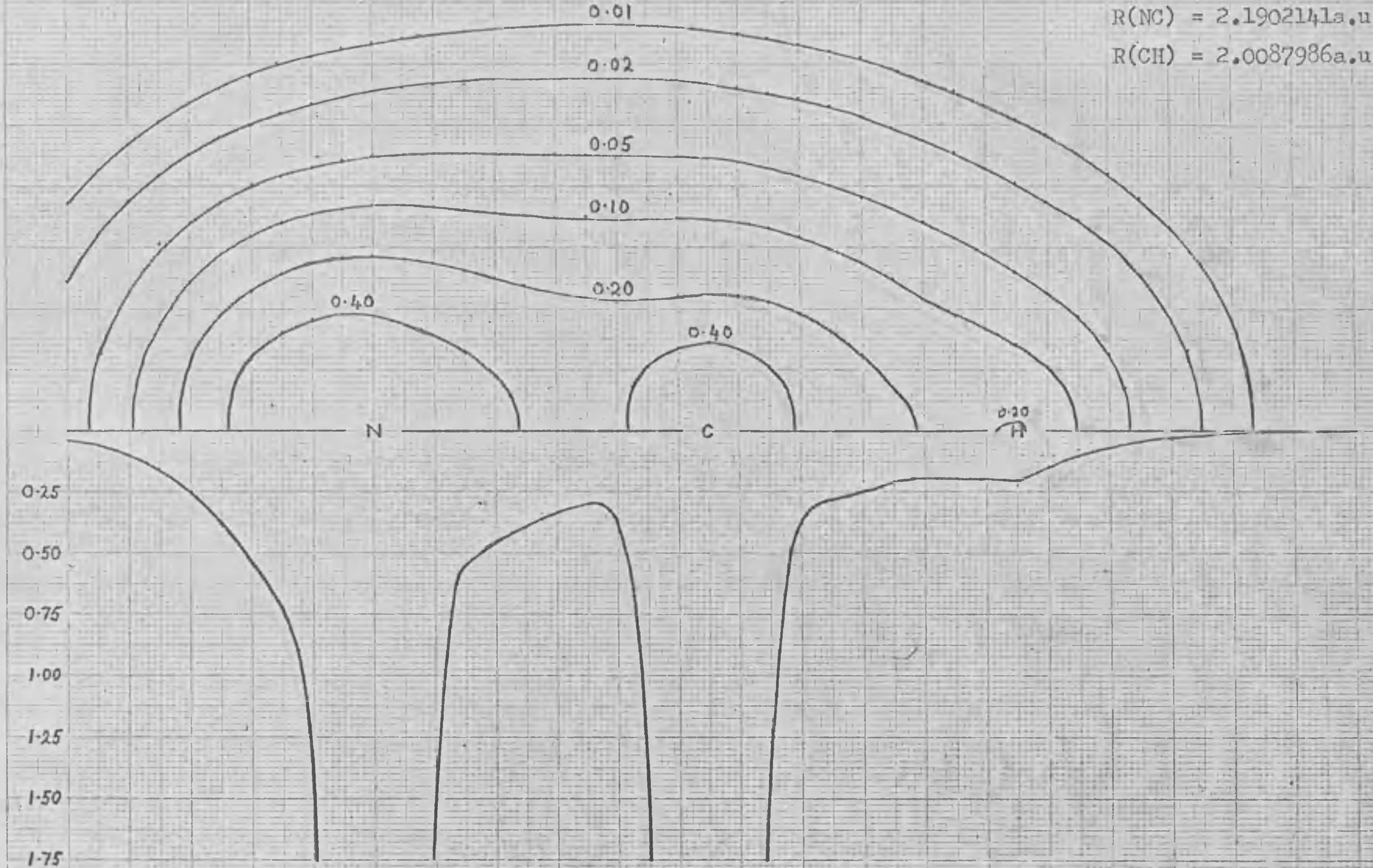

CONTOUR DIAGRAM 14.

P_{HCN}

R(NC) = 2.1902141a.u.

R(CH) = 2.20a.u.

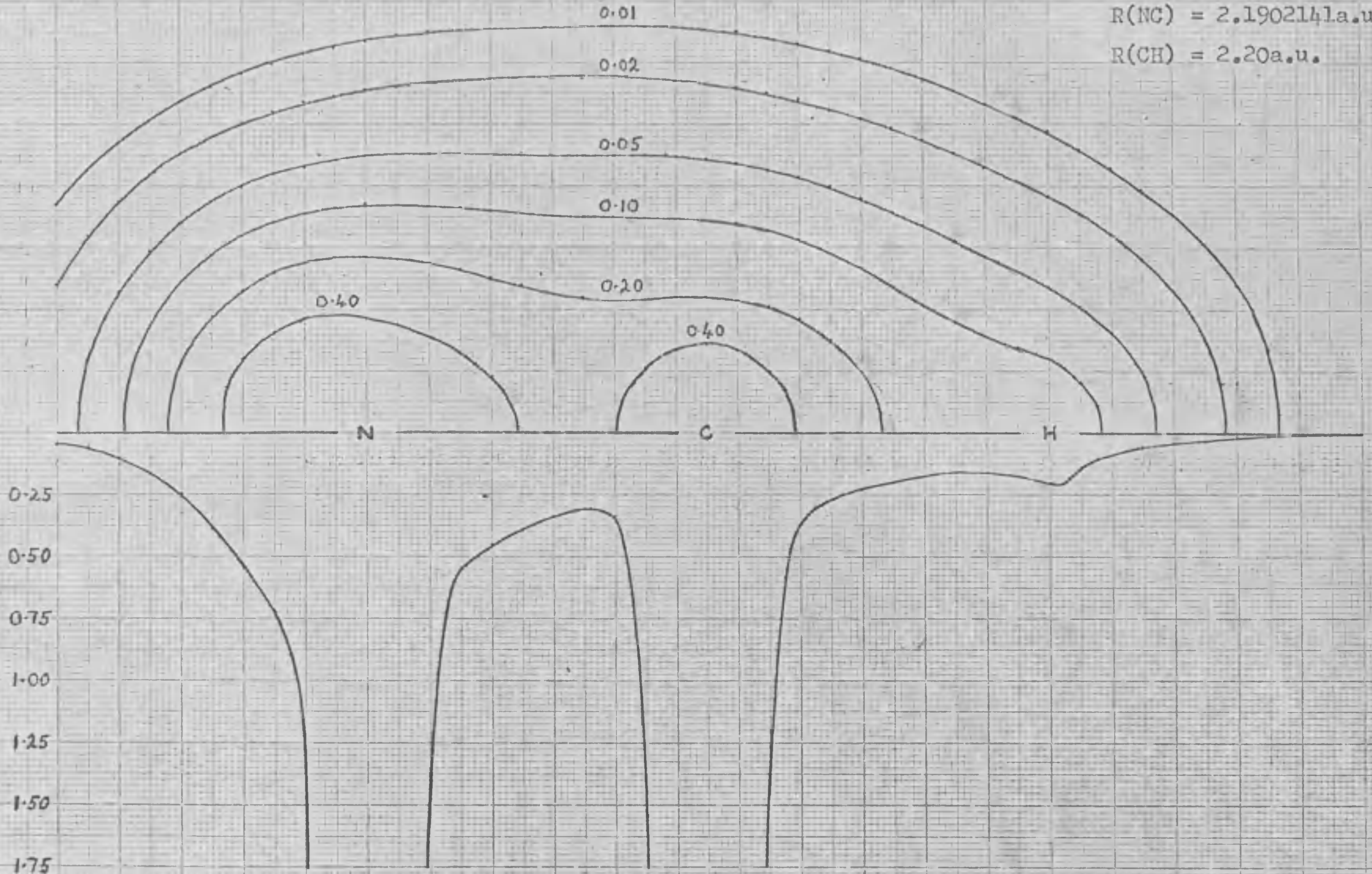

CONTOUR DIAGRAM 15.

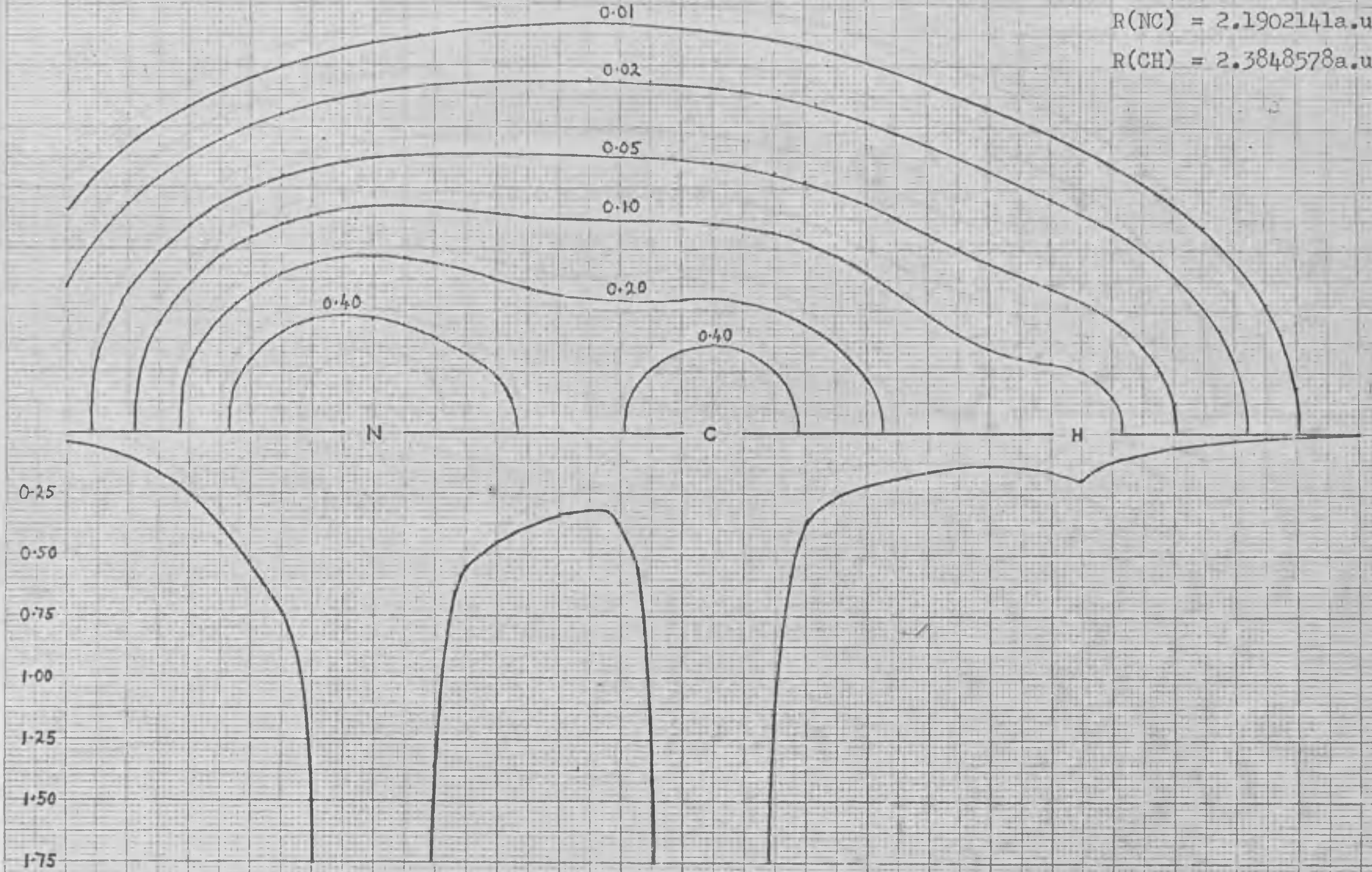

P_{HCN}

R(NC) = 2.1902141a.u.

R(CH) = 2.3848578a.u.

CONTOUR DIAGRAM 16.

P_{HCN}

R(NC) = 2.1902141a.u.

R(CH) = 2.0087986a.u.

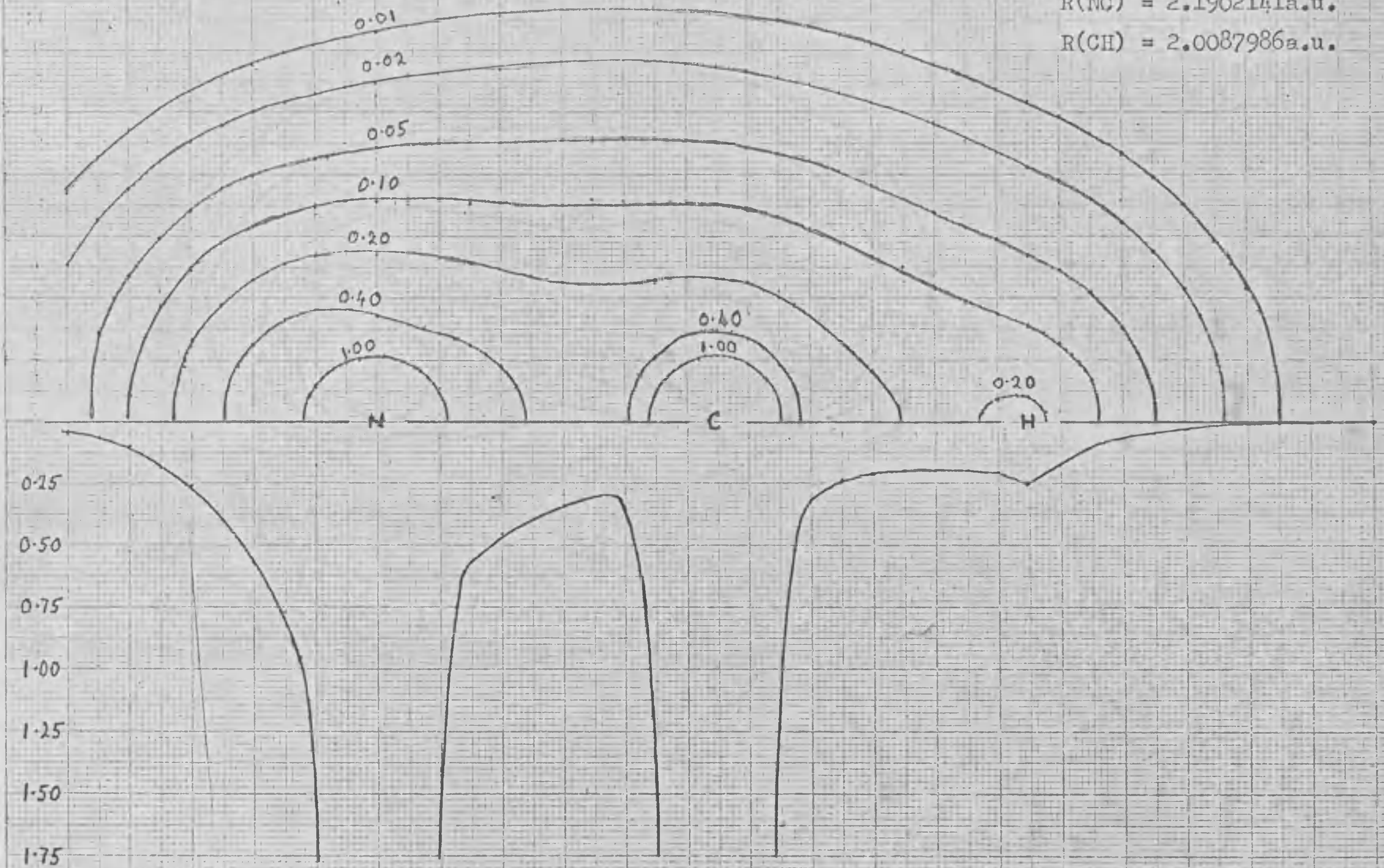

CONTOUR DIAGRAM 17.

P_{HCN}

R(NC) = 2.1902141a.u.

R(CH) = 2.0087986a.u.

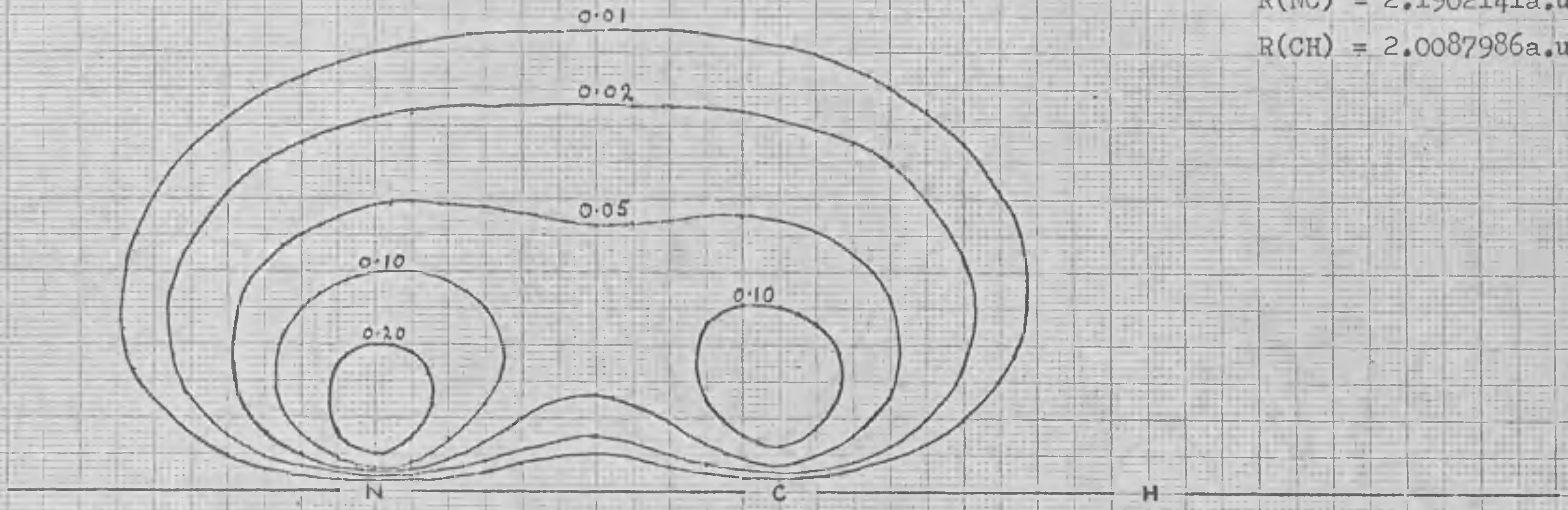

CONTOUR DIAGRAM 18.

$P_{HCN} - P_{atoms}$

R(NC) = 2.1902141a.u.

R(CH) = 2.0087986a.u.

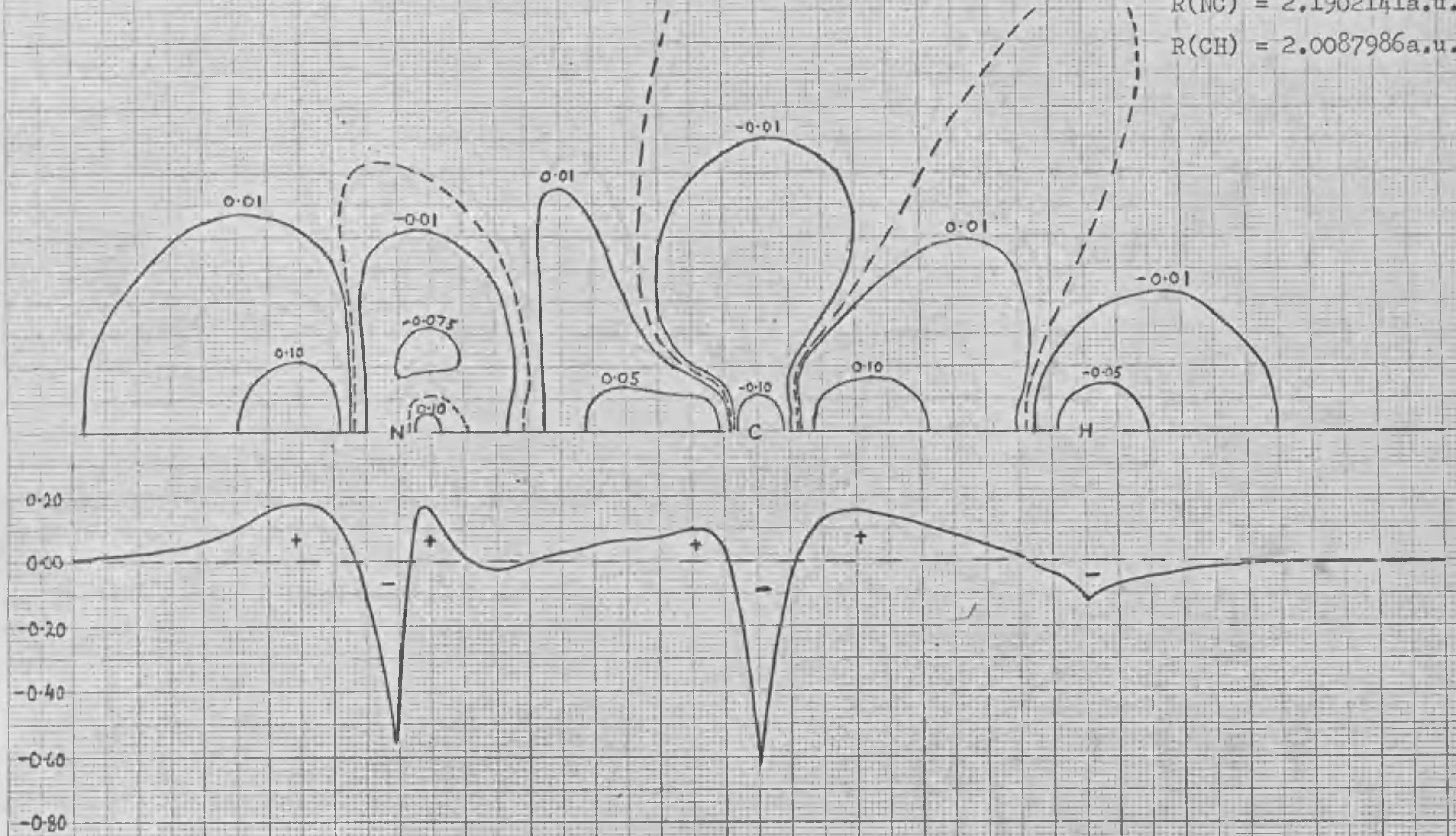

CONTOUR DIAGRAM 19.

$P_{HCN} - P_{atoms}$

R(NC) = 2.1902141a.u.

R(CH) = 2.0087986a.u.

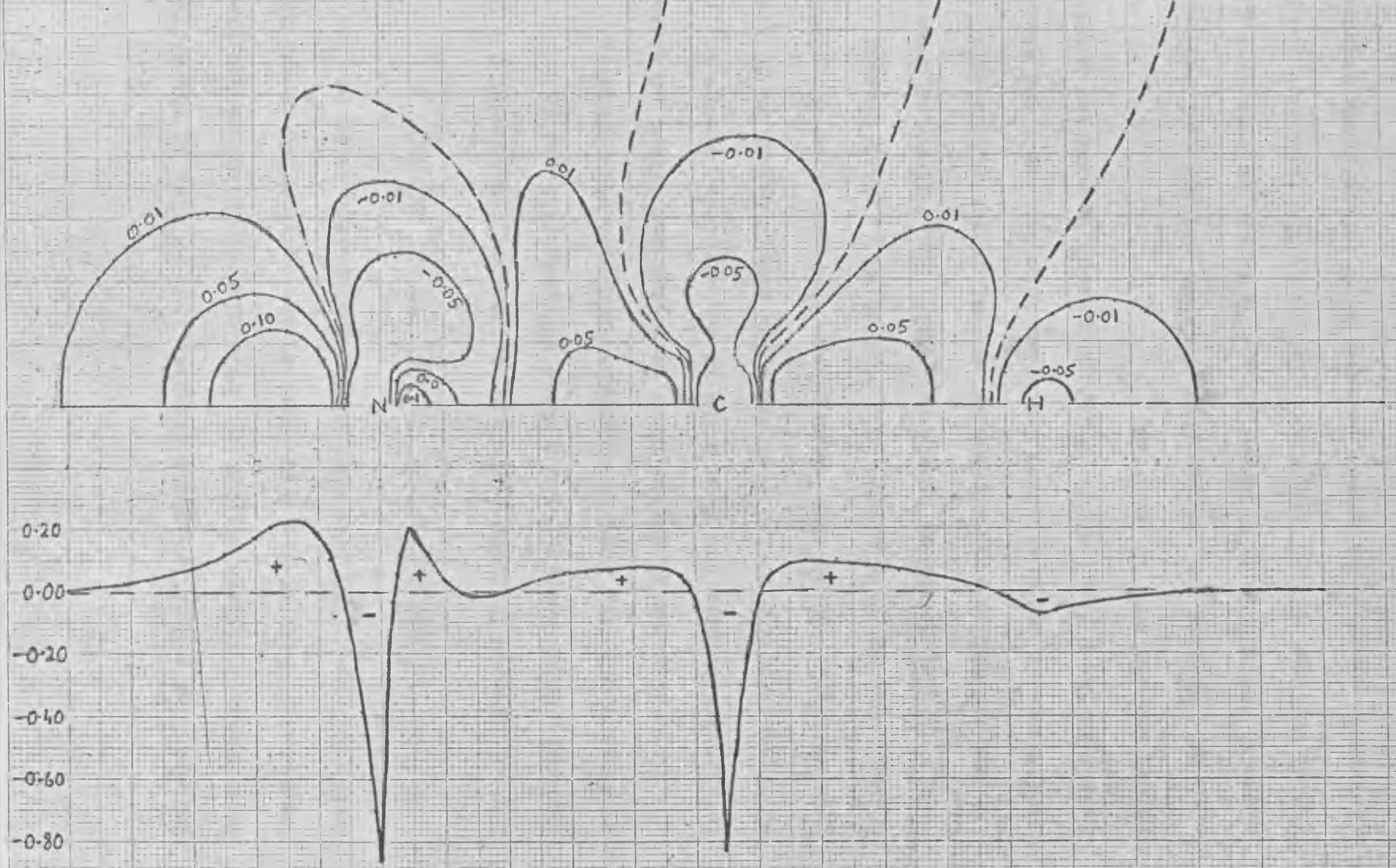

calculations respectively, ΔP diagrams and profiles of the difference charge densities between the molecular distribution and the theoretical state of the free atoms at the equilibrium ground state configuration. The free atom configurations are taken as

$$1s_H^1\ 1s_C^2\ 2s_C^2\ 2z_C^0\ 2x_C^1\ 2y_C^1\ 1s_N^2\ 2s_N^2\ 2z_N^1\ 2x_N^1\ 2y_N^1$$

Contour diagram 20 gives a similar picture for the closest C - H distance, using the IMA method where the Doggett I and II population analyses predict a negative hydrogen atom density.

From diagrams 18 and 19 it is seen that the effect of allowing interaction between the free atoms is as expected: charge is displaced from the vicinity of the atoms and is deposited in the bond regions. It is also clearly seen that charge is deposited in what appears to be a lone pair orbital on N, which closely resembles a classical sp hybrid orbital. The difference between the FLA and IMA methods appears to be that in the FLA calculation more charge is displaced from the atoms into the bonds and slightly less into the N lone pair. This again seems to show the Mulliken population analysis to be wrong.

By comparing the positions of the node and the 0.01 contour close to the H atom in diagrams 19 and 20 it can be seen that H indeed has more charge associated with it at the innermost C - H distance. However it cannot be said quantitatively how negative H actually is. It seems unlikely that it is as much as the -0.5

CONTOUR DIAGRAM 20.

$P_{HCN} - P_{atoms}$

R(NC) = 2.1902141a.u.

R(CH) = 1.60a.u.

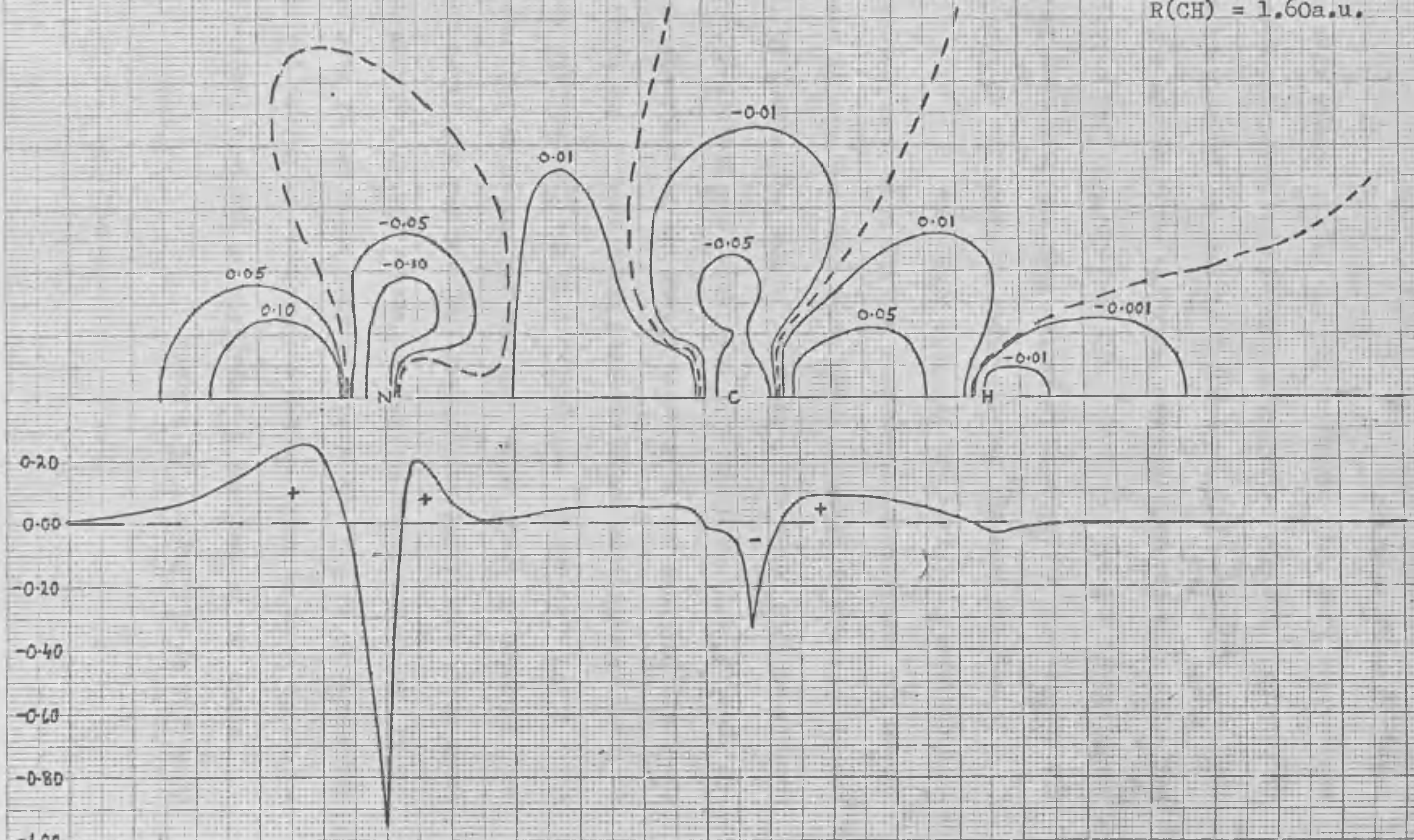

predicted by the Doggett II method.

Table IV. 20 contains a comparison of the main results of this work with those of other recent calculations by McLean [4] and Bonaccorsi et al [61] who used a minimal basis set of best atom STO's; Palke and Lipscomb [62] who used a Slater exponent minimal basis set; and Moffat and Collens [34] and Pan and Allen [33] who used Gaussian AO basis sets. McLean and Yoshimine [63] use $R_{CN} = 2.1791$a.u. and $R_{CH} = 2.0143$a.u. as the internuclear separations in their calculations using extended basis sets. The total energies for their DZ, DZ+P and BA+P calculations are respectively -92.8369a.u. -92.9089a.u. and -92.9147a.u. The latter two yielded dipole moments of 3.20 Debye and 3.29 Debye. The improvement in total energy obtained by using extended basis sets can thus be seen from McLean and Yoshimine's double-zeta and big atom calculations both with optimised polarisation orbitals added in.

It appears from the results shown in table IV. 20 that the FLA double-zeta calculation is better than the best atom STO calculations and the two poorer STO [62] and GTF [34] calculations, but worse than the STO extended basis set calculations and the molecular optimised GTF calculation of Pan and Allen (last column of table). The FLA calculation and Pan and Allen's simpler calculation have much in common but the dipole moment from the GTF calculation is superior.

Table

Comparison of Results of Recent

	This Work (FLA)	McLean [4]	Bonaccorsi [61]
R_{CN}	2.1902141	2.187	2.187
R_{CH}	2.0087986	2.000	2.000
E_{el}	-116.57417	-116.4236	-116.4234
E	-92.74404	-92.5474	-92.5471
T	91.83104	-	91.3268
$-2T/V$	0.99505	-	0.9934
$\epsilon(1\sigma)$	-15.77383	-15.7402	-15.7363
$\epsilon(2\sigma)$	-11.49190	-11.4277	-11.4303
$\epsilon(3\sigma)$	-1.32598	-1.2522	-1.2515
$\epsilon(4\sigma)$	-0.82330	-0.7965	-0.7975
$\epsilon(5\sigma)$	-0.63919	-0.5582	-0.5566
$\epsilon(6\sigma)$	0.28841	0.3648	-
$\epsilon(7\sigma)$	0.96532	1.0860	-
$\epsilon(1\pi)$	-0.57615	-0.5074	-0.5071
$\epsilon(2\pi)$	0.15536	0.2516	-
1st I.P.(eV)	15.67	13.81	13.81
μ_{calc}(Debye)	2.486	2.100	2.07
q_N	7.242	7.082	7.082
q_C	6.156	6.156	6.156
q_H	0.602	0.761	0.761

IV. 20.

Calculations on the Ground State of HCN.

Palke and Lipscomb [62]	Moffat and Collens [34]	Pan and Allen [33]	
2.187	2.187	2.1775	2.1775
2.000	2.000	2.000	2.000
-116.4665	-116.5676	-116.63513	-116.79248
-92.5903	-92.6914	-92.67131	-92.82866
92.6803	-	-	-
-	-	-	-
-15.6471	-15.6182	-15.7830	-15.6265
-11.3353	-11.3464	-11.5266	-11.3100
-1.2181	-1.2773	-1.3355	-1.2699
-0.7770	-0.8089	-0.8544	-0.8130
-0.5287	-0.5583	-0.6319	-0.5758
0.4882	0.2169	0.3295	0.2491
1.2173	-	-	-
-0.4764	-0.4794	-0.5811	-0.5032
0.2949	0.2009	0.1543	0.1656
12.95	13.05	15.81	13.69
2.11	-	2.712	3.366
7.075	-	-	-
6.141	-	-	-
0.784	-	-	-

The $\underset{\sim}{R}$ matrix for the FLA calculation on HCN at the experimental internuclear separations is presented in Table IV. 21.

Table IV. 21.

R Matrix for HCN FLA Calculation 3: R(CH) = 2.0087986a.u.

$\underset{\sim}{R}_{\sigma}$	1.0034	0.0027	−0.0349	0.0020	−0.0191	0.0200	0.0171
		0.9197	−0.2933	−0.0295	−0.0876	−0.0381	0.0602
			0.5576	−0.0255	0.2770	−0.2074	−0.2244
				1.0040	−0.0322	0.0072	0.0077
					0.5410	0.1542	0.0663
						0.2861	0.2171
							0.1778
$\underset{\sim}{R}_{\pi}$	0.3844	0.3665					
		0.3495					

4.4. Molecular Electronic Structure Calculations on FCN.

In this section, results are presented for molecular electronic structure calculations performed at the five internuclear distances of the C – F bond given in 3.2. A minimal basis set of double-zeta AO's is again used and all two-centre integrals are evaluated accurately. As in 4.3, two sets of calculations are performed in which the three-centre integrals are evaluated either by the invariant Mulliken approximation or by the full Löwdin approximation. In addition, one calculation was performed on FCN at its experimental configuration using the partial Löwdin approximation to the three-centre integrals.

A comparison of various calculated molecular properties is presented in Tables IV. 22 and IV. 23. Calculation 6 of Table IV. 23 contains the results of the PLA calculation. Tables IV. 22 and IV. 23 indicate how the molecular properties vary as the C – F separation is increased. A minimum in E is predicted close to 2.20a.u. for the IMA calculation and between 2.40 and 2.60a.u. for the FLA calculation. Figure IV. 7 shows the variation of E with R_{CF} more clearly. It is immediately obvious that the FLA calculation at the FCN experimental internuclear separations is out of step with the others. This fact can also be seen in Table IV. 23 from the value of μ; a value of about 1.55 Debye would have been expected not 1.32 Debye. A comparison of the total energies of calculations 3 and 6 shows that the FLA value is lower than the

Table IV.22.

Some Calculated Molecular Properties for FCN at Five Internuclear Distances of the CF Bond (Invariant Mulliken Approximation).

Calculation	1	2	3	4	5
R_{CF}	2.00	2.20	2.3848578	2.60	2.80
Electronic Energy E_{el}	-253.44387	-250.34058	-247.84498	-245.30843	-243.24301
Total Energy E	-192.23263	-192.26882	-192.25564	-192.21118	-192.15638
Kinetic Energy T	191.14301	190.71859	190.46405	190.26275	190.11101
Potential Energy V	-383.37564	-382.98741	-382.71969	-382.47393	-382.26708
-2T/V	0.99716	0.99595	0.99532	0.99491	0.99465
Dipole Moment μ_{HCN}	2.122	1.747	1.506	1.336	1.133

Table IV.23.

Some Calculated Molecular Properties for FCN at Five Internuclear Distances of the CF Bond (Full Löwdin Approximation)*.

Calculation	1	2	3	4	5	6*
R_{CF}	2.00	2.20	2.3848578	2.60	2.80	2.3848578
Electronic Energy E_{el}	-252.63941	-249.57648	-247.26464	-244.66105	-242.62658	-247.25501
Total Energy E	-191.42817	-191.50472	-191.67530	-191.56380	-191.53995	-191.66567
Kinetic Energy T	191.50504	191.00430	190.90212	190.48131	190.30397	190.35313
Potential Energy V	-382.93321	-382.50902	-382.57742	-382.04511	-381.84392	-382.01880
-2T/V	1.00020	0.99869	0.99798	0.99717	0.99676	0.99656
Dipole Moment μ_{FCN}	2.191	1.856	1.318	1.408	1.316	1.679

*Column 6 contains the results of the PLA Calculation at the same R_{CF} as calculation 3.

FIGURE IV.7.

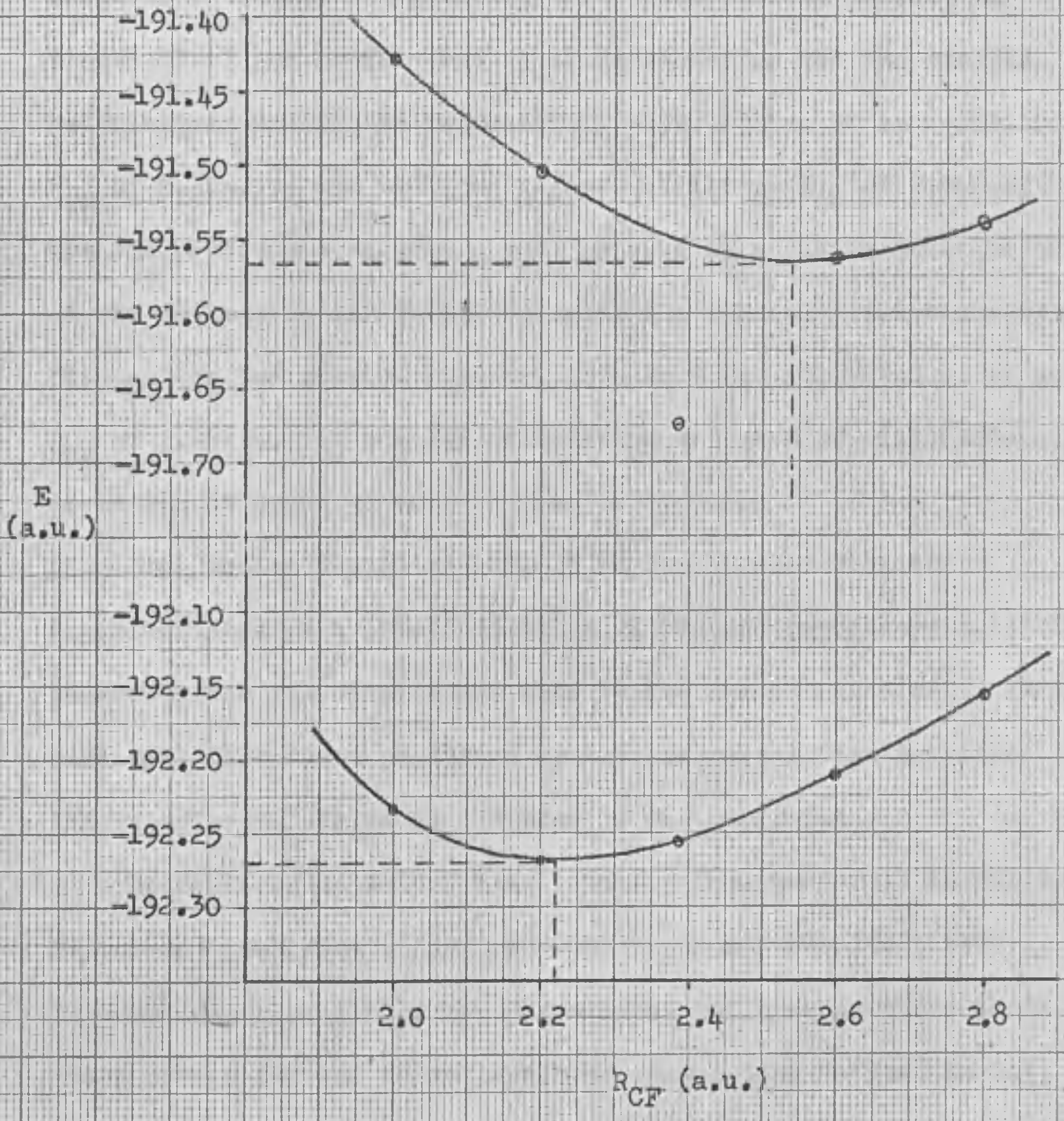

Diagram to show Variation of E with R_{CF} for FCN.

PLA, which is a complete reversal of the trends noted in the previous sections. Neglecting this point for the moment, in figure IV. 7 the minimum energy predictions for the IMA and FLA calculations on FCN are respectively -192.270a.u. at an equilibrium R_{CF} of 2.22a.u., and -191.566 at an equilibrium R_{CF} of 2.54a.u. The FLA prediction, however, must be open to a little doubt because of the estimation involved in drawing the figure. Least squares fits on the two sets of results yield an E of -192.2624a.u. at an R_{CF} of 2.26a.u. for the IMA calculation and an E of -191.6180a.u. at an R_{CF} of 2.48a.u. for the FLA calculation.

From Tables IV. 22 and IV. 23 it can be seen that the experimental dipole moment of 2.17a.u. [5], is reproduced a little better by the FLA calculation than by the IMA calculation. It is also seen that the μ predicted by the PLA calculation is closer to the experimental value than either of the other two.

Accurate calculations have recently been performed on FCN by McLean and Yoshimine [63]. As with their HCN results little information is available for comparison, but they do quote their total energy for the three levels of calculation defined in 4.3; i.e. the DZ, DZ+P and BA+P. The values are respectively -191.6275a.u., -191.7668a.u. and -191.7798a.u. The dipole moments are quoted for the last two levels and are 2.24 and 2.28 Debye's. Unfortunately as with HCN they do not quote their double-zeta value. It is possible that it is close to the PLA or FLA derived values because McLean and Yoshimine's value for their BA calculation is 1.67 Debye. It seems likely, then, that the inclusion of polarisation orbitals is necessary to improve the calculated dipole moment of FCN.

The question must now be answered as to why the FLA calculation broke down as shown by the results of calculation 3. The clue was obtained by examination of the elements of the bond asymmetry matrix, $\underset{\sim}{\lambda}$, where a value of -4.97 occurred for the $\lambda_{2z_C 2z_F}$ element.

It can be seen from (II. 62) that the calculation of λ is open to the possibility of a singularity since it is theoretically possible for the denomimator to be zero. It is conceivable, therefore, that for certain choices of basis set and internuclear separations the method may be close to breakdown. That this is much more the exception rather than the rule was confirmed to some degree by examining the λ elements for the other four C – F internuclear separations and finding them to be quite stable. So far, it has been impossible to find any rules to predict when a singularity will occur. The best method of avoiding it seems to be to carry out a search of the $\underset{\sim}{\lambda}$ matrices at various internuclear separations, before performing the SCF calculations, and avoiding any separations which could lead to a breakdown.

The one-electron MO energies from the IMA calculation are shown in Table IV. 24 and those from the FLA and PLA calculations are presented in Table IV. 25. It can again be seen that the FLA

Table IV. 24.

One Electron MO Energies for IMA Calculations on FCN.

Calculation	1	2	3	4	5
R_{CF}	2.00	2.20	2.3848578	2.60	2.80
1σ	-26.46549	-26.43017	-26.41308	-26.40636	-26.39911
2σ	-15.75407	-15.77884	-15.79504	-15.80691	-15.81648
3σ	-11.73295	-11.69703	-11.67226	-11.65007	-11.64166
4σ	-1.96377	-1.85125	-1.77209	-1.70673	-1.66270
5σ	-1.44145	-1.42417	-1.41123	-1.39813	-1.38912
6σ	-0.99181	-0.95297	-0.91924	-0.88171	-0.84861
7σ	-0.63831	-0.65269	-0.66097	-0.66516	-0.66703
8σ	0.94921	0.72276	0.54728	0.38352	0.26300
9σ	1.81718	1.58297	1.41266	1.26122	1.14367
1π	-1.09658	-1.02294	-0.97156	-0.92774	-0.89512
2π	-0.70712	-0.71709	-0.72310	-0.72677	-0.72763
3π	0.62558	0.55502	0.50892	0.47040	0.43896
G	-125.19050	-124.53436	-124.06646	-123.64818	-123.34042
$\pi-\pi^A$ gap	1.33270	1.27211	1.23202	1.19717	1.16659
1st I.P.(eV)	17.36	17.76	17.98	18.10	18.15

Table IV. 25.

One Electron MO Energies for FLA and PLA* Calculations on FCN.

Calculation	1	2	3	4	5	6*
R_{CF}	2.00	2.20	2.3848578	2.60	2.80	2.3848578
1σ	-26.52569	-26.47794	-26.45249	-26.43497	-26.42642	-26.45927
2σ	-15.76382	-15.76382	-15.75893	-15.79583	-15.80616	-15.77489
3σ	-11.67113	-11.65235	-11.58786	-11.61553	-11.61315	-11.62303
4σ	-1.94826	-1.84177	-1.75851	-1.70328	-1.66435	-1.76795
5σ	-1.32999	-1.33994	-1.32549	-1.34719	-1.35208	-1.36525
6σ	-1.02355	-0.96547	-0.96500	-0.87791	-0.83532	-0.93911
7σ	-0.65056	-0.65634	-0.68545	-0.66622	-0.66383	-0.65812
8σ	0.41334	0.31703	0.29946	0.16838	0.09455	0.47309
9σ	1.15944	1.04154	1.23034	0.98788	0.95003	1.31903
1π	-0.92507	-0.86429	-0.81192	-0.78519	-0.76294	-0.81582
2π	-0.53882	-0.55581	-0.55393	-0.57631	-0.58484	-0.56176
3π	0.19799	0.17011	0.17040	0.14517	0.13702	0.16193
G	-123.62024	-123.07566	-122.53086	-122.32686	-122.11374	-121.56204
$\pi-\pi^A$ gap	0.73681	0.72592	0.72433	0.72148	0.72186	0.72369
1st I.P.(eV)	14.66	15.12	15.07	15.68	15.91	15.28

*Column 6 contains the results of the PLA Calculation at the same R_{CF} as calculation 3.

calculation 3 values are slightly varied from the trend predicted by the other four. However, the most important point obtained from the two tables is that the Mulliken approximation has transposed the 7σ and 2π MO energies. This is a rather serious effect and one which again shows the superiority of the PLA and FLA methods over the MA.

Although McLean and Yoshimine's values for the MO energies of their calculations have not been published some of their results have been made available privately. The ordering of their MO energy levels is exactly as predicted by the FLA and PLA calculations; i.e. with the 2π higher than the 7σ.

It is also seen that the π bonding-antibonding gap is reasonably constant as R_{CF} varies in the FLA calculations but varies much more in the IMA calculations. No experimental value for the first ionisation potential of FCN could be traced but the value of about 15.40eV interpolated from the FLA calculations seems reasonable, especially when considering the trends in experimental ionisation potentials of the series HCN, (FCN), ClCN, BrCN and ICN: these are, respectively, 13.86eV, 12.49eV, 11.95eV and 10.98eV. A value of about 13.1eV might be expected if FCN fitted in to the series trend.

Tables IV. 26 and IV. 27 contain the results of a Mulliken population analysis on respectively, the IMA and FLA calculations. The set of PLA populations and densities are included for

Table IV. 26.

Mulliken Population Analysis of IMA FCN Calculations.

R_{CF}		Atom/Bond Populations.						Gross Atom Charge Densities.		
		N	C	F	NC	CF	NF	N	C	F
2.00	sigma	4.776	2.908	5.159	0.741	0.535	-0.118	5.088	3.545	5.367
	pi	1.610	1.523	3.925	1.090	-0.098	-0.050	2.130	2.019	3.851
	total	6.386	4.431	9.084	1.830	0.436	-0.167	7.217	5.564	9.218
2.20	sigma	4.805	2.979	5.085	0.681	0.535	-0.087	5.102	3.588	5.310
	pi	1.565	1.511	3.944	1.083	-0.070	-0.033	2.089	2.018	3.893
	total	6.370	4.491	9.030	1.764	0.466	-0.120	7.192	5.605	9.203
2.385	sigma	4.829	3.054	5.032	0.634	0.517	-0.066	5.113	3.629	5.258
	pi	1.534	1.500	3.965	1.079	-0.055	-0.023	2.062	2.012	3.926
	total	6.363	4.554	8.997	1.713	0.461	-0.089	7.175	5.641	9.183
2.60	sigma	4.850	3.141	4.983	0.587	0.488	-0.049	5.119	3.678	5.202
	pi	1.512	1.487	3.984	1.076	-0.045	-0.014	2.042	2.003	3.955
	total	6.362	4.628	8.967	1.663	0.443	-0.063	7.162	5.681	9.157
2.80	sigma	4.853	3.197	4.961	0.551	0.475	-0.038	5.110	3.711	5.180
	pi	1.504	1.476	3.985	1.072	-0.028	-0.009	2.035	1.998	3.966
	total	6.357	4.674	8.946	1.623	0.447	-0.047	7.145	5.709	9.146

Table IV. 27.

Mulliken Population Analysis of FLA and PLA* FCN Calculations.

R_{CF}		Atom/Bond Populations.						Gross Atom Charge Densities.		
		N	C	F	NC	CF	NF	N	C	F
2.00	sigma	4.964	3.274	5.324	0.189	0.324	-0.076	5.021	3.531	5.448
	pi	1.715	1.484	3.781	1.060	0.017	-0.057	2.216	2.023	3.761
	total	6.679	4.758	9.106	1.250	0.341	-0.133	7.237	5.554	9.209
2.20	sigma	4.945	3.236	5.222	0.273	0.388	-0.063	5.050	3.566	5.384
	pi	1.660	1.475	3.821	1.057	0.026	-0.040	2.169	2.017	3.814
	total	6.605	4.711	9.042	1.330	0.414	-0.103	7.219	5.583	9.198
2.385	sigma	4.959	3.667	5.155	-0.008	0.247	-0.020	4.945	3.787	5.268
	pi	1.728	1.353	3.861	1.053	0.033	-0.027	2.241	1.896	3.864
	total	6.687	5.020	9.015	1.045	0.280	-0.047	7.186	5.683	9.132
2.60	sigma	4.910	3.376	5.061	0.311	0.374	-0.033	5.049	3.719	5.232
	pi	1.623	1.409	3.910	1.061	0.014	-0.017	2.144	1.947	3.909
	total	6.532	4.786	8.972	1.372	0.389	-0.050	7.193	5.666	9.141
2.80	sigma	4.896	3.392	5.008	0.349	0.382	-0.027	5.057	3.757	5.186
	pi	1.607	1.396	3.937	1.061	0.011	-0.012	2.132	1.932	3.936
	total	6.503	4.788	8.944	1.410	0.393	-0.038	7.189	5.689	9.122
2.385*	sigma	4.817	3.220	5.063	0.508	0.439	-0.047	5.048	3.693	5.259
	pi	1.576	1.506	3.871	1.061	0.014	-0.028	2.092	2.043	3.864
	total	6.393	4.726	8.934	1.569	0.453	-0.074	7.140	5.737	9.123

*PLA Calculation results.

comparison. In discussing trends the FLA calculation 3 results will be ignored in general. The important points to notice are as follows: there is little or no bonding between the carbon and fluorine pi orbitals; the NC bond population from the FLA series is seen to increase as R_{CF} increases whereas the opposite trend is shown in the IMA series; and in both series the atom populations on N and F decrease as R_{CH} increases, while on C the charge density increases in the IMA series, and increases after passing through a minimum in the FLA series. It is interesting to note again the opposing trends of the σ and π electronic charges. It is clearly seen from the gross atom charge densities that as the σ charge increases the π charge decreases.

The effective atomic charges, as evaluated by the Mulliken, Löwdin, Doggett I and Doggett II population analyses, are presented in Tables IV. 28 and IV. 29 for the IMA and FLA series respectively. The trends shown by the Doggett II method are of little value because of the singularity at the experimental R_{CF} distance. In general N appears to be negatively charged but loses some of this charge as R_{CF} increases. C is positively charged and F is negatively charged. On the whole C tends to gain electronic charge as R_{CF} increases but it is not clear what happens to the charge on F. The Mulliken method predicts a loss of charge from F; the Löwdin method predicts a gain in charge on F and the Doggett I method oscillates very slightly but tends to predict a minimum

Table IV. 28.

Effective Atomic Charges for IMA FCN Calculations.

R_{CF}		Mulliken	Löwdin	Doggett I	Doggett II
	N	-0.218	-0.186	-0.206	-0.176
2.00	C	+0.436	+0.222	+0.294	+0.266
	F	-0.218	-0.026	-0.088	-0.090
	N	-0.192	-0.144	-0.166	-0.143
2.20	C	+0.395	+0.204	+0.241	+0.353
	F	-0.203	-0.060	-0.075	-0.210
	N	-0.175	-0.118	-0.138	-0.118
2.3848578	C	+0.358	+0.194	+0.202	-1.068
	F	-0.183	-0.076	-0.064	+1.186
	N	-0.162	-0.094	-0.110	-0.093
2.60	C	+0.319	+0.174	+0.164	-0.064
	F	-0.157	-0.080	-0.054	+0.157
	N	-0.145	-0.074	-0.076	-0.056
2.80	C	+0.291	+0.162	+0.144	-0.011
	F	-0.146	-0.088	-0.068	+0.067

Table IV. 29.

Effective Atomic Charges for FLA and PLA* FCN Calculations.

R_{CF}		Mulliken	Löwdin	Doggett I	Doggett II
2.00	N	-0.237	-0.212	-0.017	+0.044
	C	+0.446	+0.202	+0.068	+0.054
	F	-0.209	+0.010	-0.051	-0.098
2.20	N	-0.219	-0.172	-0.030	+0.023
	C	+0.417	+0.212	+0.088	+0.208
	F	-0.198	-0.040	-0.058	-0.231
2.3848578	N	-0.186	-0.132	+0.115	+0.208
	C	+0.317	+0.164	-0.138	-2.033
	F	-0.131	-0.032	+0.023	+1.825
2.60	N	-0.193	-0.120	-0.005	+0.052
	C	+0.334	+0.184	+0.032	-0.244
	F	-0.141	-0.064	-0.027	+0.192
2.80	N	-0.189	-0.110	-0.015	+0.040
	C	+0.311	+0.178	+0.048	-0.141
	F	-0.122	-0.068	-0.033	+0.101
2.3848578*	N	-0.140	-0.104	0.000	+0.050
	C	+0.263	+0.126	-0.010	-1.545
	F	-0.123	-0.022	+0.010	+1.495

* PLA Calculation Results.

in the effective charge.

The trends in electron density movement as R_{CF} increases, are shown in pictorial form for the FLA series, in contour diagrams 21 to 25. As expected charge is depleted from the region of the CF bond. It can be seen from Table IV. 27 that this trend is not clearly displayed by the population analysis. The only other trend discernible is that C loses electronic charge as well. It is not obvious that N and F gain the charge.

Contour diagram 26 shows the electron density distribution for the IMA calculation at the experimental internuclear separations. The main difference from the FLA series seems to be that the charge in the vicinity of N is polarised more towards C. Contour diagram 27 shows the pi electronic charge distribution of the FLA calculation at the experimental internuclear separations. It shows clearly both the lack of bonding between the C and F atoms, and the build up of electronic charge on the N atom as compared with the C atom. Contour diagram 28 is interesting as it shows the difference density between taking convergence at 50 cycles and 100 cycles of the SCF iteration scheme for the FLA equilibrium geometry calculation. The main changes in the charge distribution appear to have taken place in the region of the N atom. Otherwise the contours are small in magnitude and cover small areas.

For the same calculation, contour diagram 29 shows how the electronic charge has rearranged from the theoretical state of the

CONTOUR DIAGRAM 21.

P_{FCN}
$R(NC) = 2.1902141$
$R(CF) = 2.00$a.u.

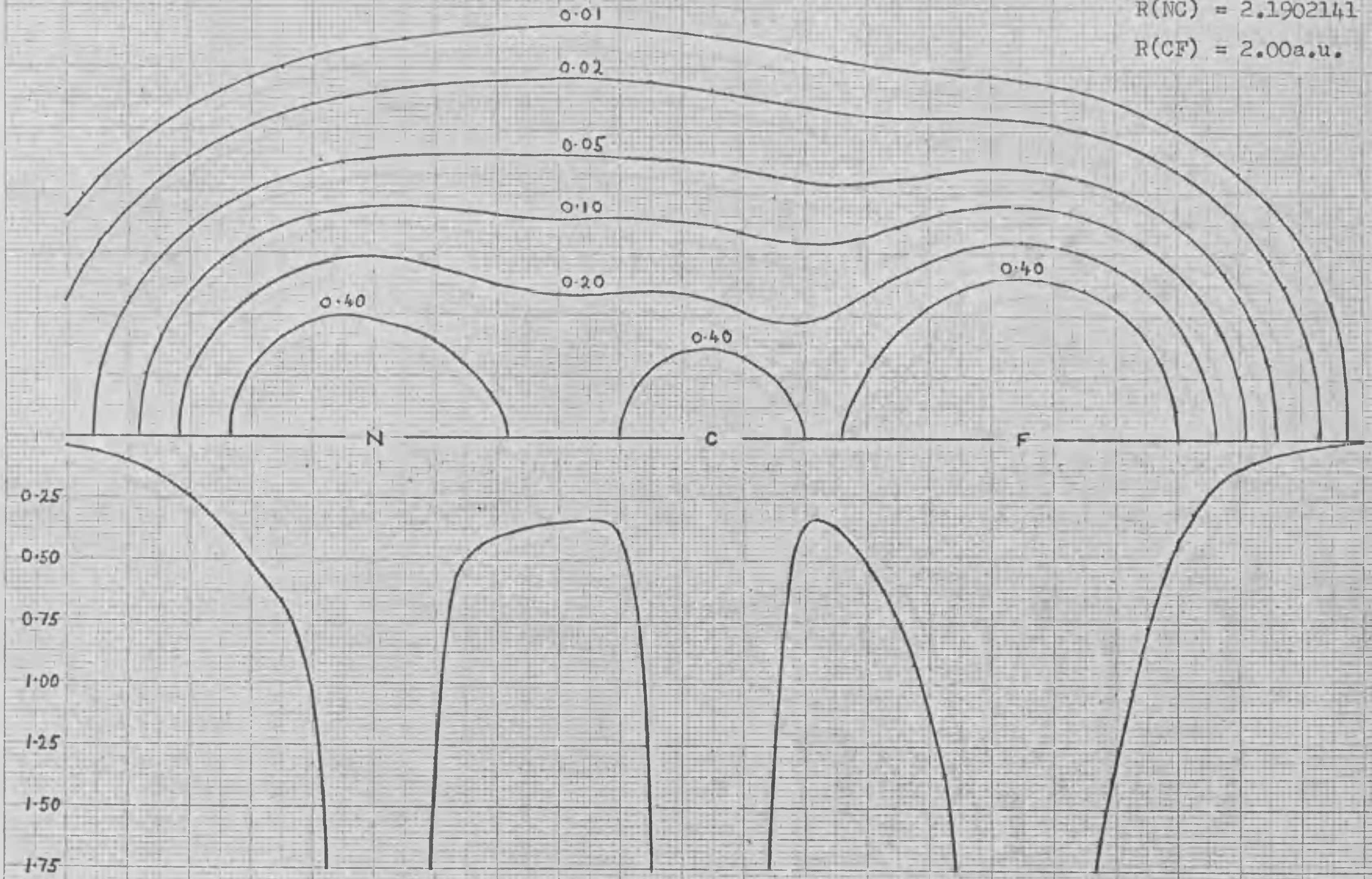

CONTOUR DIAGRAM 22.

P_{FCN}

$R(NC) = 2.1902141a.u.$

$R(CF) = 2.20a.u.$

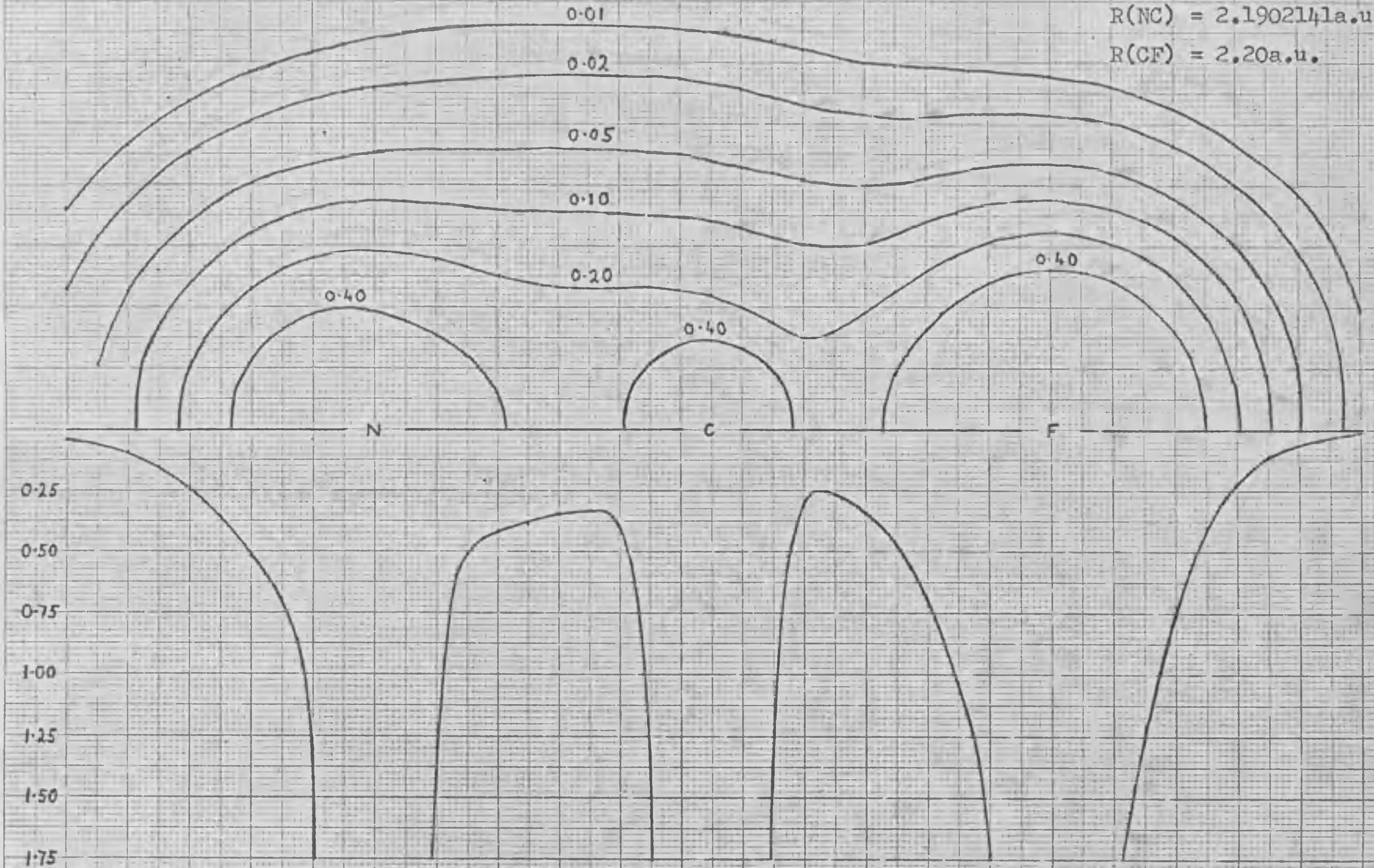

CONTOUR DIAGRAM 23.

P_{FCN}

R(NC) = 2.1902141a.u.

R(CF) = 2.3848578a.u.

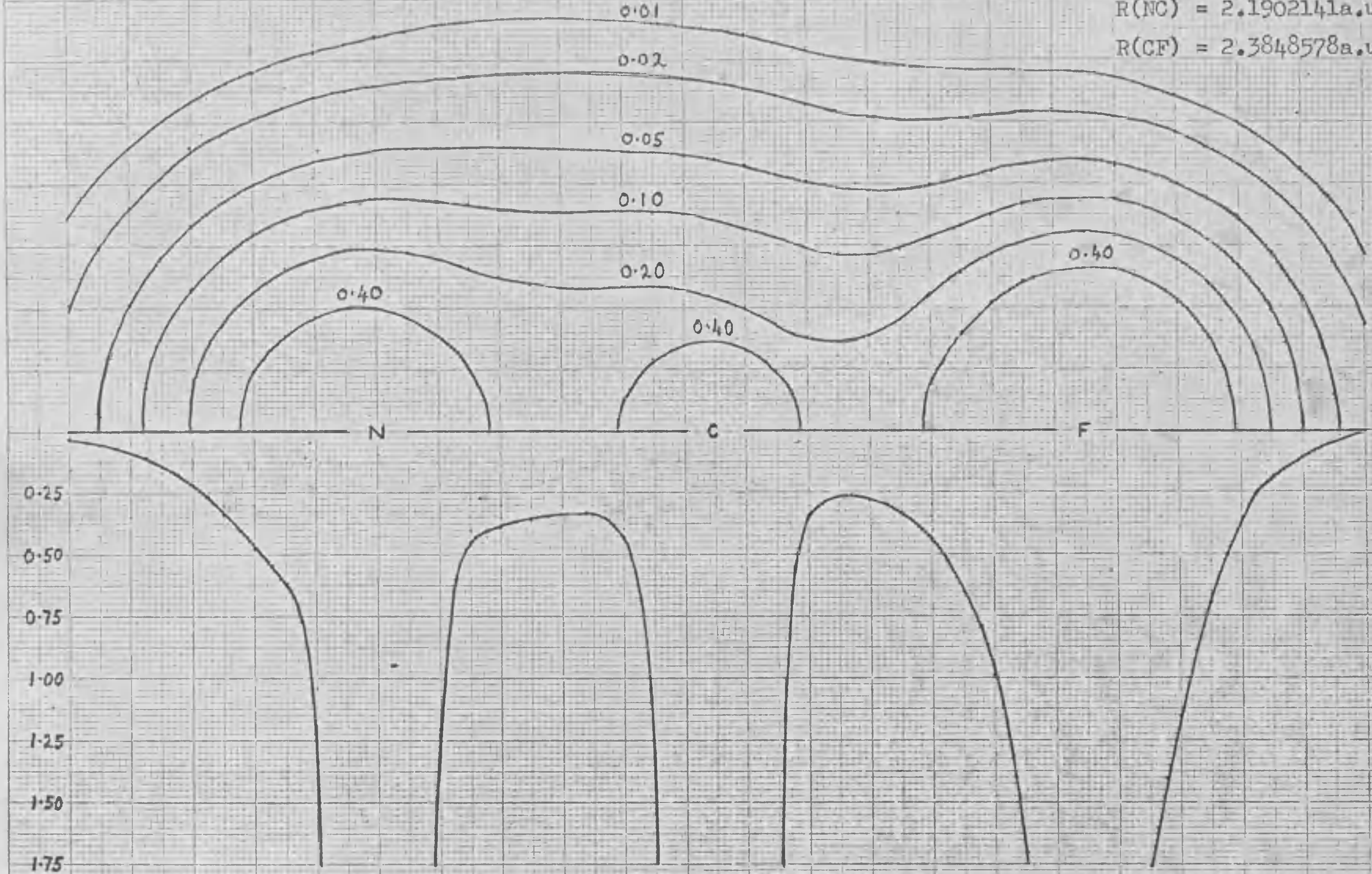

CONTOUR DIAGRAM 24.

P_{FCN}

$R(NC) = 2.1902141$a.u.

$R(CF) = 2.60$a.u.

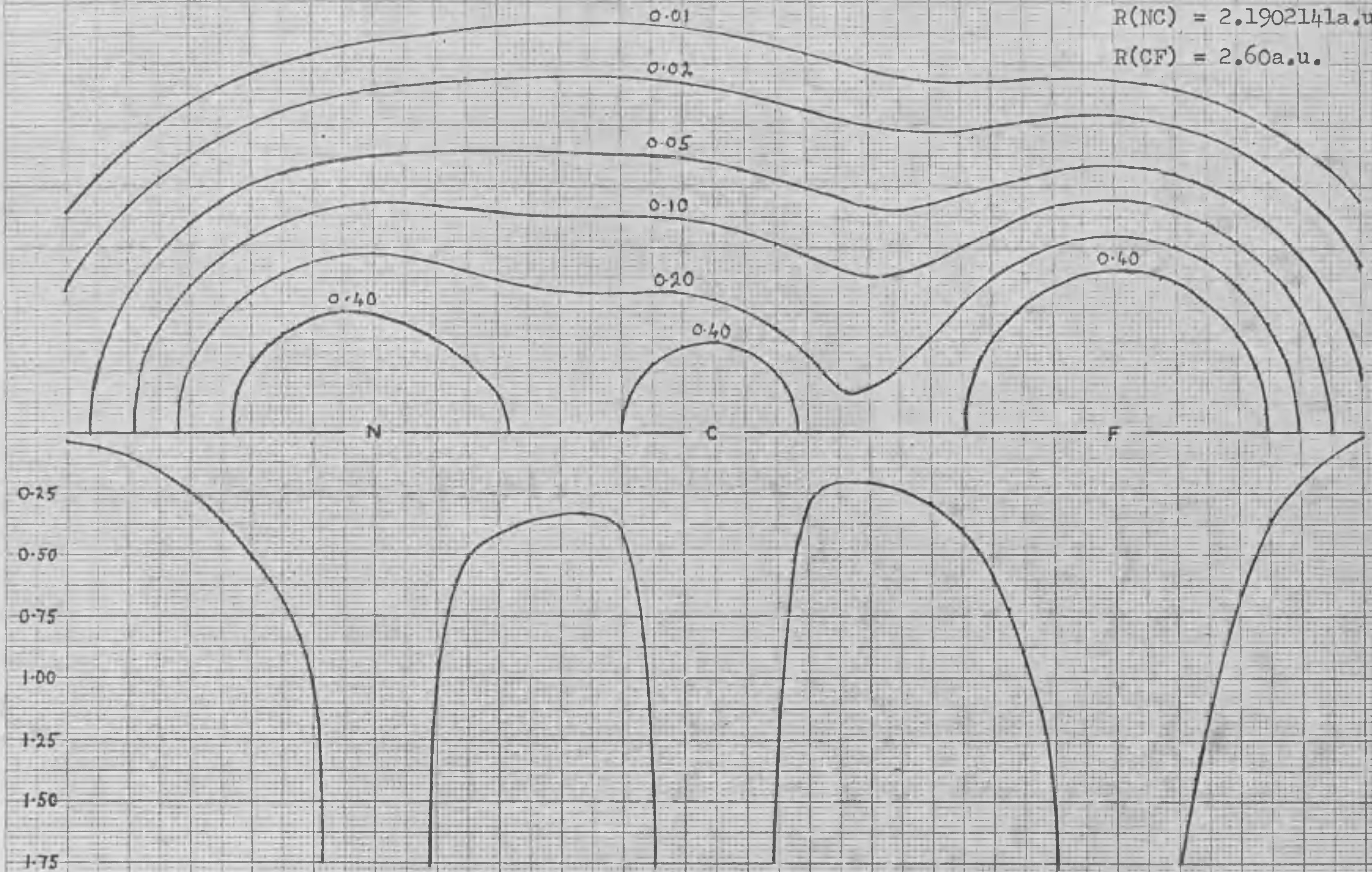

CONTOUR DIAGRAM 25.

P_{FCN}

R(NC) = 2.1902141a.u.

R(CF) = 2.80a.u.

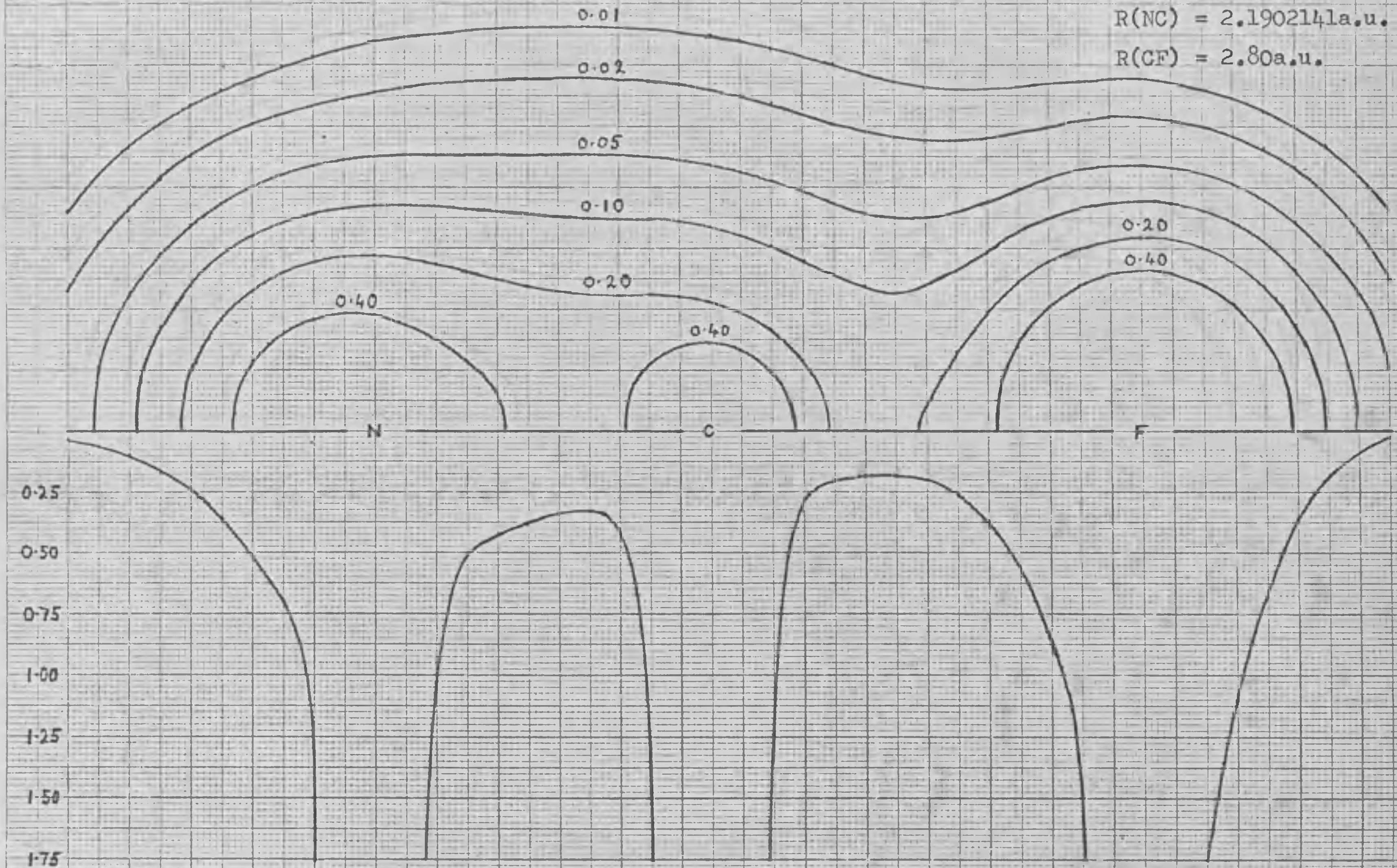

CONTOUR DIAGRAM 26.

P_{FCN}

R(NC) = 2.1902141a.u.

R(CF) = 2.3848578a.u.

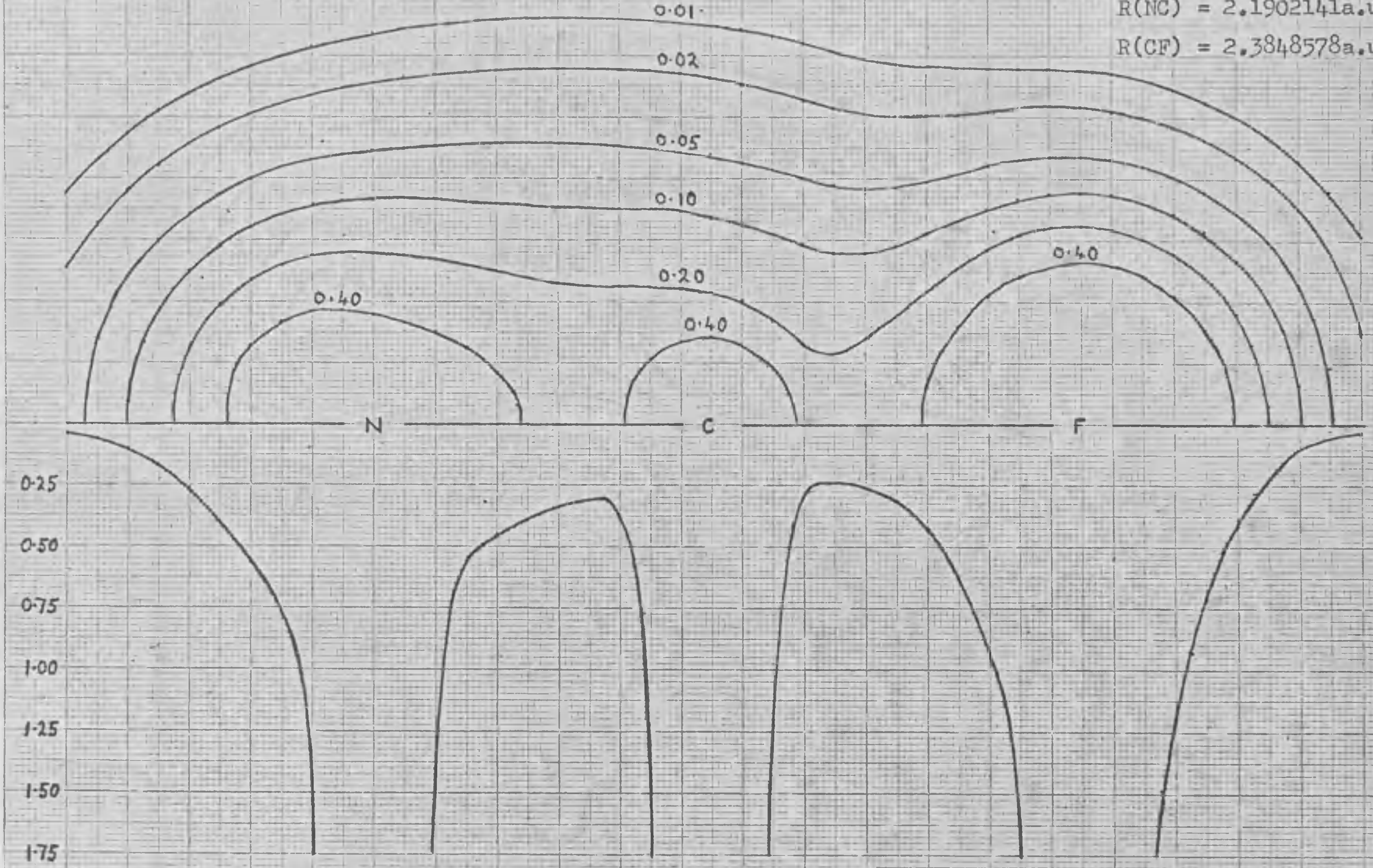

CONTOUR DIAGRAM 27.

P_{FCN}

$R(NC) = 2.1902141$ a.u.

$R(CF) = 2.3848578$ a.u.

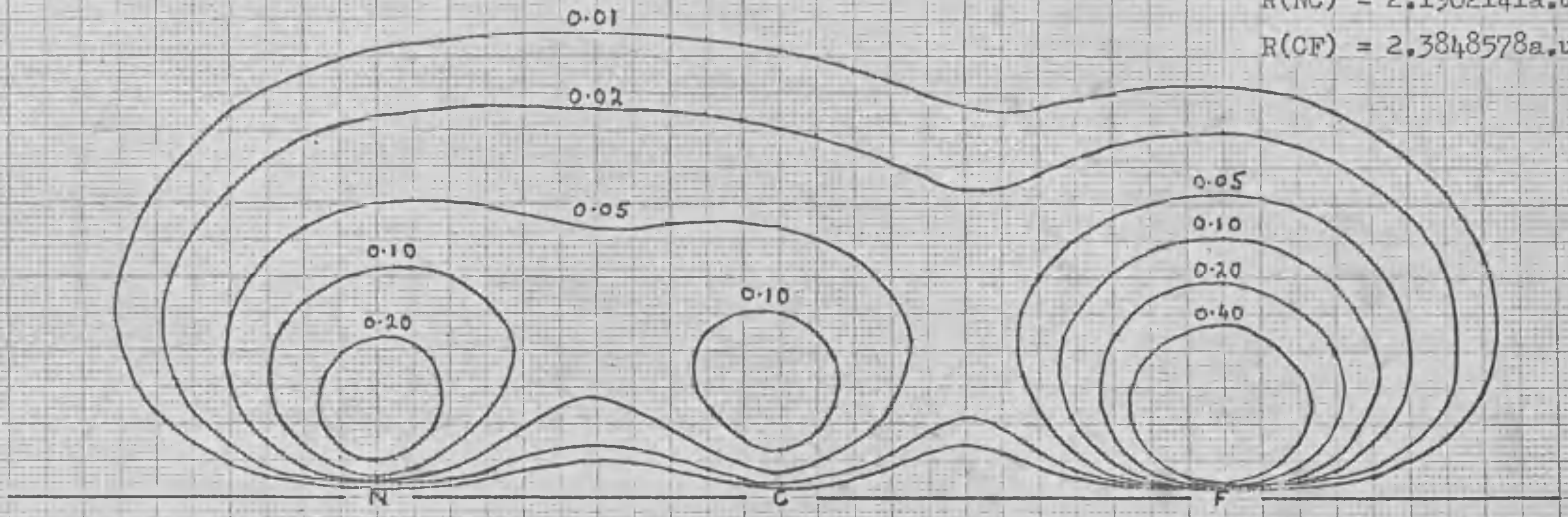

CONTOUR DIAGRAM 28. P_{FCN} (100cycles - 50cycles) R(NC) = 2.1902141a.u.

R(CF) = 2.3848578a.u.

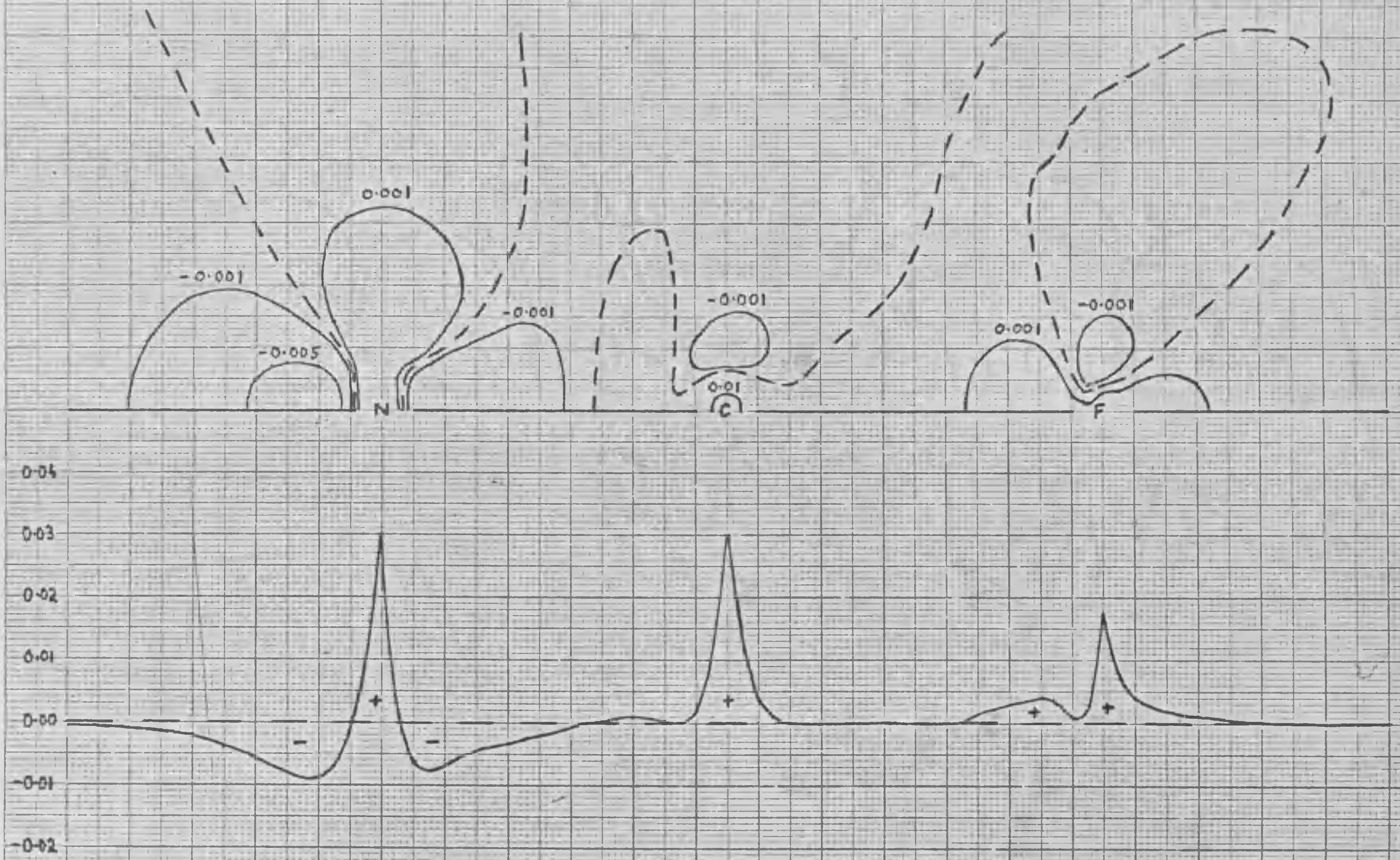

CONTOUR DIAGRAM 29.

$P_{FCN} - P_{atoms}$

R(NC) = 2.1902141a.u.

R(CF) = 2.3848578a.u.

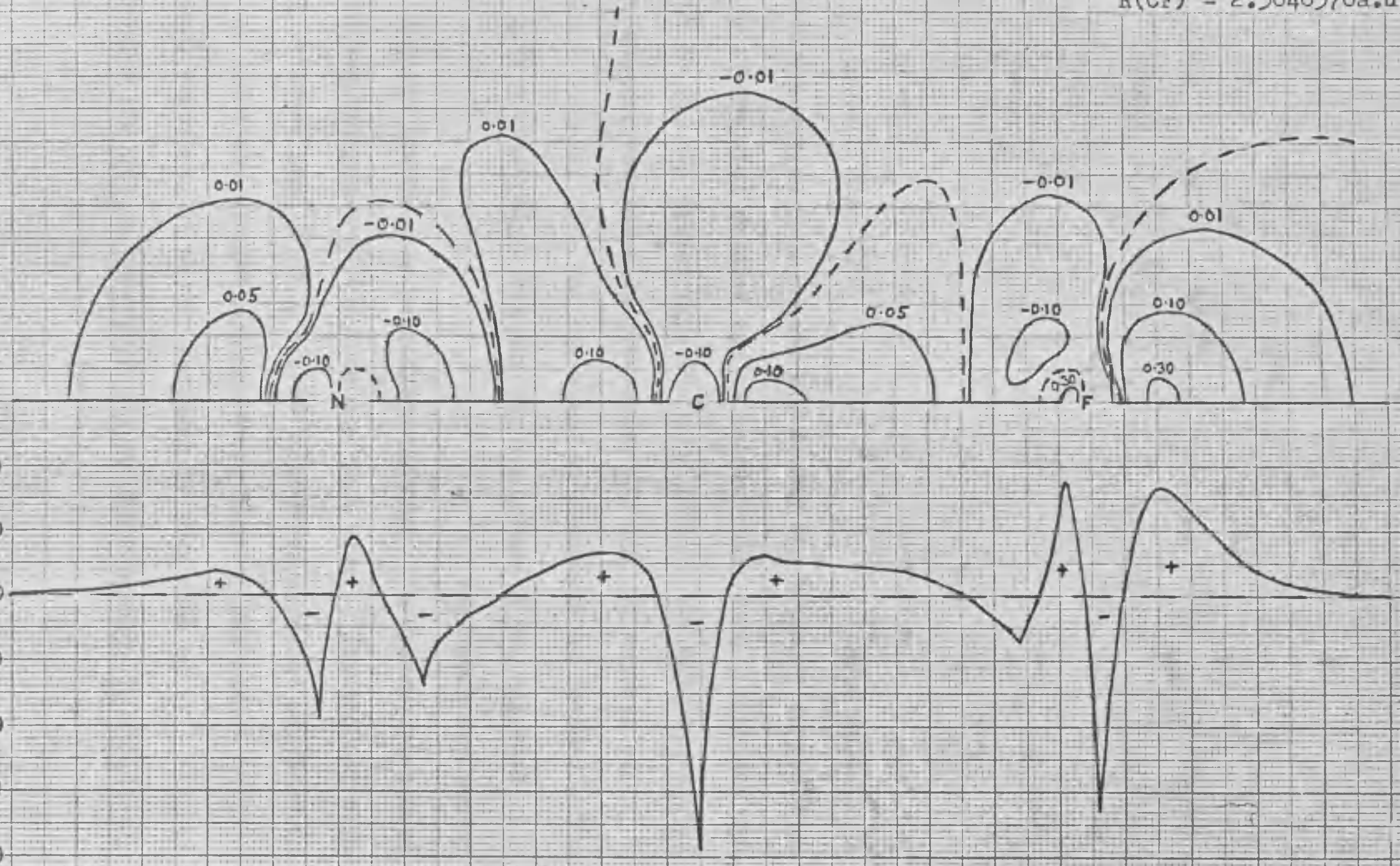

free atoms at bonding internuclear distances to the FCN molecule itself. It is seen that as expected charge is displaced from the regions around the atoms and deposited either in the bonds or in the regions normally thought of as the N and F lone pairs. It is also interesting to note that the bond charge densities are both polarised towards C. This is unexpected from simple electronegativity concepts.

Finally, the $\underset{\sim}{R}$ matrix for the FCN FLA calculation 4 with R_{CF} = 2.6a.u. is presented in Table IV. 30.

The results for FCN are reasonably encouraging although the calculations do not predict an R_e as efficiently for FCN as they did for HCN. Once again, however, the general improvement obtained by invoking the FLA or PLA rather than Mulliken's method is clearly shown.

Table IV. 30.

R Matrix for FCN FLA Calculation 4: R(CF) = 2.60 a.u.

$$\begin{array}{cccccccccc}
\underset{\sim}{R}_{\sigma} & 1.0049 & 0.0129 & -0.0401 & 0.0026 & -0.0318 & 0.0261 & -0.0004 & -0.0044 & -0.0148 \\
 & & 0.9917 & -0.3221 & -0.0291 & -0.1684 & 0.0100 & 0.0037 & -0.0611 & -0.0434 \\
 & & & 0.4584 & -0.0235 & 0.2856 & -0.2410 & 0.0038 & -0.0111 & 0.1748 \\
 & & & & 1.0049 & -0.0309 & 0.0133 & 0.0001 & 0.0142 & 0.0032 \\
 & & & & & 0.4505 & -0.0199 & -0.0118 & 0.1126 & -0.2337 \\
 & & & & & & 0.2328 & -0.0107 & 0.0231 & -0.2812 \\
 & & & & & & & 1.0009 & -0.0043 & 0.0187 \\
 & & & & & & & & 1.0125 & -0.1992 \\
 & & & & & & & & & 0.5172
\end{array}$$

$$\begin{array}{cccc}
\underset{\sim}{R}_{\pi} & 0.4057 & 0.3651 & -0.1537 \\
 & & 0.3524 & 0.0093 \\
 & & & 0.9776
\end{array}$$

4.5. Discussion of the Electronic Structure of the XCN system.

In this section the trends in the redistribution of the electronic charge among the molecules CN^-, HCN and FCN are discussed. In addition to the results presented in 4.2, 4.3 and 4.4, four other ΔP diagrams are presented to help elucidate the features of charge redistribution. Contour diagrams 30 and 31 present ΔP diagrams and profiles for $[P_{HCN} - P_{CN^-}]$ from the FLA and IMA calculations on HCN, respectively. They show how electronic charge has redistributed itself as a proton is allowed to bond with the CN^- ion.

Diagrams 30 and 31 are very similar in outline. They both show that charge has been transferred from the vicinity of the N atom, from the CN bond and from the region normally referred to as the C lone pair, to the region around the proton, as would be expected. Charge has also built up in the region of the C atom. The only major difference between the two calculations appears to be that the FLA causes a slight build up of charge close to the N nucleus.

In contour diagrams 32 and 33, ΔP diagrams and profiles are presented for the difference densities between FCN and CN^- and between FCN and HCN where $R_{CF} = R_{CH}$, respectively. Since HCN and CN^- are isoelectronic and have eight electrons fewer than FCN, it is not surprising that there is some resemblance between the diagrams.

CONTOUR DIAGRAM 30.

$P_{HCN} - P_{CN^-}$

R(NC) = 2.1902141a.u.

R(CH) = 2.0087986a.u.

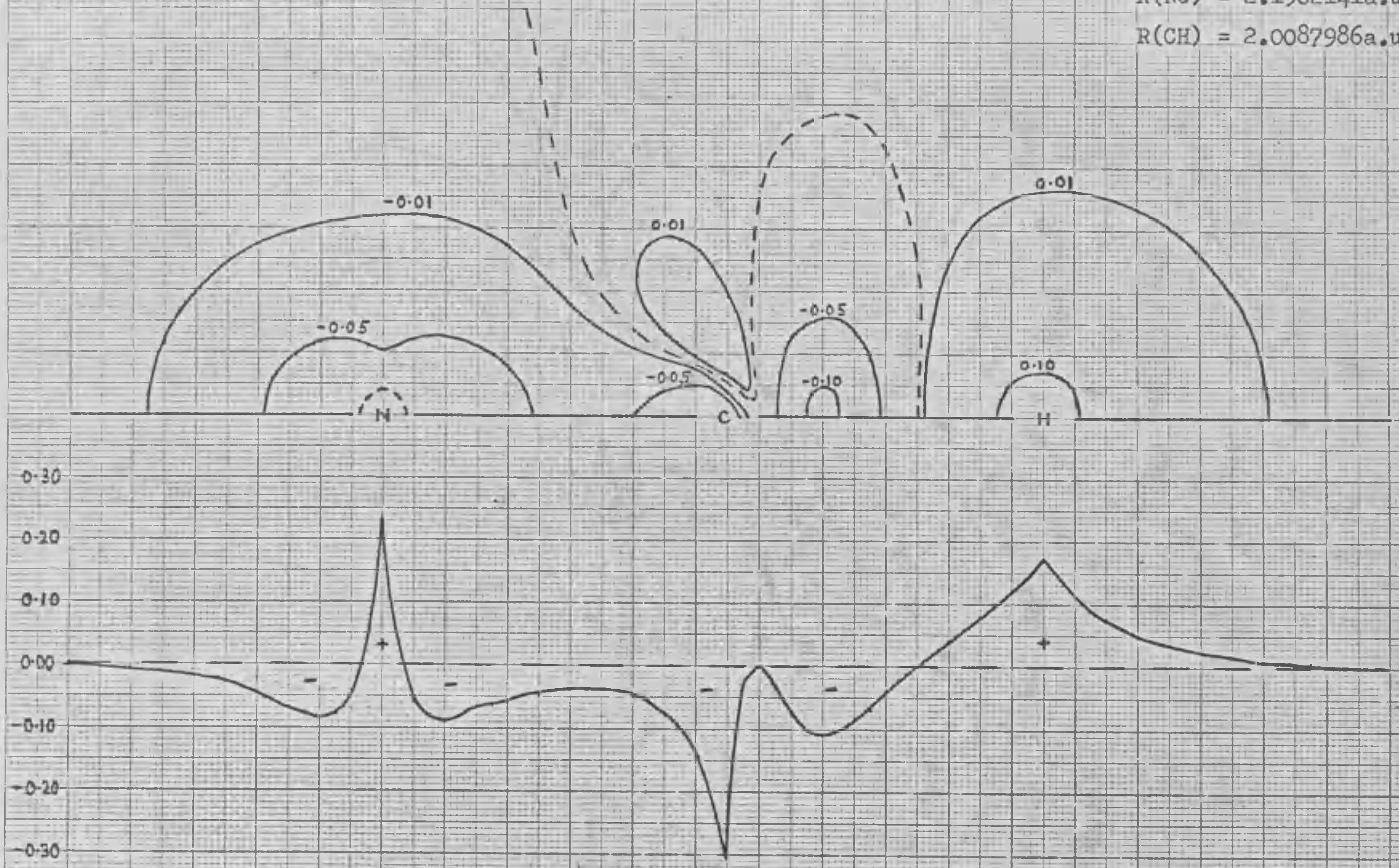

CONTOUR DIAGRAM 31. $P_{HCN} - P_{CN^-}$ R(NC) = 2.1902141a.u. R(CH) = 2.0087986a.u.

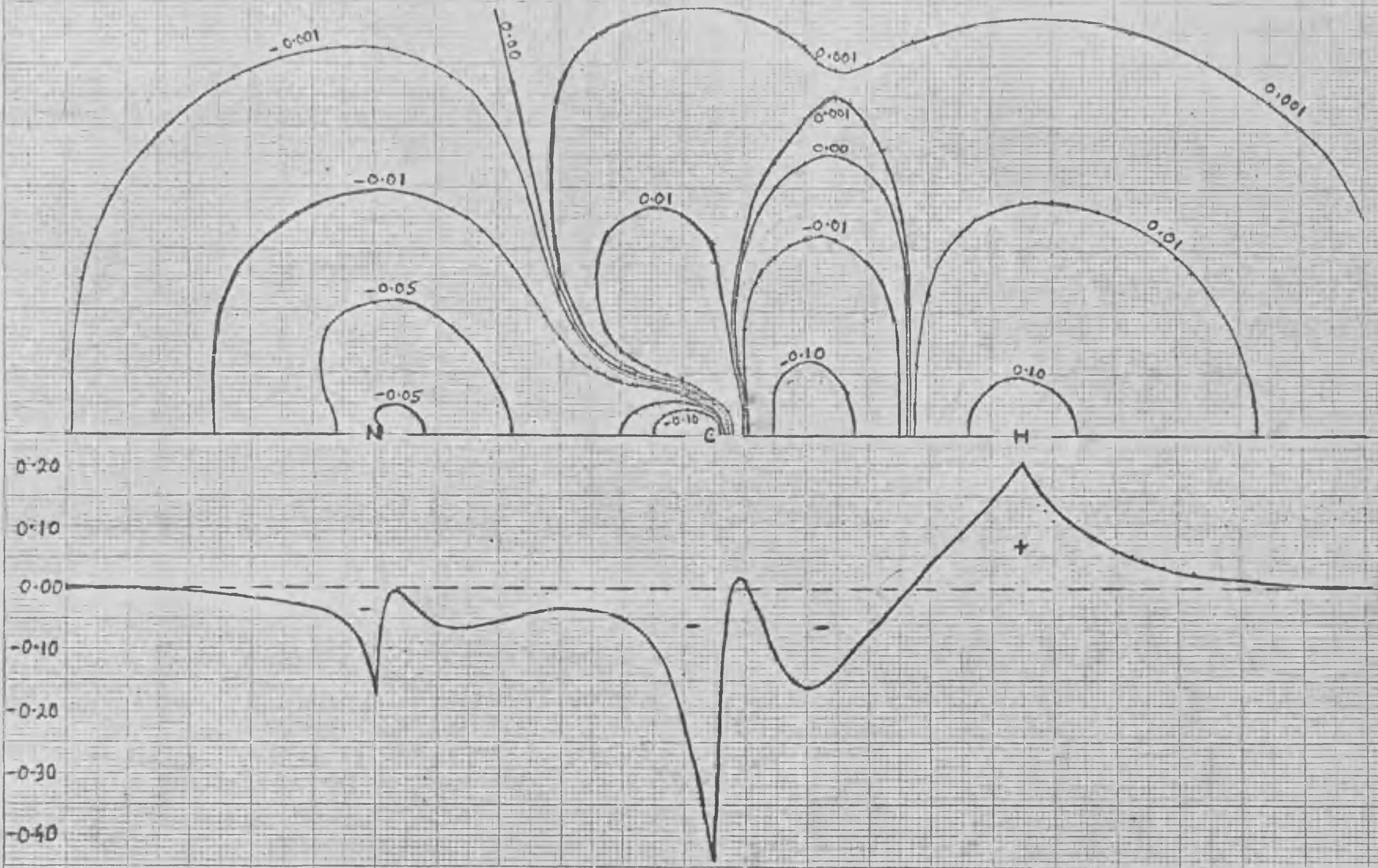

CONTOUR DIAGRAM 32.

$P_{FCN} - P_{CN^-}$

R(NC) = 2.1902141a.u.

R(CF) = 2.3848578a.u.

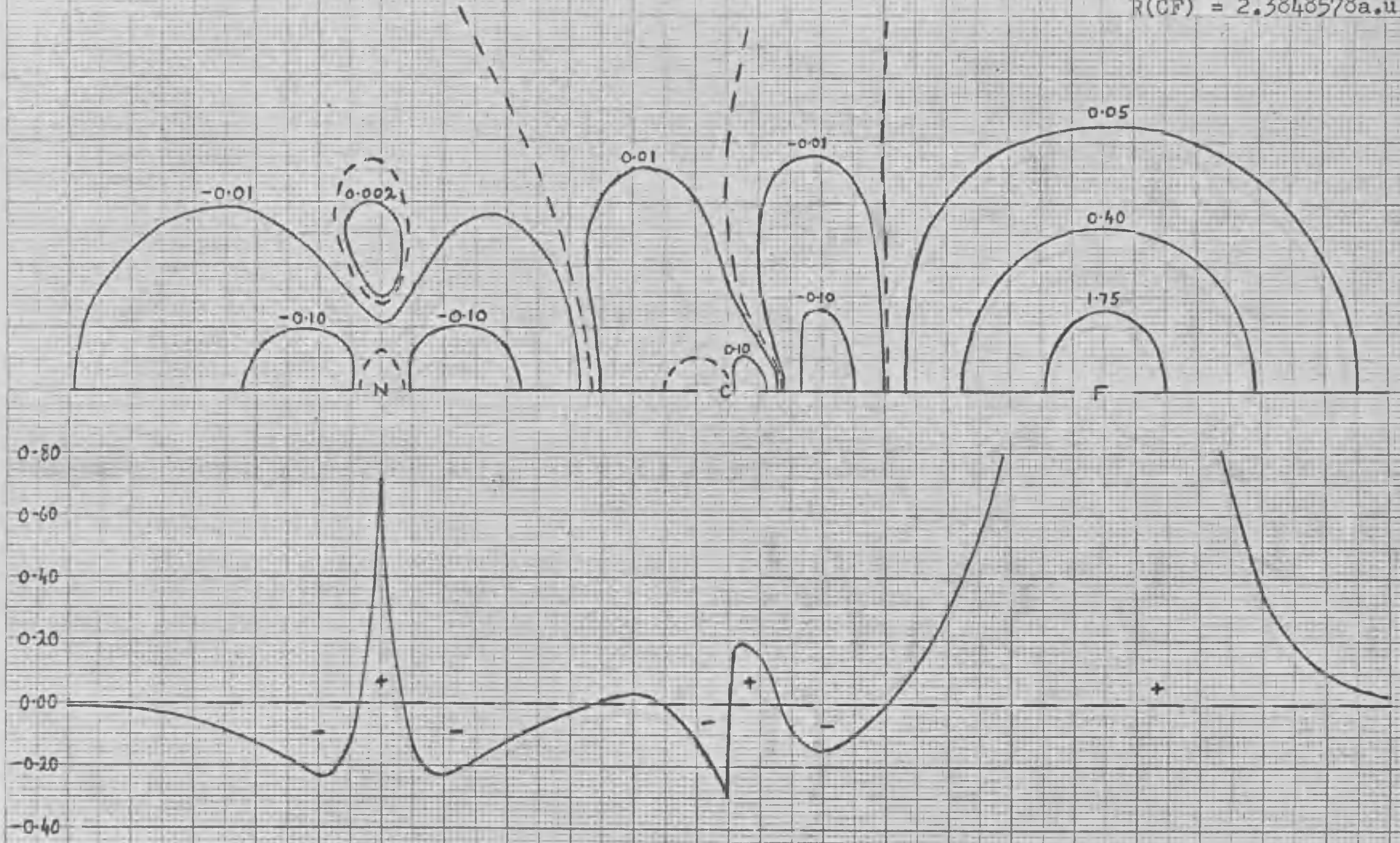

CONTOUR DIAGRAM 33.

$P_{FCN} - P_{HCN}$

R(NC) = 2.1902141a.u.

R(CF/CH) = 2.3848578a.u.

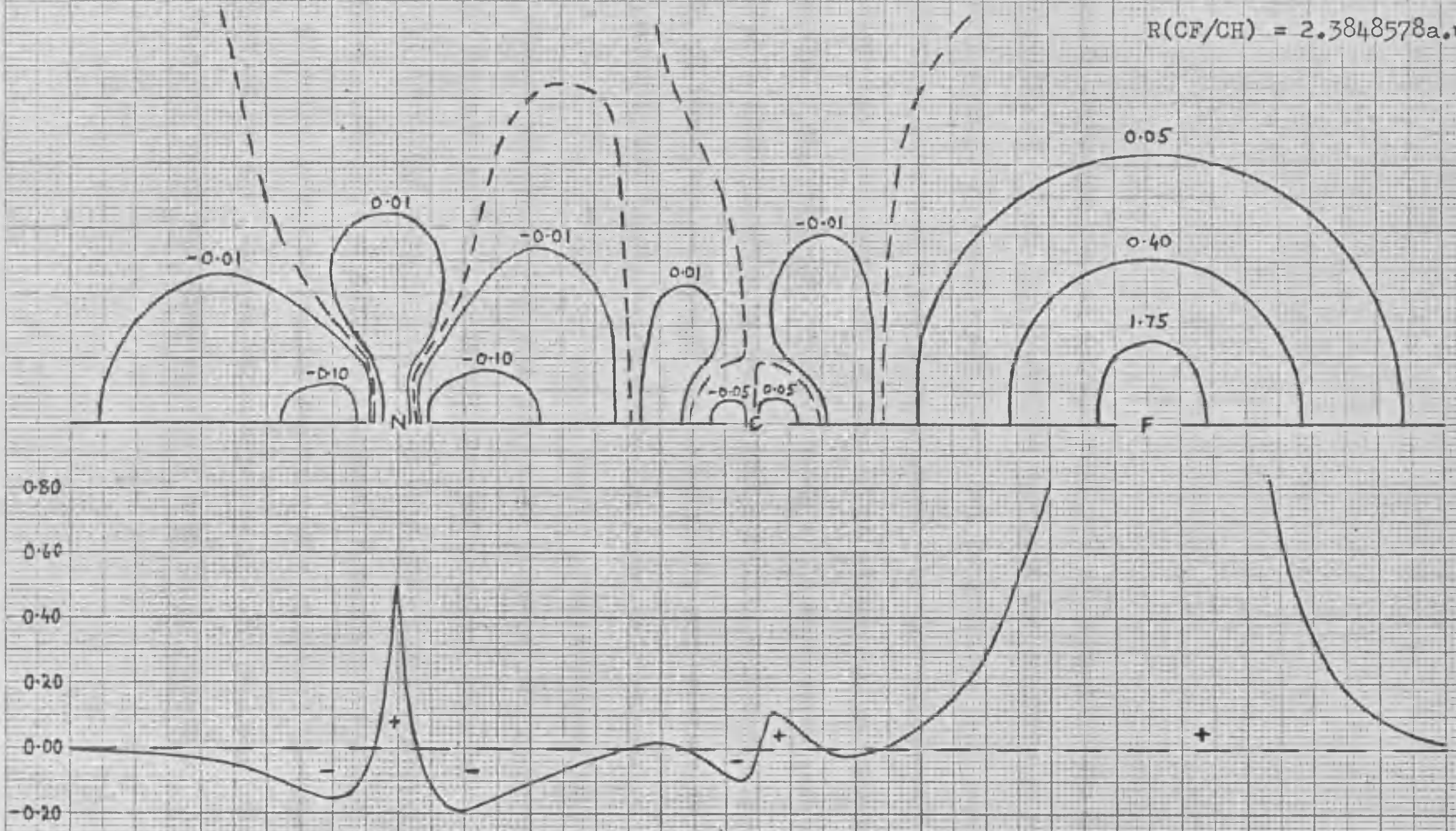

In general it is seen that electronic charge is built up round the F atom. It is interesting to note that charge is also built up, though to a much lesser degree, in the vicinity of the N nucleus. Electronic charge is depleted in the region normally ascribed to the N lone pair as is shown in both diagrams.

The high electronegativity effect of F can be seen as the NC and CF bond electron densities have been polarised towards C and F, respectively.

From the results of the foregoing sections, and this section, it is obvious that the value of the population analyses, in the elucidation of electronic structures, is difficult to assess. In most cases trends are shown to be in agreement but a quantitative estimate of the charge on an atom is not possible. The pictorial representations of the charge density are a much more reliable method of investigating the electronic structures of molecules, and ΔP diagrams and profiles are especially useful in detecting the redistribution of electron density between molecular systems.

4.6. Evaluation of the Multicentre Integral Approximations.

The multicentre integral approximations considered in this thesis are evaluated in this section from two separate viewpoints. The main evaluation is based on the results of the electronic structure calculations presented in the previous five sections.

In 4.1 it is seen that the two asymmetric partitioning methods, the PLA and the FLA undoubtedly give much improved results as compared with the Mulliken approximation. This trend is confirmed by 4.2 and 4.3 although the IMA calculation is shown to be surprisingly good for HCN. However, the possible danger in using the IMA is highlighted in 4.3 by the unacceptable ordering of the MO energy levels in FCN when 7σ instead of 2π is the highest energy bonding orbital.

It is not so simple to choose between the PLA and the FLA, however. Both have their merits. Although the FLA suffers from the danger of breakdown due to the possible singularity in choosing the bond asymmetry parameter, λ, as is shown in 4.4, it is still obviously very useful in that provided a near singularity does not occur the resultant calculated molecular properties are close to those deduced from *ab initio* calculations.

Provided that exploratory calculations are performed first of all to detect a possible breakdown, this danger can be avoided by making a different choice for the internuclear separations. The possibility of a breakdown can be determined by examining the bond asymmetry matrix, $\underset{\sim}{\lambda}$. If any elements vary markedly from the range 0.0 to 1.0, the internuclear separations which correspond to that λ, should be avoided. For example, the $\lambda_{2z_C 2z_F}$ value, in the FLA calculation on FCN which is close to breakdown, is -4.97.

The PLA does not suffer from the difficulty of this singularity, yet also gives results close to those of ab initio calculations, although in general it is slightly inferior to the FLA. Before recommending the use of the PLA further investigation of its effects on observables such as the dipole moment, and on the predicted minimum energy and equilibrium configuration, would have to be carried out. From this work it would appear that the use of the FLA and PLA should preferably be complementary.

In the second evaluation of the various multicentre integral approximations comparisons are made with accurate values of some three-centre one-electron integrals obtained from a program being developed in Glasgow [64]. A few integral values are presented in Table IV.31 for the molecules HCN and FCN, using double-zeta AO's. It is clear from this table that the FLA is consistently the best of the approximations. In the cases where it does not yield the value closest to the accurate integral, it provides a value which is still acceptable. Although the PLA is in general poorer than the FLA it also yields integrals much more accurately than the IMA.

Because of the dearth of accurate three-centre two-electron

Table IV.31.

Comparison of Approximated Three-Centre One-Electron Integrals with Accurate Values.

Integral	Accurate	MA	IMA	PLA	FLA
$(1s^N \vert 1/r_H \vert 1s^C)$	0.00011	0.00013	0.00013	0.00012	0.00012
$(1s^N \vert 1/r_H \vert 2s^C)$	0.01482	0.02152	0.02267	0.01515	0.01357
$(1s^N \vert 1/r_H \vert 2z^C)$	0.02506	0.04069	0.03873	0.02579	0.02566
$(2s^N \vert 1/r_H \vert 1s^C)$	0.02869	0.02308	0.02328	0.02983	0.02853
$(2s^N \vert 1/r_H \vert 2s^C)$	0.14774	0.17045	0.18117	0.16287	0.13401
$(2s^N \vert 1/r_H \vert 2z^C)$	0.12280	0.20362	0.19548	0.14170	0.12846
$(2z^N \vert 1/r_H \vert 1s^C)$	0.05280	0.04233	0.04195	0.05451	0.05429
$(2z^N \vert 1/r_H \vert 2s^C)$	0.16996	0.15667	0.16347	0.19203	0.17505
$(2z^N \vert 1/r_H \vert 2z^C)$	0.04877	0.08206	0.07748	0.09179	0.06214
$(2x^N \vert 1/r_H \vert 2x^C)$	0.10570	0.11773	0.11773	0.11442	0.11442
$(1s^N \vert 1/r_C \vert 1s^H)$	0.00372	0.00357	0.00357	0.00352	0.00352
$(2s^N \vert 1/r_C \vert 1s^H)$	0.07600	0.05387	0.05573	0.05360	0.07074
$(2z^N \vert 1/r_C \vert 1s^H)$	0.11489	0.07386	0.07148	0.07306	0.08108
$(1s^C \vert 1/r_N \vert 1s^H)$	0.03611	0.02905	0.02905	0.03696	0.03696
$(2s^C \vert 1/r_N \vert 1s^H)$	0.18363	0.19890	0.20903	0.19883	0.17108
$(2z^C \vert 1/r_N \vert 1s^H)$	0.10153	0.19047	0.18167	0.11283	0.11535
$(2x^N \vert 1/r_F \vert 2x^C)$	0.09600	-	0.10561	0.10284	0.10284
$(2z^N \vert 1/r_F \vert 2s^C)$	0.14965	-	0.14350	0.16667	0.15340
$(2s^N \vert 1/r_C \vert 2s^F)$	-0.01892	-	-0.01246	-0.01165	-0.01750
$(2s^C \vert 1/r_N \vert 2z^F)$	-0.10296	-	-0.10745	-0.11833	-0.09952
$(2z^C \vert 1/r_N \vert 2s^F)$	0.10289	-	0.15231	0.11692	0.10617

integrals, no useful comparisons for these integrals can yet be made. However, it would be expected that the trends shown in Table IV.31 would be confirmed for the two-electron integrals also.

Ellison [42] has suggested that different approximations should be used to evaluate specific classes of integrals on the grounds that some multicentre integral approximations are better equipped to evaluate certain types of integrals than are others.

From the point of view of consistency it would seem better to use only one approximation in a given calculation. An attempt was made in this work to perform a calculation where the one-electron integrals were evaluated by the PLA and the two-electron integrals by the IMA, but the method failed to converge to a minimum.

Although a fuller investigation of this topic is necessary it would appear that the use of more than one integral approximation per calculation should be approached with caution.

4.7. Conclusion.

Perhaps the first question pertinent to this work, which has to be answered, is whether it is now worthwhile to perform approximate calculations. Clementi [65] has recently suggested that, since there are now quite a few computer programs capable of performing accurate ab initio calculations, the effort put into semi-empirical calculations should at least be reduced.

Although such a viewpoint must be agreed with on theoretical grounds, it is not always a practical proposition. As discussed in chapter five, only now are the computers being installed in parts of the world other than North America which allow the running of these ab initio programs. The second restriction is that the amount of computer time available in many institutions is limited.

For this reason, alone, it seems necessary to search for reliable approximate methods. Also there is still a limit on the size of molecule whose structure can be elucidated, and tested approximate methods will almost certainly play a part when molecules larger than pyridine are studied.

An additional impetus to find a reliable multicentre integral approximation is provided by the desirability of using a basis set of STO's rather than one of GTF's of which many more are required to adequately reproduce the molecular properties.

Accepting that the above approach is worthwhile, there still remains the problem of deciding whether it is reasonable to employ accurate one- and two-centre integrals, and improved basis sets, when multicentre integral approximations are being invoked. From the results presented in this thesis it is felt that such improvements are definitely important provided the integral approximations are accurate enough. It is well known that the use of restricted basis sets does not yield good values for observables such as the dipole moment. It is shown here that in addition to obtaining a better total energy, the use of the double-zeta functions, in conjunction with either of the Löwdin approximations, yields a dipole moment close to the ab initio value. It is therefore, reasonably confidently predicted that further improvements to the basis set by adding in polarisation orbitals will lead to molecular properties close to those obtained by the most accurate ab initio calculations of the type performed by McLean and Yoshimine [63].

The other main objective of this work was to investigate the reliability of population analyses as guides to the electronic structure of molecules. From the results of the various population analyses presented in this chapter, it is seen that the trends shown are often at variance with each other and only one trend can be correct. Until adequate proof of which method, if any, always predicts the correct trend, the results of population analyses should be treated with caution. It is more desirable, though, of course, more time consuming, to investigate trends in electronic charge redistribution by the use of P and ΔP diagrams and profiles. However, bearing in mind results of the evaluation of the multicentre integral approximations and the more complex nature of the Doggett II method, it seems likely that the Doggett I method may be the most useful of the existing methods of determining gross atom charge densities.

CHAPTER FIVE

COMPUTER PROGRAMMING

5.1. Introduction.

Undoubtedly one of the most important developments in theoretical chemistry in the past ten or fifteen years has been the ever increasing use of the electronic digital computer. Computers have allowed the chemist to undertake calculations which would otherwise be virtually impossible or at least very time consuming and prone to error. As well as allowing him to cover much more work, machine calculation has minimised the time spent at a subprofessional level operating desk calculators.

Computers can also aid the theoretical chemist more adventurously in the fields of experimental design, simulation and evaluation but it is in the first respect which they have been used in this work.

The University of Glasgow has installed an English Electric Leo Marconi KDF9 computer which became operational just prior to the start of this work. Programming was carried out in ALGOL as defined in the KDF9 ALGOL programming manual [66].

Initially few programs were available at Glasgow and it was decided that a system of programs to effect electronic structure calculations of various degrees of complexity should be built up. During the period of this work some advances in the availability of quantum chemical computer programs were achieved both internationally and in Britain.

The Quantum Chemistry Program Exchange scheme was inaugurated in 1965 and is administered from the University of Indiana. This project is a welcome start towards the goal of saving needless duplication of programs, but at present suffers from restrictions imposed by the incompatibility of the various computers involved. Often programs are too large for some university computers or are written in whole, or in part, in specific machine codes in order to reduce run times. Computer configuration is a restriction in some cases: for example, the McLean-Yoshimine LCAO program [67] is written, partly in machine code, for an IBM 7094, a computer configuration which, as far as can be determined, is not readily available in Britain at the moment. This particular restriction will soon be removed as the program is at present being rewritten for the new IBM 360 series.

The British project, involving the 'KDF9 universities' and administered from Nottingham, is in its early stages yet but should be very useful as there are no compatibility problems here. It is hoped the computer programs described below can make a useful contribution, either in part or as a whole, to this scheme.

5.2. The Program System.

In designing the program system a compromise had to be made between the desire for generality and the problem of keeping down computer store requirements and run times. With this in mind, the programs were written so that they could be run not only in close succession, i.e. effectively as one large program, but also as individual entities realising specific results useful in other calculations. Algol procedures were written where possible as these could be useful in future programs. In this system, input data are read in from paper tape and the results are output on line print. Large matrices which are required by subsequent programs are stored on magnetic tape. Also in most programs there is the option of having these large matrices output on paper tape.

The major programs in the system are listed below and are designated by their computer identifier and a program title:

DD023AA00KP5	SCF CONTROL PROGRAM
DD023I607KP5	INVARIANT MULLIKEN ONE ELECTRON MATRICES
DD023I705KP5	PARTIAL LÖWDIN ONE ELECTRON MATRICES
DD023I804KP5	FULL LÖWDIN ONE ELECTRON MATRICES
DD023N100KP5	TWO ELECTRON INTEGRALS
DD023N200KP5	LABEL TWO ELECTRON MATRICES
DD023N301KP5	INVARIANT MULLIKEN THREE CENTRE γ INTEGRALS
DD023N401KP5	PARTIAL LÖWDIN THREE CENTRE γ INTEGRALS
DD023M306KP5	FULL LÖWDIN THREE CENTRE γ INTEGRALS
DD023N500KP5	ENERGY MINIMISATION USING $\bar{\gamma}$
DD023E206KP5	ENERGY MINIMISATION USING γ
DD023D400KP4	MO ENERGIES
DD023C106KP4	ELECTRONIC PROBABILITY DENSITIES
DD023F103KP4	MOLECULAR PROPERTIES

The function of each program is described in more detail in the succeeding paragraphs. If a program was developed in collabaration with another author, an acknowledgement is made to this effect.

Flow diagram 1 shows how the programs are linked together. The various routes can be chosen by the user, via the input data tape, by varying the parameter "scf".

5.3. The One-electron Matrices Programs: I6, I7 and I8.

Description. The purpose of each of these programs is to set up all the one electron matrices required in the SCF calculation; namely, the overlap matrix $\underset{\sim}{S}$; the matrix required for the Löwdin symmetrical orthogonalisation procedure, $\underset{\sim}{S}^{-\frac{1}{2}}$; the dipole moment matrix $\underset{\sim}{d}$; the kinetic energy matrix $\underset{\sim}{K}$; the nuclear attraction matrices $\underset{\sim}{ra}$, $\underset{\sim}{rb}$, $\underset{\sim}{rc}$; and the one-electron Hamiltonian matrices in the natural and orthogonal bases, $\underset{\sim}{f}$ and $\underset{\sim}{\bar{f}}$, respectively.

The calculation procedure is shown in flow diagram 2.

Procedure. The program first reads in general data concerning the setting up of array bounds, and the route to be taken is designated by the decision parameters. Specific data about the first diatomic fragment of the molecule are then read in: the number of AO's on centre A; the number of AO's on centre B; the internuclear distance, R_{AB} in atomic units; the Clementi double-zeta data for the AO's on A and B. All one-electron integrals involving orbitals on atoms A and B are then evaluated using Gaussian quadrature. (see appendix 1). The program then forks. If a triatomic molecule is being studied then further data are read in: the number of orbitals

FLOW DIAGRAM 1.

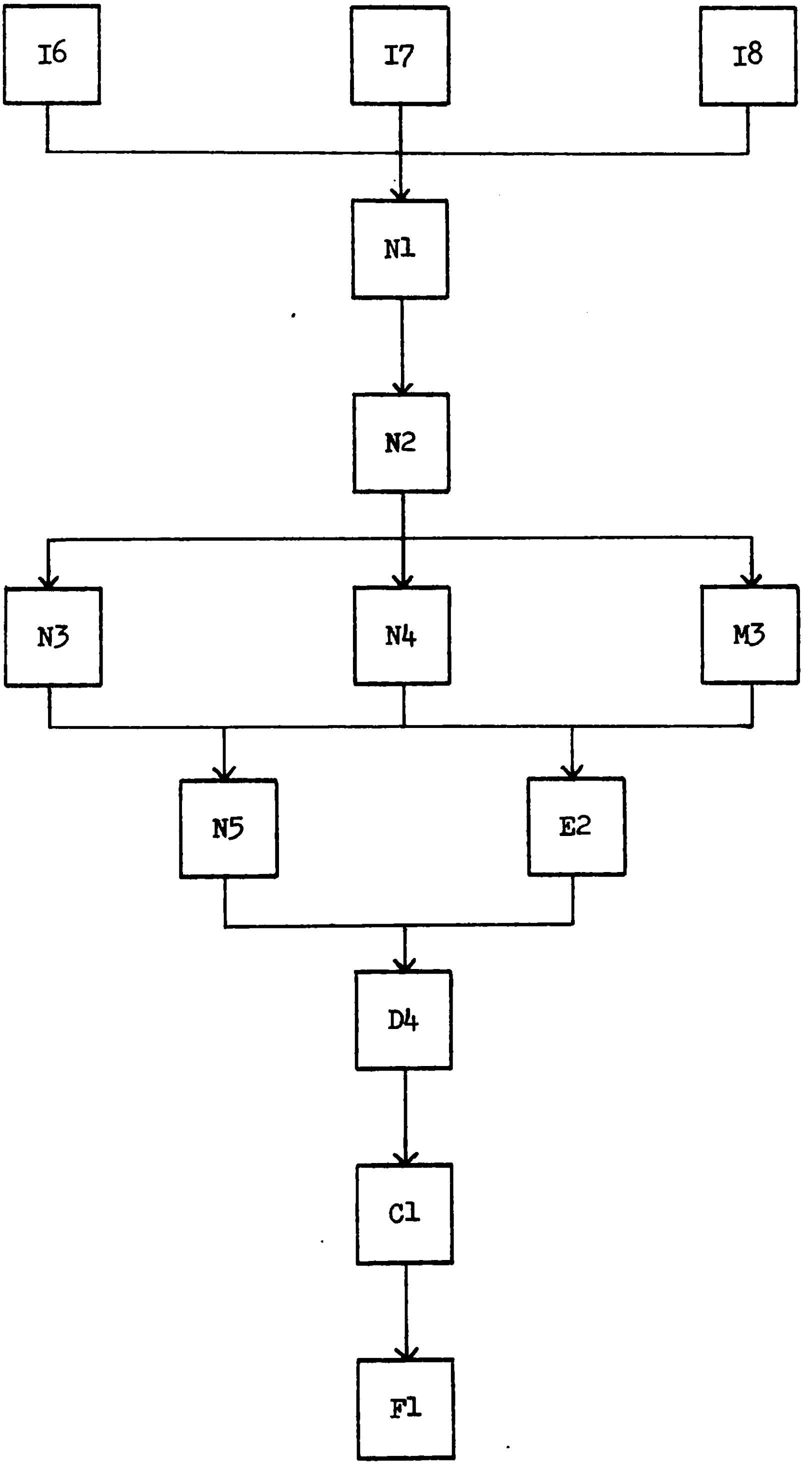

FLOW DIAGRAM 2.

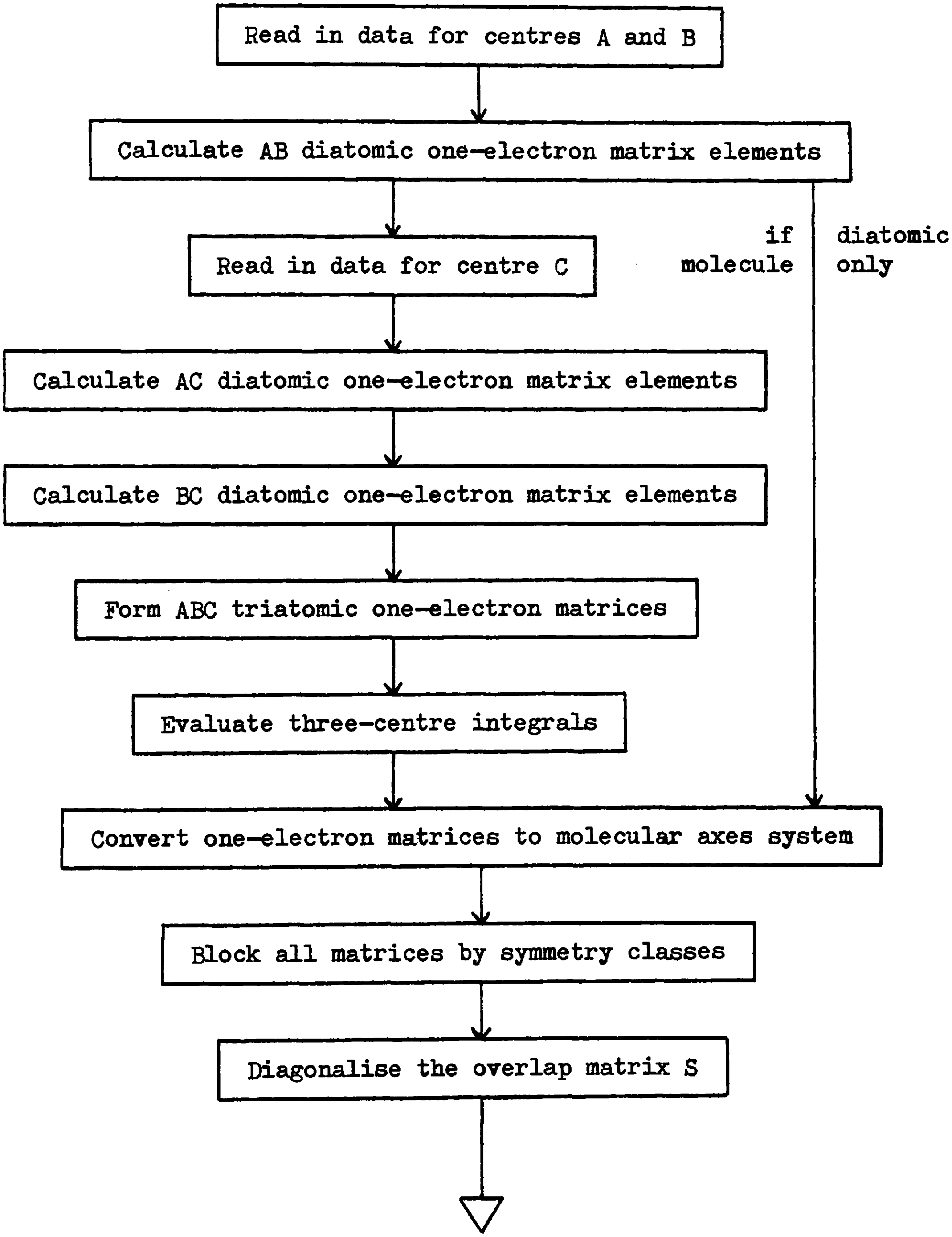

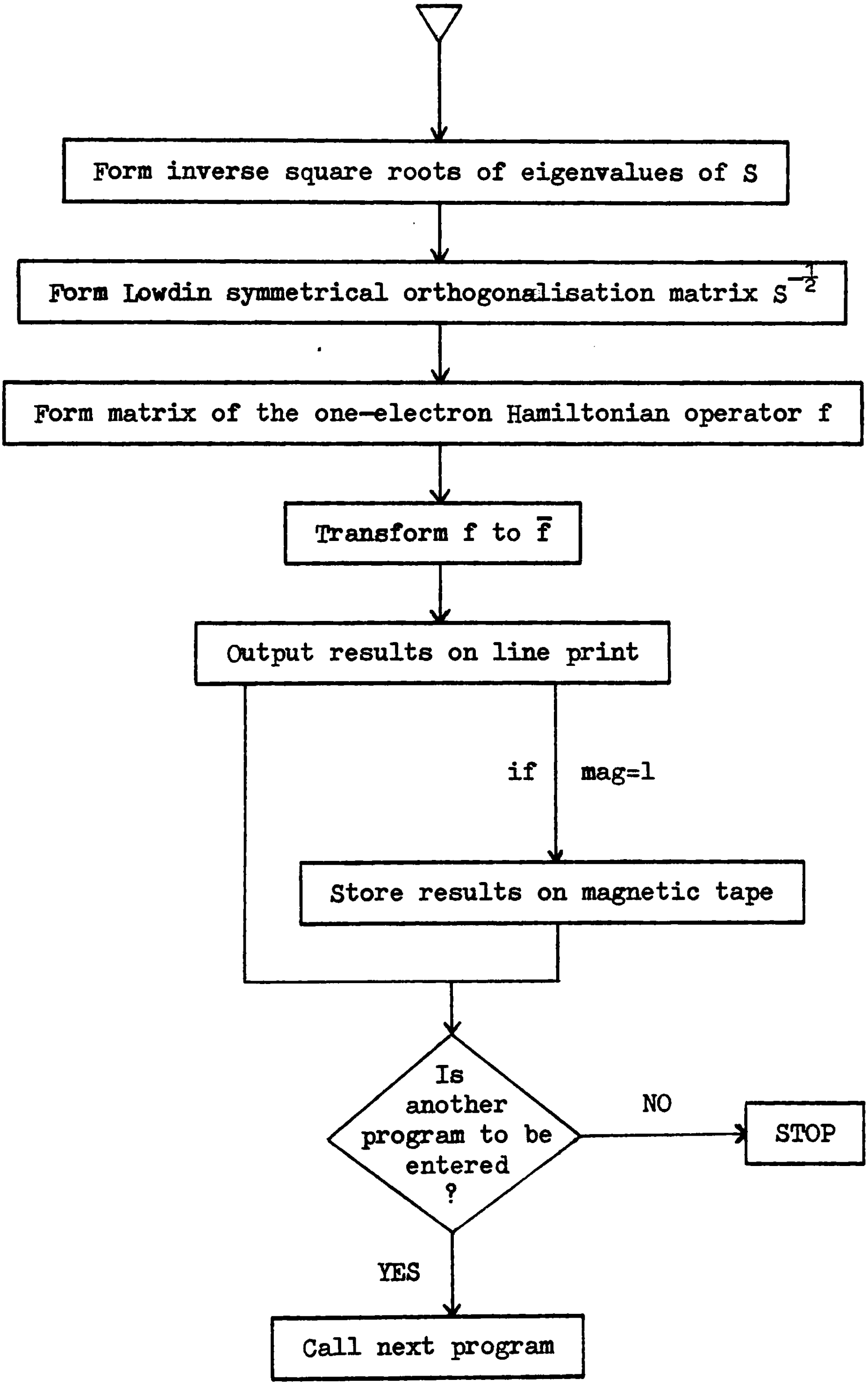
Form inverse square roots of eigenvalues of S
Form Lowdin symmetrical orthogonalisation matrix $S^{-\frac{1}{2}}$
Form matrix of the one-electron Hamiltonian operator f
Transform f to $\bar{f}$
Output results on line print
if mag=1
Store results on magnetic tape
Is another program to be entered ?
NO
STOP
YES
Call next program

on centre C; the internuclear separation R_{AC}; the Clementi double-zeta AO data for centres A and C. The one electron integrals for the A and C AO's are then evaluated. The orbital data for centres B and C, prefixed by the internuclear separation, R_{BC}, is then read in and the one-electron BC integrals are evaluated.

The one electron matrices for ABC are formed, and the integral signs are modified to allow for the change in frame of axes from the local diatomic system to the molecular frame. The next step is the evaluation of the three centre integrals. This is where the main difference in I6, I7 and I8 lies. I6 evaluates these integrals using the Mulliken approximation which has been made invariant to transformations of the basis set (Chapter 2.5). I7 provides the option of using the Mulliken approximation or the Partial Löwdin approximation, neither of which is invariant. I8 evaluates the integrals by using the Full Löwdin approximation which is invariant.

The fork ends here and if a diatomic molecule is the subject of the calculation, the one-electron matrix elements are corrected to allow for the change of axes to the molecular frame.

The one-electron MO's in a linear molecule can be classified according to the value of the component of angular momentum, λ, along the internuclear axis, taken here as the Z-axis. For $\lambda = 0$ and 1 the one-electron MO's are said to have σ and π symmetry respectively. For example, s and p_z AO's combine to give σ MO's, while p_x and p_y AO's yield π MO's. The fact that matrix elements between AO's of different symmetries are zero, can now be used to factorise the one-electron matrices.

In forming these one-electron matrices the basis functions on each atom were indexed sequentially. However, it is more convenient to index the AO's as in chapter three. In this case only AO's in the same symmetry class on an atom are numbered sequentially. This leads to the required symmetry factorisation of the matrices. As a result of this factorisation, computer store is saved and, since the effective size of the matrices being handled is now less, computer time is additionally saved.

In the programs this is achieved by interchanging rows and columns of a given matrix, $\underset{\sim}{M}$, to yield the symmetry blocked matrix, $\underset{\sim}{W}$. This is accomplished in matrix terminology by applying the following transformation:

$$\underset{\sim}{W} = \underset{\sim}{A}\,\underset{\sim}{M}\,\underset{\sim}{A}^{\dagger} \tag{V.1}$$

where A is the matrix describing how the AO's have been reordered.

$$\begin{bmatrix} 1 & 0 & 0 & 0 & 0 & 0 & 0 & 0 & 0 \\ 0 & 1 & 0 & 0 & 0 & 0 & 0 & 0 & 0 \\ 0 & 0 & 1 & 0 & 0 & 0 & 0 & 0 & 0 \\ 0 & 0 & 0 & 0 & 0 & 0 & 0 & 1 & 0 \\ 0 & 0 & 0 & 1 & 0 & 0 & 0 & 0 & 0 \\ 0 & 0 & 0 & 0 & 1 & 0 & 0 & 0 & 0 \\ 0 & 0 & 0 & 0 & 0 & 1 & 0 & 0 & 0 \\ 0 & 0 & 0 & 0 & 0 & 0 & 0 & 0 & 1 \\ 0 & 0 & 0 & 0 & 0 & 0 & 1 & 0 & 0 \end{bmatrix}$$

A for an HCN calculation is given above as an example.

It is to be noted that in these programs the p_y AO's are not considered explicitly since the integrals involving them are identical to those involving p_x AO's.

$\underset{\sim}{S}^{-\frac{1}{2}}$ is then formed by diagonalising $\underset{\sim}{S}$, taking the inverse square root of the eigenvalues in $\underset{\sim}{\Delta}$ to give $\underset{\sim}{\Delta}^{-\frac{1}{2}}$ and then performing a unitary transformation on $\underset{\sim}{\Delta}^{-\frac{1}{2}}$ with the matrix of eigenvectors $\underset{\sim}{U}$. In matrix notation, if

$$\underset{\sim}{U}^{\dagger}\,\underset{\sim}{S}\,\underset{\sim}{U} = \underset{\sim}{\Delta} \tag{V.2}$$

then

$$\underset{\sim}{S}^{-\frac{1}{2}} = \underset{\sim}{U}\,\underset{\sim}{\Delta}^{-\frac{1}{2}}\,\underset{\sim}{U}^{\dagger} \tag{V.3}$$

The Jacobi method is used to diagonalise matrices in these programs. Successive elementary orthogonal transformations chosen to nullify each off-diagonal element in turn are applied to the matrix to be diagonalised. The procedure then iterates until all off-diagonal elements are less than a previously specified allowable threshold. It is a slower method than the more preferable Givens and Householder methods but this is not too significant as the order of matrices being handled is not large, and the actual number of diagonalisations per SCF calculation is only two.

$\underset{\sim}{f}$, is then formed by the algebraic addition of its constituent one-electron integral matrices. Using $\underset{\sim}{S}^{-\frac{1}{2}}$, $\underset{\sim}{f}$ is transformed to $\underset{\sim}{\bar{f}}$, the corresponding matrix in the LOAO basis.

Finally, the results are output and if desired the next program in the system is entered.

Discussion. Rigorous tests were applied to these three programs to ensure their correct execution, and experience has shown them to be very reliable. Testing was carried out by requiring the programs to reproduce the results of hand calculations involving small matrices. In the case of the one-electron integration procedure the results were checked with the values published in Sahni and Cooley's tables [68].for single STO's. Integrals formed from double-zeta AO's were checked with results from the MI DIAT program on the Atlas computer. Table V.1 compares various integrals of double-zeta AO's as evaluated by I6, I7 or I8 and by MI DIAT.

TABLE V.1.

Comparison of One-Electron Molecular Integrals in a Double-Zeta basis as evaluated by the Glasgow Programs and by MIDIAT.

Integral	I6/I7/I8 Value	MIDIAT Value
$(2z^N \vert 2s^C)$	0.4317284	0.4317284
$(1s^C \vert -\frac{1}{2}\nabla^2 \vert 1s^C)$	16.0494005	16.0494007
$(1s^N \vert 1/r_N \vert 1s^N)$	6.6527985	6.6527985
$(2s^N \vert 1/r_C \vert 2z^N)$	0.1465831	0.1465831
$(2z^C \vert 1/r_H \vert 1s^H)$	0.5048310	0.5048310
$(2p_X^C \vert 1/r_F \vert 2p_X^F)$	0.1449265	0.1449265
$(2s^N \vert -\frac{1}{2}\nabla^2 \vert 2z^F)$	0.0099810	0.0099810

The integrals are evidently reliable to seven places of decimals and the tolerance parameter for the diagonalisation procedure was set to be compatible with this accuracy.

5.4. The Two-Electron Integral Program N1.

Description. This program evaluates the one- and two-centre two-electron coulomb and hybrid molecular integrals by the method of Gaussian quadrature, i.e. integrals of the type (AA|AA), (AA|BB) and (AA|AB). This program is designed explicitly for Clementi type AO's, but it will also evaluate the molecular integrals for single STO's. All non-zero integrals between 1s, 2s, $2p_Z$, $2p_X$ and $2p_Y$ orbitals on each of two centres are evaluated. The input data are read in from paper tape and the results output to line printer, and to magnetic tape if required. The calculation procedure is shown in flow diagram 3.

Procedure. After reading in the decision parameters, the program sets up the Gaussian quadrature mesh. (See Appendix 1). Specific data about the first diatomic fragment of the molecule are then read in. Only the number of components in the minimal basis set need be given, along with the internuclear separation and specific orbital data.

At this point the program evaluates each unique exponential which arises in the integral expressions over all mesh points. This saves the unnecessary evaluation of exponentials at every mesh point and as exponentiation is relatively costly in computer

FLOW DIAGRAM 3.

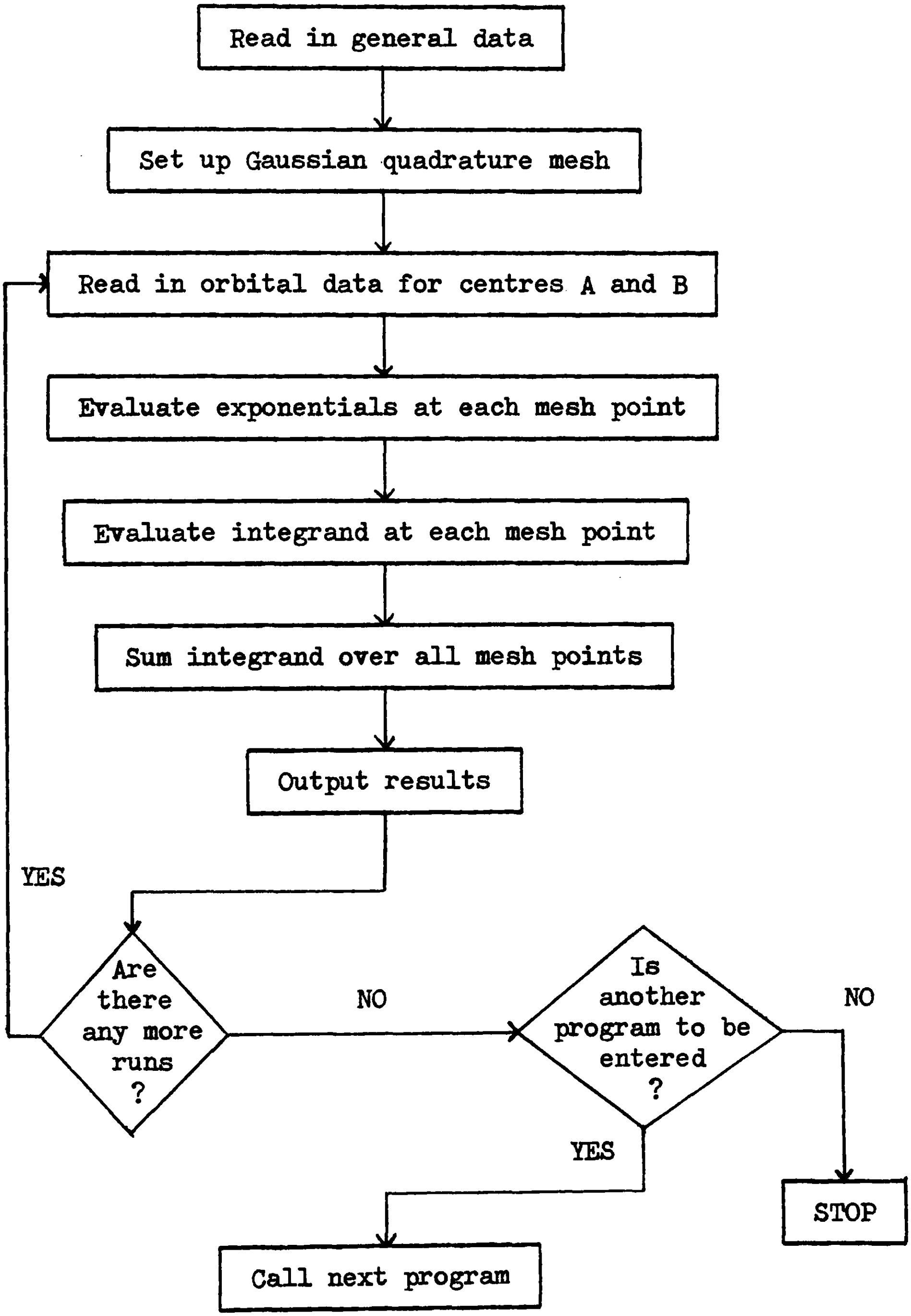

time this is an important saving.

The Gaussian quadrature consisting of (2 x 16) x 16 = 512 mesh points is then set up, the Gaussian weighted integrand evaluated at each point and then summed over all mesh points as given in appendix 1. In ALGOL such loops are easily programmed as nested for statements, i.e.

```
for i:=1 step 1 until 16 do for j:=1 step 1 until 32 do .....;
```

This part of the program consumes the most time and every computing technique which will minimise the time has been used within these for statements. The Clementi integrand

$$\sum_{abcd} \chi'_a(1)\, \chi'_b(1) \frac{1}{r_{12}}\, \chi'_c(2)\, \chi'_d(2)$$

was expressed in its two constituent parts, the Clementi potential

$$\sum_{ab} \chi'_a(1)\, \chi'_b(1) \frac{1}{r_{12}} \quad \text{and the orbital density} \quad \sum_{cd} \chi'_c(2)\, \chi'_d(2).$$

The two double summations were then performed together using another two nested for statements i.e. the summations over c and d were performed in the same loops as the summations over a and b.

Although it is convenient practice to consider two-electron integrals and orbital densities as elements of four and two dimensional arrays this is impracticable since the computer manipulation of such higher dimensioned arrays is not efficient. Consequently only one dimensional arrays are used within the multiple for statements and whenever possible single variables are substituted even for elements of these one-dimension arrays. For example, an array element appearing in an inner for statement but which remains constant throughout its execution since it depends on an outer for parameter, is assigned to a real variable whose access time in the computer is significantly less.

The results are output to the line printer and magnetic tape and optionally to the paper tape punch. N1 can then enter the SCF control program if desired.

Discussion. At the start of this research work the coulomb and hybrid integrals were obtained, as the exchange integrals still are, from the MIT diatom program [52] available at the SRC ATLAS computing laboratory at Didcot. Although the integrals were accurate enough there was the physical problem of transferring the integral values from line printer or paper tape output to suitably ordered input for KDF9. It was decided to eliminate most of this time consuming data handling by writing this program. At the same time the chance was taken to use a Gaussian rather than a Simpson grid thus yielding greater accuracy for comparable grid sizes.

The integral values were tested by comparing them with the published tables of coulomb integrals by Sahni and Cooley [68] and of hybrid integrals by Preuss [69] and Kotani [70]. In addition, the integrals from N1 were checked with those from Corbató and Switendick's MIDIAT program. A few examples of this last integral comparison are given in Table V.2.

TABLE V.2.

Comparison of Two-Electron Molecular Integrals in a Double-Zeta basis as evaluated by the Glasgow Programs and by MIDIAT.

Integral	N1 Value	MIDIAT Value
$(1s^C2z^C\|1/r_{12}\|2s^F2z^F)$	0.00592684	0.00592684
$(2z^N2x^N\|1/r_{12}\|2z^F2x^F)$	0.00083697	0.00083697
$(2s^C2z^C\|1/r_{12}\|2s^C2z^C)$	0.11460861	0.11460861
$(1s^C2s^F\|1/r_{12}\|2s^F2s^F)$	-0.01272423	-0.01272429
$(1s^C2z^C\|1/r_{12}\|1s^H1s^H)$	0.01404553	0.01404553
$(1s^H1s^H\|1/r_{12}\|1s^H2s^C)$	0.31256598	0.31256596
$(1s^N2z^N\|1/r_{12}\|1s^H2z^N)$	0.00247795	0.00247794

All two-centre coulomb and hybrid integrals are accurate to seven or eight decimal places. In most cases the one-centre integrals have a similar accuracy, but in a few one-centre integrals involving highly contracted 1s AO's, some accuracy is lost. The diatomic mesh is inadequate for these integrals but the accuracy only falls below five decimal places for one-centre integrals involving the Fluorine 1s AO. Although integrals accurate to five decimal places are probably sufficient for molecular computations, this is a possible limitation on the extension of this program to elements of the second row of the periodic table.

Table V.3 compares some one-centre integrals evaluated by N1 and

MIDIAT with accurate analytic values.

TABLE V.3.

Comparison of Analytically obtained One-Centre Two-Electron Molecular Integrals in a Double-Zeta basis with those evaluated by N1 and MIDIAT.

Integral	MIDIAT Value	N1 Value	Analytic Value
$(1s^N 1s^N \vert 1/r_{12} \vert 1s^N 1s^N)$	4.12841405	4.12497454	4.12497823
$(1s^N 1s^N \vert 1/r_{12} \vert 1s^N 2s^N)$	-0.40564392	-0.40502596	-0.40502650
$(1s^N 1s^N \vert 1/r_{12} \vert 2s^N 2s^N)$	0.97063772	0.97027951	0.97027958
$(1s^N 2s^N \vert 1/r_{12} \vert 1s^N 2s^N)$	0.06448263	0.06437717	0.06437726
$(1s^N 2s^N \vert 1/r_{12} \vert 2s^N 2s^N)$	-0.01708425	-0.01701217	-0.01701218
$(2s^N 2s^N \vert 1/r_{12} \vert 2s^N 2s^N)$	0.68323552	0.68320893	0.68320893
$(1s^N 1s^N \vert 1/r_{12} \vert 2z^N 2z^N)$	0.94921442	0.94897163	0.94897163
$(1s^N 2s^N \vert 1/r_{12} \vert 2z^N 2z^N)$	-0.01150523	-0.01145178	-0.01145178
$(2s^N 2s^N \vert 1/r_{12} \vert 2z^N 2z^N)$	0.66904289	0.66903122	0.66903122
$(1s^C 1s^C \vert 1/r_{12} \vert 1s^C 1s^C)$	3.50903057	3.50893809	3.50893004
$(1s^C 1s^C \vert 1/r_{12} \vert 1s^C 2s^C)$	-0.33567295	-0.33565721	-0.33565671
$(1s^C 1s^C \vert 1/r_{12} \vert 2s^C 2s^C)$	0.81090513	0.81089585	0.81089484
$(1s^C 2s^C \vert 1/r_{12} \vert 1s^C 2s^C)$	0.05187206	0.05186950	0.05186945
$(1s^C 2s^C \vert 1/r_{12} \vert 2s^C 2s^C)$	-0.01332651	-0.01332473	-0.01332473
$(2s^C 2s^C \vert 1/r_{12} \vert 2s^C 2s^C)$	0.57244152	0.57244089	0.57244089
$(1s^C 1s^C \vert 1/r_{12} \vert 2z^C 2z^C)$	0.77688788	0.77688149	0.77688568

TABLE V.3 continued.

Integral	MIDIAT Value	N1 Value	Analytic Value
$(1s^C2s^C\|1/r_{12}\|2z^C2z^C)$	-0.00840630	-0.00840498	-0.00840502
$(2s^C2s^C\|1/r_{12}\|2z^C2z^C)$	0.55461666	0.55461639	0.55462033
$(1s^F1s^F\|1/r_{12}\|1s^F1s^F)$	5.37250504	5.35699773	5.35714532
$(1s^F1s^F\|1/r_{12}\|1s^F2s^F)$	0.55031953	0.54735516	0.54738500
$(1s^F1s^F\|1/r_{12}\|2s^F2s^F)$	1.29782875	1.29614476	1.29615037
$(1s^F2s^F\|1/r_{12}\|1s^F2s^F)$	0.09136712	0.09082921	0.09083570
$(1s^F2s^F\|1/r_{12}\|2s^F2s^F)$	0.02540711	0.02504907	0.02505023
$(2s^F2s^F\|1/r_{12}\|2s^F2s^F)$	0.91001835	0.90988003	0.90988026
$(1s^F1s^F\|1/r_{12}\|2z^F2z^F)$	1.25886631	1.25778258	1.25778246
$(1s^F2s^F\|1/r_{12}\|2z^F2z^F)$	0.01729283	0.01703815	0.01703813
$(2s^F2s^F\|1/r_{12}\|2z^F2z^F)$	0.88301559	0.88295654	0.88295654

It can be seen from Table V.3 that the diatomic mesh used in MIDIAT gives a much poorer integration of the one-centre integrals than does N1 although both are chosen to give two-centre integrals accurate to at least six decimal places. Improved values of these integrals can be obtained from MIDIAT, of course, by choosing a different mesh but this is inconvenient. As stated elsewhere, these analytically obtained integrals were used in the SCF calculations reported in chapter four.

Nl takes about 0.4 seconds to evaluate an integral of single STO's but, as it is written specifically for Clementi's double-zeta AO's which can implicitly contain the weighted sum of 256 STO's, Nl takes only 0.785 seconds per "Clementi" integral.

5.5. The Labelling Program N2.

Description. This program is complementary to Nl. It takes the output of Nl, reorders the integrals and assigns them to their unique positions in the reduced two-electron integral matrices. It also accepts the exchange integrals from paper tape input and assigns them similarly. The manipulation procedure is shown in flow diagram 4.

Procedure. The general input data are read in and it is from this that the array sizes of the reduced two-electron matrices are calculated. This is an important space saving procedure and is discussed below.

Since the complete matrix of two-electron integrals, $\underset{\sim}{\gamma}$, can be regarded as a direct product matrix, its order is the square of the total number of AO's in the basis set. For example in HCN with a minimal basis set, a one-electron matrix would be an 11 x 11 containing 121 elements while the two-electron matrix would be a 121 x 121 containing 14,641 elements. Obviously this would be impracticable since most computers have immediate access stores of only 8K, 16K or 32K. Certainly complicated handling procedures

FLOW DIAGRAM 4.

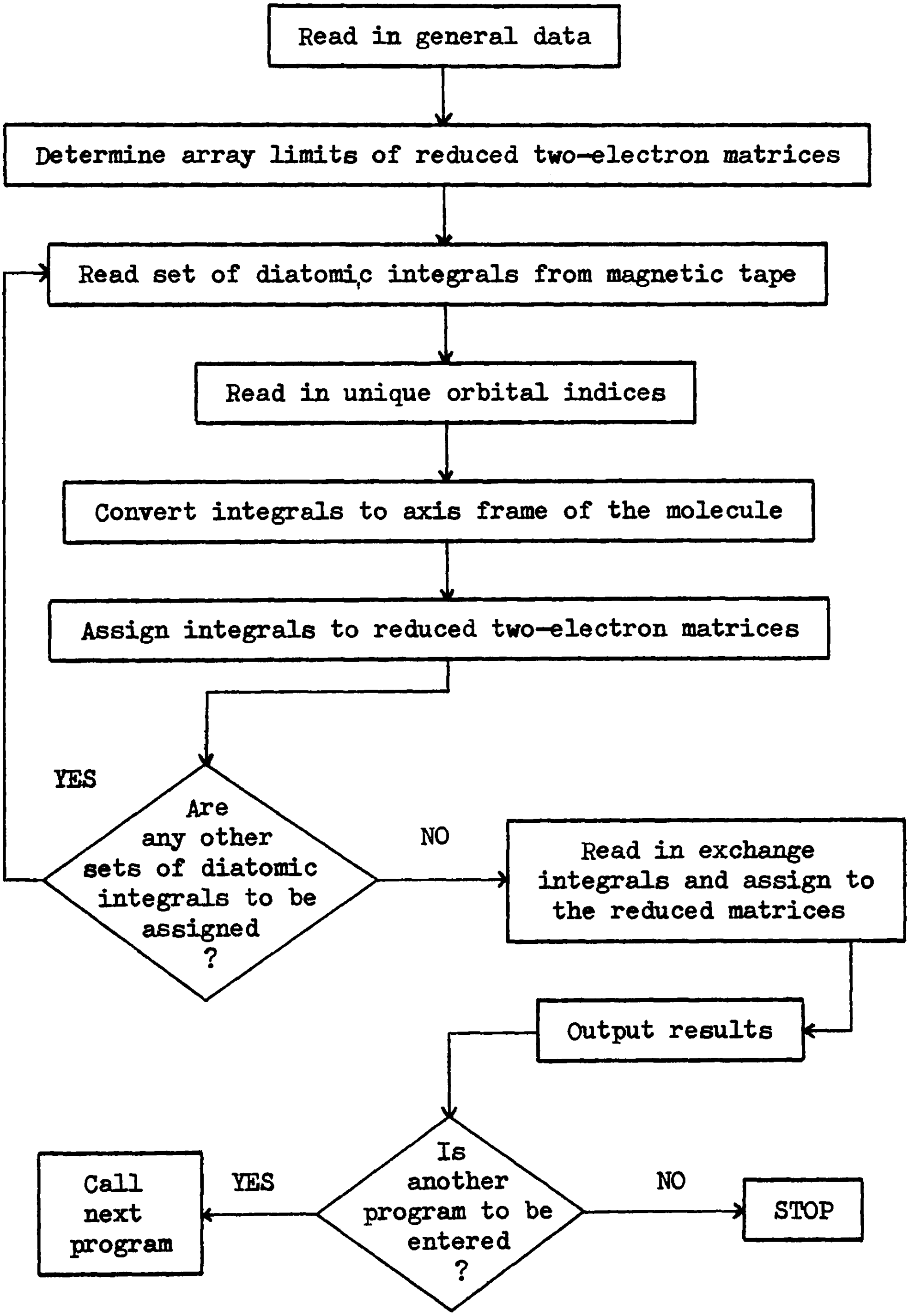

involving backing store would have to be used.

However many of these 14,641 elements are zero by symmetry and by rearranging rows and columns this matrix can be factorised into blocks as shown in figure V.1. The six unique blocks which contain all integrals between AO's in a linear molecule can be denoted by $(\sigma\sigma|\sigma\sigma)$, $(\sigma\sigma|\pi\pi)$, $(\pi\pi|\pi\pi)$, $(\pi\pi|\pi'\pi')$, $(\sigma\pi|\sigma\pi)$ and $(\pi\pi'|\pi\pi')$. The largest of these is the $(\sigma\sigma|\sigma\sigma)$ block containing in the case of HCN, $7^2 x 7^2 = 2{,}401$ elements. This is an improvement but is still impracticable for core store usage, especially when molecules such as FCN are to be studied.

Each element of these arrays containing the two-electron integrals is designated by four subscripts i, j, k, l. These can occur in any order. For example, in the sigma matrix, if i=j=k=l there is only one element with the value of the integral γ_{ijkl} but if $i \neq j \neq k \neq l$ there are eight positions containing the same integral value. What is wanted, therefore, is either a one dimensional matrix containing only the unique integral value or a two dimensional array with the unique values stored in the upper triangle. The conditions for such an element are fourfold, $i \leqslant j$, $k \leqslant l$, $i \leqslant k$, and when i=k then j=l.

These unique elements can be stored in the upper triangle of a $n(n+1)/2 \times n(n+1)/2$ matrix involving in the case of HCN only 406 stores.

The formula for reducing the element of a four dimensional

FIGURE V.1.

Diagram to show Factorisation of Υ Matrix by Symmetry.

<table>
<tr><td>σσσσ</td><td>σσππ</td><td>σσπ'π'</td><td colspan="2" rowspan="3">0</td><td colspan="2" rowspan="3">0</td><td colspan="2" rowspan="3">0</td></tr>
<tr><td>ππσσ</td><td>ππππ</td><td>πππ'π'</td></tr>
<tr><td>π'π'σσ</td><td>π'π'ππ</td><td>π'π'π'π'</td></tr>
<tr><td colspan="3" rowspan="2">0</td><td>σπσπ</td><td>σππσ</td><td colspan="2" rowspan="2">0</td><td colspan="2" rowspan="2">0</td></tr>
<tr><td>πσσπ</td><td>πσπσ</td></tr>
<tr><td colspan="3" rowspan="2">0</td><td colspan="2" rowspan="2">0</td><td>σπ'σπ'</td><td>σπ'π'σ</td><td colspan="2" rowspan="2">0</td></tr>
<tr><td>π'σσπ'</td><td>π'σπ'σ</td></tr>
<tr><td colspan="3" rowspan="2">0</td><td colspan="2" rowspan="2">0</td><td colspan="2" rowspan="2">0</td><td>ππ'ππ'</td><td>ππ'π'π</td></tr>
<tr><td>π'πππ'</td><td>π'ππ'π</td></tr>
</table>

All off-diagonal blocks which are unnamed contain integrals whose values are zero by symmetry.

matrix of the symmetry type $(\lambda\lambda|\lambda\lambda)$ to its unique two dimensional counterpart is as follows. In reducing the matrix element (i,j,k,l) to the element (p,q) the expression for q in terms of k and l is identical to the expression for p in terms of i and j.

$$p = \tfrac{1}{2}(b-1)(2n-b+2)+a+1 \tag{V.4}$$

where $a = |i-j|$, $b = \frac{1}{2}(i+j-a)$ and n^2 is the order of the two-electron matrix. In the case of the matrices of the symmetry type $(\lambda\lambda|\mu\mu)$, the element (i,j,u,v) is reduced to (p,x) in the same manner as given above. However, the conditions for such a matrix are different since now only $i \leqslant j$ and $u \leqslant v$. This results in every element (p,x) in the reduced matrix being filled. For matrices of the symmetry type $(\lambda\mu|\lambda\mu)$ the elements of the reduced matrix are stored in the upper triangle. Here, the element (i,u,j,v) is reduced to (p,q) and the conditions for this matrix are that $i \leqslant j$ and for $i = j$, $u \leqslant v$. p is given in terms of i and u by (V.5).

$$p = \tfrac{1}{2}(m_\lambda-m_\mu+1)(i+u-a)+a+1 \tag{V.5}$$

where $a = |i-u|$ and m_λ and m_μ are the number of orbitals with symmetry λ and μ respectively.

After setting up the two-electron reduced matrices, and zeroing them, the program reads the first set of diatomic integrals from magnetic tape. The orbital numbering appropriate to the two atoms involved is then read in and the integrals are assigned by the above formulae to their correct position in the arrays. If one of the atoms is hydrogen the program forks through a shorter route thus cutting down the run time. The integrals are also axis corrected from the local diatomic system to the molecular system in this section of the program.

N2 then cycles back if more sets of diatomic integrals are to be read in and repeats the above process until all integrals have been assigned to their appropriate array position. The exchange integrals which are evaluated using the MIDIAT program are read in from paper tape and assigned to their array positions.

The reduced arrays which now lack only the three-centre integrals are output on line print and stored on magnetic tape. N2 then enters the next program in the system.

Discussion. This program was tested by the only method available, namely by following through the procedure by hand and checking to ensure that each integral value occupied the correct array site.

The main limitation of this program is that it is specifically designed for linear molecules. However the method and procedures are quite general and N2 could easily be adapted to study simple molecules of any configuration.

5.6. The Multicentre Integral Approximations and Orthogonal Transformation Programs N3, N4 and M3.

Description. These programs evaluate the two-electron three-centre integrals by various approximate methods. N3 uses the well-known Mulliken Approximation which has been additionally made invariant to transformations of the basis set. N4 has the option of two approximations: either the simple Mulliken Approximation or the Partial Löwdin method, neither of which is invariant to orthogonal transformations of the basis set. M3 uses the Full Löwdin method which is an invariant procedure. If desired, these programs can also transform the integrals from the basis of natural AO's to one of LOAO's.

Input is again from magnetic tape and the results are output on line print and stored either on magnetic tape or on paper tape. The calculation procedure is shown in flow diagram 5.

Procedure. The general input data is read in and the array stores reserved. The two-electron reduced matrices and the Löwdin orthogonalisation matrix are then read from magnetic tape. If three-centre integrals are to be evaluated the overlap matrix is read from magnetic tape. In the case of N4 and M3, the bond asymmetry matrix is also read in. The three-centre integrals are then evaluated by the appropriate integral approximations, as given in 2.5, and assigned to the empty array stores.

An additional optional facility is included in the program at

FLOW DIAGRAM 5.

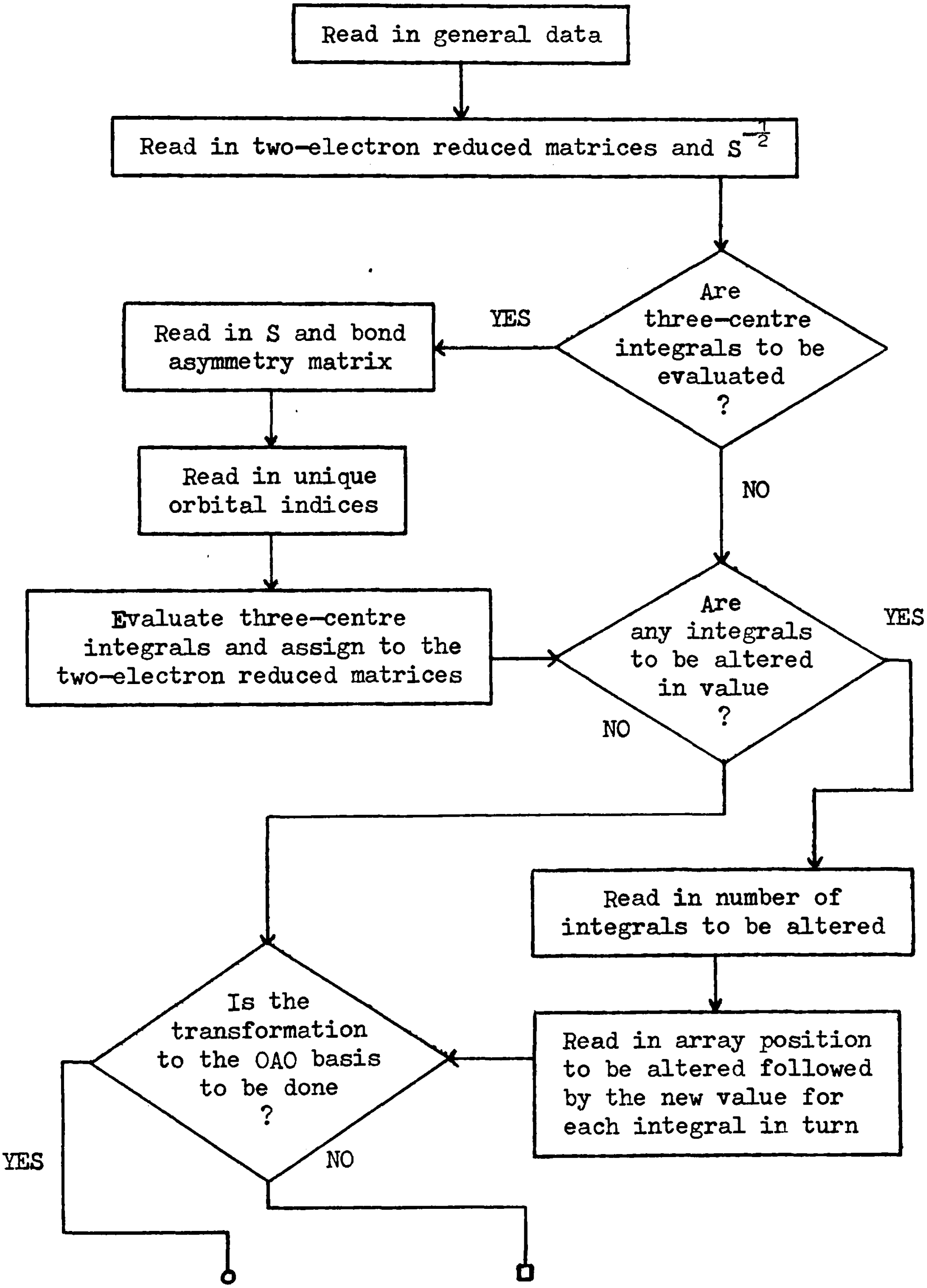

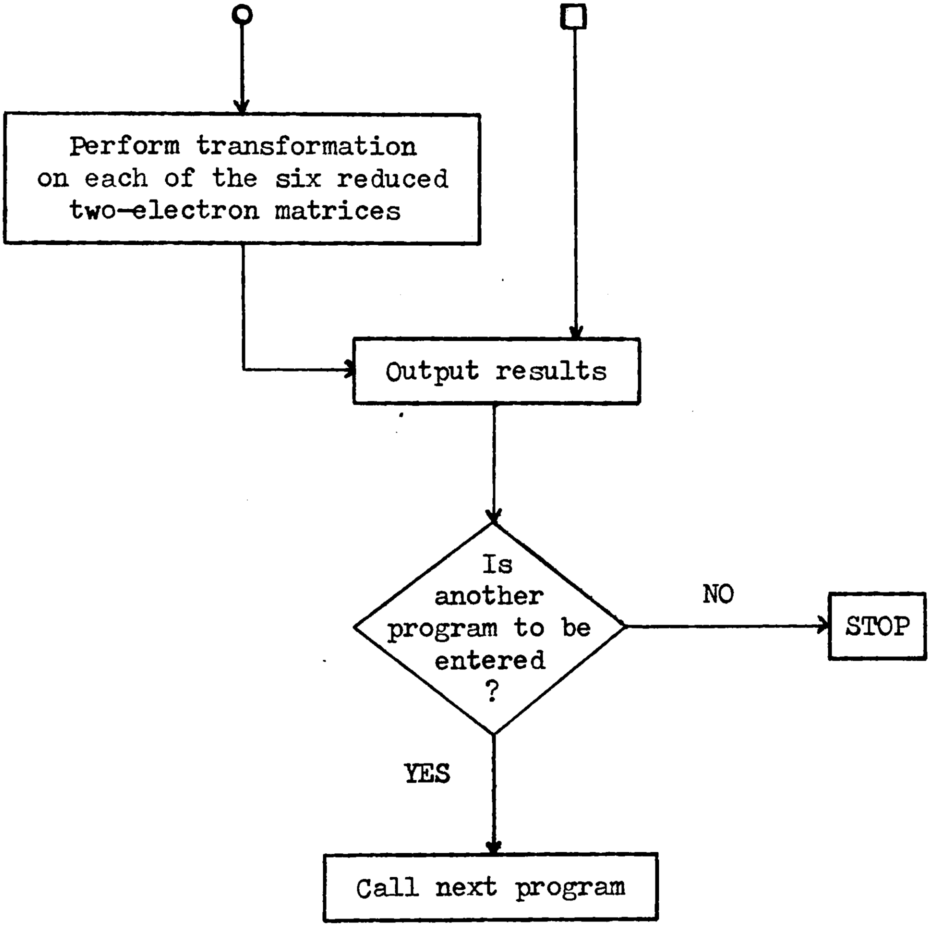
Perform transformation on each of the six reduced two-electron matrices
Output results
Is another program to be entered ?
NO
STOP
YES
Call next program

this point. This facility allows the value of any integral in any of the two-electron arrays to be changed if desired. This could be useful if, for example, accurate multi-centre integrals were to become available from some other source. Another use would be for overwriting any integral value which is suspected of being inaccurate. To effect such a change the program reads the number of integrals to be changed from paper tape, together with the four dimensional subscripts for each integral followed by the new values. The switch facility in ALGOL is used to choose the array in which the desired alteration is to be made.

The final section of the program is also optional. Here, two-electron integrals which have been evaluated in the basis of natural AO's can be transformed to one of orthogonalised AO's as in 2.3.

$$\bar{\underset{\sim}{Y}} = (\underset{\sim}{S}^{-\frac{1}{2}} x \underset{\sim}{S}^{-\frac{1}{2}}) \underset{\sim}{Y} (\underset{\sim}{S}^{-\frac{1}{2}} x \underset{\sim}{S}^{-\frac{1}{2}}) \qquad (V.6)$$

This equation, although simple to programme, requires a considerable amount of computer storage. An entirely equivalent if less concise way of writing the above equation is

$$(ij|kl) = \sum_p \sum_q \sum_r \sum_s S_{ip}^{-\frac{1}{2}} S_{jq}^{-\frac{1}{2}} S_{rk}^{-\frac{1}{2}} S_{sl}^{-\frac{1}{2}} (pq|rs) \qquad (V.7)$$

A large amount of core store is saved by specifying only the unique elements of $\underset{\sim}{S}^{-\frac{1}{2}}$ and (pq|rs) i.e. by using $\underset{\sim}{S}^{-\frac{1}{2}}$ as a one-dimensional matrix of n(n+1)/2 elements and (pq|rs) in the two-dimensional reduced form as described earlier. It is, however, questionable if much, if indeed any, time is saved because of the complex nested <u>for</u> statements which are required for the evaluation.

In order that all the integrals of $\underset{\sim}{\Upsilon}$ are summed with their correct coefficients, (V.7) has to be modified slightly.

$$(ij|kl) = \sum_{(pq)\leqslant(rs)}\sum \left\{ \begin{array}{c} [S_{ip}^{-\frac{1}{2}}S_{jq}^{-\frac{1}{2}} \oplus S_{iq}^{-\frac{1}{2}}S_{jp}^{-\frac{1}{2}}][S_{rk}^{-\frac{1}{2}}S_{sl}^{-\frac{1}{2}} \oplus S_{sk}^{-\frac{1}{2}}S_{rl}^{-\frac{1}{2}}] \\ \oplus [S_{ir}^{-\frac{1}{2}}S_{js}^{-\frac{1}{2}} \oplus S_{is}^{-\frac{1}{2}}S_{jr}^{-\frac{1}{2}}][S_{pk}^{-\frac{1}{2}}S_{ql}^{-\frac{1}{2}} \oplus S_{qk}^{-\frac{1}{2}}S_{pl}^{-\frac{1}{2}}] \end{array} \right\} (pq|rs) \tag{V.8}$$

where, symbolically,
$$\begin{aligned} f(pq)\oplus f(qp) &= f(pq)+f(qp) && \text{if } p\neq q \\ &= f(pp) && \text{if } p=q \end{aligned}$$

and
$$\begin{aligned} f(pq,rs)\oplus f(rs,pq) &= f(pq,rs)+f(rs,pq) && \text{if } (pq)\neq(rs) \\ &= f(pq,pq) && \text{if } (pq)=(rs). \end{aligned}$$

The five rules for the ordering of these indices and indice pairs are as follows:

a) $p \leqslant q$

b) $r \leqslant s$

c) $p \leqslant r$

d) $(pq) < (rs)$ if $p < r$ or if $p = r$ and $q < s$

e) $(pq) = (rs)$ if $p = r$ and $q = s$ or if $p = q = r = s$

This analysis has been given previously by Nesbet [71].

By suitable choice of the parameter 'scf' read in at the beginning of the program, the next program in the series may be entered.

Discussion. The run times for any of these programs is negligible compared with the complete SCF calculation if the OAO transformation is not required. Otherwise these programs account for about 40% of the SCF calculation time.

The programs were carefully tested by hand using small matrices. The evaluation of the multi-centre integrals was also checked by hand calculation.

5.7. The Energy Minimisation Programs, N5 and E2.

Description. These programs carry out the SCF iterations to obtain the minimum in the electronic energy. McWeeny's Density Matrix method is used to obtain the best descent on the energy surface for each cycle. The programs additionally perform a Mulliken population analysis. Data are read in from paper tape and magnetic tape and the results are output on line print and optionally stored on paper tape or magnetic tape.

The calculation procedure is shown in flow diagram 6.

Procedure. After the general data are read in, the required one- and two-electron matrices are read from magnetic tape. The iterative SCF procedure requires a trial density matrix, $\underset{\sim}{\bar{R}}$, as a first approximation and this is read in from paper tape. $\underset{\sim}{\bar{R}}$ is first of all made idempotent and is then used to calculate $\underset{\sim}{\bar{G}}$. It is in this step that the programs N5 and E2 differ.

FLOW DIAGRAM 6.

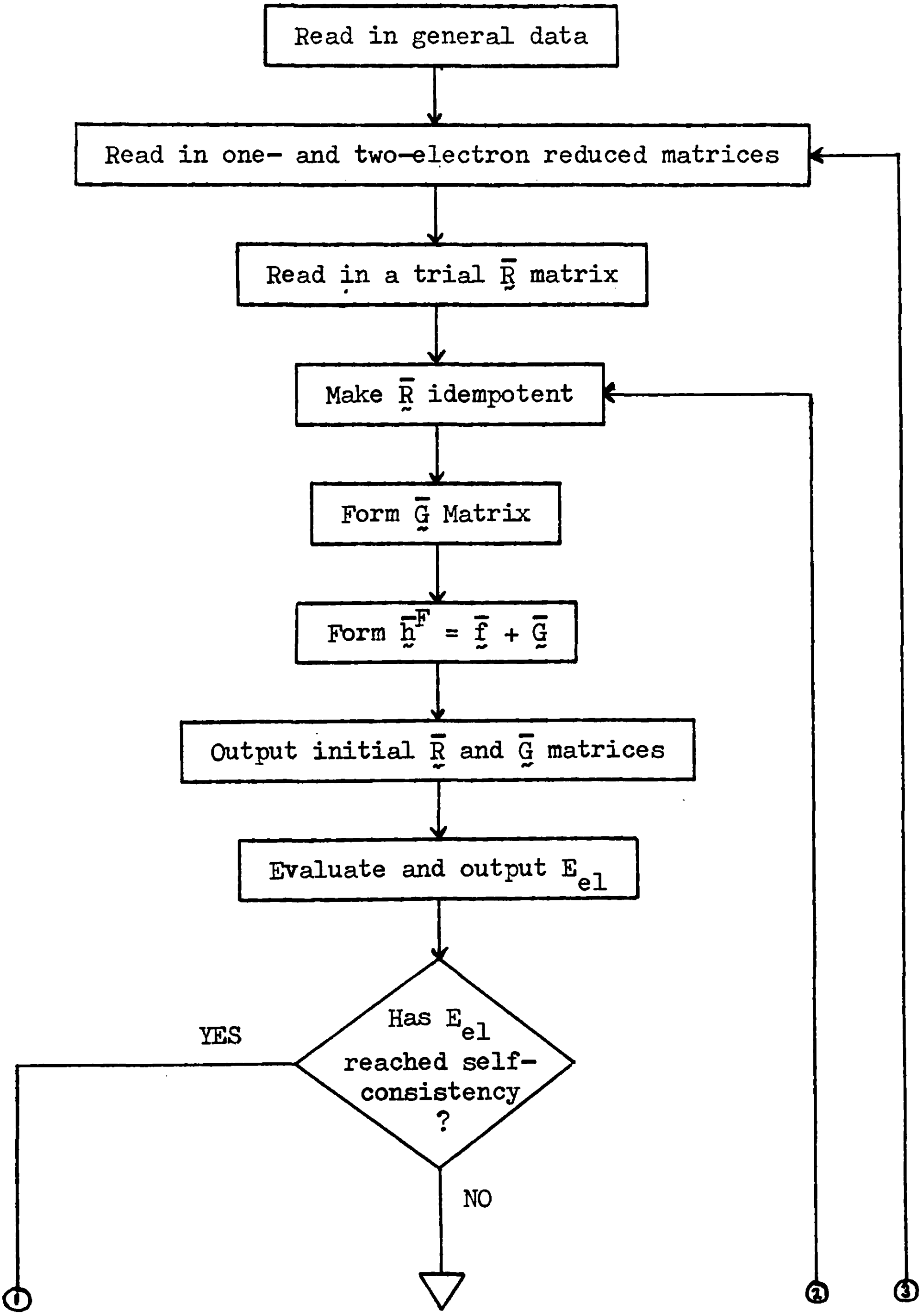

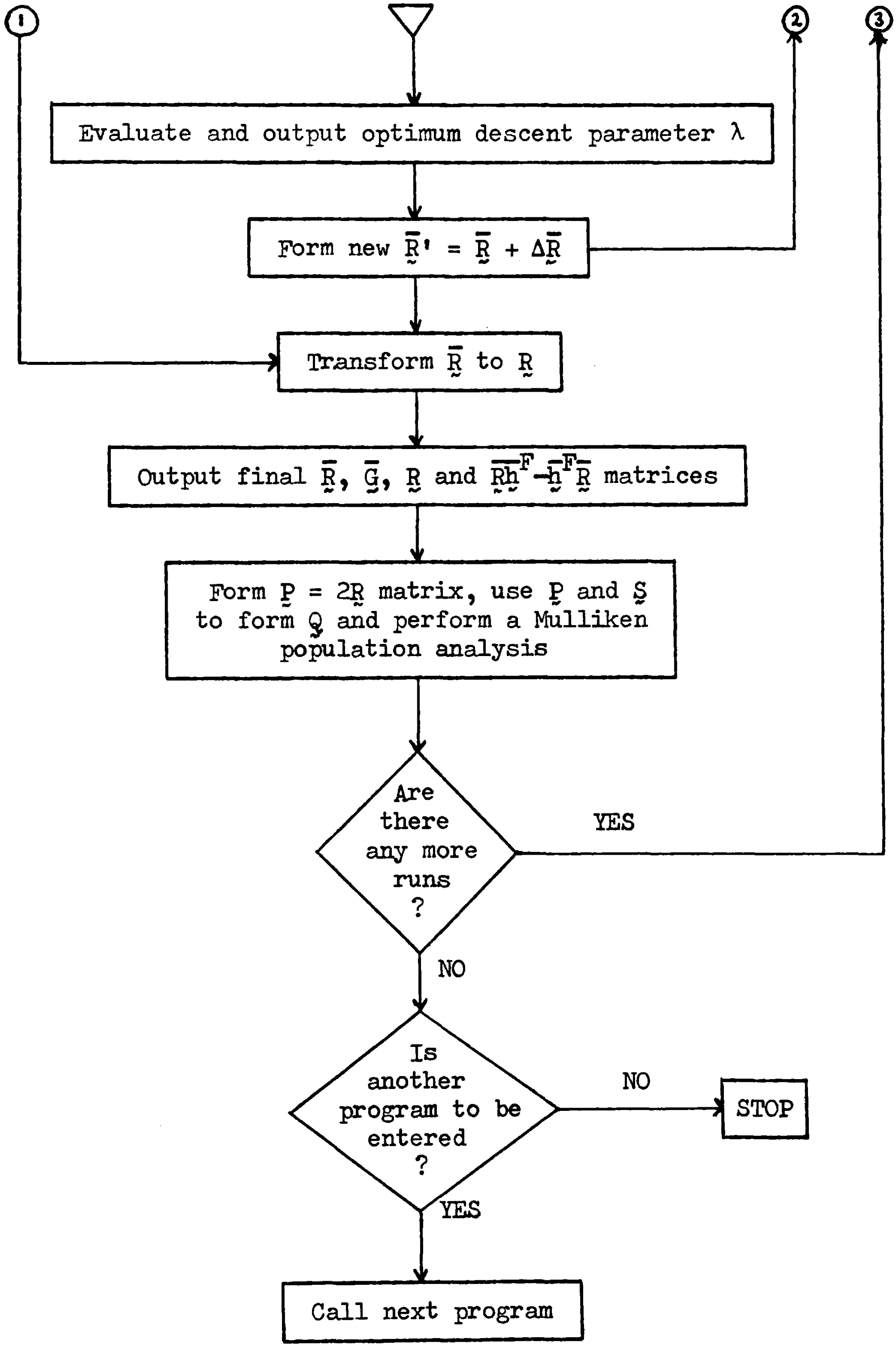
①
②
③
Evaluate and output optimum descent parameter λ
Form new $\bar{R}' = \bar{R} + \Delta\bar{R}$
Transform $\bar{R}$ to R
Output final $\bar{R}$, $\bar{G}$, R and $\overline{Rh^F - h^F R}$ matrices
Form $P = 2R$ matrix, use P and S to form Q and perform a Mulliken population analysis
Are there any more runs ?
YES
NO
Is another program to be entered ?
NO
STOP
YES
Call next program

N5 evaluates $\underset{\sim}{\bar{G}}$ directly from $\underset{\sim}{\bar{R}}$ and the OAO transformed two-electron integrals $\underset{\sim}{\bar{\Upsilon}}$. But as was pointed out in 5.6 it is very time consuming to obtain $\underset{\sim}{\bar{\Upsilon}}$, and E2 was developed to avoid this. E2 first of all transforms $\underset{\sim}{\bar{R}}$ to $\underset{\sim}{R}$, the representation of the density matrix in the natural AO basis and evaluates $\underset{\sim}{G}$ using $\underset{\sim}{R}$ and $\underset{\sim}{\Upsilon}$ which is also in the natural AO basis. $\underset{\sim}{\bar{G}}$ is then formed from $\underset{\sim}{G}$ using (II.32).

The matrix of the Hartree-Fock Hamiltonian, $\underset{\sim}{\bar{h}}^F$, is formed and the total electronic energy is evaluated from the equation,

$$E_{el} = 2 \operatorname{tr} \underset{\sim}{\bar{R}}\, \underset{\sim}{\bar{f}} + \operatorname{tr} \underset{\sim}{\bar{R}}\, \underset{\sim}{\bar{G}}$$

Normally the test for self-consistency is that the LCAO MO coefficients from successive iterations should be identical within the accuracy of the calculation. In N5 and E2 these coefficients appear implicitly in $\underset{\sim}{\bar{R}}$, and it is more convenient to terminate the calculation when two successive values of the total electronic energy are self-consistent to any required accuracy. Experience has shown that an E self-consistent to six decimal places is roughly equivalent to $\underset{\sim}{\bar{R}}$ being self-consistent to three decimal places. In this case the commutator $\overline{\underset{\sim}{R}\underset{\sim}{h}}^F - \overline{\underset{\sim}{h}^F\underset{\sim}{R}}$ is zero to at least three decimal places.

If self-consistency has not been reached the programs follow the method of steepest descents outlined by McWeeny [11]. From the optimum value of the steepest descent parameter, λ, the best correction $\Delta\underset{\sim}{\bar{R}}$ is formed and a new trial matrix $\underset{\sim}{\bar{R}}'$ is set up. The program then cycles back to make $\underset{\sim}{\bar{R}}'$ idempotent.

The total electronic energy is output to line printer at each cycle as is λ_{opt}. The current $\underset{\sim}{\bar{R}}$ and the commutator $(\underset{\sim}{\bar{R}}\underset{\sim}{\bar{h}}^F-\underset{\sim}{\bar{h}}^F\underset{\sim}{\bar{R}})$, which should be zero at the energy minimum, are also output every five iterations. When self-consistency has been attained, $\underset{\sim}{\bar{R}}$, $\underset{\sim}{\bar{G}}$, $\underset{\sim}{R}$ and $(\overline{\underset{\sim}{R}\underset{\sim}{h}}^F-\underset{\sim}{\bar{h}}^F\underset{\sim}{\bar{R}})$ are output on line print. There is also the option here of storing the $\underset{\sim}{\bar{h}}^F$ and $\underset{\sim}{R}$ matrices on magnetic tape and on paper tape.

The programs end by performing a Mulliken population analysis. The orbital population matrix, the atom and bond charge densities, the gross orbital charge densities and the gross atom charge densities are all evaluated. If it is desired, the next program in the system may then be entered.

Discussion. The density matrix iteration scheme is much faster and converges more quickly than the conventional SCF scheme which involves a matrix diagonalisation at each cycle. Approximate speeds range between 10 and 30 seconds for one iteration in the case of HCN, with N5 tending to be quicker than E2.

Again the testing was quite rigorous, the first few cycles being evaluated by hand for simple matrices of small order. A more satisfactory test applied was the reproduction of a published calculation as discussed in 5.11.

5.8. The Molecular Orbital Energies Program D4.

Description. This program diagonalises the self-consistent matrix, $\bar{\underset{\sim}{h}}^{F}$, yielding the MO energies and the LCAO MO coefficients. These coefficients are used to reconstruct $\bar{\underset{\sim}{R}}$ for comparison with the self-consistent $\bar{\underset{\sim}{R}}$ obtained from E2 or N5, thus testing to ensure the iterations have been effected for the ground state.

Input is from paper tape and magnetic tape and the results are output on line print. The calculation procedure is shown in flow diagram 7.

Procedure. After the general data have been read in, $\bar{\underset{\sim}{h}}^{F}$ and $\underset{\sim}{S}^{-\frac{1}{2}}$ are read from magnetic tape. $\bar{\underset{\sim}{h}}^{F}$ is diagonalised using the method of Jacobi [72], as in I6, I7 and I8, and the eigenvalues, which are the one electron MO energies, are ordered in increasing energy.

The eigenvectors of $\bar{\underset{\sim}{h}}^{F}$, which are the LCAO MO coefficients in the OAO basis stored in the columns of $\bar{\underset{\sim}{U}}$, and the Löwdin orthogonalisation matrix are then used to obtain the LCAO MO coefficients in the natural AO basis by forming the product $\underset{\sim}{U} = \underset{\sim}{S}^{-\frac{1}{2}}\bar{\underset{\sim}{U}}$.

D4 finishes by reforming the density matrix $\bar{\underset{\sim}{R}}$ from the occupied LCAO MO coefficients which are stored in $\bar{\underset{\sim}{T}}$. If the calculation has iterated to the ground state of the molecule this $\bar{\underset{\sim}{R}}$ and the final $\bar{\underset{\sim}{R}}$ from N5 or E2 should be identical.

The next program in the system can then be entered from D4.

FLOW DIAGRAM 7.

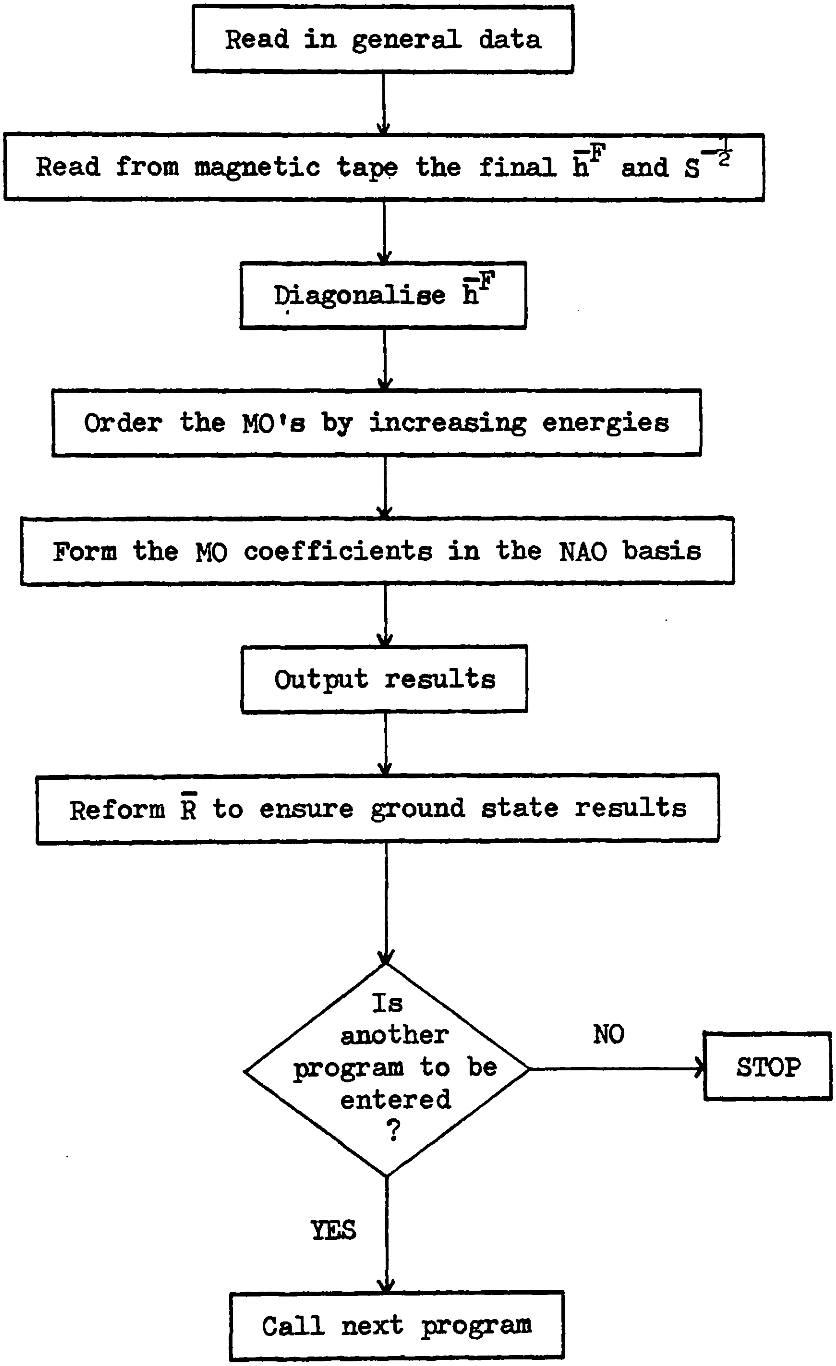

Discussion. As mentioned above the method of Jacobi is again used to obtain the eigenvalues and eigenvectors of a symmetric matrix. Although it is slower than other available methods, it should be pointed out that, for a molecule such as HCN, the computer times used by D4 and E2 are in the ratio of 1:150 which requires little improvement for such small molecules.

5.9. The Electron Density Program, C1.

Description. This program uses the AO basis set data in conjunction with the representation of the one-electron density matrix in the natural AO basis corresponding to the molecular energy minimum, $\underset{\sim}{R}$, to evaluate the electron density at each point of a chosen grid.

$$P_1(1) = 2 \sum_p \sum_q \chi_p(1)\, \chi_q(1)\, R_{pq}$$

C1 can also evaluate the difference electron density between two chemical systems, $\Delta P_1(1)$.

$$\Delta P_1(1) = 2 \sum_p \sum_q \chi_p(1)\, \chi_q(1)\, [\, R_{pq} - R'_{pq}\,]$$

Input is from paper tape and magnetic tape and the results are output on line print. The calculation procedure is outlined in flow diagram 8.

Procedure. General data are first of all read in from paper tape. This information includes the initial and final values of

FLOW DIAGRAM 8.

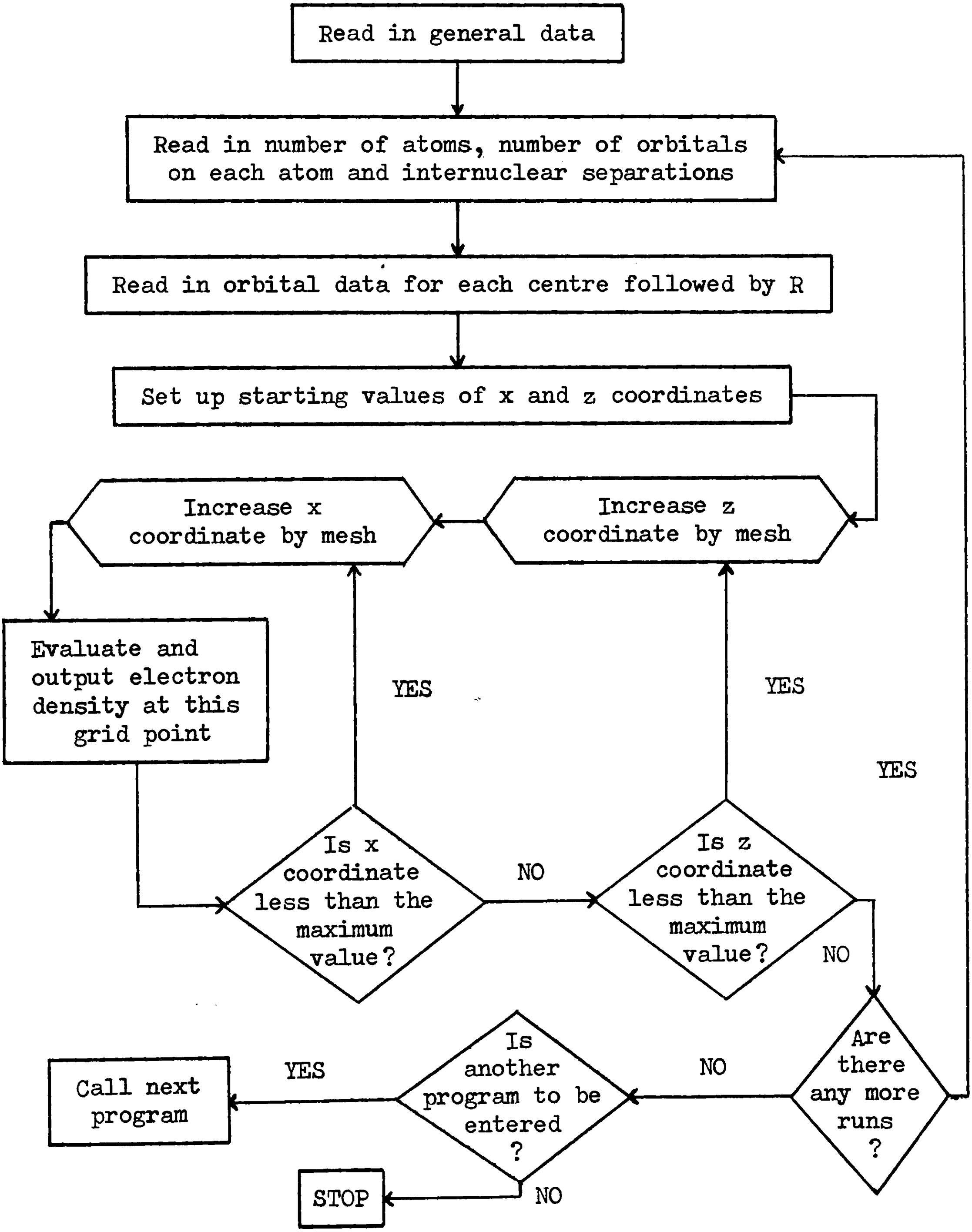

the abcissa, z, and ordinate, x, of the grid of points together with the desired mesh size. All parameters are expressed in atomic units of length.

The atomic orbital data, which is read in a form similar to that required for the one-electron matrices programs, is preceded by parameters recording the number of atoms present in the molecule; the number of orbitals present on each atom and the internuclear separations.

C1 then reads in $\underset{\sim}{R}$ from magnetic or paper tape. If a difference electron density calculation is to be performed, the density matrix of the second system is also read in and subtracted from the first. The order of these two matrices must of course be the same and rows and columns of zeros are added to one of them if this is not the case.

The program then enters two loops: the outer loop increases the abcissa by one mesh value and the inner loop the ordinate by a similar amount. This leads to the evaluation of the electron densities at all ordinate values for one particular abcissa value, in the inner loop.

The electronic charge density is then evaluated at each grid point according to one of the two equations given above, and the value of $P_1(1)$ or $\Delta P_1(1)$ is output on line print. The program then checks to see if the ordinate is below the maximum value required and, if it is, the inner loop is continued until the test is satisfied. A similar check is then applied to the outer loop. When this check is eventually satisfied the program can return to the beginning and begin a new calculation if this is required. Cl can then call the next program in the system if desired.

Discussion. This program was tested by reproducing a hand calculation on the hydrogen molecule. It normally requires from about one quarter to one half of the computer time used in the energy minimisation programs. Specific details of times for various molecules and mesh sizes are given in Table V.4.

Table V.4.

Sample Computer Run Times for Cl.

Molecule	Electron Density	Number of Grid Points	Time	Time per Mesh Point
CN^-	total	1134	3m 33s	0.188s
CN^-	total	1701	5m 18s	0.187s
CN^-	total	2140	6m 41s	0.187s
CN^-	pi	1809	1m 07s	0.037s
CN^-	sigma	1809	4m 55s	0.163s
HCN	total	2241	7m 45s	0.207s
HCN	total	2691	9m 21s	0.208
HCN	pi	2241	1m 21s	0.036s
FCN	total	2241	13m 30s	0.362s
FCN	pi	2241	2m 04s	0.055s

The times for difference electron densities are only a second or two longer than those quoted above.

5.10. The Molecular Properties Program, F1.

Description. This program is a beginning towards the goal of a program for evaluating molecular properties after an SCF calculation. By using the ALGOL switch facility, F1 can be very readily extended by the addition of small self-contained units.

At present F1 evaluates the molecular dipole moment, μ, the mean molecular kinetic energy T and the ratio $-2T/V$, where V is the mean potential energy, as a test of the Virial Theorem. In addition this program performs a population analysis according to the Doggett I and Doggett II methods whichever is desired.

Input is from paper and magnetic tape while the results are output on line print. The calculation procedure is outlined in flow diagram 9.

Procedure. F1 first reads in the general data from which all the array bounds are set. This is followed by the final $\underset{\sim}{R}$ matrix of N5 or E2, read from magnetic tape, which is converted into the matrix $\underset{\sim}{P}$, where $\underset{\sim}{P} = 2\underset{\sim}{R}$. The program then reads in the fork parameter to choose which of the program sections is to be entered via the switch mechanism.

The first section (iff=1) deals with the dipole moment evaluation. The dipole moment matrix, $\underset{\sim}{D}$, calculated in I7 or I8

FLOW DIAGRAM 9.

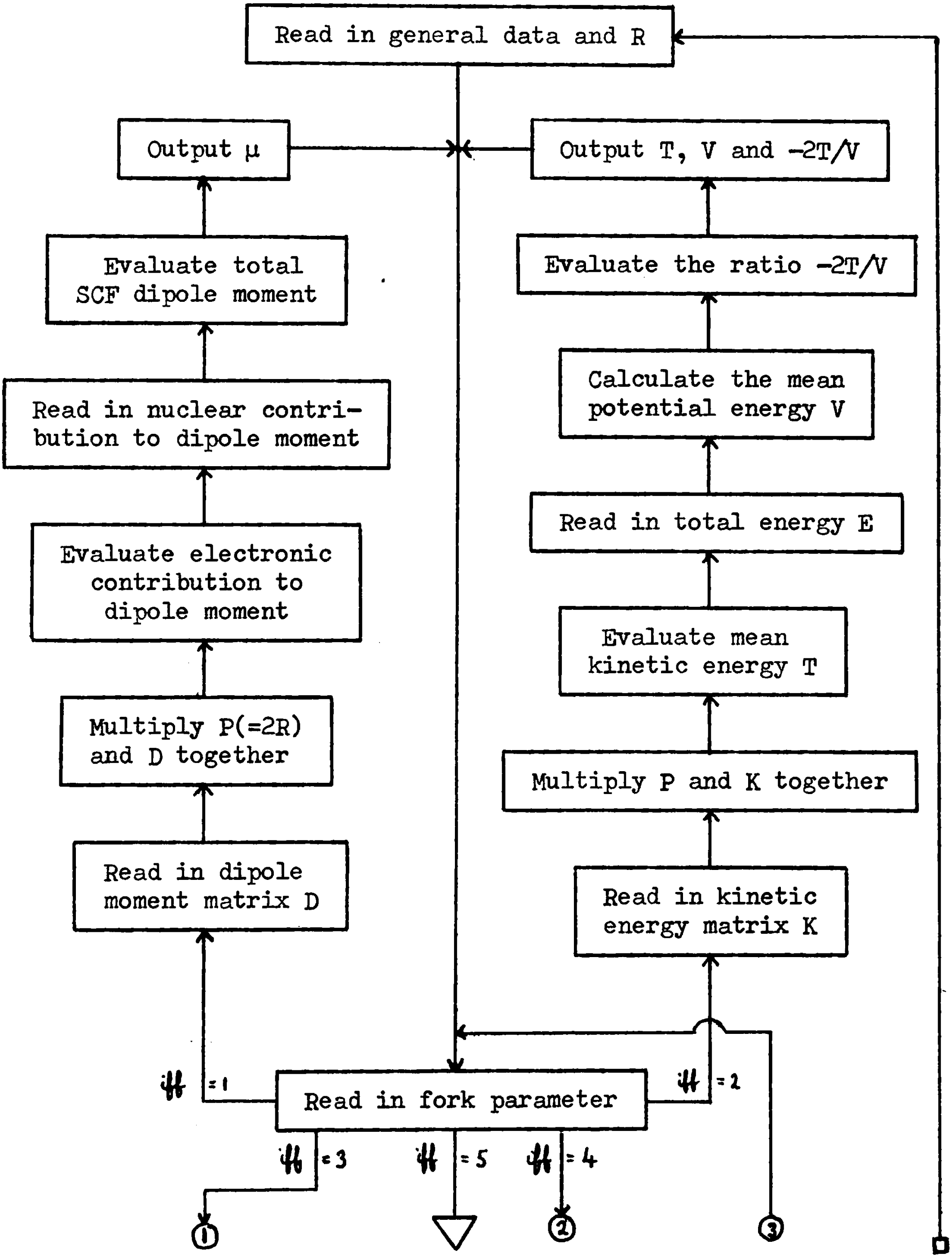

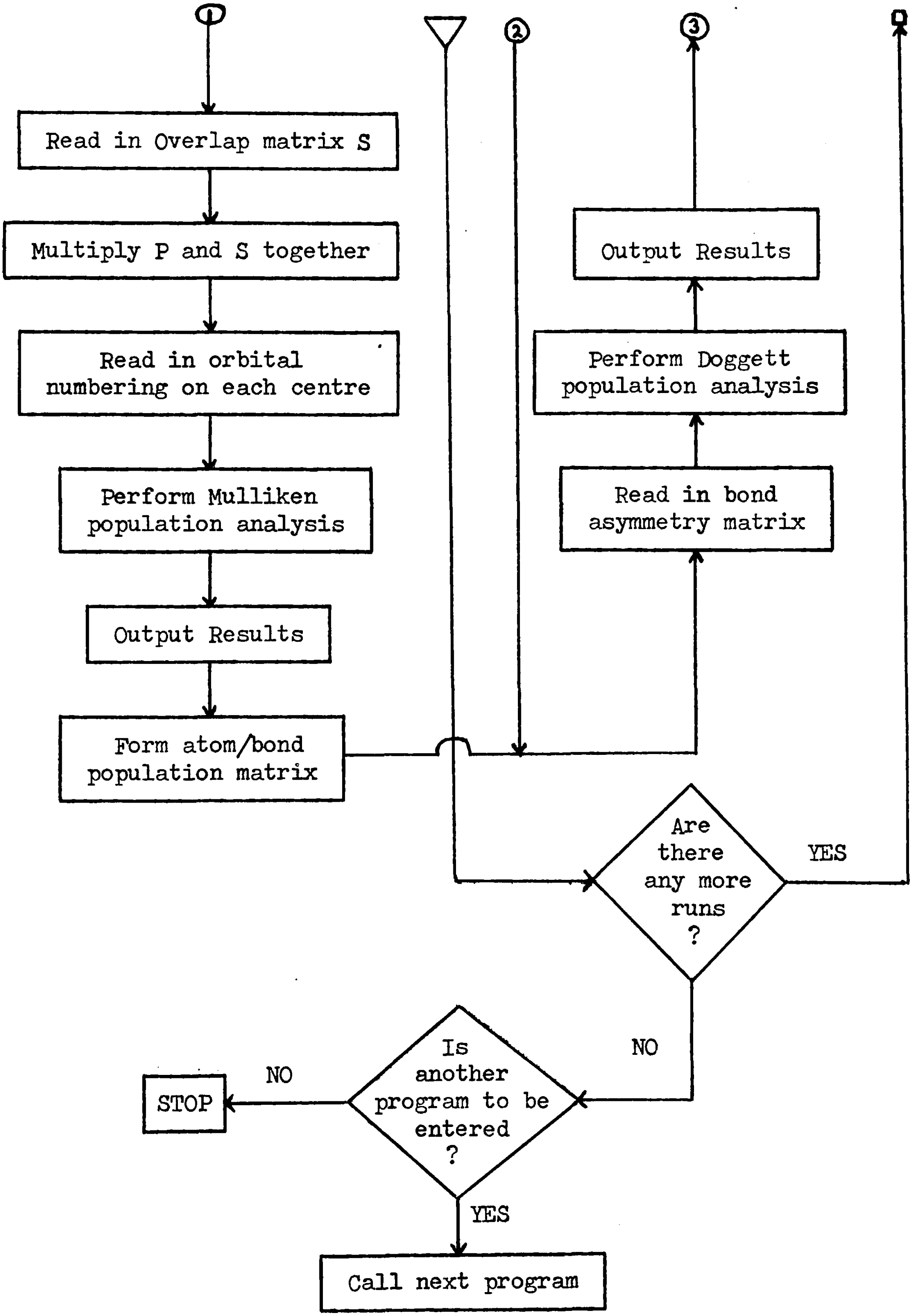
①
②
③
Read in Overlap matrix S
Multiply P and S together
Read in orbital numbering on each centre
Perform Mulliken population analysis
Output Results
Form atom/bond population matrix
Output Results
Perform Doggett population analysis
Read in bond asymmetry matrix
Are there any more runs ?
YES
NO
Is another program to be entered ?
NO
STOP
YES
Call next program

is read from magnetic tape and the electronic contribution to the molecular dipole moment is calculated from

$$\mu_e = 2\,\mathrm{tr}\,\underset{\sim}{R}\,\underset{\sim}{D} = \mathrm{tr}\,\underset{\sim}{P}\,\underset{\sim}{D} \qquad (\mathrm{V.9})$$

The nuclear contribution is read in from paper tape and the dipole moment in Debye units is calculated from the expression

$$\mu = (-\mu_e' + \mu_N) \times 2.5416 \qquad (\mathrm{V.10})$$

The second section (iff = 2) evaluates the total mean kinetic energy. The kinetic energy matrix evaluated in I6, I7 or I8, is read in from magnetic tape and the mean kinetic energy, T, is evaluated from the relationship,

$$T = 2\,\mathrm{tr}\,\underset{\sim}{R}\,\underset{\sim}{K} = \mathrm{tr}\,\underset{\sim}{P}\,\underset{\sim}{K} \qquad (\mathrm{V.11})$$

The total energy E is read in from paper tape allowing the potential energy V to be calculated since

$$V = E - T \qquad (\mathrm{V.12})$$

The ratio $-2T/V$ is then evaluated.

The final two sections of the present program are linked together in that section four is automatically performed after three. However, having performed section three once, section four can be entered again without going through three by choosing iff = 4.

Section three (iff = 3) has two purposes: firstly, a Mulliken Population analysis is performed for comparison with the results of section four, and secondly the orbital population matrix, $\underset{\sim}{Q}$, is evaluated for use in that section.

The overlap matrix is read from magnetic tape and the sigma orbital indexing on each centre is read in from paper tape. $\underset{\sim}{P}$ and $\underset{\sim}{S}$ are multiplied together and since $\mathrm{tr}\underset{\sim}{P}\underset{\sim}{S} = n$, the total number of electrons in the molecule, the diagonal elements when summed for each atom give the Mulliken gross atom charges, as discussed in 2.8. The $\underset{\sim}{Q}$ matrix is then formed according to the relationship,

$$Q_{ij} = P_{ij}S_{ij}(2-\delta_{ij}) \qquad (V.13)$$

Section four which is then entered performs a population analysis according to the Doggett I method which asymmetrically partitions each overlap electron density.

The bond asymmetry matrix is read from magnetic tape and using the orbital population matrix a Doggett I population analysis is performed as described in 2.8.

Section four may be entered again (iff=4) if the Doggett II method is also to be performed. The copytext facility allows the results on line print to show which method has been used for a given set of results.

At the end of each section the program returns to the point where another fork parameter is read in. This parameter can also be the EXIT value (iff=5) which will terminate any particular run.

F1 can then cycle back to the beginning to perform another run if desired.

Discussion. This program has the useful feature that it can be very easily extended in the future. It is also a very fast running program: a full evaluation on HCN, for example, takes only four seconds.

F1 was tested by checking with the results of hand calculations.

5.11. Discussion on the Program System.

There is one other program in the system not described above; namely, the SCF Control Program AA. It can be entered from any of the programs described above as an alternative to directly entering the succeeding program of the series. This is effected by giving 'scf' the value 9.

The functioning of AA is very simple. It uses the switch facility thus giving it the feature of being easily extended for future additions to the system. A key number is read in from paper tape defining which program is to be entered. A second advantage of AA is that non-sequential programs can be entered. For example, when effecting similar calculations using different multicentre integral approximations it is only necessary to enter N1 and N2 once and it is therefore desirable to enter N3, N4 or M3 direct from I6, I7 or I8.

The most important factor when compiling a series of programs is to be sure that they give the correct results. The first step is, of course, the rigorous testing of procedures and the individual programs themselves thus ensuring, for example, accurate integrals and correct matrix diagonalisations. However, the final test must be the reproduction of reliable quantities from a well known published work.

The first test applied to this program system was the simple molecule NH as published by B. J. Ransil [3] using an STO basis set. The second test applied was the HCN isoelectronic system CO, again the work of Ransil, using an STO basis set. The results of these comparisons were very encouraging and are shown in Tables V.5 and V.6 for NH and CO respectively.

Table V.5.

Comparison of Total Energy and One-Electron MO Energies for NH.

	Glasgow Programs	Ransil's Calculation
Total Energy E	-54.25979	-54.25984
ε (1σ)	-15.31753	-15.31801
ε (2σ)	-0.87018	-0.87022
ε (3σ)	0.00295	0.00293
ε (4σ)	0.58472	0.58475
ε (1π)	-0.23758	-0.23778

Table V.6.

Comparison of Total Energy and One-Electron MO Energies for CO.

	Glasgow Programs	Ransil's Calculation
Total Energy E	-112.34323	-112.34357
ε (1σ)	-20.70574	-20.70597
ε (2σ)	-11.35331	-11.35323
ε (3σ)	-1.49879	-1.49881
ε (4σ)	-0.73228	-0.73234
ε (5σ)	-0.48079	-0.48078
ε (6σ)	0.93370	0.93222
ε (1π)	-0.58304	-0.58308
ε (2π)	0.26077	0.26082

The third and last test applied was against an earlier best atom Slater calculation on HCN by McLean [4]. This calculation could not be exactly reproduced since exact multicentre integrals were used by McLean: nevertheless the published quantities give a valuable guide to the accuracy of the present calculations and incidently to the overall effect of the multicentre approximations.

The results and comparisons using various approximations are presented and discussed in 4.1. and are perfectly satisfactory from the test viewpoint.

Another important point of modern quantum chemistry computing is the time involved in performing a calculation. Some statistics are shown in Table III.7 of chapter three for various calculations. The computing times of this system compare very favourably indeed with those of the McLean-Yoshimine program [67,73,74], where comparisons are possible. There are, however, two important factors which affect this comparison. The present system is much more limited in its field of application than the McL-Yosh program and increasing flexibility nearly always involves increasing run times. But, since much of the McL-Yosh Linear Program is written in machine code this should compensate for the long run times imposed by the generality of the program.

It is difficult to make comparisons with the other major program systems, IBMOL [75,76], POLYATOM which was reviewed recently by Csizmadia et al [77] or the more recent MOSES [78], except to note that they all use Gaussian type functions in the AO basis set. The present program system, however, does not compare well in terms of run times with a recently reported double-zeta calculation on F_2[79] which took 3.27 minutes. This exceptional time must be due solely to the use of a Univac 1108 computer and it is doubtful if any of the above program systems would be comparable with such times.

The tests and comparisons made on the present system lead to the conclusion that the system, although limited in scope, is correct, accurate and reasonably fast.

CHAPTER SIX

FUTURE WORK

Arising out of the results and experience obtained from this work, a few proposals as to its possible extension are now put forward.

The major extension of this work must be in the direction of extending the basis set to include polarisation orbitals. This should lead to more accurate values for experimental observables and also allow the study of molecules containing second row elements. The system of computer programs must also be extended in order to study non-linear and open shell molecules.

However, a more immediate extension of this work would be in a fuller examination of the potential of the partial Löwdin approximation. It would also be useful if a set of rules could be found to determine whether the full or partial Löwdin method should be used for a given nuclear configuration.

Perhaps the greatest scope for expansion is in the information which can be obtained from the contour diagrams and profiles. It would be very useful if some of the qualitative observations made on such diagrams could be given a quantitative basis. For example, the electron probability density could be integrated over some defined region of space to yield quantities similar to gross atom charges and bond populations. These regions, for example, could be spheres centred on the nuclei, or better still, cylinders of a given length and radius. The total number of electrons resulting from such an integration procedure would be less than reality and it would be necessary to scale the resulting charges accordingly. In the case of difference densities the total charge between the nodes might give more quantitative ideas of charge transfer on molecular formation but the integration procedure would be rather complex.

As was noted throughout chapter four, the total energy resulting from calculations involving multicentre integral approximations is lower than that of accurate calculations. It was also seen that the calculated dipole moments are lower than the experimental values. Consequently, it would seem useful to investigate a constrained variation calculation where the resulting wave function is constrained to reproduce the experimental dipole moment. Because of the additional constraint imposed, the total energy would be a little higher and this would take it closer to the value from an accurate calculation. The expectation would be that other molecular properties would be obtained more accurately using this constrained wave function.

The goal of any such extensions must be to obtain as accurate molecular properties as possible with the minimum possible computation. The careful exploitation of the results obtained to yield simple new chemical concepts must be a complementary objective to the calculations themselves.

Appendix One.

This appendix contains descriptions of the coordinate system used in the evaluation of the molecular integrals and the method of Gaussian numerical quadrature.

Prolate Spheroidal Coordinates.

As discussed in chapter two the molecular integrals are expressed in elliptical coordinates before performing the Gaussian quadrature. This coordinate system is defined below where the two centres are designated by a and b and their internuclear separation by R.

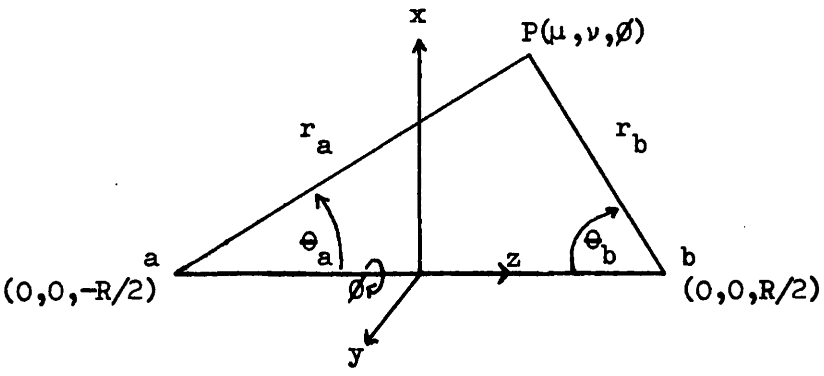

All other symbols are defined in the above diagram. The elliptical coordinates of P are defined as follows:

$$\mu = \frac{r_a + r_b}{R} \tag{A1.1}$$

$$\nu = \frac{r_a - r_b}{R} \qquad \text{(A1.2)}$$

$$\phi = \phi_a = \phi_b \qquad \text{(A1.3)}$$

The formulae for converting from spherical coordinates, on either a or b, to prolate spheroidal coordinates are as follows

$$r_a = \frac{R}{2}(\mu + \nu) \qquad \text{(A1.4)}$$

$$r_b = \frac{R}{2}(\mu - \nu) \qquad \text{(A1.5)}$$

$$\cos\theta_a = \frac{1 + \mu\nu}{\mu + \nu} \qquad \text{(A1.6)}$$

$$\cos\theta_b = \frac{1 - \mu\nu}{\mu - \nu} \qquad \text{(A1.7)}$$

$$\sin\theta_a = \frac{[\,(\mu^2-1)(1-\nu^2)\,]^{\frac{1}{2}}}{(\mu+\nu)} \qquad \text{(A1.8)}$$

$$\sin\theta_b = \frac{[(\mu^2-1)(1-\nu^2)]^{\frac{1}{2}}}{(\mu-\nu)} \qquad (A1.9)$$

For volume integration the conversion is

$$r^2\sin\theta \, dr d\theta d\phi = \frac{R^3}{8}(\mu^2-\nu^2) \, d\mu d\nu d\phi \qquad (A1.10)$$

and the integration limits are

ϕ : $0 \rightarrow 2$

μ : $1 \rightarrow \infty$

ν : $-1 \rightarrow 1$

Gaussian Numerical Quadrature.

In the numerical integration of the definite integral $\int_a^b f(x)dx$ from a given number of values of $f(x)$, the first problem is to decide how the interval (a,b) should be divided to obtain the greatest possible accuracy. Conventionally, for example, in Simpson's or Weddle's rules, equally spaced ordinates are used. However, Gauss showed that, for optimum accuracy, the ordinates should not be equidistant although they should be symmetrically placed with respect to the mid-point of the interval of integration.

Let $I = \int_a^b ydx$ denote the integral to be evaluated. On changing the variable by the substitution,

$$x = \frac{(b-a)}{2}u + \frac{(b+a)}{2} \qquad (A1.11)$$

the limits of integration become ±1.

Then $y = f(x) = f\left\{\left(\frac{b-a}{2}\right)u + \left(\frac{b+a}{2}\right)\right\} = \emptyset(u)$, say, and since

$dx = \left(\frac{b-a}{2}\right)du$ then,

$$I = \left(\frac{b-a}{2}\right)\int_{-1}^{+1}\emptyset(u)\,du = \left(\frac{b-a}{2}\right)J \qquad (A1.12)$$

Gauss's formula is

$$J = \int_{-1}^{+1}\emptyset(u)\,du = R_1\emptyset(u_1) + R_2\emptyset(u_2) + \dots + R_n\emptyset(u_n) \qquad (A1.13)$$

where $u_1, u_2, \dots, u_n$ are the points of subdivision in the interval $u=-1$ to $u=+1$. The corresponding values of x are,

$$x_i = \left(\frac{b-a}{2}\right)u_i + \left(\frac{b+a}{2}\right)$$

and the value of $\int_a^b f(x)\,dx$ is given by

$$I = \int_{-1}^{+1}\left(\frac{b-a}{2}\right)[R_1\emptyset(u_1) + R_2\emptyset(u_2) + \dots + R_n\emptyset(u_n)] \qquad (A1.14)$$

Assuming that $\phi(u)$ can be expanded in a convergent power series in the interval $-1 < u < +1$,

$$J = \int_{-1}^{+1} \phi(u)\,du = \int_{-1}^{+1} (a_0 + a_1 u + a_2 u^2 + \dots + a_m u^m + \dots)\,du$$

$$= 2a_0 + \frac{2}{3}a_2 + \frac{2}{5}a_4 + \dots \qquad \text{(A1.15)}$$

Also
$$\begin{aligned} \phi(u_1) &= a_0 + a_1 u_1 + a_2 u_1^2 + \dots + a_m u_1^m + \dots \\ \phi(u_2) &= a_0 + a_1 u_2 + a_2 u_2^2 + \dots + a_m u_2^m + \dots \\ &\vdots \\ \phi(u_n) &= a_0 + a_1 u_n + a_2 u_n^2 + \dots + a_m u_n^m + \dots \end{aligned} \qquad \text{(A1.16)}$$

On substituting (A1.16) into (A1.13)

$$\begin{aligned} J = {} & R_1(a_0 + a_1 u_1 + a_2 u_1^2 + \dots . a_m u_1^m) \\ & + R_2(a_0 + a_1 u_2 + \dots\dots\dots . a_m u_2^m) \\ & + R_3(a_0 + \dots\dots \end{aligned} \qquad \text{(A1.17)}$$

or
$$\begin{aligned} J = {} & a_0(R_1 + R_2 + \dots + R_n) + a_1(R_1 u_1 + R_2 u_2 + \dots + R_n u_n) + \\ & a_2(R_1 u_1^2 + R_2 u_2^2 + \dots + R_n u_n^2) + \dots \end{aligned} \qquad \text{(A1.18)}$$

Now, for (A1.18) to be identical to (A1.15), the coefficients of a_0, a_1 etc., must also be identical. Therefore,

$$R_1 + R_2 + \dots + R_n = 2$$

$$R_1u_1 + R_2u_2 + \dots + R_nu_n = 0$$

$$R_1u_1^2 + R_2u_2^2 + \dots + R_nu_n^2 = \frac{2}{3} \text{ etc.} \qquad \text{(A1.19)}$$

By taking 2n of these equations and solving them simultaneously, it is theoretically possible to find the 2n quantities, u_1 to u_n and R_1 to R_n. This is very laborious and the following method is preferentially used. It can be shown that if $\phi(u)$ is a polynomial of degree not greater than 2n-1, then u_1, u_2 ... u_n are the zero's of the Legendre polynomial $P_n(u)$; i.e. the roots of $P_n(u) = 0$.

$$P_n(u) = C \frac{d^n}{du^n} (u^2-1)^n = 0 \qquad \text{(A1.20)}$$

where C is a constant. It is necessary, therefore, to solve the equation

$$\frac{d^n}{du^n} (u^2-1)^n = 0 \qquad \text{(A1.21).}$$

For a particular n, the u_i can be found and substituted into equations (A1.19) to yield the R_i. The u_i and R_i for n = 16 which are used in the numerical integration of the molecular integrals in this thesis are given in Table A1.1.

Table A1.1.

The Gaussian u and R values for n = 16.

u_1	0.98940094	R_1	0.02715246
u_2	0.94457502	R_2	0.06225352
u_3	0.86563120	R_3	0.09515851
u_4	0.75540441	R_4	0.12462897
u_5	0.61787624	R_5	0.14959599
u_6	0.45801678	R_6	0.16915652
u_7	0.28160355	R_7	0.18260342
u_8	0.09501251	R_8	0.18945061
u_9	−0.09501251	R_9	0.18945061
u_{10}	−0.28160355	R_{10}	0.18260342
u_{11}	−0.45801678	R_{11}	0.16915652
u_{12}	−0.61787624	R_{12}	0.14959599
u_{13}	−0.75540441	R_{13}	0.12462897
u_{14}	−0.86563120	R_{14}	0.09515851
u_{15}	−0.94457502	R_{15}	0.06225352
u_{16}	−0.98940094	R_{16}	0.02715246

After performing the ϕ integration analytically the molecular integrals are dependent on the two remaining elliptical coordinates, μ and ν. This double integration is effected by two applications of Gaussian quadrature; i.e. a two dimensional grid is set up, and the integrand is evaluated at each grid point, followed by the summation, over all mesh points, of each integrand multiplied by the appropriate weight factor. For example, $I = \int_{-1}^{+1}\int_{1}^{\infty} f(\mu,\nu)d\mu d\nu$ represents a typical molecular integral where the limits of μ run from 1 to ∞. To change the limits to -1 to $+1$ a change of variable is made.

The integration over μ is divided into two ranges: from 1 to D and from D to E. In this work D and E are taken as 2.5 and 13 respectively as suggested by Magnusson and Zauli [80]. Thus

$$I = I_1 + I_2 = \int_{-1}^{+1}\int_{1}^{D} f(\mu,\nu)d\mu d\nu + \int_{-1}^{+1}\int_{D}^{E} f(\mu,\nu)d\mu d\nu \qquad \text{(A1.22)}$$

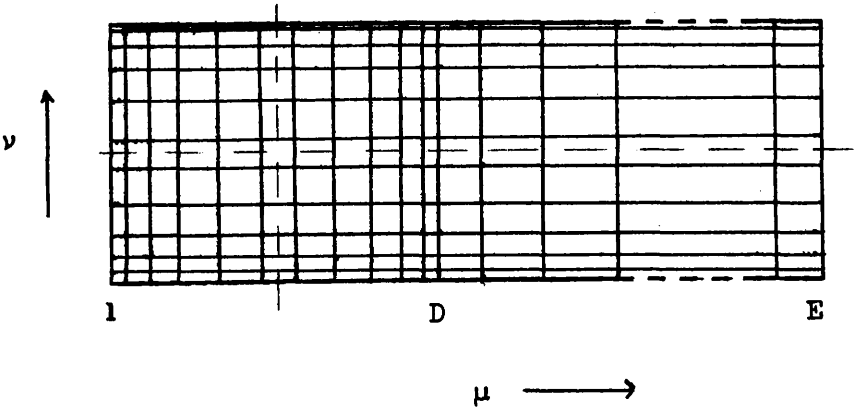

For the first range, $\frac{b-a}{2} \equiv \frac{D-1}{2} = H$, say, then the contribution to the integral I for a particular ν_j, I^j, is given by

$$I^j = H[R_1\phi(u_1\nu_j) + R_2\phi(u_2\nu_j) + \dots + R_n\phi(u_n\nu_j)] \qquad \text{(A1.23)}$$

where
$$\phi(u_i\nu_j) = f(Hu_i + H + 1, \nu_j) \qquad \text{(A1.24)}$$

The complete integral is then obtained by summing over the ν_j to give

$$\begin{aligned} I_1 = {} & H[R_1R_1\phi(u_1\nu_1) + R_2R_1\phi(u_2\nu_1) + \dots + R_1R_2\phi(u_1\nu_2) \\ & + \dots + R_iR_j\phi(u_i\nu_j) + \dots + R_nR_n\phi(u_n\nu_n)] \end{aligned} \qquad \text{(A1.25)}$$

The analysis is repeated for the second range of μ, but H is now given by $\frac{E-D}{2}$.

APPENDIX TWO.

This appendix contains the values of all the molecular one- and two-electron integrals which were used in the improved calculation on HCN with the nuclei in their equilibrium ground state configuration as given in chapter three. The molecular axis convention is also given in that chapter.

All multicentre integrals quoted here were evaluated according to the full Löwdin approximation as shown in chapter two. The values of the elements of a few important one-electron matrices which occurred in the computation, are also included below. The integrals and matrix elements are indexed according to the nomenclature introduced in chapter three.

The following symbols for the various one-electron matrices are used in the table headings:

S : Overlap matrix
D : Dipole moment matrix
KE : Kinetic energy matrix
R(N) : Matrix of nuclear attraction integrals of form $(p|1/r_N|q)$
R(C) : Matrix of nuclear attraction integrals of form $(p|1/r_C|q)$
R(H) : Matrix of nuclear attraction integrals of form $(p|1/r_H|q)$
$S^{-\frac{1}{2}}$: Löwdin orthogonalisation matrix
μ : Partial Löwdin bond asymmetry matrix
λ : Full Löwdin bond asymmetry matrix
f : Matrix of the one-electron Hamiltonian operator over NAO's
$\bar{f}$: Matrix of the one-electron Hamiltonian operator over LOAO's
$\bar{G}$: Matrix of the two-electron Hamiltonian operator over LOAO's at the SCF energy minimum

Index	S	D	KE	R(N)	R(C)	R(H)
11	1.00000	0.00000	22.14032	6.65280	0.45658	0.23815
12	0.00000	0.00000	-5.93114	-0.91915	-0.00001	-0.00002
13	0.00000	0.06989	0.00000	0.00000	0.01454	0.00396
14	0.00034	0.00035	-0.00193	0.00055	0.00045	0.00012
15	0.06039	0.00711	-0.00103	0.19339	0.02911	0.01357
16	-0.10318	-0.00857	-0.02822	-0.33679	-0.04912	-0.02566
17	0.00770	0.00115	-0.00193	0.02403	0.00352	0.00192
22	1.00000	0.00000	2.24545	1.07832	0.45015	0.23813
23	0.00000	0.77706	0.00000	0.00000	0.14658	0.04400
24	0.06271	0.12556	-0.01293	0.03141	0.16884	0.02853
25	0.47846	0.45374	0.10357	0.31519	0.28003	0.13401
26	-0.51628	-0.13155	-0.25961	-0.40514	-0.28122	-0.12846
27	0.11698	0.19143	-0.01041	0.06049	0.07074	0.04808
33	1.00000	0.00000	1.87870	0.95894	0.51362	0.25139
34	0.11299	0.23196	0.02182	0.05542	0.31415	0.05429
35	0.43173	0.81998	0.22833	0.25402	0.32059	0.17505
36	-0.20462	-0.29532	-0.33764	-0.20058	-0.20476	-0.06214
37	0.15004	0.39277	0.00702	0.06242	0.08108	0.08204
44	1.00000	2.19021	16.04940	0.45658	5.66398	0.49781
45	0.00000	0.00000	-4.17365	-0.00002	-0.76063	-0.00004
46	0.00000	0.07815	0.00000	-0.01623	0.00000	0.01928
47	0.08367	0.19463	0.00303	0.03696	0.22926	0.04487
55	1.00000	2.19021	1.54334	0.44169	0.89744	0.47438
56	0.00000	0.93471	0.00000	-0.15987	0.00000	0.17807
57	0.58538	1.87083	0.12615	0.17108	0.34358	0.41884
66	1.00000	2.19021	1.25433	0.51089	0.78417	0.55067
67	0.50876	2.19671	0.25045	0.11535	0.27514	0.50483
77	1.00000	4.19901	0.50000	0.23787	0.47086	1.00000
88	1.00000	0.00000	1.87870	0.95894	0.41106	0.23144
89	0.36309	0.35848	0.16811	0.20615	0.19257	0.11442
99	1.00000	2.19021	1.25433	0.39236	0.78417	0.41708

Index	$S^{-\frac{1}{2}}$	μ	λ	f	$\bar{f}$	$\bar{G}$
11	1.01361	0.00000	0.00000	-27.40688	-27.29046	11.59836
12	0.08076	0.00000	0.00000	0.50298	0.83992	-0.56369
13	0.04932	0.00000	0.00000	-0.09119	0.14062	0.00588
14	-0.00709	0.46248	0.46248	-0.00852	-0.05055	0.02657
15	-0.06633	0.05374	0.19840	-1.54296	-0.69653	0.15269
16	0.11496	0.03791	0.05054	2.64967	1.16844	-0.21481
17	-0.03503	0.03556	0.03556	-0.19315	-0.19266	0.04220
22	1.49157	0.00000	0.00000	-8.24182	-8.35544	7.69156
23	0.31464	0.00000	0.00000	-0.92350	-0.82732	0.97697
24	-0.07733	0.91416	0.76205	-1.27432	-0.42008	0.00029
25	-0.48167	0.43298	0.51442	-3.91694	0.06552	-0.56756
26	0.63094	0.11633	-0.05283	4.39216	0.19253	0.44052
27	-0.18349	0.38971	0.19976	-0.90637	-0.06055	-0.07685
33	1.21793	0.00000	0.00000	-8.16700	-7.96183	7.58958
34	-0.09056	0.93727	0.92188	-2.30531	-0.74748	0.04338
35	-0.39838	0.86717	1.17355	-3.64841	-0.25848	-0.26415
36	0.32476	0.65898	0.30344	2.35715	0.47415	-0.03129
37	-0.08004	0.62341	0.55947	-0.99845	0.12789	-0.13367
44	1.01644	0.00000	0.00000	-21.62830	-21.51079	10.10557
45	0.09153	0.00000	0.00000	0.39032	0.75253	-0.47533
46	-0.02555	0.00000	0.00000	0.09435	0.04835	-0.10865
47	-0.05947	0.06766	0.06766	-1.67615	-0.81824	0.31906
55	1.54109	0.00000	0.00000	-7.40747	-7.19068	6.76718
56	-0.10525	0.00000	0.00000	0.94104	0.34514	-0.48737
57	-0.43140	0.50065	0.16159	-3.55174	-0.27138	-0.01618
66	1.58428	0.00000	0.00000	-7.57753	-7.35864	7.23159
67	-0.56626	1.05911	1.12901	-2.71266	0.07474	-0.54380
77	1.47608	0.00000	0.00000	-4.99024	-4.29383	4.17734
88	1.05477	0.00000	0.00000	-7.53168	-7.57503	7.35250
89	-0.19825	0.45078	0.45078	-2.54478	0.02686	-0.39241
99	1.05477	0.00000	0.00000	-6.61424	-6.59040	6.39214

THE TWO-ELECTRON INTEGRALS.

$(\sigma\sigma|\sigma\sigma)$

1111	4.12497	1214	-0.00002	1322	0.00000	1427	0.00002
1112	-0.40503	1215	-0.01016	1323	0.03105	1433	0.00027
1113	0.00000	1216	0.01784	1324	0.00109	1434	0.00004
1114	0.00048	1217	-0.00125	1325	0.00688	1435	0.00012
1115	0.15776	1222	-0.01701	1326	-0.00724	1436	-0.00010
1116	-0.27394	1223	0.00000	1327	0.00120	1437	0.00002
1117	0.01965	1224	-0.00000	1333	0.00000	1444	0.00039
1122	0.97628	1225	0.00016	1334	0.00191	1445	-0.00001
1123	0.00000	1226	-0.00036	1335	0.01413	1446	-0.00001
1124	0.03142	1227	0.00002	1336	-0.01909	1447	0.00003
1125	0.32162	1233	-0.01145	1337	0.00248	1455	0.00021
1126	-0.41650	1234	-0.00001	1344	0.01454	1456	-0.00005
1127	0.06128	1235	-0.00070	1345	-0.00001	1457	0.00009
1133	0.94897	1236	0.00097	1346	-0.00102	1466	0.00023
1134	0.05542	1237	-0.00008	1347	0.00116	1467	0.00006
1135	0.25364	1244	-0.00001	1355	0.01151	1477	0.00012
1136	-0.20005	1245	-0.00000	1356	-0.00602	1515	0.00722
1137	0.06238	1246	0.00001	1357	0.00345	1516	-0.01245
1144	0.45658	1247	-0.00000	1366	0.01362	1517	0.00102
1145	-0.00003	1255	-0.00064	1367	0.00182	1522	0.05443
1146	-0.01623	1256	0.00107	1377	0.00392	1523	0.00259
1147	0.03696	1257	0.00014	1414	0.00000	1524	0.00201
1155	0.44097	1266	-0.00182	1415	0.00003	1525	0.02002
1156	-0.15861	1267	0.00003	1416	-0.00004	1526	-0.02577
1157	0.17126	1277	-0.00001	1417	0.00000	1527	0.00394
1166	0.50868	1313	0.02875	1422	0.00025	1533	0.05459
1167	0.11539	1314	0.00002	1423	0.00006	1534	0.00354
1177	0.23786	1315	0.00163	1424	0.00002	1535	0.01636
1212	0.06438	1316	-0.00225	1425	0.00012	1536	-0.01341
1213	0.00000	1317	0.00018	1426	-0.00014	1537	0.00385

1544	0.02912	1677	-0.02531	2236	-0.15881	2424	0.00671
1545	0.00000	1717	0.00010	2237	0.05836	2425	0.01899
1546	-0.00108	1722	0.00686	2244	0.44950	2426	-0.01930
1547	0.00235	1723	0.00030	2245	-0.00064	2427	0.00443
1555	0.02761	1724	0.00028	2246	-0.01422	2433	0.03419
1556	-0.00983	1725	0.00276	2247	0.03641	2434	0.01227
1557	0.01071	1726	-0.00352	2255	0.41352	2435	0.02181
1566	0.03156	1727	0.00049	2256	-0.11902	2436	-0.01463
1567	0.00687	1733	0.00687	2257	0.17458	2437	0.00518
1577	0.01426	1734	0.00043	2266	0.44684	2444	0.13811
1616	0.02146	1735	0.00145	2267	0.11607	2445	-0.00859
1617	-0.00195	1736	-0.00150	2277	0.23721	2446	-0.00192
1622	-0.09350	1737	0.00050	2323	0.13737	2447	0.01093
1623	-0.00348	1744	0.00352	2324	0.00987	2455	0.04735
1624	-0.00339	1745	0.00000	2325	0.04351	2456	-0.00315
1625	-0.03407	1746	-0.00012	2326	-0.03882	2457	0.02386
1626	0.04396	1747	0.00031	2327	0.00911	2466	0.04679
1627	-0.00638	1755	0.00339	2333	0.00000	2467	0.01277
1633	-0.09369	1756	-0.00115	2334	0.01753	2477	0.02713
1634	-0.00598	1757	0.00237	2335	0.07633	2525	0.13459
1635	-0.02755	1766	0.00390	2336	-0.08406	2526	-0.15434
1636	0.02242	1767	0.00255	2337	0.01684	2527	0.03272
1637	-0.00650	1777	0.00191	2344	0.14536	2533	0.27747
1644	-0.04912	2222	0.68321	2345	-0.00110	2534	0.03386
1645	0.00001	2223	0.00000	2346	-0.00729	2535	0.12876
1646	0.00182	2224	0.03028	2347	0.01158	2536	-0.09331
1647	-0.00398	2225	0.27508	2355	0.09809	2537	0.03417
1655	-0.04673	2226	-0.34277	2356	-0.02964	2544	0.28540
1656	0.01670	2227	0.05494	2357	0.03945	2545	0.00010
1657	-0.01821	2233	0.66903	2366	0.09840	2546	-0.00773
1666	-0.05349	2234	0.05363	2367	0.02036	2547	0.02305
1667	-0.01231	2235	0.22165	2377	0.04266	2555	0.24158

2556	-0.04972	2755	0.06038	3466	0.08469	3747	0.00694
2557	0.11042	2756	-0.01204	3467	0.02429	3755	0.06951
2566	0.24643	2757	0.03452	3477	0.05133	3756	0.00006
2567	0.06696	2766	0.06419	3535	0.13992	3757	0.03892
2577	0.13805	2767	0.03505	3536	-0.10281	3766	0.07408
2626	0.18784	2777	0.04261	3537	0.02910	3767	0.03394
2627	-0.02976	3333	0.70600	3544	0.33087	3777	0.06837
2633	-0.34160	3334	0.06064	3545	0.00032	4444	3.50894
2634	-0.03409	3335	0.23481	3546	-0.00780	4445	-0.33566
2635	-0.13771	3336	-0.16937	3547	0.02674	4446	0.00000
2636	0.10930	3337	0.06188	3555	0.26263	4447	0.18686
2637	-0.03332	3344	0.51133	3556	-0.03904	4455	0.81090
2644	-0.28078	3345	-0.00195	3557	0.12786	4456	0.00000
2645	0.00081	3346	-0.01717	3566	0.26078	4457	0.35101
2646	0.01346	3347	0.04130	3567	0.08061	4466	0.77688
2647	-0.02263	3355	0.43678	3577	0.16485	4467	0.27471
2655	-0.24088	3356	-0.11992	3636	0.09945	4477	0.46966
2656	0.07831	3357	0.18663	3637	-0.01966	4545	0.05187
2657	-0.09693	3366	0.46932	3644	-0.20409	4546	0.00000
2666	-0.25658	3367	0.12142	3645	0.00120	4547	-0.01177
2667	-0.06315	3377	0.24893	3646	0.01621	4555	-0.01332
2677	-0.12872	3434	0.02246	3647	-0.01628	4556	0.00000
2727	0.00654	3435	0.03905	3655	-0.15171	4557	0.00020
2733	0.05596	3436	-0.02567	3656	0.06740	4566	-0.00840
2734	0.00788	3437	0.00904	3657	-0.05166	4567	-0.00079
2735	0.02849	3444	0.25557	3666	-0.15989	4577	-0.00103
2736	-0.01696	3445	-0.01622	3667	-0.03141	4646	0.02150
2737	0.00865	3446	-0.00285	3677	-0.06379	4647	0.00186
2744	0.07051	3447	0.02023	3737	0.01257	4655	0.00000
2745	-0.00022	3455	0.08591	3744	0.08076	4656	0.02428
2746	-0.00188	3456	-0.00449	3745	-0.00027	4657	0.00751
2747	0.00504	3457	0.04397	3746	-0.00034	4666	0.00000

4667	0.01547	4777	0.04103	5657	0.04873	6666	0.57892
4677	0.01405	5555	0.57244	5666	0.00000	6667	0.25167
4747	0.01202	5556	0.00000	5667	0.08694	6677	0.45192
4755	0.06333	5557	0.29621	5677	0.11362	6767	0.19602
4756	0.00303	5566	0.55462	5757	0.18569	6777	0.33893
4757	0.03038	5567	0.23622	5766	0.29841	7777	0.62500
4766	0.06236	5577	0.42338	5767	0.17797		
4767	0.02476	5656	0.11461	5777	0.31257		

$(\sigma\sigma|\pi\pi)$

1188	0.94897	2288	0.66903	3488	0.04899	4788	0.03337
1189	0.20588	2289	0.18247	3489	0.02225	4789	0.01678
1199	0.39235	2299	0.38416	3499	0.08383	4799	0.06184
1288	−0.01145	2388	0.00000	3588	0.20958	5588	0.39489
1289	−0.00050	2389	0.02475	3589	0.08506	5589	0.16690
1299	−0.00004	2399	0.08855	3599	0.25088	5599	0.55462
1388	0.00000	2488	0.02765	3688	−0.14778	5688	−0.11181
1389	0.00326	2489	0.01244	3689	−0.05722	5689	−0.02862
1399	0.00903	2499	0.04615	3699	−0.13893	5699	0.00000
1488	0.00023	2588	0.26638	3788	0.05567	5788	0.16796
1489	0.00007	2589	0.08998	3789	0.02167	5789	0.07982
1499	0.00019	2599	0.22928	3799	0.06456	5799	0.28303
1588	0.05420	2688	−0.33286	4488	0.41104	6688	0.42591
1589	0.01258	2689	−0.10114	4489	0.19230	6689	0.16508
1599	0.02461	2699	−0.22397	4499	0.77688	6699	0.52039
1688	−0.09315	2788	0.05323	4588	−0.00007	6788	0.11328
1689	−0.02142	2789	0.01975	4589	−0.00050	6789	0.05854
1699	−0.04165	2799	0.05583	4599	−0.00840	6799	0.21964
1788	0.00683	3388	0.63484	4688	−0.01163	7788	0.23097
1789	0.00186	3389	0.17941	4689	−0.00380	7789	0.11075
1799	0.00302	3399	0.40522	4699	0.00000	7799	0.39527

(σπ|σπ)

1818	0.02875
1819	0.00115
1828	0.03105
1829	0.00536
1838	0.00000
1839	0.00326
1848	0.00009
1849	0.00052
1858	0.01027
1859	0.00494
1868	-0.01583
1869	-0.00351
1878	0.00155
1879	0.00000
1919	0.00004
1928	0.00185
1929	0.00041
1938	0.00026
1939	0.00031
1948	0.00001
1949	0.00006
1958	0.00066
1959	0.00044
1968	-0.00096
1969	-0.00028
1978	0.00000
1979	0.00000
2828	0.13737
2829	0.03531
2838	0.00000
2839	0.02475
2848	0.00068
2849	0.00504
2858	0.04877
2859	0.04306
2868	-0.06795
2869	-0.02365
2878	0.00846
2879	0.00000
2929	0.01809
2938	0.00986
2939	0.01974
2948	0.00072
2949	0.00778
2958	0.01939
2959	0.03757
2968	-0.02151
2969	-0.01020
2978	0.00000
2979	0.00000
3838	0.03558
3839	0.01485
3848	0.00041
3849	0.00333
3858	0.00999
3859	0.01983
3868	-0.00885
3869	-0.00876
3878	0.00184
3879	0.00000
3939	0.02532
3948	0.00104
3949	0.01209
3958	0.01880
3959	0.05006
3968	-0.01779
3969	-0.00867
3978	0.00000
3979	0.00000
4848	0.00008
4849	0.00119
4858	0.00057
4859	0.00196
4868	-0.00051
4869	-0.00037
4878	0.00000
4879	0.00000
4949	0.02150
4958	0.00515
4959	0.02428
4968	-0.00380
4969	0.00000
4978	0.00000
4979	0.01050
5858	0.02299
5859	0.03423
5868	-0.02783
5869	-0.01201
5878	0.00000
5879	0.00000
5959	0.11461
5968	-0.02862
5969	0.00000
5978	0.00000
5979	0.05072
6868	0.03691
6869	0.01683
6878	0.00000
6879	0.00000
6969	0.02926
6978	0.00000
6979	0.00997
7878	0.00093
7879	0.00000
7979	0.02803

(ππ|ππ)

8888	0.70600
8999	0.16836
8889	0.18712
9999	0.57892
8899	0.37495
8989	0.06615

$(\pi\pi|\pi'\pi')$

881010	0.63484	891010	0.17208	991010	0.36203
881011	0.17208	891011	0.05952	991011	0.15495
881111	0.36203	891111	0.15495	991111	0.52039

$(\pi\pi'|\pi\pi')$

810810	0.03558	811811	0.00331	910910	0.00331
810811	0.00752	811910	0.00331	910911	0.00670
810910	0.00752	811911	0.00670	911911	0.02926
810911	0.00646				

REFERENCES.

[1] Mulliken, R.S., J. Chem. Phys., 3, 720 (1935).

[2] Pauling, L., "The Nature of the Chemical Bond", Cornell University Press, Ithaca, N.Y., 1940, 3rd ed.,1960.

[3] Ransil, B.J., Revs. Modern Phys., 32, 245 (1960).

[4] McLean, A.D., J. Chem. Phys., 37, 627 (1962).

[5] Tyler, J.K., and Sheridan, J., Trans. Faraday Soc., 59, 2661 (1963).

[6] Born, M., and Oppenheimer, J.R., Ann. Physik, 84, 457 (1927).

[7] Heitler, W., and London, F., Z. Physik, 44, 455 (1927).

[8] Hund, F., Z. Physik, 40, 742; 42, 93; 43, 805 (1927); 51, 759 (1928), etc.

[9] Mulliken, R.S., Phys. Rev., 32, 186; 32, 761 (1928); 33, 730 (1929), etc.

[10] Roothaan, C.C.J., Revs. Modern Phys., 23, 69 (1951).

[11] McWeeny, R., Revs. Modern Phys., 32, 335 (1960).

[12] Hoffmann, T.A., Phil. Trans. A, 257, 309 (1965).

[13] Veillard, A., and Clementi, E., Theoret. Chim. Acta, 7, 2 (1967).

[14] Clementi, E., J. Chem. Phys., 46, 3842 (1967).

[15] Brillouin, L., Actualités Sci. et Ind., 71, 159 (1933).

[16] Cook, D.B., Hollis, P.C., and McWeeny, R., Mol. Phys., 13, 553 (1967).

[17] Allen, T.L., and Shull, H., J. Chem. Phys., 35, 1644 (1961); J. Phys. Chem., 66, 2281 (1962).

[18] Lykos, P.G., and Parr, R.G., J. Chem. Phys., 24, 1166 (1956).

[19] Pariser, R., and Parr, R.G., J. Chem. Phys., 21, 466 (1953).

[20] Pople, J.A., Trans. Faraday Soc., 49, 1375 (1953).

[21] Pople, J.A., Santry, D.P., and Segal, G.A., J. Chem. Phys., 43, S129 (1965).

[22] Pople, J.A., and Segal, G.A., J. Chem. Phys., 43, S136 (1965).

[23] Löwdin, P.O., J. Chem. Phys., 18, 365 (1950).

[24] Pople, J.A., Beveridge, D.L., and Dobosh, P.A., J. Chem. Phys., 47, 2026 (1967).

[25] Sahni, R.C., and Sawhney, B.C., Internat. J. Quantum Chem., 1, 251 (1967).

[26] Matcha, R.L., J. Chem. Phys., 47, 4595 (1967).

[27] Clementi, E., I.B.M. J. Res. Develop. Suppl., 9, 2 (1965).

[28] Mulliken, R.S., J. Chem. Phys., 36, 3428 (1962).

[29] Ballinger, R.A., Mol. Phys., 2, 139 (1959).

[30] Karo, A.M., and Allen, L.C., J. Chem. Phys., 31, 968 (1959).

[31] Clementi, E., J. Chem. Phys., 45, 2595 (1966); 46, 3851 (1967); etc.

[32] Boys, S.F., Proc. Roy. Soc. London, A, 200, 542 (1950).

[33] Pan, D.C., and Allen, L.C., J. Chem. Phys., 46, 1797 (1967).

[34] Moffat, J.B., and Collens, R.J., Canad. J. Chem., 45, 655 (1967).

[35] Sklar, A.L., J. Chem. Phys., 7, 984 (1939).

[36] Mulliken, R.S., J. Chim. Phys., 46, 497 (1949); 46, 675 (1949).

[37] Rudenberg, K., J. Chem. Phys., 19, 1433 (1951).

[38] Löwdin, P.O., J. Chem. Phys., 21, 374 (1953).

[39] Cizek, J., Mol. Phys., 6, 20 (1963).

[40] Harris, F.E., and Rein, R., Theoret. Chim. Acta, 6, 73 (1966).

[41] Roach, A.R., Ph.D Thesis, University of Glasgow, (1967).

[42] Ellison, F.O., J. Chem. Phys., 23, 2358 (1955).

[43] Löwdin, P.O., Adv. Phys., 5, 1 (1956).

[44] Wahl, A.C., Science, 151, 961 (1966).

[45] Ransil, B.J., and Sinai, J., J. Chem. Phys., 46, 4050 (1967).

[46] Bader, R.F.W., Keaveny, I., and Cade, P.E., J. Chem. Phys., 47, 3381 (1967).

[47] Mulliken, R.S., J. Chem. Phys., 23, 1833 (1955).

[48] Cusachs, L.Ch., and Politzer, P., Chem. Phys. Letts., 1, 529 (1968).

[49] Doggett, G., J. Chem. Soc., A, (in press).

[50] Berthier, G., Tetrahedron, 19, Symp. Suppl. 2, 1 (1963).

[51] Moreau, C., and Serre, J., Theoret. Chim. Acta, 2, 40 (1964).

[52] Switendick, A.C., and Corbato, F.J., Quarterly Progress Report, Solid State and Molecular Theory Group, M.I.T., Oct. 15, 1959, pp 70-85.

[53] Roothaan, C.C.J., J. Chem. Phys., 19, 1445 (1951).

[54] Barnett, M.P., and Coulson, C.A., Phil. Trans., A243, 221(1951).

[55] Ruttink, P.J.A., Theoret. Chim. Acta, 6, 83 (1966).

[56] Koopmans, T.A., Physica, 1, 104 (1933).

[57] Newton, M.D., Progress Report, Wave mechanics Group, Mathematical Institute, Oxford, 1966-67, p.48.

[58] Cohen, E.R., Dumond, JWM., Layton, T.W., and Rollett, J.S., Revs. Modern Phys., 27, 363 (1955).

[59] Melrose, M.P., Ph.D. Thesis, University of London, (1964).

[60] Vedeneyev, V.I., et al, "Bond Energies, Ionisation Potentials and Electron Affinities", Edward Arnold, London, 1966.

[61] Bonaccorsi, R., Petrongolo, C., Scrocco, E., and Tomasi, J., J. Chem. Phys., 48, 1500 (1968).

[62] Palke, W.E., and Lipscomb, W.N., J. Amer. Chem. Soc., 88, 2384 (1966).

[63] McLean, A.D., and Yoshimine, M., Internat. J. Quantum Chem., 1S, 313 (1967).

[64] These values are obtained from a multicentre integral program being developed by R. Emanuel. The three-centre one-electron integrals are accurate to at least four or five decimal places.

[65] Clementi, E., Chem. Revs., 68, 341 (1968).

[66] Green, J.S., "KDF9 ALGOL programming", English Electric-Leo-Marconi Computers Ltd., Kidsgrove.

[67] McLean, A.D., and Yoshimine, M., I.B.M. J. Res. Develop., 12, 206 (1968).

[68] Sahni, R.C., and Cooley, J.W., "Tables of Molecular Integrals", Supplements 1 and 2, NASA Tech. Note, Washington, 1960.

[69] Preuss, H., "Integraltafeln zur Quantenchemie", 4 vols., Springer-Verlag OHG, Berlin, 1956-1961.

[70] Kotani, M., Amemiya, A., Ishiguro, E., and Kimura, T., "Tables of Molecular Integrals", Maruzen, Tokyo, 2nd edit., 1963.

[71] Nesbet, R.K., Revs. Modern Phys., 35, 552 (1963).

[72] Pope, D.A., and Tomkins, C., J. Assoc. Comp. Mach., 4, 459 (1957).

[73] McLean, A.D., and Yoshimine, M., "Tables of Linear Molecule Wave Functions", published as a supplement to [67].

[74] McLean, A.D., and Yoshimine, M., McL-Yosh. Linear Molecule Program 1 - User Manual.

[75] Clementi, E., and Davis, D.R., J. Computational Phys., 2, 223 (1967).

[76] IBMOL: Special I.B.M. Technical Report, I.B.M. Research Laboratory, San Jose, California, 1966.

[77] Csizmadia, I.G., Harrison, M.C., Moskowitz, J.W., and Sutcliffe, B.T., Theoret. Chim. Acta, 6, 191 (1966).

[78] Sachs, L.M., and Geller, M., Internat. J. Quantum Chem., 1S, 445 (1967).

[79] Harris, F.E., and Michels, H.H., Internat. J. Quantum Chem., 1S, 329 (1967).

[80] Magnusson, E.A., and Zauli, C., Proc. Phys. Soc., 78, 53 (1961).